



UNITED KINGDOM • CHINA • MALAYSIA

**Encapsulation of room temperature
ionic liquids by miniemulsion
polymerisation for application in low-
emitting latex coating**

By
Yiyang Kong

A thesis submitted to the University of Nottingham for
the degree of Doctor of Philosophy

July 2016

Abstract

Latex coating has gained increasing attention. It is prepared by mixing latex, a dispersion of polymer particles in water, with pigments, fillers, and additives. As water is used as solvent, emission of VOCs can be minimised. However, coalescing agent emission and excessive surfactant residual hinder its further applications. To solve these two problems, we tried to use room temperature ionic liquid (RTIL), a potential multi-functional additive with non-volatility, to replace coalescing agent, and employed silica nanoparticle as emulsifier to stabilise the latex.

The preparation of latex containing 1-octyl-3-methylimidazolium hexafluorophosphate (C_8mimPF_6), the target RTIL in this study, could be achieved by encapsulating C_8mimPF_6 inside particles *via* miniemulsion polymerisation. Two kinds of emulsifiers, surfactant and silica nanoparticle were employed to stabilise miniemulsion/latex. To achieve this encapsulation, three steps were carried out in succession: preparation of miniemulsion, miniemulsion polymerisation, and characterisation of latex containing C_8mimPF_6 . Factors, especially C_8mimPF_6 , on initial droplet size and stability of miniemulsion, yield and stability of polymerisation process, and final functionality of latexes were systemically investigated.

For miniemulsion stabilised by surfactant, sodium dodecyl sulfonate (SDSO), initial droplet size decreased apparently with the addition of C_8mimPF_6 up to 1 wt% due to the effect of C_8mimPF_6 on oil phase viscosity and interfacial tension. During storage, C_8mimPF_6 above 10 wt% led to the frequent coalescence of droplet as it decreased the absolute zeta potential. During polymerisation, when initiated by hydrophobic 2, 2-azobis (isobutyronitrile) (AIBN), C_8mimPF_6 had a promoting effect on the reaction rate at low concentrations, but this effect might reverse upon certain

C₈mimPF₆ concentrations, *e.g.* 10 wt%; while initiated by hydrophilic hydrogen peroxide/ascorbic acid (H₂O₂/AAc), this promoting effect faded even at low C₈mimPF₆ concentrations. The different limiting factors, kinetic or transfer of radicals, might determine the reaction rate with different types of initiator. The final particle size depended on the nucleation mechanism as well as the coalescence of droplets/particles during polymerisation. For the final latex, C₈mimPF₆ promoted the decrease in glass transition temperature (T_g) and the deformation of particles, due to its function as an external plasticiser with low T_g and compatibility with poly (methyl methacrylate) (PMMA) inside particles; the film became more flexible and had better thermal stability in the present of C₈mimPF₆.

To solve excessive surfactant residual, silica nanoparticles were employed as emulsifiers to stabilise miniemulsion. Adding 1 wt% C₈mimPF₆ resulted in a sharp decline in droplet size, due to the combined effects of C₈mimPF₆ on the viscosity of oil phase and interfacial tension. Because of the low absolute zeta potential, creaming or sediment occurred at different C₈mimPF₆ concentrations, determined by the density difference between the oil and water phases. During polymerisation, a higher yield could be achieved by AIBN, compared with H₂O₂/AAc. The change of C₈mimPF₆ concentration had a greater impact on product stability *e.g.* only above 10 wt% C₈mimPF₆, stable products could be achieved. For product yield, there was only small effects, varying from 85 wt% to 91 wt% with C₈mimPF₆ changing from 0 to 30 wt%. For the final latex, the T_g of the obtained polymer decreased with the increase of C₈mimPF₆ concentration, indicating its function as an external plasticiser, but deformation of particles was limited, probably due to obstacles of silica nanoparticles on the surface of particles. Compared with bulk PMMA, films containing C₈mimPF₆ had a better thermal stability at temperatures ranging from 300 °C to 450 °C.

Affirmation

The work reported in this thesis is the solely work of the author and has been published or is to be submitted in the following publications.

Published SCI Journal papers:

1. Hu, B.*; Kong, Y.; Zheng, R.; Dong, J.; Choy, K.-L.; Zhao, H., Effect of C8mimPF6 on miniemulsion polymerisation for application in new latex coating products. Faraday discussions, 2016, 190, 487-508.

2. Kong, Y.; Hu, B.*; Guo, Y.; Wu, Y., Effect of ionic liquids on stability of O/W miniemulsion for application of low emission coating products. Chinese Journal of Chemical Engineering, 2016, 24, 196-201.

3. Kong, Y.; Hu, B.*; Choy, K.-L.; Li, X.; Chen, G., Study of miniemulsion formulation containing 1-octyl-3-methylimidazolium hexafluorophosphate for its application in low-emitting coating products. Soft matter, 2015, 11, 1293-1302.

Submitted SCI Journal papers:

1. Kong, Y.; Hu, B.*; Choy, K.-L., Characterisation of latex in the presence of room temperature ionic liquids for application in low-emitting latex coating.

Conference paper:

1. Kong, Y.; Choy, K.-L.; Hu, B.*, The role of room temperature ionic liquids in miniemulsion stabilized by silica nanoparticles. Chemeca 2016, 25-28 September 2016, Adelaide Australia.

International conference:

1. Kong, Y.; Choy, K.-L.; Hu, B.*; The role of room temperature ionic liquids in miniemulsion stabilized by silica nanoparticles. Chemeca 2016, 25-28 September 2016, Adelaide Australia, oral presentation.
2. Kong, Y.; Hu, B.*; Choy, K.-L., Study on Pickering miniemulsion polymerisation containing room temperature ionic liquids: a step towards low-VOCs, non-surfactant latex coating. 26th EUCHEM on Molten Salts and Ionic Liquids, 3-8 July 2016, Vienna Austria, poster.
3. Hu, B.*; Kong, Y.; Zheng, R.; Dong, J.; Choy, K.-L.; Zhao, H., Effect of C₈mimPF₆ on miniemulsion polymerisation for application in new latex coating products. Faraday Discussion on Liquid Salts for Energy and Materials, 11-13 May 2016, Ningbo, oral presentation.
4. Hu, B.*; Kong, Y.; Choy, K.-L.; Bi, X., Study of Room Temperature Ionic Liquid on Miniemulsion Polymerisation for Application in Low-Emitting Waterborne Coating Products. Polymer Reaction Engineering IX (PRE9), 10-15 May 2015, Cancun Mexico, oral presentation.
5. Hu, B.*; Kong, Y.; Choy, K.-L., Encapsulation of ionic liquids in O/W miniemulsion for application of low emission coating products. 6th Global Chinese Symposium of Chemical Engineering, 16-19 July 2014, Hong Kong, oral presentation.
6. Kong, Y.; Hu, B.*; Choy, K.-L., Development of New Paint Formula for Emission Control. 7th International Conference for Atmosphere Science and Emission control, 9-11 October 2013, Ningbo, oral presentation.

Acknowledgements

First of all, I would like to thank the University of Nottingham Ningbo China, especially the Faculty of Science and Engineering for the opportunity to carry out my research project. I would also like to acknowledge the Low Carbon Automation Manufacture Innovation Team for PhD studentship and financial support.

I would also like to express my sincerest thanks and appreciation to my supervisors, Associate professor Binjie Hu and Professor Kwang-Leong Choy for sharing their precious time and knowledge with me. It would be impossible to complete this thesis without their guidance and encouragement.

Furthermore, I would like to extend my acknowledgement to all of the technical staff of the Faculty of Science and Engineering, especially Mr. Julian Zhu, Ms. Jane Zhang, Ms. Helen Xu and Ms. Carey Tao for their technical support.

Last but not least, I would like to express my deepest appreciation to my parents, Mr. Xiang Kong and Mrs. Xia Hong for giving me endless support and motivation all the time. I would also like to extend my acknowledgement to friends, thank you all for the wonderful memories.

Table of contents

Abstract	i
Affirmation	iii
Acknowledgements	v
Table of contents	vi
List of figures	xi
List of tables	xviii
List of abbreviations	xx
Chapter 1 Introduction	1
1.1 Background of latex coating	1
1.1.1 Preparation of latex coating	1
1.1.2 Film formation of latex coating	7
1.1.3 Challenges of latex coating and solutions	9
1.2 Motivation	11
1.3 Research aims and objectives	13
1.4 Scope of this thesis	13
Chapter 2 Literature review	15
2.1 Introduction	15
2.2 Ionic liquids	15
2.2.1 Overview of ionic liquids	15
2.2.2 Potential application of ionic liquid related to coating field	18
2.2.2.1 ILs as solvents for solvent polymerisation	18
2.2.2.2 ILs as functional plasticisers for polymer	20
2.2.2.3 ILs as electrolytes for polymer electrolytes and their applications in solventborne coating as conductive agents	25
2.2.2.4 ILs as surface modification agents for silica nano-particle modification	28
2.2.2.5 ILs as dispersing agents for dispersion of pigment and exfoliation agent for filler in liquid medium	30
2.2.2.6 ILs as antimicrobial agents for marine antifouling coatings	32
2.2.3 The choice of ionic liquid in this study	33
2.3 Miniemulsion stabilised by surfactant	35
2.3.1 Classification of oil in water dispersions	36

2.3.2	Preparation of miniemulsion	37
2.3.2.1	Introduction of miniemulsion	37
2.3.2.2	Essential components for miniemulsion	38
2.3.2.3	Homogenisation devices	40
2.3.3	Factors affecting initial droplet size of miniemulsion	44
2.3.3.1	Homogeniser type	45
2.3.3.2	Operation condition	47
2.3.3.3	Properties of liquid media	48
2.3.4	Mechanism of miniemulsion instability	50
2.3.4.1	Reversible change	50
2.3.4.2	Irreversible change	51
2.4	Polymerisation of miniemulsion stabilised by surfactant	54
2.4.1	Mechanism of free radical polymerisation	55
2.4.1.1	Mechanism of free radical polymerisation	55
2.4.1.2	Kinetics of free radical polymerisation	57
2.4.1.3	Decomposition of initiators	59
2.4.2	Mechanism of miniemulsion polymerisation	61
2.4.2.1	Miniemulsion polymerisation initiated by hydrophilic initiator	61
2.4.2.2	Miniemulsion polymerisation initiated by hydrophobic initiator	63
2.4.3	Factors affecting stability of miniemulsion during polymerisation	64
2.4.4	Factors affecting reaction rate of miniemulsion polymerisation	65
2.5	Miniemulsion stabilised by silica nanoparticles and its polymerisation process	68
2.5.1	Adsorption of nanoparticles on oil water interface	68
2.5.2	Effect of silica nanoparticle on droplet size and stability of miniemulsion	70
2.5.3	Interaction between auxiliary co-monomer and silica nanoparticle during polymerisation	71
2.5.3.1	Pickering emulsion polymerisation	72
2.5.3.2	Pickering miniemulsion polymerisation	74
2.5.4	The possibility of ILs acting as an auxiliary co-monomer	75
Chapter 3	Factors on initial droplet size and stability of miniemulsion	76
3.1	Introduction	76
3.2	Materials and methods	76
3.2.1	Materials	76

3.2.2 Preparation of miniemulsion	77
3.2.2.1 Miniemulsion stabilised by surfactant	77
3.2.2.2 Miniemulsion stabilised by silica nanoparticle	80
3.2.3 Characterisation of miniemulsion	83
3.2.3.1 Droplet size measurement	83
3.2.3.2 Stability of miniemulsion during storage	83
3.2.3.3 Viscosity measurement	84
3.2.3.4 Interfacial tension measurement	85
3.2.3.5 Zeta potential measurement	85
3.3 Results and discussion	86
3.3.1 Miniemulsion stabilised by surfactant	86
3.3.1.1 Factors affecting initial droplet size of miniemulsion	86
3.3.1.2 Factors affecting stability of miniemulsion	97
3.3.2 Miniemulsion stabilised by silica nanoparticles	110
3.3.2.1 Factors affecting initial droplet size of miniemulsion	110
3.3.2.2 Factors affecting stability of miniemulsion	120
3.4 Conclusion	128
Chapter 4 Factors on polymer yield and stability of miniemulsion polymerisation	131
4.1 Introduction	131
4.2 Materials and methods	131
4.2.1 Materials	131
4.2.2 Preparation of miniemulsion	132
4.2.2.1 Miniemulsion stabilised by surfactant	132
4.2.2.2 Miniemulsion stabilised by silica nanoparticle	133
4.2.3 Miniemulsion polymerisation	134
4.2.3.1 Miniemulsion stabilised by surfactant	134
4.2.3.2 Miniemulsion stabilised by silica nanoparticle	135
4.2.4 Characterisation	135
4.2.4.1 Determination of yield of polymer	135
4.2.4.2 Droplet/particle size measurement	137
4.2.4.3. Viscosity measurement	137
4.2.4.4. Morphology observation	137
4.3 Results and discussion	138

4.3.1 Miniemulsion stabilised by surfactant	138
4.3.1.1 Factors affecting yield of polymer during miniemulsion polymerisation	140
4.3.1.2 Factors affecting stability of miniemulsion during polymerisation...	152
4.3.2 Miniemulsion stabilised by silica nanoparticle	164
4.3.2.1 Factors affecting yield of polymer during miniemulsion polymerisation	164
4.3.2.2 Factors affecting stability of miniemulsion during polymerisation...	170
4.4 Conclusion	184
Chapter 5 Characterisation of latex containing C₈mimPF₆	188
5.1 Introduction	188
5.2 Materials and methods	188
5.2.1 Materials	188
5.2.2 Preparation of miniemulsion	189
5.2.2.1 Miniemulsion stabilised by surfactant	189
5.2.2.2 Miniemulsion stabilised by silica nanoparticle	190
5.2.3 Miniemulsion polymerisation	191
5.2.3.1 Miniemulsion stabilised by surfactant	191
5.2.3.2 Miniemulsion stabilised by silica nanoparticle	192
5.2.4 Characterisation	192
5.2.4.1 Stability of latex	192
5.2.4.2 Zeta potential measurement	193
5.2.4.3 Glass transition temperature measurement	193
5.2.4.4 Spectroscopic analyses	194
5.2.4.5 Morphology observation	194
5.2.4.6 Molecular weight and distribution measurement	195
5.2.4.7 Mechanical property analysis	195
5.2.4.8 Thermogravimetric analysis	196
5.3 Results and discussion	196
5.3.1 Latexes stabilised by surfactant	196
5.3.1.1 Effect of C ₈ mimPF ₆ concentration on stability of latex during storage	196
5.3.1.2 Effect of C ₈ mimPF ₆ concentration on T _g of polymer and particle deformation	201

5.3.1.3 Effect of C ₈ mimPF ₆ concentration on molecular weight and distribution	212
5.3.1.4 Effect of C ₈ mimPF ₆ concentration on mechanical properties of film	213
5.3.1.5 Effect of C ₈ mimPF ₆ concentration on thermal properties of film	217
5.3.2 Latexes stabilised by silica nanoparticle.....	218
5.3.2.1 Effect of C ₈ mimPF ₆ concentration on stability of latex	218
5.3.2.2 Effect of C ₈ mimPF ₆ concentration on T _g of polymer and particle deformation	220
5.3.2.3 Effect of C ₈ mimPF ₆ concentration on molecular weight and distribution	228
5.3.2.4 Effect of C ₈ mimPF ₆ concentration on thermal properties of film	229
5.4 Conclusion	230
Chapter 6 Conclusions	232
6.1 Conclusions	232
6.1.1 Preparation of miniemulsion	232
6.1.2 Miniemulsion polymerisation	233
6.1.3 Characterisation of latex	235
6.2 Future work	237
Reference	240

List of figures

Fig.1.1 Preparation process of latex coating.....	2
Fig.1.2 Schematic illustration of emulsion polymerisation: (a), dispersion stage; (b), particle formation stage (stage I); (c), particle growth stage (stage II); (d), completion stage (stage III).	3
Fig.1.3 Schematic illustration of thermoplastic latex film formation process.....	8
Fig.2.1 Some commonly used ILs system (Stark and Seddon, 2007)	16
Fig.2.2 Effect of traditional and IL plasticisers on glass transition temperatures of PMMA (bmimPF ₆ : C ₄ mimPF ₆ , hmimPF ₆ : C ₆ mimPF ₆). (Scott et al., 2003).....	22
Fig.2.3 Variation of T _g with weight fraction of polymer in C ₂ mimTFSI for 125K and 335K PMMA (125K PMMA: number-average molecular weights 125 kg/mol, 335 K PMMA: number-average molecular weights 335 kg/mol). (Mok et al., 2011) 23	23
Fig.2.4 TG curves for MMA network polymers with different mole fractions of dissolved EMITFSI and EMITFSI bulk at a heating rate of 10 °C min ⁻¹ (EMITFSI: C ₂ mimTFSI) (Susan et al., 2005a).....	25
Fig.2.5 Routes of preparation of ILs-based polymer electrolytes (Ye et al., 2013)	27
Fig.2.6 Schematic diagram of ionic liquid [EMIM][PF ₆] (C ₂ mimPF ₆) immobilised on a silica surface (Liu et al., 2010).....	29
Fig.2.7 Proposed interfacial structure for the SBR/silica/MimMa composites (Lei et al., 2010)	30
Fig.2.8 Commercially available ILs dispersant (Weyershausen et al., 2005)	31
Fig.2.9 Schematic illustrations of the procedures for preparing SWCNT/PDMS composites (Oh et al., 2013)	32
Fig.2.10 Preparation of miniemulsion (Asua, 2002)	38
Fig.2.11 Schematic of sonication process (Asua, 2002).....	42
Fig.2.12 Schematic of a rotor-stator system (Maa and Hsu, 1996)	43
Fig.2.13 Schematic of the Microfluidizer and Interaction Chamber (Casey, 2009)	44
Fig.2.14 Different forms of breakup (Saygı-Arslan, 2010).....	45

Fig.2.15 Droplet size distribution for different emulsification methods: emulsion composition was Hi-Cap (10%) and MD (30%), pre-emulsified with 10% limonene by IKA mixer or Silverson (rotor-stator). Final emulsification was done by microfluidization (high pressure homogeniser) (20 MPa, one cycle) or ultrasonication (sonicator) at the highest power (20 s). (Jafari et al., 2007)	46
Fig.2.16 Effect of the consumed power on d_{32} : MA, mechanical agitation; US, ultrasound with gentle mechanical pre-emulsification (Montanox 60, 10 g/L, $\Phi=0.25$, $t_c = 30$ s). (Canselier et al., 2002).....	47
Fig.2.17 Decrease of the droplet size with sonication time, 20 wt % organic phase, 50 wboop % alkyd resin, and 2 wt % surfactant (compared to dispersed phase). (López et al., 2008)	48
Fig.2.18 Variations of d_{32} as a function of the surfactant concentration (MA: mechanical agitation, US: power ultrasound) ($t=30$ s, $\Phi=0.25$, $P_{MA}=170$ W, $P_{US}=130$ W) (Abismaïl et al., 1999)	49
Fig.2.19 Z-average drop diameter vs. viscosity ratio for miniemulsions prepared with 0.5 vol % oil/water ratio and SDS concentrations of 1.0 and 2.5 g/l.(Nazarzadeh and Sajjadi, 2010)	50
Fig.2.20 Destabilisation phenomena in emulsions (Abismaïl et al., 1999)	51
Fig.2.21 Schematic representation of miniemulsion polymerisation mechanism (Casey, 2009)	62
Fig.2.22 Entry and exit of free radical through a particle.....	66
Fig.2.23 Scheme of three phase contact angle.....	70
Fig.2.24 Reaction scheme for the formation of PMMA-silica nanoparticles (Chen et al., 2004)	73
Fig.2.25 Structure of 1-VID and C_8mimPF_6	75
Fig.3.1 Procedure for the preparation of miniemulsion.....	77
Fig.3.2 Image of a sonicator (Xinzhi Scientz II)	79
Fig.3.3 Position of plastic container and ultrasound probe	80
Fig.3.4 Image of a high speed disperser (IKA T25)	81
Fig.3.5 Illustration of stator/rotor structure	82
Fig.3.6 Position of baker and tip of rotor.....	82
Fig.3.7 Image of a bottle placed upside down in order to measure the height of sediment.	84

Fig.3.8 Initial droplet size of miniemulsion as a function of input duration with different input powers ranging from 57 W to 133 W.	88
Fig.3.9 Variation of droplet sizes as a function of surfactant concentration for miniemulsions containing 10 wt% C ₈ mimPF ₆ stabilised with SDSO	89
Fig.3.10 Variation of interfacial tension as a function of surfactant concentration	90
Fig.3.11 Variation of droplet sizes as a function of C ₈ mimPF ₆ concentration for miniemulsions stabilised with SDSO.....	92
Fig.3.12 Variation of viscosity ratio between oil phase and water phase as a function of C ₈ mimPF ₆ concentration	93
Fig.3.13 Variation of interfacial tensions as a function of C ₈ mimPF ₆ concentration at 0, 0.1, 30 mM SDSO in water phase	94
Fig.3.14 Variation of droplet sizes as a function of time for miniemulsions containing 10 wt% C ₈ mimPF ₆ stabilised with different surfactants upon aging at 20°C	100
Fig.3.15 Variation of droplet sizes as a function of time for miniemulsions containing different C ₈ mimPF ₆ concentrations at 20°C.....	103
Fig.3.16 Droplet size distribution at 0 h and 288 h aging time for miniemulsions containing different concentrations of C ₈ mimPF ₆	105
Fig.3.17 Variation of zeta potentials of droplet sizes as a function of C ₈ mimPF ₆ concentration.....	107
Fig.3.18 Variation of droplet sizes as a function of storage time for miniemulsion containing 10 wt% C ₈ mimPF ₆ at different temperatures.	110
Fig.3.19 Initial droplet size of miniemulsion as a function of input duration with different stirring speed ranging from 16000 rpm to 24000 rpm.	111
Fig.3.20 Variation in droplet sizes as a function of water phase pH for miniemulsions stabilised with silica nanoparticles	113
Fig.3.21 Variation in zeta potential of silica nanoparticles in water phase as a function of pH of water phase.....	113
Fig.3.22 Variation in droplet sizes as a function of silica nanoparticle concentration for miniemulsions containing 10 wt% C ₈ mimPF ₆	115
Fig.3.23 Variation in droplet sizes as a function of C ₈ mimPF ₆ concentration for miniemulsions stabilised by silica nanoparticle.....	116
Fig.3.24 Variation in the viscosity ratio between oil phase and water phase as a function of C ₈ mimPF ₆ concentration.	118

Fig.3.25 Variation in the interfacial tensions as a function of C ₈ mimPF ₆ concentration at 0, 50 g/l silica nanoparticles in water phase.....	119
Fig.3.26 Variation of viscosity as a function of shear rate for miniemulsions prepared under different pH of water phase	121
Fig.3.27 A typical image of creaming and sedimentation (the cylindrical glass bottle is held horizontally to see the creaming at the top of sample or the sediment at the bottom of sample)	123
Fig.3.28 Variation in height ratio of sediment with miniemulsion as a function of aging time for miniemulsions containing 10 wt%, 20 wt%, and 30 wt% C ₈ mimPF ₆	123
Fig.3.29 Variation in the zeta potentials of droplet sizes as a function of C ₈ mimPF ₆ concentration.....	126
Fig.3.30 Variation of droplet sizes as a function of storage time for miniemulsion containing 10 wt% C ₈ mimPF ₆ at different temperatures.	128
Fig.4.1 Yield of polymer as a function of reaction time for miniemulsion containing 10 wt% C ₈ mimPF ₆ at different temperatures initiated by AIBN.	141
Fig.4.2 Yield of polymer as a function of reaction time for miniemulsion containing 10 wt% C ₈ mimPF ₆ at different temperatures initiated by H ₂ O ₂ /AAc.....	142
Fig.4.3 Yield of polymer as a function of reaction time for miniemulsions containing different C ₈ mimPF ₆ concentrations initiated by AIBN.....	145
Fig.4.4 Dimensional Group [M]·N as a function of C ₈ mimPF ₆ concentration for miniemulsions initiated by AIBN	149
Fig.4.5 Yield of polymer as a function of reaction time for miniemulsions containing different C ₈ mimPF ₆ concentrations initiated by H ₂ O ₂ /AAc.	150
Fig.4.6 Dimensional group [M]·N as a function of C ₈ mimPF ₆ concentration for miniemulsions initiated by H ₂ O ₂ /AAc	152
Fig.4.7 Variation of droplet/particle sizes as a function of reaction time for miniemulsion containing 10 wt% C ₈ mimPF ₆ at different temperatures initiated by H ₂ O ₂ /AAc.	154
Fig.4.8 Droplet/particle size distribution at different reaction time for miniemulsion containing 10wt% C ₈ mimPF ₆ at different temperatures initiated by H ₂ O ₂ /AAc.	155
Fig.4.9 Variation of droplet/particle sizes as a function of reaction time for miniemulsion containing 10wt% C ₈ mimPF ₆ at different temperatures initiated by AIBN.....	156

Fig.4.10 Droplet/particle size distribution at different reaction time for miniemulsion containing 10wt% C ₈ mimPF ₆ at different temperatures initiated by AIBN.....	157
Fig.4.11 Variation of droplet size as a function of reaction time for miniemulsion containing 10wt% C ₈ mimPF ₆ at different H ₂ O ₂ /AAc concentrations.	159
Fig.4.12 Droplet size distribution at different reaction time for miniemulsion containing 10wt% C ₈ mimPF ₆ at different H ₂ O ₂ /AAc concentrations.	160
Fig.4.13 Variation of droplet size as a function of reaction time for miniemulsion containing 10wt% C ₈ mimPF ₆ at different AIBN concentrations.	161
Fig.4.14 Droplet size distribution at different reaction time for miniemulsion containing 10wt% C ₈ mimPF ₆ at different AIBN concentrations	161
Fig.4.15 Variation of droplet/particle sizes as a function of reaction time for miniemulsions containing different C ₈ mimPF ₆ concentrations initiated by AIBN. ...	163
Fig.4.16 Variation of droplet/particle sizes as a function of reaction time for miniemulsions containing different C ₈ mimPF ₆ concentrations initiated by H ₂ O ₂ /AAc.	164
Fig.4.17 Yield of polymer as a function of reaction time for miniemulsion containing 10 wt% C ₈ mimPF ₆ stabilised by silica nanoparticles in the initiation of AIBN and H ₂ O ₂ /AAc at 40 °C.	165
Fig.4.18 Yield of polymer as a function of reaction time for miniemulsion containing 10 wt% C ₈ mimPF ₆ at different temperatures initiated by AIBN.	167
Fig.4.19 Yield of polymer as a function of reaction time for the miniemulsion containing 10 wt% C ₈ mimPF ₆ at different pH of water phase.	169
Fig.4.20 Yield of polymer as a function of reaction time for miniemulsion containing different C ₈ mimPF ₆	170
Fig.4.21 Variation of droplet/particle sizes as a function of reaction time for miniemulsion containing 10 wt% C ₈ mimPF ₆ at different temperatures initiated by AIBN.....	171
Fig.4.22 Variation of droplet/particle sizes as a function of reaction time for miniemulsion containing 10wt% C ₈ mimPF ₆ at different pH of water phase.	173
Fig.4.23 Morphologies of products after polymerisation at different of pH of water phase.....	174
Fig.4.24 Variation of viscosities as a function of shear rate for products prepared under different water phase pH.....	176
Fig.4.25 Polymerisation process of miniemulsion at difference pH of water phase	177

Fig.4.26 Variation of droplet/particle sizes as a function of reaction time for miniemulsions containing different C ₈ mimPF ₆	178
Fig.4.27 Morphologies of products after polymerisation	179
Fig.4.28 Droplet/particle size distribution at different reaction time for miniemulsion containing different C ₈ mimPF ₆	180
Fig.4.29 Images of products after polymerisation	181
Fig.4.30 Variation of viscosities as a function of shear rate for products prepared under different C ₈ mimPF ₆ concentrations.....	182
Fig.5.1 Variation in the particle sizes as a function of time for latexes containing different C ₈ mimPF ₆ concentrations at 20°C	198
Fig.5.2 Particle size distribution at 0 h and 576 h of aging time for latexes containing different concentrations of C ₈ mimPF ₆	199
Fig.5.3 Variation in the zeta potentials of latexes as a function of C ₈ mimPF ₆ concentration.....	201
Fig.5.4 Glass transition temperature of particles containing different C ₈ mimPF ₆ concentrations.	202
Fig.5.5 Deformation of particles containing different C ₈ mimPF ₆ under different storage temperature for 2 h. (a) 0 wt% C ₈ mimPF ₆ ; (b) 10 wt% C ₈ mimPF ₆ ; (c) 20 wt% C ₈ mimPF ₆ ; (d) 30 wt% C ₈ mimPF ₆	205
Fig.5.6 FTIR spectra for C ₈ mimPF ₆ and PMMA.	207
Fig.5.7 FTIR spectra for particles containing different C ₈ mimPF ₆ concentrations and pure C ₈ mimPF ₆	208
Fig.5.8 Illustration of a homogeneous particle and a particle with a core-shell structure.....	210
Fig.5.9 TEM images of particles containing different C ₈ mimPF ₆ concentrations	211
Fig.5.10 Molecular weight distributions of polymers prepared from polymerisation of miniemulsions containing different C ₈ mimPF ₆ concentrations....	213
Fig.5.11 Stress–strain curves of films formed from latexes containing different C ₈ mimPF ₆ concentrations	214
Fig.5.12 stress–strain curves of glassy polymer at different temperatures.....	216
Fig.5.13 Young’s modulus of films formed latexes containing different C ₈ mimPF ₆ concentrations	217

Fig.5.14 TG curves for films formed from latexes containing different C ₈ mimPF ₆ concentrations.	218
Fig.5.15 Variation in height ratio of sediment with latexes as a function of aging time for latexes containing 10 wt%, 20 wt%, and 30 wt% C ₈ mimPF ₆	220
Fig.5.16 Glass transition temperature of particles containing different C ₈ mimPF ₆ concentrations.	221
Fig.5.17 Deformation of particles containing different C ₈ mimPF ₆ under different storage temperatures for 2 h. (a) 0 wt% C ₈ mimPF ₆ ; (b) 10 wt% C ₈ mimPF ₆ ; (c) 20 wt% C ₈ mimPF ₆ ; (d) 30 wt% C ₈ mimPF ₆	223
Fig.5.18 FTIR spectra for particles containing different C ₈ mimPF ₆ concentrations and pure C ₈ mimPF ₆	225
Fig.5.19 TEM images of particles containing different C ₈ mimPF ₆ concentrations	227
Fig.5.20 Molecular weight distributions of polymers prepared from polymerisation of miniemulsions containing different C ₈ mimPF ₆ concentration.	229
Fig.5.21 TG curves for films formed from latexes containing different C ₈ mimPF ₆ concentrations.	230

List of tables

Table.1.1 Function of coating layer containing polymer corresponding to its monomer	2
Table.1.2 Roles of additives	6
Table.2.1 the comparison between ILs and organic solvents (Plechkova and Seddon, 2008)	17
Table.2.2 The solubility and other properties of ionic liquid with PF ₆ anion or Tf ₂ N anion.....	35
Table.2.3 Comparison of properties of O/W dispersions (Anderson and Daniels, 2003)	36
Table.3.1 Formula of oil phases	78
Table.3.2 Formula of water phases containing surfactant	78
Table.3.3 Formula of water phases containing silica nanoparticle.....	80
Table.3.4 Mass ratio of separated oil phase with miniemulsion containing different concentrations of C ₈ mimPF ₆ and surfactants	99
Table.3.5 Droplet sizes of miniemulsions containing different concentrations of C ₈ mimPF ₆ before and after 288 h storage.....	102
Table.3.6 Stability of miniemulsions containing different C ₈ mimPF ₆ concentrations with different aging time. (-: stabilisation; *: creaming; : sedimentation)	122
Table.3.7 Density of oil phase containing different concentrations of C ₈ mimPF ₆ and water phase containing different concentrations of silica nanoparticles at 20 °C	124
Table.4.1 Formula of oil phase	132
Table.4.2 Formula of water phases containing surfactant	133
Table.4.3 Formula of water phases containing silica nanoparticle.....	134
Table.4.4 Formula of H ₂ O ₂ /AAc initiator solution.....	135

Table.4.5 Final yield of polymer in miniemulsion containing 10 wt% C ₈ mimPF ₆ initiated by different concentrations of AIBN at 40 °C	143
Table.4.6 Final yield of polymer in miniemulsion containing 10 wt% C ₈ mimPF ₆ initiated by different concentrations of H ₂ O ₂ /AAc at 40 °C	144
Table.4.7 Interfacial tensions between water phase and oil phase containing different concentrations of C ₈ mimPF ₆ at 40 °C	151
Table.5.1 Formula of oil phases	189
Table.5.2 Formula of water phases containing surfactant	189
Table.5.3 Formula of oil phase	190
Table.5.4 Formula of water phases containing silica nanoparticle.....	191
Table.5.5 Formula of H ₂ O ₂ /Ac initiator solution.....	192
Table.5.6 Number-average molecular weight and polydispersity of polymers prepared from polymerisation of miniemulsions containing different C ₈ mimPF ₆ concentrations.	212
Table.5.7 Stability of latexes containing different C ₈ mimPF ₆ concentrations with different aging time. (-: stabilisation; +: thickness; *: coagulation; : sedimentations)	219
Table.5.8 Number-average molecular weight and polydispersity of polymers prepared from polymerisation of miniemulsions containing different C ₈ mimPF ₆ concentration.....	228

List of abbreviations

AA	acrylic acid
AAM	acrylamide
AIBN	2, 2-azobis (isobutyronitrile)
AN	acrylonitrile
APTES	3-aminopropyl trimethoxy silane
BF ₄ ⁻	tetrafluoroborate anion
BPO	benzoyl peroxide
CA	cetyl alcohol
CMC	critical micelle concentration
C ₂ mimBF ₄	1-ethyl-3-methylimidazolium tetrafluoroborate
C ₂ mimEtSO ₄	1-ethyl-3-methylimidazolium ethyl sulphate
C ₂ mimPF ₆	1-ethyl-3-methylimidazolium hexafluorophosphate
C ₂ mimTFSI	1-ethyl-3-methylimidazolium bis(trifluoromethylsulfonyl)-imide
C ₄ mimBF ₄	1-butyl-3-methylimidazolium tetrafluoroborate
C ₄ mimPF ₆	1-butyl-3-methylimidazolium hexafluorophosphate
C ₄ mimTFSI	1-butyl-3-methylimidazolium bis(trifluoromethylsulfonyl) -imide
C ₆ mimPF ₆	1-hexyl-3-methylimidazolium hexafluorophosphate
C ₈ mimBMSI	1-octyl-3-methylimidazolium bis(perfluoromethylsulfonyl)imide
C ₈ mimPF ₆	1-octyl-3-methylimidazolium hexafluorophosphate
C ₈ mim ⁺	1-octyl-3-methylimidazolium cation
C ₁₂ mimBMSI imide	1-dodecyl-3-methylimidazolium bis(perfluoromethylsulfonyl)- imide
C ₁₂ mimCl	1-dodecyl-3-methylimidazolium chloride
C ₁₂ Br bromide	N,N-dimethyl-N-n-dodecyl-N-2-methacryloyloxyethylammonium bromide
DMA	dodecyl methacrylate

DOP	dioctylphthalate
DSC	differential scanning calorimetry
DTAB	dodecyltrimethylammonium bromide
EMITFSI	1-ethyl-3-methylimidazolium bis(trifluoromethylsulfonyl)-imide
FTIR	Fourier Transform Infrared
HD	hexadecane
HLB	hydrophile–lipophile balance
H ₂ O ₂	hydrogen peroxide
H ₂ O ₂ /AAc	hydrogen peroxide/ascorbic acid
IL-SWCNT	ionic liquid-based single-walled carbon nanotube
ILs	ionic liquids
IPA	isopropyl alcohol
IR	infrared
KH570	3-methacryloxypropyl trimethoxy silane
KPS	potassium persulfate
LSW	Lifshitz-Slyozov-Wagner
MAA	methacrylic acid
MFFT	minimum film formation temperature
MimMa	1-methylimidazolium methacrylate
MMA	methyl methacrylate
MPTS	3-mercaptopropyl trimethoxy silane
MS	modified starch
MTC	2-(methacryloyl)ethyltrimethylammonium chloride
O/W	oil in water
PDMAEMA	poly[(dimethylamino)ethyl methacrylate]
PDMS	polydimethylsiloxane
PF ₆ ⁻	hexafluorophosphate anion

PhmimBF ₄	1-benzyl-3-methylimidazolium tetrafluoroborate
PILs	polymeric ionic liquids
PLP	Pulse Laser Polymerisation
PMMA	poly (methyl methacrylate)
PVC	poly (vinyl chloride)
RTIL	room temperature ionic liquid
SBR	styrene butadiene rubber
SDBS	sodium dodecyl benzene sulfonate
SDS	sodium dodecyl sulfate
SDSO	sodium dodecyl sulfonate
SEM	field emission scanning electron microscope
SMA	stearyl methacrylate
SWCNT	single-walled carbon nanotube
TEM	transmission electron microscope
TESPD	bis-(3-(trimethoxysilyl)-propyl) -disulfide
TESPT	silane coupling agents are bis-(3-(triethoxysilyl)-propyl)-tetrasulfide
TFSI ⁻	bis(trifluoromethylsulfonyl)-imide anion
T _g	glass transition temperature
TG	thermogravimetric
TPM	3-methacryloxypropyl trimethoxysilane
UV	ultraviolet
AAc	L-Ascorbic acid
VOCs	volatile organic compounds
V50	2,2'-azobis(2-amidinopropane) dihydrochloride
W/O	water in oil
XPS	X-ray photoelectron spectroscopy
1-VID	1-vinylimidazole

2-VP	2-vinylpyridine
4-VP	4-vinylpyridine
[EMIM][PF ₆]	1-ethyl-3-methylimidazolium hexafluorophosphate

Chapter 1 Introduction

1.1 Background of latex coating

As legislations against emission of volatile organic components (VOCs) become more stringent, latex coating has attracted increasing attention. Latex coating is prepared by mixing latex with fillers, pigments, and additives. The term latex is used to describe a dispersion of polymer particles, the main film formation materials, in water. Compared with solventborne coating, latex coating has two advantages. First, molecular weights of polymers in latex are generally high, commonly with a weight average molecular weight higher than 1000000.(Zeno W. Wicks et al., 2007) Unlike solventborne coating which may cause considerable increase in viscosity at such high molecular weight, the molecular weight of polymers in particles does not affect the viscosity of latex coating. Second, water is used in substitution of organic solvent as dispersion medium, thus preventing the VOCs emission. The largest fraction of latex coating is applied in architectural field, including interior coating, exterior coating, and wood paint.

1.1.1 Preparation of latex coating

Preparation process of latex coating is shown in Fig.1.1. Latexes are mainly prepared by emulsion polymerisation (Zeno W. Wicks et al., 2007). The latex obtained from emulsion polymerisation is then mixed with fillers, pigments, and additives to form a specific latex coating.(Barbosa et al., 2013a) Choice of monomers, emulsion polymerisation process, and choice of additives are critical for successful preparation of latex coating. These will be introduced in the following content.

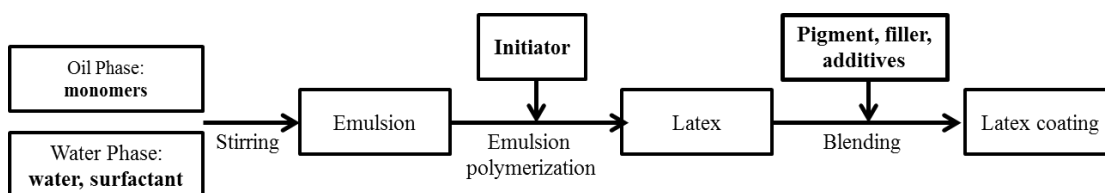


Fig.1.1 Preparation process of latex coating

Monomers The monomers for synthesising polyacrylic based latex include acrylic monomers, methacrylic monomers, and other compounds containing double bond such as styrene or vinyl ether. Due to the chemically stable carbon-carbon backbone of polyacrylic, polyacrylic based latexes show excellent properties in UV resistance, chemical resistance, and gloss retention.

The choice of monomers is critical in designing latexes. An important consideration is to make proper combination of monomers, as the function of coating layer depends on the type of monomer being used. Relationships between monomers and functions of coating layers are tabulated in Table.1.1.(Wang and Bao, 2005)

Table.1.1 Function of coating layer containing polymer corresponding to its monomer

Type of monomer	Functions of coating layer
Methyl methacrylate, styrene, acrylic acid, acrylonitrile, methacrylic acid	Hardness, adhesion, stain resistance
Acrylonitrile, acrylic acid, acrylamide, methacrylic acid	Solvent resistance
Ethyl acrylate, acrylate-2-ethylhexyl acrylate, butyl acrylate	Flexibility
Methyl methacrylate, long chain alkyl methacrylate, styrene	Water resistance
Methacryamide, acrylamide	Abrasion resistance
Methacrylate, acrylate	Weather resistance, transparency
Short chain alkyl acrylate, methyl methacrylate, styrene	Stain resistance

Monomers with cross-linking groups such as hydroxyl or carbamate groups are commonly polymerised with other acrylic monomers for synthesising polymers with cross-linking groups. By reacting with cross-linker, polymers with network structure can be obtained, thus promoting the film with rigidity or glassiness. (Streitberger and Dössel, 2008)

Emulsion polymerisation According to the reaction mechanism, emulsion polymerisation can be divided into four stages, which are dispersion stage, particle formation stage (stage I), particle growth stage (stage II), completion stage (stage III) shown in Fig.1.2. (Zeno W. Wicks et al., 2007, Schork et al., 2005)

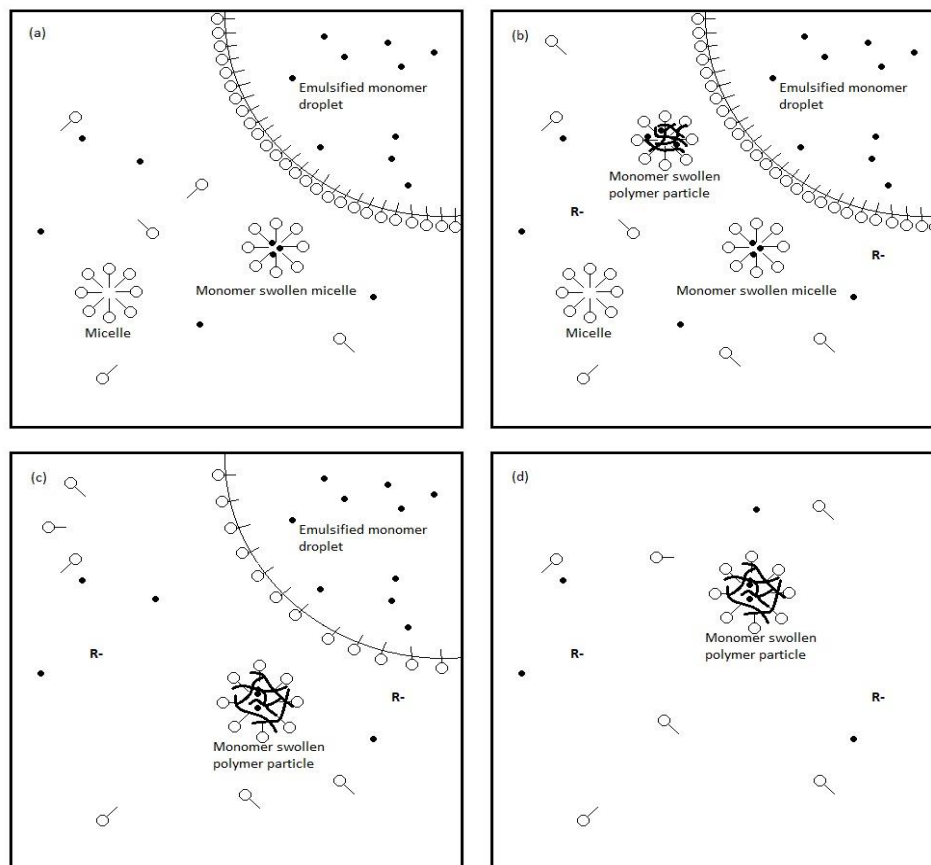


Fig.1.2 Schematic illustration of emulsion polymerisation: (a), dispersion stage; (b), particle formation stage (stage I); (c), particle growth stage (stage II); (d), completion stage (stage III).

Dispersion stage is to mix monomer, surfactant, and water by stirring. During this process, monomers will be dispersed into droplets. Surfactants are adsorbed on the water droplet interface, thus stabilising the droplets. Some monomers may diffuse into the water phase as single molecule. In addition, monomers dissolving in the water phase will partly absorb into micellae and form a monomer swollen micelle due to the solubilisation effect of micelle. Such diffusion process will continue until a dynamic equilibrium is reached among droplet, water phase, and monomer swollen micelle.

Stage I is a nucleation process begins after adding hydrophilic initiator. The initiator in water decomposes and generates radicals. Radicals are more likely to encounter micelles or monomer swollen micelles compared with droplets, as the total surface area of micelles is overwhelmingly larger than that of droplets. The superiority in surface area is because the number of micelles ($10^{17} \sim 10^{18} / \text{cm}^3$) is six to seven orders of magnitude larger than that of droplets ($10^{10} \sim 10^{12} / \text{cm}^3$), though the size of micelle (4~5 nm) or monomer swollen micelle (6~10 nm) is much smaller than droplet (1~10 μm). After entering micelles, radicals initiate the free radical polymerisation, and micelles are transforming into particles. During polymerisation, monomers will diffuse from droplets into particles to complement the consumption of monomers. This nucleation process is called micelle nucleation, which is the dominating mechanism for emulsion polymerisation. Other nucleation mechanisms, including homogeneous nucleation and droplet nucleation, may also occur during emulsion polymerisation. Homogeneous nucleation refers to nucleation occurs in water phase. Polymerisation is carried out among monomers which dissolved in water phase. Molecular chains continue to grow until become insoluble in water. These insoluble molecular chains may aggregate with other growing chains or be surrounded by surfactants. Then they swell with monomers and become polymerisation sites.

Droplet nucleation occurs when polymerisation carries out in droplets due to absorption of free radical.

At Stage II, the number of particles remains constant. As monomers continuously diffuse from droplets into particles through water phase to support polymerisation, the concentration of monomers in particles remains constant. The disappearance of droplets is the end of stage II.

At stage III, both micelles and droplets disappear. Only two phases remain: particles and water phase. Due to the disappearance of droplets, monomers stored in particles become the only source for further polymerisation. With the continuous generation of polymers, viscosity inside particles increases dramatically. Such high viscosity reduces the mobility of the molecular chains. So the growing chains are less to react with each other and terminate growth. Chain termination rate decreases dramatically at this stage.

Additives Additives are essential minor constituents. The type of additives used depends on the purpose of application of coating product, which are listed in Table.1.2. Additives can efficiently avoid film defect, and make the production and construction process controllable. It may also add special functions for the coating product. The amount of additive is various, depending on the formula and application. Taking coalescing agent for example, its dosage is determined by the requirement in minimum film formation temperature, and normally between 0 wt% ~ 10 wt% based on solid content.(Toussaint et al., 1997, Lahtinen et al., 2003, Raja et al., 2010)

It has to be mentioned that some representatives shown in Table.1.2 are VOCs, thus complete elimination of VOCs cannot be fulfilled. Among VOCs additives, coalescing agent is the main source. It is necessary to reduce or eliminate the usage of

coalescing agent. On the other hands, most additives only have single function. To achieve a target latex coating, it is needed to add a variety of additives and adjust their combination, which is costly and laborious.

Table.1.2 Roles of additives

Process	Name	Functions of additive	Representative
Producing process	Wetting agent (Hoffarth, 1998)	Enhance the wetting of particles like pigments and fillers towards liquid	Anion surfactant, non-ionic surfactants
	Dispersing agent (Schmitz et al., 1999, Uemae and Komatsu, 1995)	Avoid the flocculation and agglomeration of particles in liquid	Polyacrylate, phosphate, silicate
	Antifoaming agent (Uchiyama and Suzuki, 1992)	Inhibit the formation of foam during producing process	Polysiloxane, mineral oil
Storage and construction	Thickening agent (Dupre, 1982)	Adjust the viscosity or rheological properties of latex coatings	Colloidal silica, cellulose, polyacrylamide
	Cross-linking agent (Streitberger and Dössel, 2008)	Link different linear polymers chemical bonds	Melamine-formaldehyde resin, urea formaldehyde resin
Film formation	Coalescing agent (Raja et al., 2012)	Reduce T_g and enhance deformation and coalescence of particles	Aromatic hydrocarbons, Texanol, glycol ether
	Leveling agent (Bieleman, 2000)	Provide latex coatings with a good leveling property	1, 2-propanediol
Functional additive	Fungicidal agent (Brix et al., 2013)	Prevent the breeding of fungus and bacteria	Substituted aromatic hydrocarbons, organometallic compounds
	Antifouling agent (Ruffolo et al., 2013)	Prevent the adhesion of marine organism	Zinc pyrithione, copper pyrithione, TF-SPC

With the development of latex coating, additive with high efficiency, low VOCs, and multi-functions has become the target for research and application.(Chang et al., 1999, Barbosa et al., 2013a, Johansson, 2006, Stout and Louis, 2005, Shibulal and Naskar, 2012)

1.1.2 Film formation of latex coating

The protective and decorative function of latex coating can work only after film formation. To form a continuous film, application temperature must be upon its minimum film formation temperature (MFFT) which is mainly controlled by the glass transition temperature (T_g) of the polymer inside particles.

Film formation mechanism of latex coating is different from solvent borne coating. For solvent borne coating, polymers stretch in solvent, and film formed directly with the evaporation of solvent. While for latex coating, polymers are restricted inside particles in an intertwined state, leading to their unique film formation mechanism. If polymers in latex do not contain crosslinking groups, this latex is called thermoplastic latex. Latex containing polymers which incorporate crosslinking groups and can undergo crosslinking reactions, is named thermosetting latex. Their film formation mechanisms have some similarities.

Since thermoplastic latexes do not contain crosslinking groups, film formation process is mainly a physical process. Such process can be divided into three steps which are overlapped with each other as shown in Fig.1.3.(Zeno W. Wicks et al., 2007, Keddie and Routh, 2010) Step one is evaporation of water, leading to a close packed layer of spheres. Assembling and packing of particles carry out from the surface of coating layer to the inner parts as water evaporates. The space volume between particles is influenced by particle size distribution. Step two is deformation

of particles. As particles approach each other, the space between them becomes smaller and forms a capillary. Capillary generates capillary forces that put pressure to adjacent particles. This force leads to the connection and deformation of particles. The rate of deformation is strongly dependent on T_g of polymers. Particles containing lower T_g polymers are with a lower modulus, thus they are more easily deformed. Step three is coalescence of deformed particles. Coalescence is a slow process that polymers restricted in different particles inter-diffuse through the boundaries of particles and entangle with each other. In this case, boundary between particles will disappear to form a continuous film. The rate of inter-diffusion is primarily affected by the difference between application temperature and T_g of polymers. When the application temperature is higher than the T_g of the particles, adequate inter-diffusion will occur. Coalescing agent, a kind of plasticiser, can reduce the T_g of polymers, thus accelerating the deformation and coalescence.

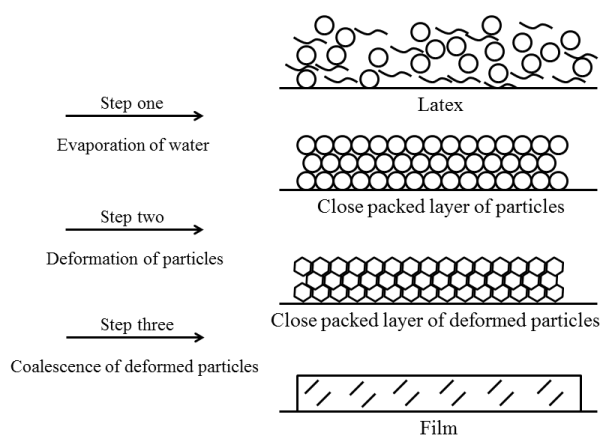


Fig.1.3 Schematic illustration of thermoplastic latex film formation process

To produce film with better properties, thermosetting latex whose polymer are incorporated with crosslinking groups could be used. The crosslinking groups

facilitate crosslinking reaction with crosslinking agent during film formation. The way how crosslinking reaction occurs depends on the method the crosslinking agent introduced. There are two methods. One is that crosslinking agents are dissolved in the water phase, and react with the polymers containing corresponding reactive groups during film formation process. The other one is blending two types of latexes associated with complementary reactive groups respectively. Crosslinking reaction takes place when polymers diffuse from one particle into an adjacent particle with corresponding reactive groups.(Keddie and Routh, 2010) In both methods, sufficient inter-diffusions are essential before crosslinking reaction takes place. Otherwise, improper crosslinking process may result in a weaker film. Compared to thermoplastic latexes, the film formed by thermosetting latexes has a cross-linked network structure, leading to the increase in durability, wear resistance, and chemical resistance.

1.1.3 Challenges of latex coating and solutions

Latex coating has several advantages. Emission of VOCs can be well eliminated due to the replacement of organic solvent with water. In addition, higher molecular weight can be achieved due to the micelles nucleation mechanism of latex, thus providing better mechanical properties.(Zeno W. Wicks et al., 2007) However, compared with an organic solvent, water as an alternative solvent to form latex exhibits some disadvantages. The major challenges of latex coating are given below:

- 1), the control of evaporation rate of water. Compared with solvent borne coating, where the evaporation rate of the solvent can be adjusted by combining solvents with different evaporation characteristics, the evaporation rate of latex coating is difficult to adjust as water is the sole solvent. On the other hand, the

evaporation rate of water is influenced by the relative humidity of the air. The change in relative humidity would cause major problems in final film formation.(Zeno W. Wicks et al., 2007)

2), the VOC emission induced by coalescence agent used in the film formation. After film formation, coalescence agent diffuses out of film and evaporates slowly. It has become the main VOCs of latex coating.(Raja et al., 2012, Keddie and Routh, 2010) Some coalescence agents, for example Texanol, release a weak, but mildly unpleasant odour that even persists for days.(Gallagher et al., 2008)

3), the residual of surfactant after film formation. Surfactant used to stabilise emulsion and polymer particles after polymerisation often remains in the dried film. The residual surfactant may migrate to the film/substrate interface and film surface, leading to the loss of adhesion and gloss of the film being formed.(Keddie, 1997, Keddie and Routh, 2010) It may also form aggregates within the film, causing poor water resistance.(Gundabala et al., 2008)

So far majority of research are focused on coalescing agent emission and surfactant residual.

Several attempts have been done to overcome coalescing agent emission. 1) reactive coalescing agents such as aliphatic epoxides containing polar groups and self-crosslinking agents. Aliphatic epoxides are dispersed in water and react with the carboxylic acid groups in polymers after water was evaporated, thus becoming a part of the film.(Hulkko et al., 2005) 2) self-crosslinking agents as co-monomers. it may become a part of polymers after polymerisation, thus enabling oxidative cure reaction with atmospheric oxygen after film formation.(Barbosa et al., 2013b) 3), coalescing agent with high boiling point, preferably above about 250 °C. These coalescing agents

include dicarboxylic/tricarboxylic, adipates, sebacates, maleates, and so on.(Yang et al., 2007)

For the surfactant residual problem, some alternatives to conventional surfactants have been attempted, including polymerisable surfactants and Pickering emulsifiers. 1) polymerisable surfactants. They are attached to polymer by polymerisation. Hence migration of surfactants can be avoided. However, the condition of polymerisation need to be redesigned whenever the monomer system changes.(Schoonbrood and Asua, 1997, Summers and Eastoe, 2003, Aramendia et al., 2003, Aramendia et al., 2005) 2) Pickering emulsifier. It is a type of solid particle as an alternative to surfactant. They can collect at the oil-water interface as a steric barrier to prevent the collision of droplets. When droplets are transforming from monomers to polymers during polymerisation, effective binding between solid particles and polymeric core is essential to keep the dispersion stable. To enhance this binding effect, an auxiliary co-monomer which has strong interaction with solid particles is needed.(Schrade et al., 2013)

1.2 Motivation

Employing coalescing agent with high boiling point is a feasible method to eliminate VOCs. Due to the non-volatility property, flash or evaporation is less to occur at expected indoor and outdoor temperature. (Yang et al., 2007) In view of non-volatility, room temperature ionic liquids (RTILs) which are composed of a bulky organic cation and an inorganic anion shall be taken into consideration. They are frequently viewed as “green solvents” in place of volatile organic solvents.(Le Bideau et al., 2011) Whether RTILs can act the same as coalescing agent with high boiling point is worth considering.

It is interesting to note that RTILs with low glass transition temperature (T_g) have been used as effective plasticisers to reduce T_g of polymer. Due to the non-volatility and plasticising effect, some RTILs indeed have the potential to replace the conventional coalescing agents, thus eliminating VOCs emission to the maximum. On the other hand, unlike coalescing agent with high boiling point, RTILs can be multi-functional, and provide the film with some special properties like thermal stability, conductivity, and antifouling property. These functions have been supported by the research in polymer/RTILs composites and solvent-borne coating. In addition, it has been proven that some RTILs and silica-nanoparticle, a type of Pickering emulsifier have a synergistic effect. This synergistic effect makes it possible to employ RTILs as “auxiliary co-monomers” to enhance the binding between silica-nanoparticle and polymeric core. So the addition of room temperature ionic liquids (RTILs) into latex coating may overcome the problems like coalescing agent emission and surfactant residual, as well as provide the final film with some special functions.

Because the process of preparing latex coating is a complex work, currently we just focus on the preparation of latex. Considering water resistance of final film, RTILs remaining in the final film must be hydrophobic. Hydrophobic RTILs cannot be directly dispersed into water phase, but encapsulated inside polymer particles. This encapsulation cannot be carried by emulsion polymerisation, the method of preparing latex coating, due to its micellar nucleation mechanism. Miniemulsion polymerisation, a method commonly used for encapsulating hydrophobic compounds, is a solution.

To the best of my knowledge, the ideas to employ RTILs in place of coalescence agents and to employ RTILs/silica nanoparticles in place of surfactant are

proposed for the first time. The method, miniemulsion polymerisation, has not been used to encapsulate RTILs. It can be seen that this research is novel and has practical value.

1.3 Research aims and objectives

This research aims to encapsulate RTILs by miniemulsion polymerisation which is stabilised by surfactant or silica nanoparticle for the preparation of latex containing RTILs.

The main objectives of this research program are as follows:

1. To prepare miniemulsion containing RTILs in the stabilisation of surfactant or silica nanoparticles, and gain an understanding of factors, especially RTILs, on initial droplet size and stability of miniemulsion.
2. To carry out polymerisation of miniemulsion containing RTILs in the stabilisation of surfactant or silica nanoparticles, and study factors, especially RTILs, on kinetics and stability of polymerisation process.
3. To characterise latexes containing RTILs in the stabilisation of surfactant or silica nanoparticles, and evaluate the function of RTILs on final properties of latexes.

1.4 Scope of this thesis

A brief description of each chapter is illustrated in the following content.

Chapter 1 introduces the research background and outlines the aims and objectives of this research. Chapter 2 reviews the existing literature discussing about applications of RTILs related to coating fields, preparation of miniemulsion,

mini-emulsion polymerisation, and mini-emulsion/mini-emulsion polymerisation stabilised by nanoparticles. This chapter illustrates the novelty and feasibility of preparing latex containing RTILs, and the choice of RTILs in this research. Furthermore, factors affecting initial droplet size and stability of mini-emulsion, kinetics and stability of polymerisation process are revealed for mini-emulsion stabilised by surfactant or nanoparticles. Chapter 3 introduces various factors on the initial droplet size and stability of mini-emulsion in the stabilisation of surfactant or silica nanoparticle. In chapter 4, various factors that have an influence on kinetics and stability of polymerisation process are described. In chapter 5, the effect of RTILs concentration on the stability of latex, the glass transition temperature of polymer, the polymer particle deformation, and the thermal and mechanical properties of final film is described. Finally, chapter 6 summarises the finding from this research and outlooks the further work to conclude this thesis.

Chapter 2 Literature review

2.1 Introduction

This chapter first reviews the key component in this study, RTILs. By giving an overview of RTILs and a discussion about applications of RTILs relative to coating fields, the novelty and feasibility of preparing latex containing RTILs, and the choice of RTILs in this research are illustrated. Then the method used in this study, miniemulsion polymerisation, is presented. It includes miniemulsion stabilised by surfactant, polymerisation of miniemulsion stabilised by surfactant, and miniemulsion stabilised by silica nanoparticles and its polymerisation process. Factors affecting initial droplet size and stability of miniemulsion, kinetics of polymerisation, and stability of miniemulsion during polymerisation are discussed.

2.2 Ionic liquids

Ionic liquids (ILs) are kinds of non-volatile organic salts with low melting points. They have been widely used as non-volatile solvents in place of volatile organic solvents in academic research and chemistry industry. (Plechkova and Seddon, 2008) In the following review, the functions of ILs related to coating fields are summarised. This may give some ideas about applying ILs as non-volatile, multi-functional coalescing agent for latex coatings. On the other hand, the target IL for this research process will be chosen after systematic analysis.

2.2.1 Overview of ionic liquids

ILs are kinds of organic salt with a low melting point. It is normally composed of organic cation with relatively large volume and inorganic anion with relatively

small volume shown in Fig.2.1.(Stark and Seddon, 2007) Due to the large volume of cation and loose structure, the interaction between cation and anion is weak, thus ILs exhibits a state of liquid consisting almost exclusively of ions at or upon ambient temperature. Especially, those in a state of liquid at or around room temperature are often referred as “room-temperature ionic liquids”.(Davis and Fox, 2003, Freemantle, 2010)

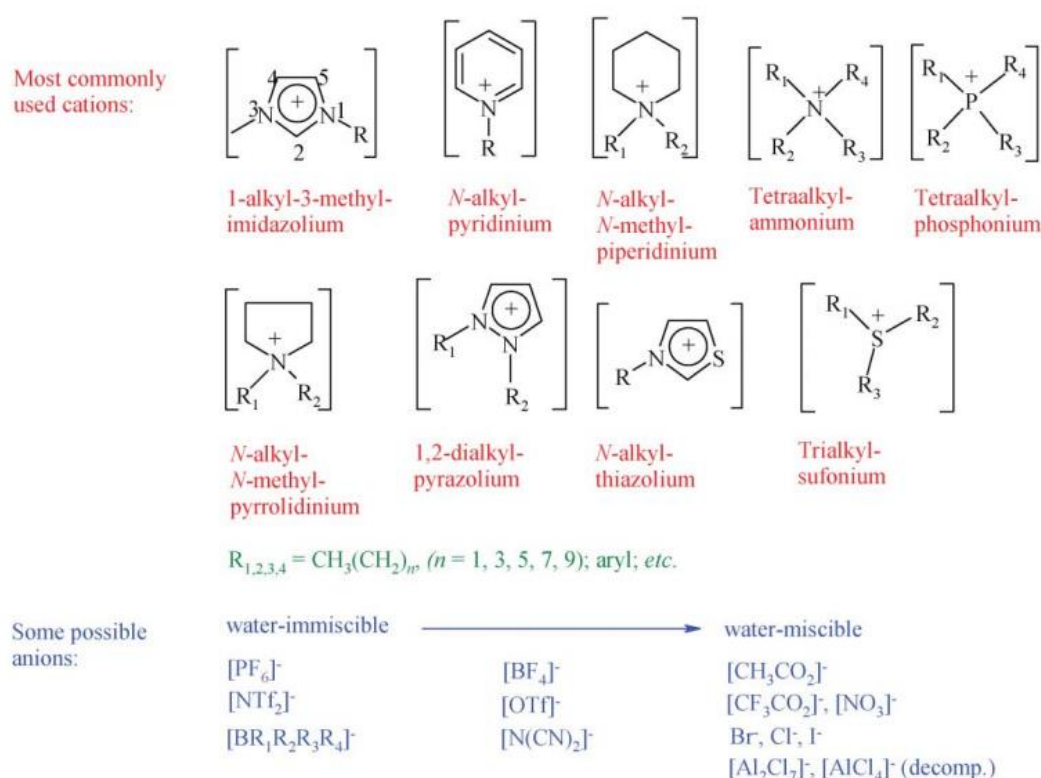


Fig.2.1 Some commonly used ILs system (Stark and Seddon, 2007)

The unique composition and structure provides ILs with some special physical and chemical properties which in turn expand their academic research fields. These properties include negligible vapour pressure, thermal and chemical stability, dissolving capacity, adjustable structure, catalytic activity, ionic conductivity, and electrochemical stability. Due to these unique properties, ILs exhibit many advantages in various applications compared with the conventional organ solvents, shown in

Table.2.1. (Plechkova and Seddon, 2008) Hence, ILs are frequently viewed as “green solvents” in place of conventional organic solvents. Moreover, they play more roles than the conventional organic solvent. Many relevant research work based on ILs has been carried out since 1990s, including electrochemistry, catalysis, inorganic chemistry, organic reaction, biotechnology, analysis, and polymer science.(Freemantle, 2010, Lu et al., 2009)

Table.2.1 the comparison between ILs and organic solvents (Plechkova and Seddon, 2008)

Property	Organic solvents	Ionic liquids
Number of solvents	>1000	>1000000
Applicability	Mainly employed as solvent	Multifunction
Catalytic ability	Rare	Common and tuneable
Chirality	Rare	Common and tuneable
Vapour pressure	Obeys the Clausius-Clapeyron equation	Negligible vapour pressure under normal conditions
Flammability	Usually flammable	Usually non-flammable
Solvation	Weakly solvating	Strongly solvating
Polarity	Conventional polarity concepts apply	Polarity concept questionable
Tuneability	Limited range of solvents available	Virtually unlimited range means "designer solvents"
Cost	Normally cheap	2 and 100 times the cost of organic solvents
Driving force for Recycle	Green imperative	Economic imperative
Viscosity/ cP	0.2-100	22-40000
Density/g.cm ⁻³	0.6-1.7	0.8-3.3
Refractive index	1.3-1.6	1.5-2.2

The applications of ILs are not only limited in academic research, but also extended into commercial application. For industrial level, the security of supply and cost of ILs must be taken into consideration.(Fitzwater et al., 2005) This supply issue has already been solved as there are many suppliers that can provide ILs from the gram scale to the multi-ton scale.(Plechkova and Seddon, 2008) The current cost of

ILs normally is about 5–20 times higher than conventional organic solvents on a lab scale, which is a key issue in industrial application. Producing ILs in a large scale, or recycling ILs during the application process could be a solution to further reduce the cost. So far, the industrial application about ILs are developing vigorously in the world wide, and many processes, such as the process for isomerisation of 3,4-epoxybut-1-ene to 2,5-dihydrofuranethylene by Eastman, the BASIL™ process by BASF, the process for dimerisation of alkenes by IFP, the process for hydrosilylation of a polydimethylsiloxane by Degussa, have been conducted successfully.(Plechkova and Seddon, 2008)

When it comes to this study, some properties of ILs may contribute to the improvement on the functionality for latex coating application. For example, due to negligible vapour pressure, ILs would eliminate emission of VOCs caused by conventional solvent if conventional solvent is replaced by ILs in latex coating. In the presence of ILs, the resistance to thermal decomposition of coating film at higher temperature may be increased because of thermal stability of ILs. The tuneable structures of ILs allow free selection of hydrophobic ILs to enhance water resistance of coating film. Certain ILs as additives presented in latex coating formula potentially could enhance ionic conductivity, hence, the electrical resistance of the coating film may be reduced and allow coating film with better conductivity. Detailed explanations will be given in the following content.

2.2.2 Potential application of ionic liquid related to coating field

2.2.2.1 ILs as solvents for solvent polymerisation

In solvent polymerisation, monomers are dissolved and polymerised directly in organic solvent. Studies on employing ILs as a substitute for organic solvent in

solvent polymerisation have been carried out. In these studies, polymerisation process follows free radical polymerisation mechanism, where single molecules react into macromolecule by the successive addition of free radicals, including chain initiation, chain propagation, chain termination, and chain transfer (shown in 2.4.1.1). The results suggested that apart from general advantages as “green solvents”, adding ILs also affected the reaction rate and the polymerisation degree. (Harrisson et al., 2002, Harrisson et al., 2003, Hong et al., 2002, Thurecht et al., 2008, Ueda et al., 2008, Cheng et al., 2004, Vygodskii et al., 2007)

Harrison et al. first studied the free radical polymerisation of methyl methacrylate (MMA) in 1-butyl-3-methylimidazolium hexafluorophosphate (C_4mimPF_6) solution by Pulse Laser Polymerisation (PLP). (Harrisson et al., 2002, Harrisson et al., 2003) It was observed that the chain propagation rate of MMA increased with the increase of C_4mimPF_6 concentration, while the chain termination rate reduced in turn. The presence of C_4mimPF_6 increased the polarity of the medium, which might contribute to the charge-transfer structure to the transition states, thus causing a decrease in the activation energy of propagation. The decrease in termination rate was due to the increasing viscosity of the medium caused by C_4mimPF_6 . These two effects may explain why high overall polymerisation rate and high molecular weight could be achieved when MMA was polymerised in ILs medium. (Hong et al., 2002) Alternative explanations for the ILs effect were put forward by a “protected” radical mechanism. In this case, parts of monomers were separated into extremely small domains by the barrier of ILs domain, so the radical could be protected in the ILs domain. There was a partition between radical protected in the ILs domain and radical formed in the monomer, thus chain termination could be well prevented. (Thurecht et al., 2008) Apart from MMA, for other monomers such as

styrene, vinyl acetate, and acrylonitrile, the reaction rates and molecular weights of polymer could be enhanced when the free radical polymerisations were carried out in ILs, compared with the one in organic solvents. (Ueda et al., 2008, Cheng et al., 2004, Vygodskii et al., 2007)

It can be seen that ILs, when applied in solvent polymerisation, may not only act as “green solvents”, but also shorten the reaction time with longer molecular chain product, offering environmental and economic advantages. However, research about the effect of ILs on reaction rate in emulsion/miniemulsion polymerisation is rare. Only Costa *et al* employed 1- dodecyl-3-methylimidazolium chloride ($C_{12}minCl$) as surfactant in emulsion polymerization of MMA and studied its effect on reaction rate when heated under microwave irradiation. It was found that under pulsed high-power microwave irradiation, slightly higher reaction rates and molecular weights could be achieved for emulsion stabilised by $C_{12}minCl$, compared with surfactant, dodecyltrimethylammonium bromide (DTAB). Due to high polarity and dielectric properties, the presence of $C_{12}minCl$ may favour the absorption of microwave energy, which may lead to an increase in propagation rate. (Costa et al., 2013) As emulsion/miniemulsion polymerisation may undergo the same free radical polymerisation mechanism as solvent polymerisation, the content summarised above may help to extend the application of ILs in latex coating.

2.2.2.2 ILs as functional plasticisers for polymer

A plasticiser is a small molecular weight compound that can reduce the glass transition temperature (T_g) of polymer. It make material more flexible with increased elongation and decreased tensile strength at room or working temperature. The mechanisms of plasticisation could be explained by the free volume theory.(Wypych,

2004) The free volume is used to describe the free space between molecules, where chain ends, side chains, and main chain can move in the space. The free volume decreases with the decrease of temperature. Especially, when temperature reduces to T_g , a critical point that polymer changes from a non-crystalline, glass-like state to a rubbery state, molecules become densely packed with negligible internal mobility, and free volume decreases into a minimum value. Plasticizer is a compatible compound with lower molecular weight. When it permeates into the space between polymers, the free spaces between polymers increase due to the motion from chain ends and side chains of plasticizer. The motion of main chain occurs more frequently due to these free spaces. All these effects lead to an increase in free volume of polymer system, that is to say, temperature can be further decreased when free volume reaches its minimum value. Thus, T_g of polymer can be reduced due to the external plasticizer. On the other hand, polymers are swollen by plasticiser, promoting the mobility of chain segments, hence soften the resulting polymer. (Oh et al., 2013, Sun et al., 2007)

In recent decades, ILs as potential substitutes for conventional plasticisers had been reported to minimise VOCs emission caused by plasticisers. This is expounded in the following sections.

Scott *et al.* reported that 1-butyl-3-methylimidazolium hexafluorophosphate (C_4mimPF_6) could act as an effect plasticiser for poly (methyl methacrylate) (PMMA) synthesised by the polymerisation of MMA in C_4mimPF_6 . C_4mimPF_6 could be compatible with PMMA at higher concentration (50 wt% based on total weight) than with a conventional plasticiser, dioctylphthalate (DOP) (30 wt%) and exhibited a linear drop in T_g .(Scott et al., 2002) Scott *et al.* further studied the plasticising effect

of 1-hexyl-3-methylimidazolium hexafluorophosphate ($C_6\text{mimPF}_6$) on PMMA, and made a comparison of T_g between products with $C_4\text{mimPF}_6$, $C_6\text{mimPF}_6$, and DOP respectively shown in Fig.2.2.(Scott et al., 2003) The PMMA also showed a linear drop in T_g with the increase of concentration of $C_6\text{mimPF}_6$, and exhibited larger reduction on T_g compared with the one containing $C_4\text{mimPF}_6$, at similar concentration up to 40 %.

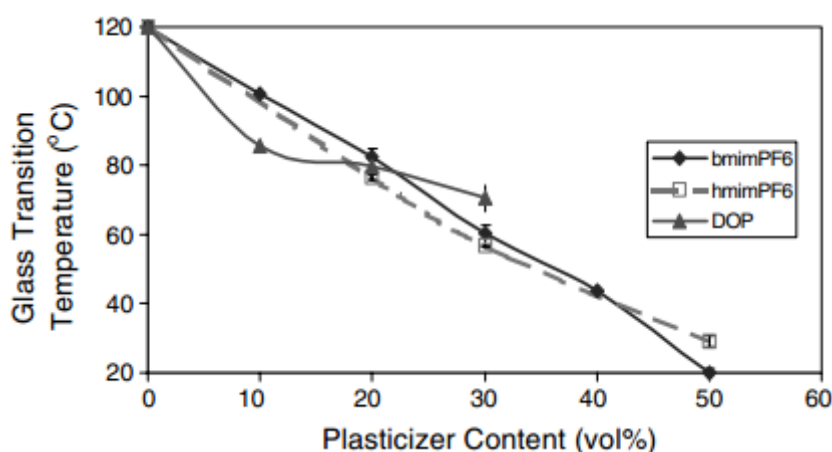


Fig.2.2 Effect of traditional and IL plasticisers on glass transition temperatures of PMMA ($C_4\text{mimPF}_6$: $C_4\text{mimPF}_6$, $C_6\text{mimPF}_6$: $C_6\text{mimPF}_6$).(Scott et al., 2003)

Mok *et al.* further studied the plasticising effect with another IL, 1-ethyl-3-methylimidazolium bis(trifluoromethylsulfonyl)-imide ($C_2\text{mimTFSI}$), which is compatible with PMMA over full range of weight ratio.(Mok et al., 2011) They prepared PMMA/ $C_2\text{mimTFSI}$ composites by dissolving PMMA and $C_2\text{mimTFSI}$ in methylene chloride, then removing methylene chloride by heating in a vacuum oven. Based on the curve, variation of T_g with weight fraction of polymer in $C_2\text{mimTFSI}$ shown in Fig.2.3, it could be found that the T_g of PMMA linearly reduces from 133 °C to -7 °C as the weight fraction of PMMA decreases of from 100 wt% to 35 wt%. Two T_g , representing $C_2\text{mimTFSI}$ and PMMA respectively, could be observed at

intermediate PMMA concentrations ranging from 30 wt% to 50 wt%, which was not reported in the studies of Scott *et al.*

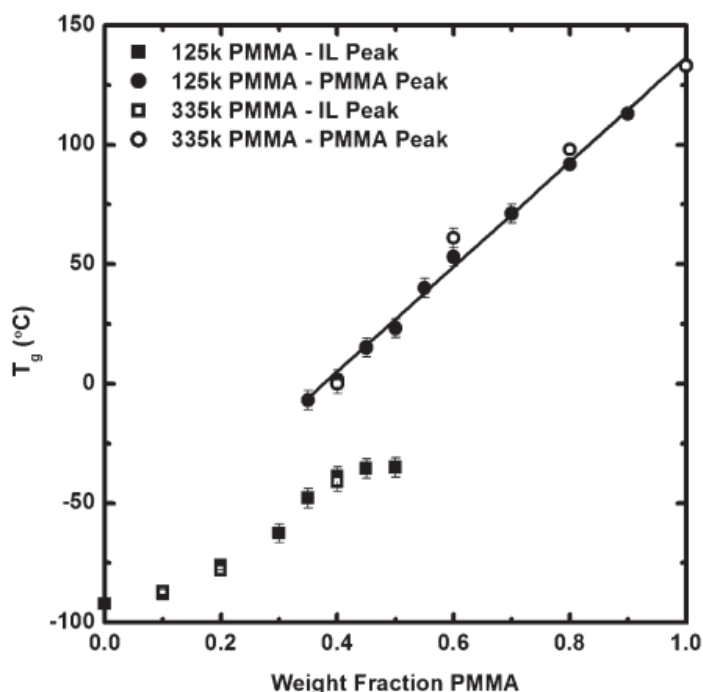


Fig.2.3 Variation of T_g with weight fraction of polymer in $C_2mimTFSI$ for 125K and 335K PMMA (125K PMMA: number-average molecular weights 125 kg/mol, 335 K PMMA: number-average molecular weights 335 kg/mol). (Mok et al., 2011)

The above studies with different type of ILs, *i.e.* C_4mimPF_6 , C_6mimPF_6 , and $C_2mimTFSI$, suggested that ILs chosen as plasticisers have a lower T_g , *i.e.* $-76\text{ }^\circ\text{C}$ for C_4mimPF_6 , $-78\text{ }^\circ\text{C}$ for C_6mimPF_6 , and $-92\text{ }^\circ\text{C}$ for $C_2mimTFSI$. (Fredlake et al., 2004, Harris et al., 2007) With similar anion group, C_6mimPF_6 has a lower T_g than C_4mimPF_6 , thus it performed better on reduction of T_g of PMMA compared with C_4mimPF_6 .

The plasticising effect of ILs also reflects on mechanical property of polymer. Rahman and Brazel employed ILs composed of ammonium, imidazolium and phosphonium cations as plasticisers for poly (vinyl chloride) (PVC). PVC plasticised by ILs was more flexible than those plasticised by conventional plasticisers and

exhibited better leaching and migration resistance. (Rahman and Brazel, 2006) Hou and Wang studied $C_4\text{mimPF}_6$ and $C_6\text{mimPF}_6$ as plasticisers for PVC paste resin. The tensile strength and elastic modulus of PVC paste resin decreased, and the elongation at break of PVC paste resin membranes was distinctly enhanced as the increase concentration of ILs. (Hou and Wang, 2011)

Apart from the typical plasticising function, ILs may provide polymers with better thermal stability and UV resistance. In terms of thermal stability, Susan *et al.* prepared networked PMMA/ $C_2\text{mimTFSI}$ composites with different mole fraction of $C_2\text{mimTFSI}$, and measured thermogravimetric curves of these composites, shown in Fig.2.4. The weight loss curves for PMMA/ $C_2\text{mimTFSI}$ is higher than that of bulk PMMA. This indicates that composites containing $C_2\text{mimTFSI}$ are less likely to decompose into volatile micro molecules at high temperature, thus the thermal stability is improved in the presence of $C_2\text{mimTFSI}$.(Susan et al., 2005a) Similar improved thermal stability was also reported by the study of $C_4\text{mimPF}_6$ / $C_6\text{mimPF}_6$ plasticised PMMA and $C_4\text{mimPF}_6$ / $C_6\text{mimPF}_6$ plasticised PVC.(Scott et al., 2003, Hou and Wang, 2011) Because the onset decomposition temperatures of ILs mentioned above ($C_2\text{mimTFSI}$, $C_4\text{mimPF}_6$, and $C_6\text{mimPF}_6$) are all higher than 400 °C,(Cao and Mu, 2014) they would not decompose into micro molecules at high temperature. The thermal stability of ILs plasticised polymer can be improved due to the contribution of ILs. As to UV resistance, Hou and Wang found elongation at break of un-plasticised PVC increased remarkably after exposure to UV ray compared with $C_4\text{mimPF}_6$ / $C_6\text{mimPF}_6$ plasticised PVC. The increase in elongation at break was mainly attributed to polymer cleavage, which indicated $C_4\text{mimPF}_6$ / $C_6\text{mimPF}_6$ plasticised had a better resistance to polymer cleavage.(Hou and Wang, 2011)

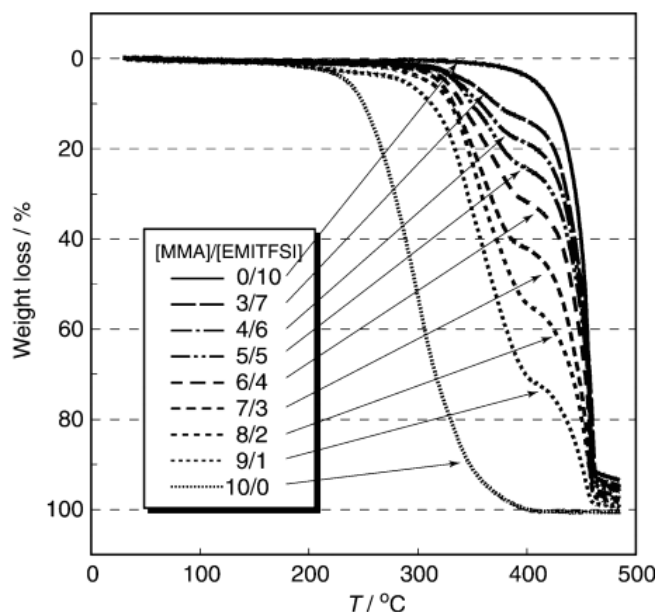


Fig.2.4 TG curves for MMA network polymers with different mole fractions of dissolved EMITFSI and EMITFSI bulk at a heating rate of $10\text{ }^{\circ}\text{C min}^{-1}$ (EMITFSI: $\text{C}_2\text{mimTFSI}$) (Susan et al., 2005a)

According to the review mentioned above, ILs are potential substitutes for conventional plasticisers which can reduce the T_g of polymer, and make polymer more flexible. Apart from the typical plasticising function, ILs may provide polymers with better thermal stability and UV stability. It can be seen that, due to plasticising effect and non-volatility, a certain ILs may act the same as conventional coalescing agents with minimum VOCs emission. In addition, film containing ILs may have a better thermal stability and UV resistance, thus extending its application temperature and outdoor lifetimes.

2.2.2.3 ILs as electrolytes for polymer electrolytes and their applications in solventborne coating as conductive agents

Ion-conducting polymer electrolyte has gained increased interest because of its thin-film forming property, transparency, and high ionic conductivity. (MacCallum, 1989) Conventional polymer electrolytes, such as polyether-based polymer electrolyte, are solid solutions of electrolyte salts in polymers. In many cases, the

rapid increase in T_g due to the higher T_g of polymer restricts the ionic mobility in polymer electrolyte, causing reduction on the conductivity of polymer electrolyte.(Susan et al., 2005a)

ILs, with high ionic conductivity and plasticising property, can be employed as electrolytes as well as enhance ionic mobility by lowering the T_g of polymer. Ionic conductivity of polymer electrolyte is positively correlated with the amount of ILs added. Especially, a continuous and interconnected ion transport domain will improve ionic conductivity. A desired ILs-based polymer electrolyte exhibited excellent properties, including high ionic conductivity, good mechanical and dimensional stability, and high ionic retention.

ILs-based polymer electrolytes can be prepared according the following routes shown in Fig.2.5: (i) doping of polymer with ILs; (ii) polymerisation/crosslinking of monomers in ILs; (iii) synthesis of polymeric ionic liquids (PILs). (Ye et al., 2013) For example, Choudhury et al. impregnated Nafion membranes with 1-butyl-3-methylimidazolium bis(trifluoromethylsulfonyl) -imide ($C_4mimTFSI$), and obtained a membrane containing 17% $C_4mimTFSI$ with a conductivity of 3.58 mS cm^{-1} at 160°C .(Mistry et al., 2009) Susan et al. synthesised polymer electrolytes by the radical polymerisation of MMA in $C_2mimTFSI$ in the present of a cross-linker. The compatibility of PMMA with $C_2mimTFSI$ hindered the phase separation between polymer and ILs, thus a self-standing, flexible, and transparent film can be achieved with ionic conductivity reaching a value close to $10^{-2} \text{ S cm}^{-1}$.(Susan et al., 2005a)

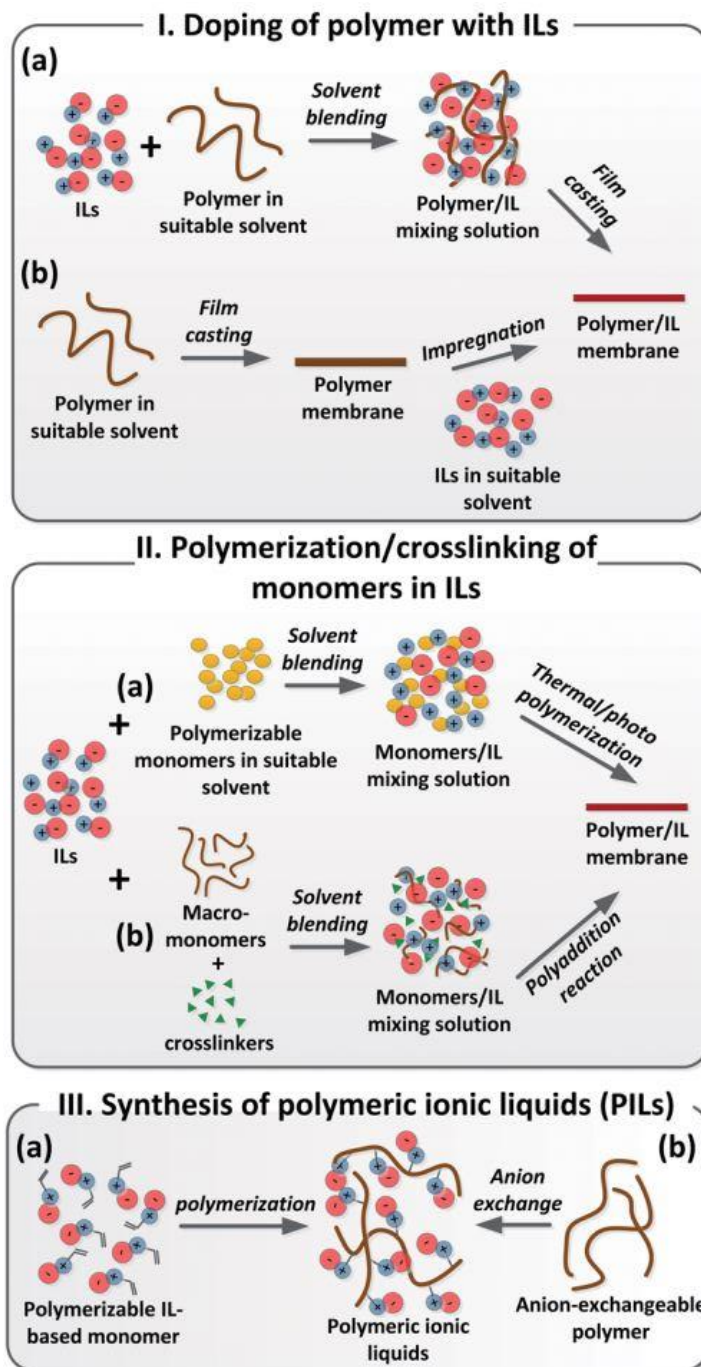


Fig.2.5 Routes of preparation of ILs-based polymer electrolytes (Ye et al., 2013)

Due to the high ionic conductivity, ILs have been employed as conductive agents in solventborne coating. After film formation, ILs would remain in the film and enhance the ionic conductivity of film. This enhancement is because ILs are ions, and their plasticising effect would enhance ionic mobility by lowering the T_g of polymer.

The methods to add ILs in solventborne coating are similar to the process of preparing ILs-based polymer electrolytes, which include dissolving ILs in solvent and incorporating polymeric ionic liquid into polymer. For example, Nagano *et al.* prepared a water-borne primer surfacer with enhanced conductivity by making use of common ILs, like 1-ethyl-3-methylimidazolium tetrafluoroborate (C_2mimBF_4). By directly adding 5 wt% ILs in water-borne primer surfacer, the electrical resistance of film fell by 4 to 5 orders of magnitude, thus solved the colour problem caused by using carbon particle conductive agent hence saved the cost for using expensive colourless conductive agent.(Nagano et al., 2009)

2.2.2.4 ILs as surface modification agents for silica nano-particle modification

Silica nano-particles are commonly used as fillers to improve the mechanical property of waterborne coating(Zhu et al., 2008). Due to its nano-scale size, high specific surface area and surface chemical bond, silica nanoparticle suffers several drawbacks: self-aggregation, poor compatibility with polymer and difficult dispersion in polymer system. Surface modification of nanoparticle by the grafting of silane coupling agent can prevent the accumulation in the dispersion media because grafted organic groups provide steric repulsion on the surface. Commonly used silane coupling agents are bis-(3-(triethoxysilyl)-propyl)-tetrasulfide (TESPT)(Choi et al., 2007), bis-(3-(trimethoxysilyl)-propyl) -disulfide (TESPD)(Kim, 2010), 3-mercaptopropyl trimethoxy silane (MPTS)(Tao and Xian-Hua, 2006), 3-aminopropyl trimethoxy silane (APTES)(Smith and Chen, 2008),3-methacryloxypropyl trimethoxy silane (KH570)(Ma et al., 2013).

Some ILs can interact with silica nano-particles via hydrogen bond and Van der Waals' force. Zhou *et al.* employed 1-butyl-3-methylimidazolium tetrafluoroborate

(C_4mimBF_4) as template to form mesoporous silica with wormhole framework. The hydrogen bond between BF_4^- and silano group of silica gel was observed and effected the formation of mesoporous silica.(Zhou et al., 2004) Liu *et al.* dispersed the mixture of silica nanoparticles and C_2mimPF_6 or the mixture of silica nanoparticles and 1-benzyl-3-methylimidazolium tetrafluoroborate ($PhmimBF_4$) in methanol then extensive grinded them. After removing methanol in vacuum oven, ILs successfully immobilised onto the surface of silica nanoparticles. Intermolecular hydrogen bonds were formed between the F atom of PF_6^- or BF_4^- anion and the hydroxyl groups of silanols. And the cations absorbed onto the surface of silica nanoparticles due to the Van der Waals force. These two interactions show in Fig.2.6, led to the decrease in the melting point of the mixture compared with pure ionic liquid.(Liu et al., 2010)

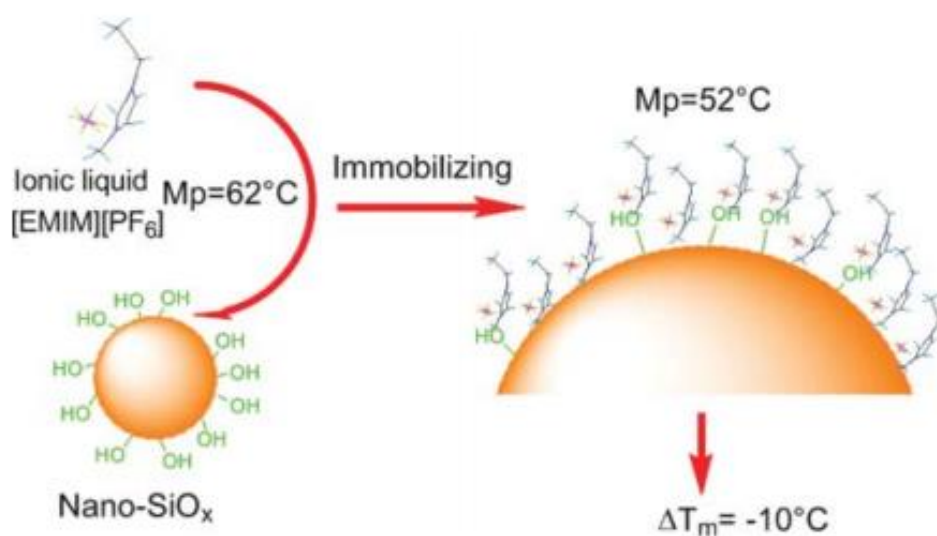


Fig.2.6 Schematic diagram of ionic liquid [EMIM][PF₆] (C_2mimPF_6) immobilised on a silica surface (Liu et al., 2010)

The interaction between ILs and silica nanoparticles showed above provides a new idea for the surface modification of silica nanoparticles. Lei *et al.* synthesised an imidazolium-based IL with double bond anion, 1-methylimidazolium methacrylate

(MimMa) and used it to modify the styrene butadiene rubber (SBR)/silica composites. The anion of MimMa could be grafted onto rubber chains by radical polymerisation. The polymerised MimMa interacted with silica nanoparticles probably by hydrogen bond thus facilitated the dispersion, restrained the filler networking of silica in rubber matrix as well as enhanced the SBR/silica interaction. After silica was added in the composite, the shift of functional group of MimMa was detected by IR spectra, and the difference of the absorption peak of Si by XPS. All of these evidences support the interaction between silica and MimMa. Fig.2.7 shows the proposed interfacial structure for the composites.(Lei et al., 2010)

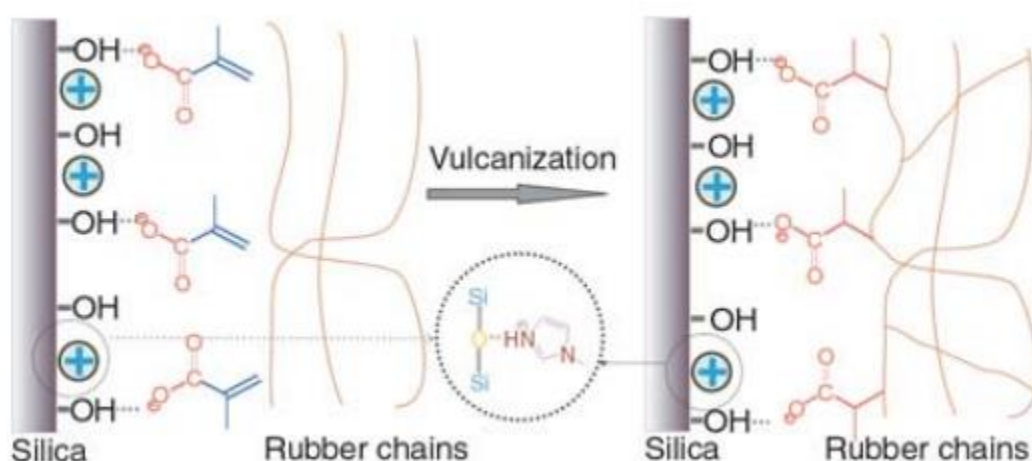


Fig.2.7 Proposed interfacial structure for the SBR/silica/MimMa composites (Lei et al., 2010)

2.2.2.5 ILs as dispersing agents for dispersion of pigment and exfoliation agent for filler in liquid medium

Dispersing agents are commonly used as homogeneously stabilise fillers and pigments in liquid media to achieve better storage stability.

Waterborne universal pigment modified with primary dispersing agent can be well dispersed in waterborne coating but cannot be used for the tinting of solvent-borne coating, which required separated mixer causing an increase on capital cost. By

employing a commercially available IL shown in Fig.2.8, waterborne universal pigment now become applicable in solvent-borne coating due to the synergistic effect between IL and primary dispersing agent (e.g. styrene oxide-based phosphorylated polyether).(Weyershausen et al., 2005)

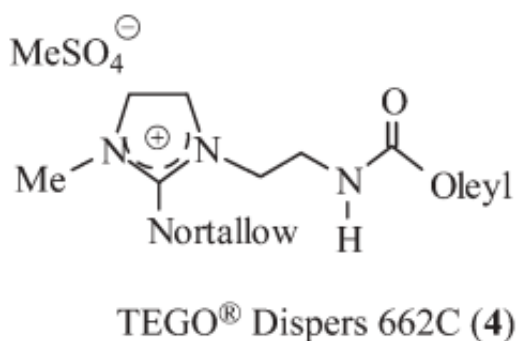


Fig.2.8 Commercially available ILs dispersant (Weyershausen et al., 2005)

ILs can also be used as exfoliation agents to disperse filler like nanotubes. Recently, Oh *et al.* synthesised a highly stretchable dielectric composite shown in Fig.2.9.(Oh et al., 2013) Ionic liquid-based single-walled carbon nanotube gel (IL-SWCNT) was employed as a dielectric and polydimethylsiloxane (PDMS) as an elastomer matrix. The whole process contains several stages. First, SWCNT was grinded in ILs to form IL-SWCNT gel, followed by dissolving this gel in toluene. Then the uniform IL-SWCNT solution was mixed with PDMS by stirring for 6 h. After and removing excess toluene, the curing agent was added into the IL-SWCNT/PDMS mixture, and cured at 150 °C for 10 min. In the presence of ILs, the SWCNTs were highly exfoliated and dispersed in the polymer matrix. The dielectric constant at 100 Hz was twice than that of composite without ILs.

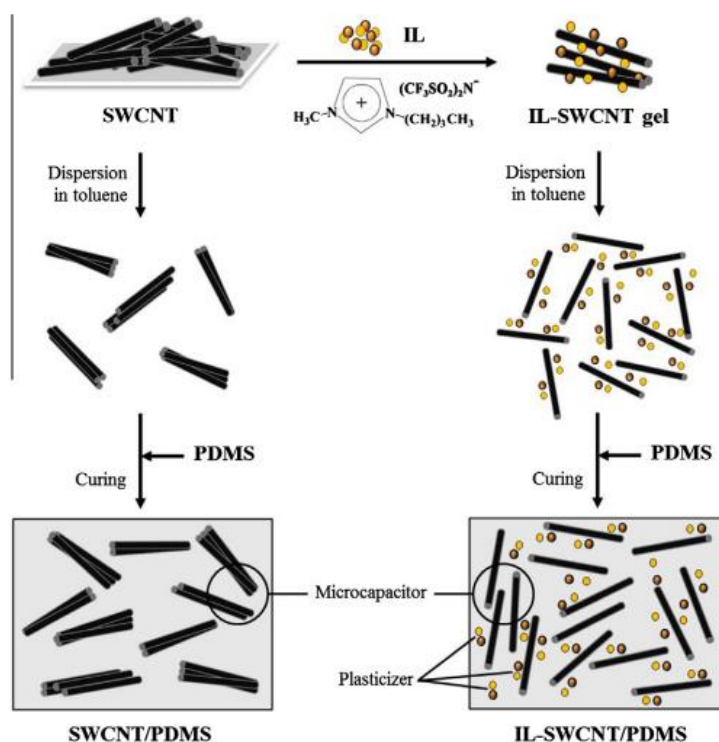


Fig.2.9 Schematic illustrations of the procedures for preparing SWCNT/PDMS composites (Oh et al., 2013)

2.2.2.6 ILs as antimicrobial agents for marine antifouling coatings

The antimicrobial characteristic of ILs has gained more and more attention recently. Studies have shown that ILs containing imidazolium, quaternary ammonium, and pyridinium cations exhibited remarkable antimicrobial activities. (Carson et al., 2009, Docherty and Kulpa, 2005) In addition, some ILs with biocidal activity can effectively resist Gram-positive and Gram-negative fungi, bacteria, and algae. (Pernak et al., 2003, Yagci et al., 2011) The antimicrobial mechanism of imidazolium based ILs is similar to that of quaternary ammonium surfactants. At a physiological pH, 7.4, the bacterial cell walls are negatively charged. This negatively charged bacterial cell will attract the cations of ILs by electrostatic interaction. The cell membrane will be disturbed by the hydrophobic components of ILs, resulting in the leakage of the

intracellular substances, followed by the death of the bacterial cell.(Riduan and Zhang, 2013) So some ILs can prevent the breeding of bacterial.

Due to the antimicrobial characteristic of ILs, ILs as antifouling agents had been reported in antifouling coating application. For example, Yu *et al.* prepared a marine antifouling coating by mixing polyurethane resin with 1-methyl-3-hexyl hexafluorophosphate (C_6mimPF_6) and coated it on the test board. After one year stored in seawater, the fouling coverage was 10%, which is a 30% reduction compared with a commercial marine antifouling coating.(Yu et al., 2011) This ILs based antifouling coating not only overcomes the pollution of organotin, a kind of biological antifouling agent, but also reduces the overall cost because of the lower price of C_6mimPF_6 compared to organotin. However, there is a drawback. The marine antifouling coating mentioned above suffered from the lack of long-term effect due to the release of small molecules ILs from film when stored in aqueous condition. To overcome the release of small molecules ILs, Pei *et al.* synthesised sorts of polymeric ILs, and incorporated these ILs into main chain by polymerisation with acrylate monomers, organosilicone monomers. This new marine antifouling coating has the same antifouling effect as international brands.(Pei et al., 2011)

2.2.3 The choice of ionic liquid in this study

From the review in 2.2.2, ILs have the potential to be non-volatility coalescing agents for latex coating. After film formation, they remain in the film and provide the film with thermal stability, UV resistance, conductivity, and antimicrobial property. To achieve these functions, a proper IL should be carefully chosen from various ILs. The prerequisites of this target IL includes:

1), it must be with low water solubility, otherwise it will release from film in aqueous condition;

2), in order to fulfil its plasticiser effect, the chosen IL should have a low T_g , and is miscible with MMA (the target monomer in this study, which is a typical acrylate monomer) before polymerisation as well as compatible with PMMA after polymerisation;

3), among ILs which meet the demands mentioned above, IL with a lower price shall be chosen.

We first try to choose the target IL, by considering their water solubility, T_g , and price. Anions like Cl^- , Br^- , and BF_4^- anions are more hydrophilic, so the target IL will be chosen from ILs with hydrophobic anions, including PF_6^- and TFSI. Table.2.2 lists physical properties of ILs with PF_6^- and TFSI. It can be seen that the solubility of PF_6^- and TFSI based ILs is at the same low level. Considering price factor, ILs with PF_6^- anion is chosen. Among three PF_6^- anion based ILs, C_8mimPF_6 has the lowest water solubility and lowest T_g . So C_8mimPF_6 is the target IL for this study.

The target IL, C_8mimPF_6 , can be miscible with MMA and compatible with PMMA after polymerisation according to the study of Li et al. and Perrier et al..(Li et al., 2007, Perrier et al., 2002) So the plasticising effect of ILs can be fulfilled if C_8mimPF_6 is chosen.

After choosing the target IL, how to balance the cost of the IL shall be taken into consideration. The price of C_8mimPF_6 (200 RMB/kg) is much higher than conventional coalescing agent *e.g.* Eastman[®] Texanol (20 RMB/kg). Even though the emission of VOCs can be reduced by replacing coalescing agent with C_8mimPF_6 , the

cost of C₈mimPF₆ is not acceptable. Such cost can be balanced by employing C₈mimPF₆ as a multi-functional additive, which plays the same role as conductive agent, UV resistance agent, and antimicrobial agent. The price of typical conductive agent, *e.g.* Moneng[®] 6002 is 104 RMB/kg. The cost of UV resistance agent, *e.g.* BASF[®] Tinuvin 622 LD is 100 RMB/kg, and that of antimicrobial agent *e.g.* Dow[®] ROCIMA 342 is 90 RMB/kg. It can be seen that the cost of C₈mimPF₆ indeed can be covered if it is employed as a multi-functional additive.

Table.2.2 The solubility and other properties of ionic liquid with PF₆ anion or Tf₂N anion

Ionic liquids		Solubility (25 °C) g/l	Density(25°C) g/cm ³	Viscosity mp.s	T _g °C
C ₄ mim	PF ₆	19.2 (Fortunato et al., 2004)	1.32 (Fortunato et al., 2004)	207 (25 °C) (Frez and Diebold, 2006)	-76 (Harris et al., 2007)
C ₆ mim		7.53 (Freire et al., 2007)	1.29 (Macchiagodena et al., 2011)	497.1 (30 °C) (Ning et al., 2012)	-78 (Harris et al., 2007)
C ₈ mim		2.26 (Fortunato et al., 2004)	1.19 (Fortunato et al., 2004)	1052 (20 °C) (Tomida et al., 2007a)	-81.9 (Harris et al., 2007)
C ₂ mim	TFS I	19.14 (Toh et al., 2006)	1.5 (Toh et al., 2006)	/	/
C ₄ mim		6.58 (Toh et al., 2006)	1.42 (Toh et al., 2006)	/	-86.8 (Harris et al., 2007)
C ₆ mim		3.18 (Toh et al., 2006)	1.33 (Toh et al., 2006)	68 (25 °C) (Muhammad et al., 2008)	/
C ₈ mim		1.9 (Toh et al., 2006)	1.31 (Toh et al., 2006)	/	/

2.3 Miniemulsion stabilised by surfactant

Considering hydrophobicity of C₈mimPF₆, it cannot be dispersed in water phase directly without the help of organic co-solvent. Encapsulating C₈mimPF₆ inside particles is a solution. However, this encapsulation cannot be achieved by emulsion

polymerisation, the main method to prepare latexes, due to its micelle nucleation mechanism. An alternative method, miniemulsion polymerisation, is a good choice.

Miniemulsion polymerisation can be divided into two steps: 1), initial formation of miniemulsion; 2), polymerisation process. The first step is focused on in the following review. Essential components and homogenisation devices for preparing miniemulsion are introduced, and effects on initial droplet size and stability of miniemulsion are discussed.

2.3.1 Classification of oil in water dispersions

Oil in water (O/W) dispersions can be classified into three types according to the range of droplet size and their long term stability: emulsion, miniemulsion, and microemulsion. A comparison of these O/W dispersions is given in Table.2.3.(Anderson and Daniels, 2003)

Table.2.3 Comparison of properties of O/W dispersions (Anderson and Daniels, 2003)

Properties	Emulsion	Miniemulsion	Microemulsion
Droplet size range	> 1 μm	50 ~ 500 nm	10 ~ 100 nm
Duration of stability	seconds to hours	hours to months	indefinitely
Diffusional stabilisation	kinetic	kinetic	thermodynamic
Nucleation mechanism	micellar, homogeneous	droplet	droplet
Emulsifier concentration	moderate	moderate	high
Co-stabiliser type	none	hexadecane, cetyl alcohol	hexanol, pentanol
Homogenisation method	none	mechanical or ultrasonic	none
Particle size range	50 ~500 nm	50 ~500 nm	10 ~100 nm

For polymerisation carried out in emulsion, it is most widely used to prepare latex. However, it is difficult to incorporate extremely hydrophobic monomers or hydrophobes lack of double bond. These components cannot transfer from droplets into micelles through water phase. While for miniemulsion, polymerisation conducts primarily according to droplet nucleation mechanism, where monomers are polymerised directly inside droplets rather than transferring from droplets to micelles. This benefits the encapsulation of hydrophobic compounds. Microemulsion is formed spontaneously from water/monomer mixture in the presence of a considerable amount of surfactant. It is a thermodynamically stable system with droplet size less than 100 nm. The high surfactant concentration might deteriorate to application. So miniemulsion polymerisation is chosen as the method for encapsulation C_8mimPF_6 .

2.3.2 Preparation of miniemulsion

2.3.2.1 Introduction of miniemulsion

The initial droplet size in emulsion is normally in the range from 1 μm to 10 μm . Such large droplets can be further broken up into miniemulsion scale, ranging from 50nm to 500 nm. (Schork et al., 2005) These smaller droplets can be obtained by the energy input from a homogenisation device such as sonicator, rotor-stator, and high pressure homogenizer, and stabilised by an effective surfactant/co-stabiliser system. Surfactants are absorbed on the surface of droplet to prevent aggregation and coalescence. As the small, numerous droplets provide enough surface area for surfactant adsorption, the free surfactant concentration in aqueous phase may be even below the CMC value. Co-stabiliser is a highly water-insoluble compound. It can slow down the diffusion of monomer from large droplet to small droplet known as Ostwald ripening, thus providing the system with stability against diffusion

degradation. Fig.2.10 describes the general procedure for the preparation of miniemulsion.(Asua, 2002)

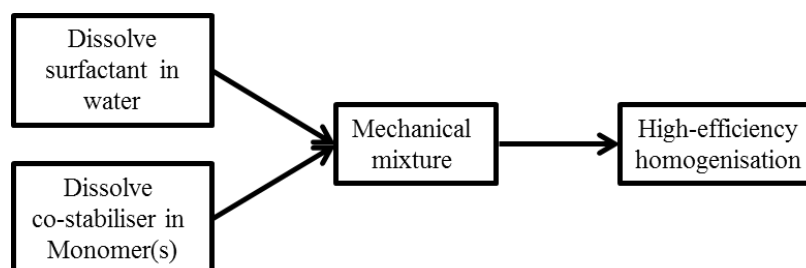


Fig.2.10 Preparation of miniemulsion (Asua, 2002)

2.3.2.2 Essential components for miniemulsion

A typical miniemulsion formulation includes water, a mixture of monomers, a co-stabiliser, and a surfactant. The water acts as a continuous phase. The mixture of monomers comprises a dispersed phase, and provides the source for polymerisation. The surfactant/co-stabiliser system hinders the instability of miniemulsion caused by coalescence and Ostwald ripening.

2.3.2.2.1 Monomers

Monomers with different water solubility have been used for the preparation of miniemulsion, including vinyl acetate (Steinmacher et al., 2015), vinyl chloride (Pham et al., 2012), methyl methacrylate (Ma and Zhang, 2014, Staudt et al., 2013, Zhu et al., 2012), butyl acrylate (Capek, 2012, Capek and Kocsisová, 2011), and styrene (Kohri et al., 2012, Boursier et al., 2011). In some cases, miniemulsion containing highly hydrophobic monomer, dodecyl methacrylate, was also synthesised for the polymerisation which was hardly carried out in emulsion polymerisation due to its difficulty in diffusion from droplet into the reaction site.(Lv et al., 2014) In addition, miniemulsion formulations containing more than one kind of monomer were

prepared for copolymerisation. Such multi-monomer includes styrene–butadiene system (Wei et al., 2012), styrene-methyl methacrylate system (Khezri et al., 2012) and so on.

2.3.2.2.2 *Surfactant*

Surfactant for stabilising droplets in miniemulsion has the same requirements as in emulsion polymerisation to some degree. Different kinds of surfactants, frequently reported in emulsion polymerisation, including anionic (Teo et al., 2014), cationic (Landfester et al., 1999b), non-ionic (Chern and Liou, 1999a), and mixed anionic/non-ionic surfactants (Masa et al., 1993) have been widely used in miniemulsion. In order to overcome the lack of gloss and poor water resistance caused by surfactant, polymerisable surfactant has been widely used to stabilise miniemulsion. Taniguchi *et al.* prepared a miniemulsion of styrene stabilised by a cationic polymerisable surfactant, N,N-dimethyl-N-n-dodecyl-N-2-methacryloyloxyethylammonium bromide (C₁₂Br), and obtained polystyrene latexes with a narrow particle size distribution after initiated by a cationic initiator 2,2'-azobis(2-amidinopropane) dihydrochloride (V50) (Taniguchi et al., 2008). Ni *et al.* synthesised a novel Y-shaped macromonomer based on poly[(dimethylamino)ethyl methacrylate] (PDMAEMA). The macromonomer could act both as a comonomer and as a pH-responsive polycationic surfactant for the miniemulsion polymerisation of styrene. (Ni et al., 2006)

2.3.2.2.3 *Co-stabiliser*

To take effect on limiting Ostwald ripening, co-stabiliser are selected according to the following requirements: low water solubility, high monomer solubility, and low molecular weight (Schork et al., 2005). Hexadecane (HD) and cetyl alcohol (CA) are the most widely used co-stabilisers. However, these co-stabilisers remain unreacted in

the final particles, thus may cause some negative effects on the final performance of product. To overcome this problem, highly water insoluble monomers were employed, acting as both co-stabilisers and comonomers in the miniemulsion polymerisation. Reimers and Schork, for the first time, employed highly water insoluble monomers, including vinyl hexanoate, p-methyl styrene, vinyl 2-ethyl hexanoate, vinyl decanoate, and vinyl stearate as co-stabilisers for the miniemulsion polymerisation of MMA. Stable miniemulsions could be formed, and polymerised under predominant droplet nucleation (Reimers and Schork, 1996a). Chern and Chen employed long chain monomers, including dodecyl methacrylate (DMA), stearyl methacrylate (SMA), as co-stabilisers for the miniemulsion polymerisation of styrene (Chern and Chen, 1998, Chern and Chen, 1997). The effectiveness of preventing Ostwald ripening was strongly dependent on the solubility of co-stabiliser in water. Due to the hydrophobicity of HD, neither of these co-stabilisers was as effective as HD. Some components which strongly affected polymerisation process, including chain transfer agents and initiators, were also used as co-stabilisers (Wang et al., 1997, Alduncin et al., 1994, Alduncin and Asua, 1994). However, the molecular weight distribution and polymerisation rate may be affected. In some cases, polymers, viewed as hydrophobes, could be used as co-stabiliser (Wang et al., 1996, Miller et al., 1995, Reimers and Schork, 1996b). But they were less efficient compared with co-stabilisers due to the high molecular weight.

2.3.2.3 Homogenisation devices

In miniemulsion system, the diameter of monomer droplet is in the range of 50~500 nm, much smaller than that of coarse emulsion produced by agitation. The

disruptive energy required for breaking up droplets into such scale is far over agitation can provide, thus additional homogenisation is needed.

Several homogenisation devices can provide the disruptive energy for homogenisation, including sonicators (Canselier et al., 2002, Mahdi Jafari et al., 2006), rotor-stators (Jasińska et al., 2014, Urban et al., 2006, Bałdyga et al., 2008), high pressure homogenisers (Mahdi Jafari et al., 2006, Qian and McClements, 2011), static mixers (Ouzineb et al., 2006), and membranes (Joscelyne and Trägårdh, 2000). As for the lab scale, sonicator, rotor-stators, and high pressure homogenisers are most used and will be introduced in the following content.

2.3.2.3.1 Sonicator

The homogenisation mechanism for sonicator is primarily based on cavitation. Ultrasound waves, including compression cycle and rarefaction cycle, are produced in sonication region shown in Fig.2.11. In rarefaction cycle, a negative pressure generates and causes the formation of voids or cavities growing in size; in the coming compression cycle, the cavitation bubbles are forced to contract, to some degree, even disappear. The collapse of the bubbles produces shock waves, causing the breakup of droplets surrounded (Canselier et al., 2002). Because ultrasound waves only affected the sonication region around the sonication tip, this may cause the heterogeneity of droplets. This heterogeneity may become less pronounced with the increase of sonication time, as more of the fluid passes through the sonication region. The droplet size decreases with the sonication time because of this, then trends towards a constant value depending on the formulation and energy input (Asua, 2002).

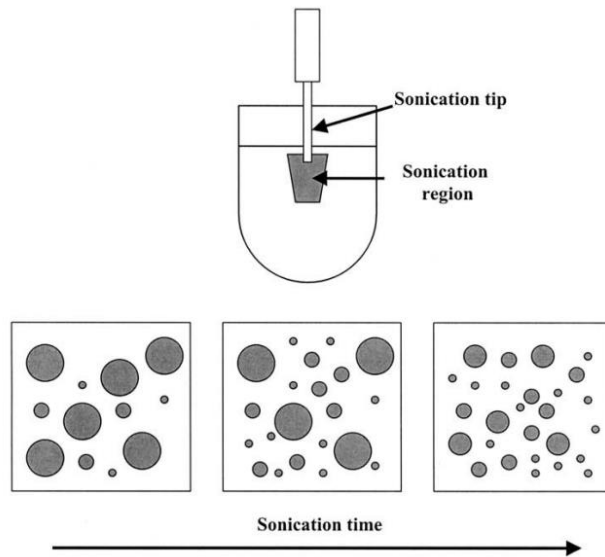


Fig.2.11 Schematic of sonication process (Asua, 2002)

2.3.2.3.2 Rotor-stator

Rotor-stator system contains a rotor with two or more blades and a stator with slots around its wall. The rotor is inserted inside the middle of the stator shown in Fig.2.12. As the rotor rotates, it leads to the circulation that draws the fluid in and out of the rotor-stator field. As the fluid accelerates, mechanical impingement against the wall can reduce the size of droplet. At the same time, shear force generates within the gap between the rotor and the stator, leading to the high turbulence in this field with eddies in different scales. The minimum droplet size relies on the smallest turbulent eddy formed, which in turn influenced by the rotor-stator shape and rotation speed (Maa and Hsu, 1996, Asua, 2002). So the homogenisation effect is strongly based on the rotor-stator design, the rotation speed, and the rotation time which decided the residence time droplets staying in the shear field.

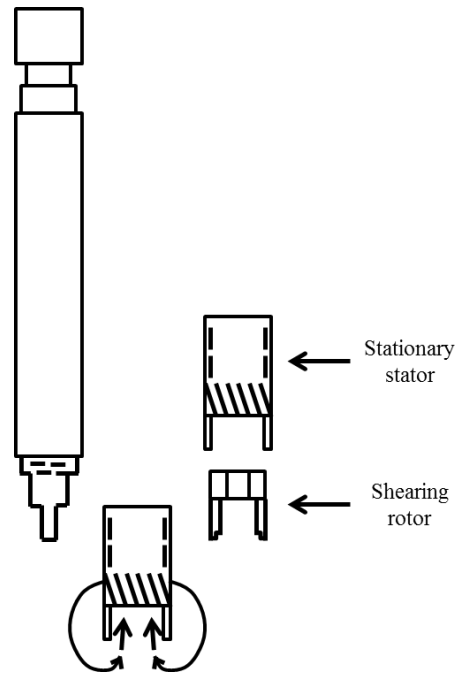


Fig.2.12 Schematic of a rotor-stator system (Maa and Hsu, 1996)

2.3.2.3.3 High pressure homogeniser

For high pressure homogeniser, microfluidizer is a commonly used device shown in Fig.2.13. First, high pressure is imparted into the liquid by intensifier with a value about 8000-9000 psi. Then the liquid is sent to the interaction chamber. In the interaction chamber, the liquid is divided into two streams with an accelerated speed close to 300 m/s. In a region created by an orifice plate, these two streams are turned at right angles and impinge on each other, followed by a pressure drop. Cavitation, shear, and impact co-exist within the interaction chamber, leading to the breakup of droplets (Casey, 2009). Typically, the droplet size tends to decrease as the increase of homogenisation pressure and number of passes (Qian and McClements, 2011).

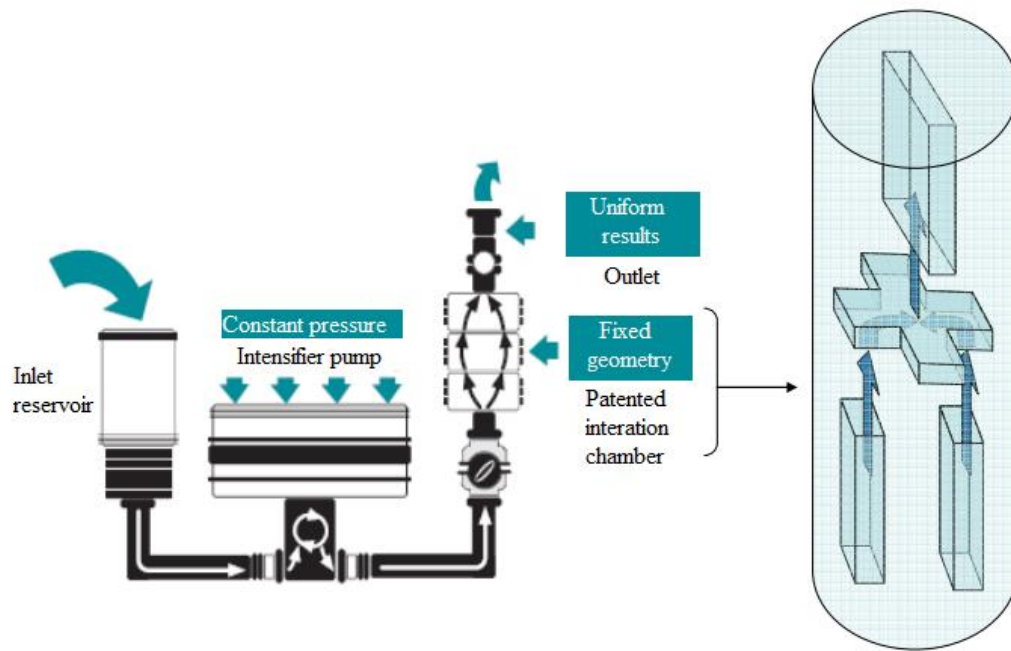


Fig.2.13 Schematic of the Microfluidizer and Interaction Chamber (Casey, 2009)

2.3.3 Factors affecting initial droplet size of miniemulsion

During homogenisation process, both droplet breakup and droplet coalescence occur. For droplet breakup, the prerequisite is the disruptive energy should overcome the surface energy controlled by interfacial tension and viscoelastic energy controlled by the viscosity of dispersed phase (Asua, 2014). The droplet breakup can be classified into three patterns, including erosive breakage, thorough breakage, and binary approximately equal breakage shown in Fig.2.14. (Saygı-Arslan, 2010) The multimodality of droplet distributions in miniemulsion is mostly under the effect of erosive breakage. In the breakup process, surfactants play important role as they decrease the interfacial tension of the monomer/water interface, thus reduce the surface energy. Droplet coalescence normally goes through two processes: collision of droplets and drainage of the liquid between the droplets. Surfactants absorbed on the surface of droplet prevent the coalescence fully carrying out. But before the breakup and coalescence meet a balance, the generation of new surfaces after droplet

breakup is much faster compared with the time of a surfactant diffusing and adsorbing at the interface surface. Therefore, since the droplets cannot be stabilised fast enough, they probably coalesce and form larger droplets again (Saygi-Arslan, 2010). The droplet size and distribution are the results of both droplet breakup and droplet coalescence.

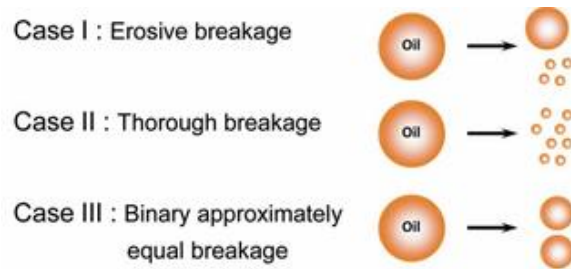


Fig.2.14 Different forms of breakup (Saygi-Arslan, 2010)

After having a better understanding of formation mechanism of droplets, factors affecting initial droplet size of miniemulsion will be discussed from the following three aspects: homogeniser type, operation condition, formulation.

2.3.3.1 Homogeniser type

Considering the energy density and homogenising time, sonicator, rotor-stator, and high pressure homogeniser share different homogenising processes. Sonicator is a high energy/long time process; High pressure homogeniser is a high energy/short time process; and rotor-stator consumes less energy but lasts longer times.(Jafari et al., 2007) Hence, the type of homogeniser employed directly affect the initial droplet size and droplet size distribution of emulsion/miniemulsion.

In order to compare the homogenising efficiency of homogenisers on initial droplet size, Jafari *et al.* produced coarse emulsion by rotor-stator (L2R, Silverson Machines Ltd., UK), and then passed this coarse emulsion through high pressure

homogeniser (Model M-110 L, Microfluidics, USA) at the minimum pressure with a value of 20 MPa for one cycle, or sonicated it by sonicator (Dr. Hielscher series, Model UP 400S) for 20 s at the highest power.(Jafari et al., 2007) It can be seen in Fig.2.15, after rotor-stator, further homogenisation by high pressure homogeniser or sonicator can move droplet into smaller size scale. Compared with sonicator, high pressure homogeniser gave smaller droplet size and narrower distribution. The efficiency in droplet reduction of high pressure homogeniser is due to its efficient droplet disruption (cavitation, shear force and inertia force) and higher energy density. On the other hand, narrower distribution observed in high pressure homogeniser is because all of the liquid flowing through high pressure homogeniser theoretically experiences the same shear history, whereas in sonicator only the liquid directly under the ultrasound probe is sheared.

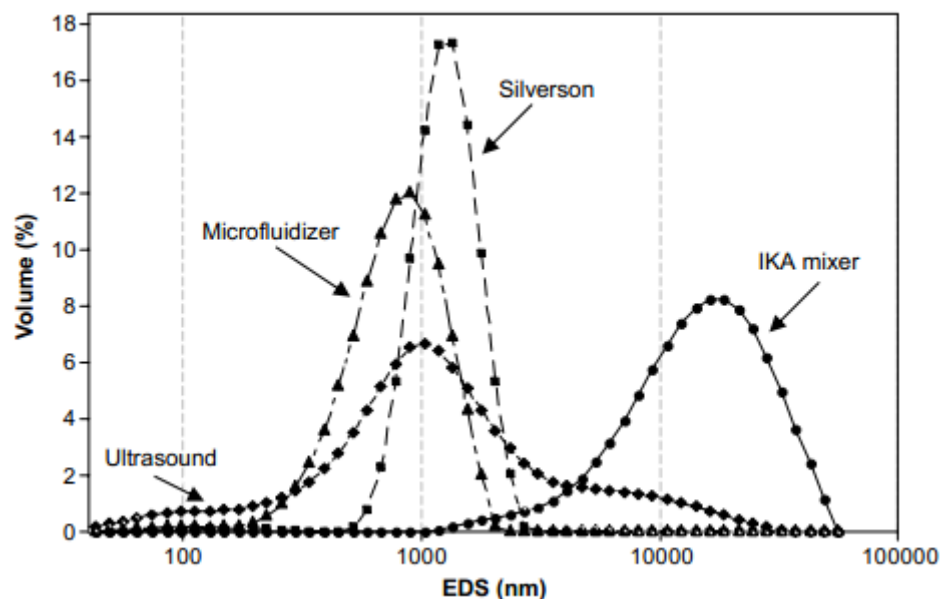


Fig.2.15 Droplet size distribution for different emulsification methods: emulsion composition was Hi-Cap (10%) and MD (30%), pre-emulsified with 10% limonene by IKA mixer or Silverson (rotor-stator). Final emulsification was done by microfluidization (high pressure homogeniser) (20 MPa, one cycle) or ultrasonication (sonicator) at the highest power (20 s). (Jafari et al., 2007)

It can be concluded that high pressure homogeniser produces miniemulsion with smaller droplets and narrower distribution compared with sonicator and rotor-stator (Asua, 2002, Mahdi Jafari et al., 2006).

2.3.3.2 Operation condition

Parameters set for homogeniser, *e.g.* energy input for sonicator, rotation speed for rotor-static, and homogenisation pressure for high pressure homogeniser, directly determine the disruptive energy input into the dispersion system, thus affecting the droplet size. For example, droplet size of kerosene-in-water emulsion stabilised by Montanox 60 was directly affected by the energy input of sonicator (Misonix Sonicator XL2020, sonotrode) shown in Fig.2.16.(Canselier et al., 2002) An increase in energy input, *e.g.* from 10 w to 60 w, yields emulsions with smaller droplet size. However, further increase in energy may have a limited effect on reduction of droplet size. Because further increase in energy led to excessive cavitation, and coalescence may become predominant.

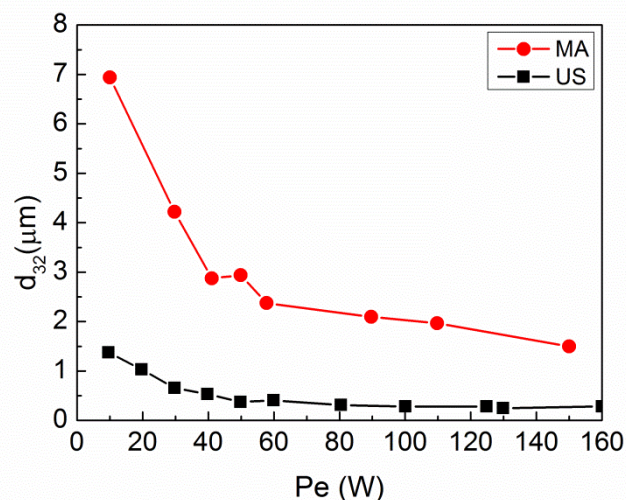


Fig.2.16 Effect of the consumed power on d_{32} : MA, mechanical agitation; US, ultrasound with gentle mechanical pre-emulsification (Montanox 60, 10 g/L, $\Phi=0.25$, $t_c = 30$ s). (Canselier et al., 2002)

Homogenising time, which is an accumulated energy input, is also important for all homogenisation devices. Taking sonicator for example, droplet size of alkyd resin/monomer-in-water miniemulsion stabilised by Dowfax 2A1 as a function of sonication time was measured and shown in Fig.2.17.(López et al., 2008) It can be seen that droplet decreases with the increase of sonication time, due to the accumulated input of disruptive energy. However, further increase in sonication time, *e.g.* 180 s, droplet size remains constant. This indicates that to achieve stable droplet, sufficient homogenising time is essential.

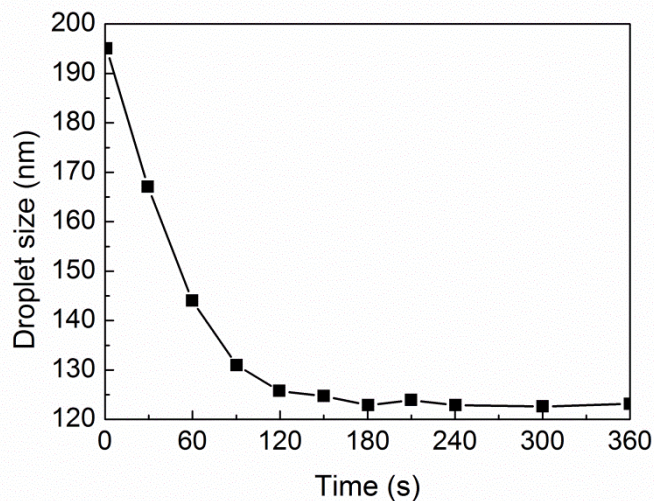


Fig.2.17 Decrease of the droplet size with sonication time, 20 wt % organic phase, 50 wt % alkyd resin, and 2 wt % surfactant (compared to dispersed phase). (López et al., 2008)

2.3.3.3 Properties of liquid media

Surfactant concentration affect the interfacial tension which controls the surface energy. After droplet breakup, surfactant would absorb on the surface of droplet to prevent coalescence. Sufficient surfactant would prevent coalescence, thus decreasing droplet size. From the result of Fig.2.18, with the same formula (only difference in surfactant concentration) and operation condition, droplet size decreased with the

increase of surfactant concentration up to 10 g/l, then trends to be stable. The decrease in droplet size at a low surfactant concentration is due to that the low surfactant concentration would lead to the incompletely covered interface, thus more surfactants were required to prevent smaller droplets from coalescence.

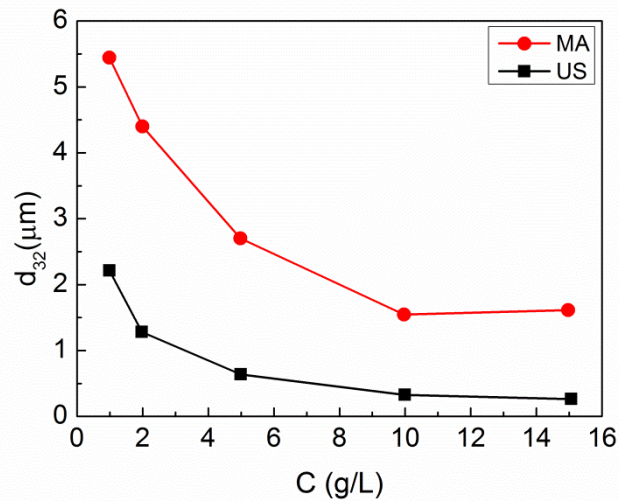


Fig.2.18 Variations of d_{32} as a function of the surfactant concentration (MA: mechanical agitation, US: power ultrasound) ($t=30$ s, $\Phi=0.25$, $P_{MA}=170$ W, $P_{US}=130$ W) (Abismail et al., 1999)

Viscosity of continuous/dispersed phase affected viscoelastic energy which prevents the breakup of droplet. From the open literature, it has been reported that increase of the viscosity of oil phase (dispersed phase) may affect miniemulsion droplet size. This is depends on the viscosity ratio between dispersed phase and continuous phase. Nazarzadeh and Sajjadi studied the viscosity effects of dispersed phase (silicon oil) on droplet size of miniemulsion prepared by ultrasound.(Nazarzadeh and Sajjadi, 2010) From the result of Fig.2.19, It can be seen that the average droplet size sharply decreased as the increase of dispersed/continuous phase ratio, reached a minimum when the viscosity ratio was around 1.0, and then remained constant, followed by a significant increase at viscosity ratio beyond 10. The reason why a minimum droplet can be achieved at a viscosity ratio around 1.0 is

due to the following reason. In a simple shear field, with lower interfacial tension for oil and water phase with similar viscosity, maximum energy transfer may be achieved. (Nazarzadeh and Sajjadi, 2010, Karam and Bellinger, 1968)

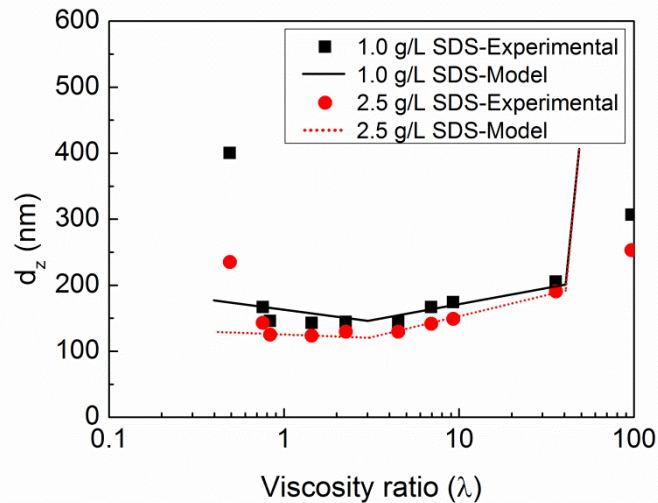


Fig.2.19 Z-average drop diameter vs. viscosity ratio for miniemulsions prepared with 0.5 vol % oil/water ratio and SDS concentrations of 1.0 and 2.5 g/l.(Nazarzadeh and Sajjadi, 2010)

2.3.4 Mechanism of miniemulsion instability

As miniemulsion has some similarities to emulsion, the study about the instability of emulsion may give us a better understanding of miniemulsion. The destabilisation of emulsion can be classified into two kinds: reversible change and irreversible change shown in Fig.2.20.(Abismaïl et al., 1999)

2.3.4.1 Reversible change

For reversible change, droplets first flocculate, followed by creaming or sedimentation. Whether creaming or sedimentation happens is determined by densities of dispersed and continuous phases.

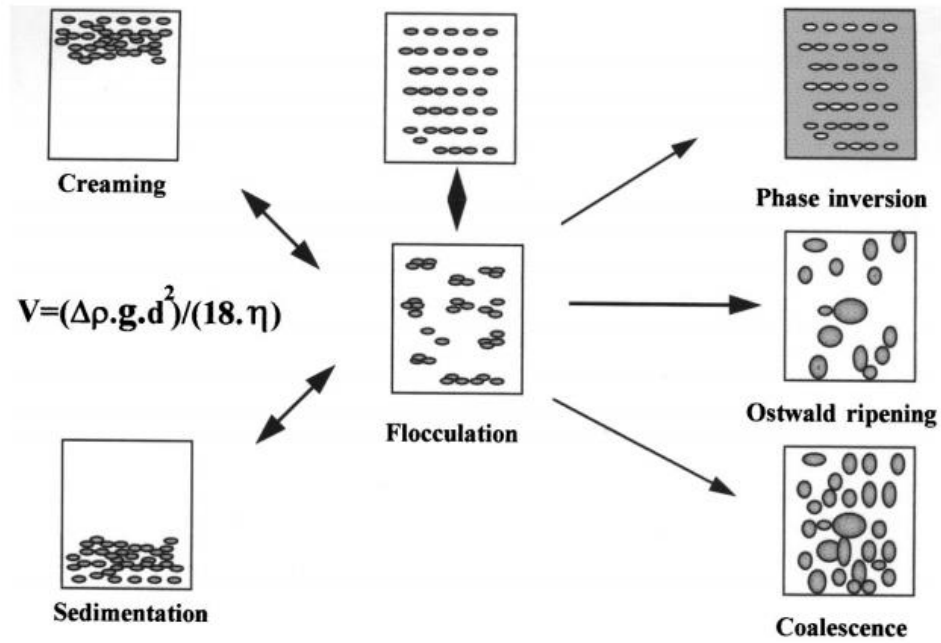


Fig.2.20 Destabilisation phenomena in emulsions (Abismaïl et al., 1999)

The migration rate of droplets follows the Stoke's law expressed as Eq.2.1:

$$V = \frac{\Delta\rho \cdot g \cdot d^2}{18 \cdot \eta} \quad \text{Eq.2.1}$$

where $\Delta\rho$ is density difference between dispersed and continuous phases; g is the gravitational acceleration; d is the diameter of droplet; η is the viscosity of continuous phase. It can be see that the degree of creaming or sedimentation is proportion to density difference between two phase and diameter of droplet, and inverse proportion to viscosity of continuous phase.

2.3.4.2 Irreversible change

Irreversible change includes coalescence and Ostwald ripening, thus lead to the formation of larger droplets. As larger droplets increases in size and number, eventually phase separation happens. Phase inversion is normally caused by the

change of temperature or composition. For the instability of miniemulsion, the most discussed is about Ostwald ripening and coalescence.

2.3.4.2.1 Ostwald ripening

Ostwald ripening is a phenomenon that monomer diffuses from small droplet to large droplet caused by the greater interfacial energy of small droplet than that of large one. Given two pure monomer droplets with the same interfacial tension, the difference in their chemical potential can be expressed as Eq.2.2:

$$\frac{\Delta\mu_{m,1-2}^{(d)}}{RT} = \frac{2\gamma\tilde{V}_m}{RT} \left(\frac{1}{r_{d,1}} - \frac{1}{r_{d,2}} \right) = \psi \left(\frac{1}{r_{d,1}} - \frac{1}{r_{d,2}} \right) \quad \text{Eq.2.2}$$

where $\Delta\mu_{m,1-2}^{(d)}$ is the difference in chemical potential; R is the gas constant; T is the absolute temperature; γ is the interfacial tension between water/oil phase; \tilde{V}_m is the molar volume of the monomer; $r_{d,1}$ is the radius of droplet one; $r_{d,2}$ is the radius of droplet two. If $r_{d,2}$ is larger than $r_{d,1}$, the difference in chemical potential is positive value, leading to the diffusion of monomer from one to two (Schork et al., 2005). Once co-stabiliser exists in the droplets, a new term will be added in Eq.2.2. After supposing that two droplets with different sizes have the same composition and the mixture of monomer and co-stabiliser acts as an ideal mixture, the difference in chemical potential between two droplets can be given by Eq.2.3:

$$\frac{\Delta\mu_{m,1-2}^{(d)}}{RT} = \ln \frac{\varphi_{m,1}}{\varphi_{m,2}} + (1 - m_{m,c})(\varphi_{m,2} - \varphi_{m,1}) + \psi \left(\frac{1}{r_{d,1}} - \frac{1}{r_{d,2}} \right) \quad \text{Eq.2.3}$$

where $\varphi_{m,1}$ is the volume fraction of monomer in droplet one; $\varphi_{m,2}$ is the volume fraction of monomer in droplet two; $m_{m,h}$ is the ratio of equivalent number of molecular segments between co-stabiliser and monomer; ψ is defined in Eq.2.2.

Considering that $\ln \varphi_m \approx \varphi_m - 1$ if the volume fraction of co-stabiliser is small, Eq.2.3 can be simplified as follows:

$$\frac{\Delta\mu_{m,1-2}^{(d)}}{RT} = m_{m,c} (\varphi_{m,1} - \varphi_{m,2}) + \psi \left(\frac{1}{r_{d,1}} - \frac{1}{r_{d,2}} \right) \quad \text{Eq.2.4}$$

The first term on the right is referred as molar energy, and second term as interfacial energy. At beginning, because the initial composition of two droplets is the same, the molar energy is zero. The difference in chemical potential is only caused by the difference in droplet size, leading to the monomer diffusing from small droplet to large one. As diffusion continuous, the volume fraction of monomer in droplet one increases, while that of droplet two decreases. Therefore the molar energy becomes positive value, thus an opposite diffusion of monomer is occurred. When it leads to equilibrium between the two energies, a balance reaches between large droplet and small droplet. (Schork et al., 2005).

Ostwald ripening is mainly affected by the type and concentration of monomer and co-stabiliser. Meliana *et al.* studied the effect of HD and CA on preventing Ostwald ripening by measuring the increase of droplet size in a short time. They found HD played a better role in preventing the Ostwald ripening compared with CA, and the function of reducing Ostwald ripening effect increased as more co-stabiliser was added (Meliana et al., 2011). Chern et al. found that the solubility of monomer was related to the rate of Ostwald ripening. Hydrophobic monomer was more effective to prevent Ostwald ripening compared with hydrophilic one (Chern et al., 2009).

2.3.4.2.2 *Coalescence*

Coalescence is a process in which, smaller droplets in liquid media collide together to form larger droplet. It may not only occur during homogenisation as described in 2.3.3, but also affect the stability of miniemulsion during storage. Both surfactant type and surfactant concentration are important in controlling coalescence during storage. To evaluate suitability of the types of surfactants, the hydrophile–lipophile balance (HLB) value is commonly used.(Griffin, 1949). If the HLB value of the surfactant chosen fits the HLB value oil phase required, the droplet is more stable as surfactant can tightly absorbed on the surface of droplet (Schmidts et al., 2010). Surfactant concentration also affects the stability of miniemulsion by controlling its initial droplet size as well as the amount of surfactant absorbed on the surface of droplet. The obstacle effect may better prevent the collision if more surfactant absorbed on the surface of droplet. Interfacial tension is a good parameter to reflect the adsorption of surfactant on the interface. Interfacial tension between water and oil phase decreases as the surfactant concentration increases until it reached a critical point. After the critical point, surfactant has been tightly arranged at the interface, thus no more surfactant can be further adsorbed (Rosen and Kunjappu, 2012). Zeta potential represents the electrostatic resistance of a droplet and it is an parameter to evaluate the stability of the colloidal dispersion system.(DOANE et al., 2011) The coalescence of droplets could be prevented when the absolute zeta potential is larger than 30 mV. (Mandzy et al., 2005)

2.4 Polymerisation of miniemulsion stabilised by surfactant

Majority of monomers with double bond are polymerised through free radical polymerisation. Different polymerisation methods, including miniemulsion

polymerisation, bulk polymerisation, solution polymerisation, suspension polymerisation, emulsion polymerisation follow the free radical polymerisation mechanism during polymerisation.

In this part, mechanism of free radical polymerisation and nucleation mechanism of miniemulsion polymerisation are introduced, and factors affecting conversion and stability of miniemulsion during polymerisation are discussed.

2.4.1 Mechanism of free radical polymerisation

2.4.1.1 Mechanism of free radical polymerisation

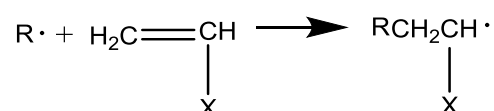
Free radical polymerisation is a micro process where single molecules transfer into macromolecule, including chain initiation, chain growth, chain termination, and chain transfer.

Chain initiation Chain initiation is a reaction process in which the monomer radicals are formed. It consists of the following two steps.

Step one: primary radicals form by initiator decomposition.

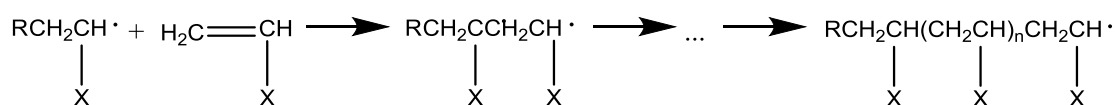


Step two: monomer radical form by addition reaction between primary radical and monomer.



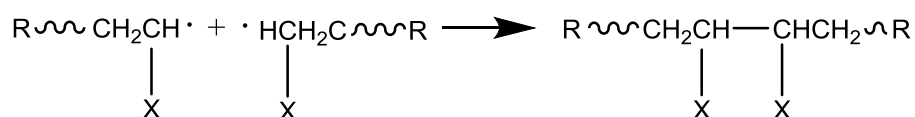
Chain growth Addition reaction carries out between monomer radical and vinyl monomer, forming a new radical. The newly formed radical continues to react

with vinyl monomers, forming long chain radical. This is a strongly exothermal reaction with low activation energy.

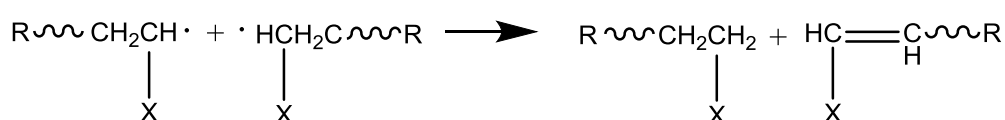


Chain termination Highly active long chain radicals cannot exist stably, and are likely to terminate with other radicals. This bi-radical termination contains coupling termination and disproportionation termination.

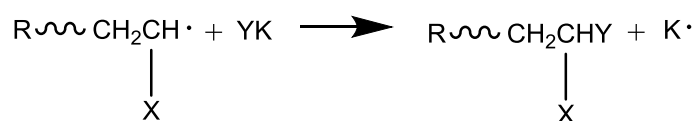
Coupling termination means single electrons from two radicals bond with each other by covalent bond.



Disproportionation termination is a process that one radical captures hydrogen atom or other atom of another radical to terminate both two radicals.



Chain transfer Long chain radicals may capture one atom from monomer, initiator, solvent, and macromolecule, and transfer one electron to the molecules losing one atom. New radicals form and continue chain growth.



2.4.1.2 Kinetics of free radical polymerisation

In free radical polymerisation, the overall reaction rate may be determined by 3 key steps, *i.e.* chain initiation, chain growth, and chain termination. Considering chain transfer only affects degree of polymerisation, it is not taken into consideration when calculating reaction rate.

Chain initiation rate Chain initiation reaction scheme can be expressed by the following two reactions:



Decomposition of the initiator is a slow reaction, controlling chain initiation rate. Because some of the initiators are consumed by side reaction, the initiator efficiency, f , is introduced. The reaction rate for chain initiation can be expressed as:

$$R_i = 2fk_d[I] \quad \text{Eq.2.5}$$

In above formulas, I , M , $R \cdot$, k represent initiator, monomer, primary radical, and rate constant, respectively; $[\]$, subscript d and i represent concentration, decomposition, and initiation, respectively.

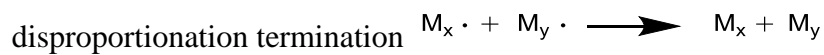
Chain growth rate Chain growth is the chain reaction of monomer radicals with amounts of monomers:



Assuming that chain length does not affect activity of chain radicals, reaction rate of every chain growth step is equal, which means $k_{p1} = k_{p2} = k_{p3} = \dots = k_{px} = k_p$. $[M\cdot]$ represents the sum concentration of radicals with different chain length $[RM\cdot]$, $[RM_2\cdot]$, $[RM_3\cdot]$, ..., $[RM_x\cdot]$. Chain growth rate equation can be expressed as:

$$R_p \equiv -\left(\frac{d[M]}{dt}\right)_p = k_p[M] \sum_{i=1}^x [RM_i\cdot] = k_p[M][M\cdot] \quad \text{Eq.2.6}$$

Chain termination rate Chain termination is process of disappearance of radicals, containing coupling termination and disproportionation termination:



Chain termination rate is the sum of coupling and disproportionation termination rate, and can be expressed as:

$$R_t \equiv -\frac{d[M\cdot]}{dt} = R_{tc} + R_{td} = 2k_{tc}[M\cdot]^2 + 2k_{td}[M\cdot]^2 = 2k_t[M\cdot]^2 \quad \text{Eq.2.7}$$

In above formulas, subscript p , t , tc , td represent chain growth, chain termination, coupling termination, and disproportionation termination, respectively.

After a period of polymerisation, initiating rate equals to termination rate ($R_i = R_t$), reaching dynamic equilibrium. In this case, concentration of radicals is constant. This concentration can be calculated by Eq.2.8:

$$[M\cdot] = \left(\frac{R_i}{2k_t}\right)^{1/2} \quad \text{Eq.2.8}$$

Polymerisation rate Polymerisation rate can be expressed by the consumption rate of monomer. Assuming that the majority of monomers are consumed by chain growth, thus polymerisation rate equals to the chain growth rate:

$$R \equiv -\frac{d[M]}{dt} = R_i + R_p \approx R_p \quad \text{Eq.2.9}$$

Universal equation of polymerisation rate can be achieved by adding radical concentration in steady state which is shown in Eq.2.8 into Eq.2.6:

$$R \approx R_p = k_p [M] \left(\frac{R_i}{2k_t} \right)^{1/2} \quad \text{Eq.2.10}$$

When initiated by initiator, by adding Eq.2.5 into Eq.2.10, the polymerisation rate can be expressed as:

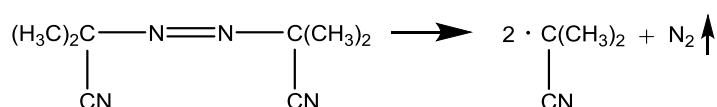
$$R = k_p \left(\frac{fk_d}{k_t} \right)^{1/2} [I]^{1/2} [M] \quad \text{Eq.2.11}$$

2.4.1.3 Decomposition of initiators

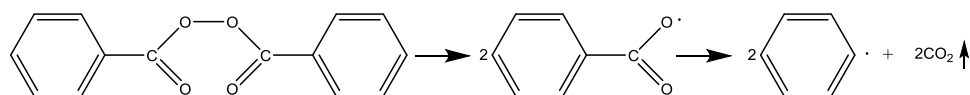
The function of initiator is to provide radicals for chain growth of vinyl monomers. The commonly used initiators are azo or peroxide compounds. Radicals form *via* thermal decomposition or redox reaction of the initiators being used.

2.4.1.3.1 Thermal decomposition initiator

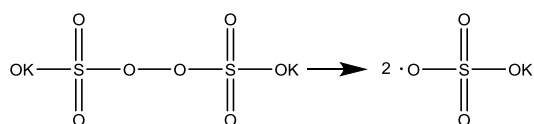
2, 2-azobis (isobutyronitrile) (AIBN) is a hydrophobic azo initiator which decomposes at 45 ~80 °C. Its thermal decomposition equation is as follows:



Benzoyl peroxide (BPO) is a hydrophobic peroxide initiator. Its decomposition temperature range is from 60 °C to 80 °C. Its thermal decomposition equation is as follows:

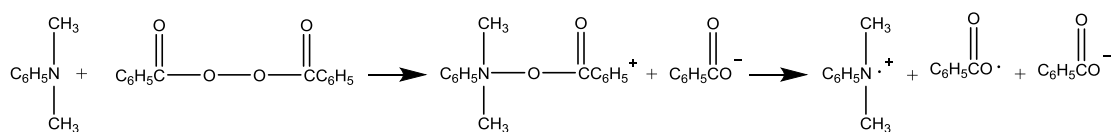


Potassium persulfate (KPS) is a hydrophilic initiator. The temperature for effective decomposition is over 60 °C. Its thermal decomposition equation is as follows:



2.4.1.3.2 Redox Initiator

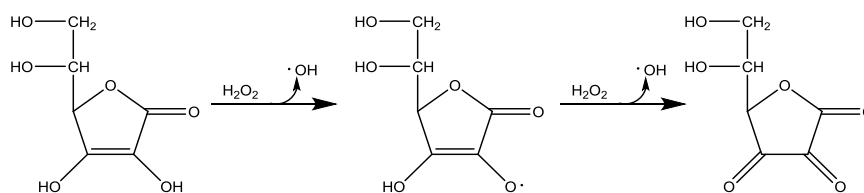
Benzoyl peroxide coupled with N,N-Dimethylaniline is a hydrophobic redox initiator. It is a high reactive redox initiator which can be used at room temperature. Its decomposition equation is as follows:



Persulfate coupled with sulfite or thiosulfate is a hydrophilic redox initiator. In the presence of the reducing agent, initiating temperature can be reduced compared with persulfate. Its decomposition equation is as follows:



Hydrogen peroxide coupled with ascorbic acid is a non-salt hydrophilic redox initiator. Its decomposition equation is as follows:



2.4.2 Mechanism of miniemulsion polymerisation

2.4.2.1 Miniemulsion polymerisation initiated by hydrophilic initiator

In emulsion polymerisation, three different mechanisms, including micellar, homogenous, and droplet nucleation co-exist. Micellar and homogenous nucleation are dominant. Droplet nucleation undoubtedly occurs in emulsion polymerisation, but its contribution is generally considered less important (explained in 1.1.1). The total area of micelles is overwhelmingly larger than that of droplets, thus makes droplets ineffective in the entry of radicals.

If the droplet size can be further reduced from micro scale to nano scale, the polymerisation process will change from emulsion polymerisation into miniemulsion polymerisation, in which two events will occur. First, the reduction in droplet size results in the remarkable increase in surface area of droplets thus making droplets comparable to micelles in the absorption of water-soluble free radicals. Second, surfactants will be adsorbed on the surface of newly formed droplets to prevent aggregation and coalescence. The free surfactant concentration in aqueous phase is much lower than that in emulsion, and even below the CMC value. Therefore, by breaking up droplet size into nano scale, the surface area of droplets increases while

the number of micelles decreases, hence the droplet nucleation become much more dominant compared with emulsion polymerisation. (Schork et al., 2005, Asua, 2002).

As for water-soluble initiator, free radicals are generated in water phase once the decomposition process of initiator starts, and are more likely to enter nano-size droplets as has been mentioned above. The radicals, which enter into droplet, will initiate free radical polymerisation. Fig.2.21 illustrates idealised miniemulsion polymerisation initiated by water-soluble initiator (Casey, 2009).

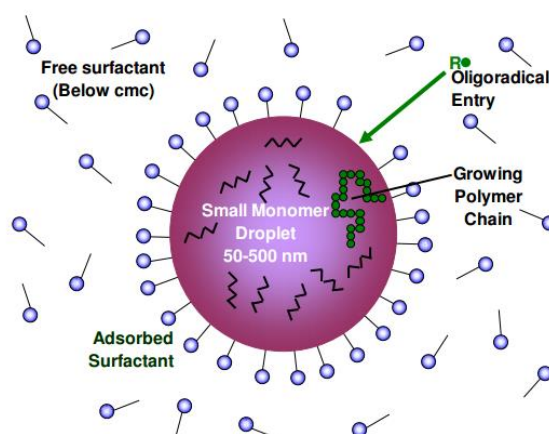


Fig.2.21 Schematic representation of miniemulsion polymerisation mechanism (Casey, 2009)

Even though droplet nucleation is the dominant nucleation mechanism for miniemulsion, homogenisation nucleation may also play some roles. Primary particles generated in the aqueous phase by the chain growth reaction of radicals with monomers dissolved in water. They were stabilised by the surfactant dissolved in water or released from droplet surface (Chern and Liou, 1999a, Schork et al., 2005). In addition, if surfactant concentration in water phase is higher than CMC value, micellar nucleation cannot be ignored (Schork et al., 2005, Asua, 2002). Theoretically, due to the droplet nucleation mechanism, the droplet size shall remain fairly constant during process changing from droplet into particle. However, the

phenomenon of decrease in droplet size after a period of time was observed in miniemulsion polymerisation of MMA initiated by hydrophilic initiator $\text{H}_2\text{O}_2/\text{AAc}$ (Romio et al., 2009a), and miniemulsion polymerisation of styrene initiated by another hydrophilic initiator sodium persulfate (Chern and Liou, 1999a). The droplet size was moving towards smaller due to the contribution of the smaller primary particles formed by homogenisation and micellar nucleation.

2.4.2.2 Miniemulsion polymerisation initiated by hydrophobic initiator

While for hydrophobic initiator, it is dissolved in oil phase before homogenisation. It will decompose in oil phase forming radicals for initiating the polymerisation. On the other hand, radicals may contact with each other and recombine into molecular before initiating polymerisation. In some cases, both initiator and radicals may diffuse into water phase, acting the same as water-soluble initiator (Mørk and Makame, 1997, Shang and Shan, 2012).

It is notable that similar trends of decrease in droplet size were also reported when the miniemulsion polymerisation of styrene was initiated by AIBN, a hydrophobic initiator (Chern and Liou, 1999c, Chern and Liou, 1999a). This indicates micellar or homogeneous nucleation still occurred even if a hydrophobic initiator is used. However, the necessary prerequisite for micellar or homogeneous nucleation is the existence of radicals in water phase which is favorable for hydrophilic initiator. While for AIBN, its decomposition was mainly carried out in droplets, which means the majority of radicals generated existed in droplets. It has been suggested that the source of free radicals in water phase were generated from the small fraction of hydrophobic initiator dissolved in water phase (Chern and Liou, 1999c, Mørk and Makame, 1997). Another source was radicals desorbed from the droplets and resided

in water phase. It has been proved that isobutyronitrile which has the same structure as radical generated from AIBN but in a state of molecular is more hydrophilic compared with AIBN (Shang and Shan, 2012). It is possible that radicals preferentially reside in water phase rather than oil phase that enhance the micellar or homogeneous nucleation.

2.4.3 Factors affecting stability of miniemulsion during polymerisation

The instability phenomenon of miniemulsion during polymerisation has some similarity to that during storage. Oil phase may separate from miniemulsion at the early stage of polymerisation. Miniemulsion may become viscous, and then coagulation of particles will separate from miniemulsion in the end of polymerisation. Sometimes product is stable and homogeneous, but particles may be bridged together when observed in microscope. (Musyanovych et al., 2007)

Factors having influence on stability of miniemulsion described in 2.3.4 also affect the stability of miniemulsion during polymerisation. Other factors including temperature and initiator type are taken into consideration when polymerisation is carried out. Temperature has a great effect on the stability of miniemulsion. The movement of droplets becomes more frequent with the increase of temperature, thus aggravating the coalescence of droplets. So stability of miniemulsion decreases with the increase of temperature. (Asua, 2002) This instability needs to be considered during polymerisation, as polymerisation is normally carried at a high temperature. The effect of initiator on stability of miniemulsion has received much attention in literature. Some of initiators are composed of salt. The adding of salt affects the zeta

potential of dispersion system.(Niriella and Carnahan, 2006) This may have an influence on stability of miniemulsion.

2.4.4 Factors affecting reaction rate of miniemulsion polymerisation

In miniemulsion polymerisation, its process can be divided into two stages. At stage I, droplets transform into particles through droplet nucleation. The efficiency of droplet nucleation is normally very high. However, micellar nucleation and homogenisation nucleation may still occur. At stage II, the effect of micellar nucleation and homogenisation nucleation fades down, thus the number of particles in aqueous phase would remain constant. Monomers stored in particles are continuously consumed with the progress of polymerisation process. Polymerisation rate at stage II can be expressed the same as the rate of free radical polymerisation shown in Eq.2.6:

$$R \equiv -\frac{d[M]}{dt} \approx R_p = k_p [M][M\cdot] . [M] \text{ represents the concentration of monomer in}$$

particles. Assuming the number of particles per unit volume of aqueous phase remains constant during polymerisation, $[M\cdot]$ can be expressed as:(Bechthold and Landfester, 2000)

$$[M\cdot] = \frac{\bar{n}N}{N_A} \quad \text{Eq.2.12}$$

where \bar{n} is average radical number per particle; N is the number of particles; N_A is Avogadro's number. After adding Eq.2.12 into Eq.2.6, polymerisation rate of stage II can be expressed as:

$$R_p = \frac{k_p [M] \bar{n} N}{N_A} \quad \text{Eq.2.13}$$

In ideal condition, \bar{n} equals to 0.5. Small particles can only contain one radical. When the second radical enters, the number of radical becomes zero due to chain termination. So the average radical number per particle is 0.5. However, for miniemulsion polymerisation \bar{n} cannot be assumed to equal to 0.5 because the particle size of miniemulsion is no longer “small”. When the initial particle size is greater than 120 nm, such large space makes it possible to contain more than one radical. Radical entry, radical exit, and radical termination happen at the same time in a particle shown in Fig.2.22. In this case, pseudo-bulk kinetic shown in Eq.2.14 better describes the real situation:

$$\frac{d\bar{n}}{dt} = \rho - k\bar{n} - 2c\bar{n}^2 \quad \text{Eq.2.14}$$

where ρ is the rate of radicals entering into the particle; k is the rate constant of radical exiting from the particle; c is the rate constant of chain termination.

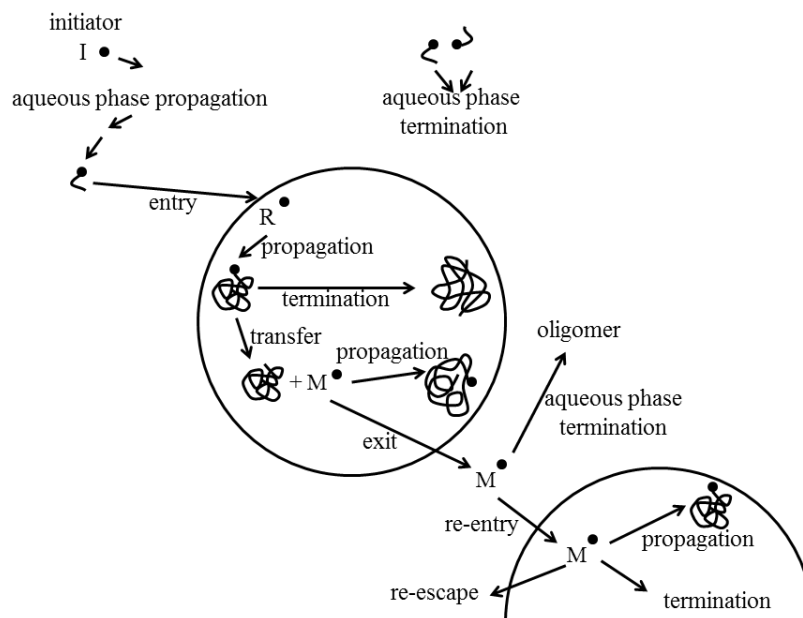


Fig.2.22 Entry and exit of free radical through a particle

After having a better understanding of kinetics of miniemulsion polymerisation, factors affecting kinetics of miniemulsion polymerisation will be discussed.

Initiator type has an influence on the rate of radicals formed. Initiator with lower activation energy may generate more radicals at the same temperature compared with initiator with higher activation energy, thus contributing to the polymerisation. Chern and Liou studied miniemulsion polymerisation of styrene in the presence of sodium dodecyl sulfate as surfactant and dodecyl methacrylate as co-stabiliser. They found polymerisation rate and conversion were higher when initiated by sodium persulfate, compared with 2,2'-azobisisobutyronitrile (AIBN). Low initiator efficiency of AIBN may be one reason leading to the low conversion. (Chern and Liou, 1999c) Temperature is another factor affecting kinetics of miniemulsion polymerisation. Decomposition rate of initiator is strongly dependent on temperature. Taking AIBN for example, it was reported in open literature that its half-life time was 80 min at 80 °C, (Perrier et al., 2005) while this time expanded to 37 h if temperature reduced to 55 °C. (Svec and Frechet, 1995) Clearly, higher temperature promoted higher efficiency in radical generation from the decomposition of AIBN, while low temperatures may cause inefficiency in radical generation, leading to the lack of radicals for further polymerisation. Choi *et al.* studied the temperature effect on the miniemulsion polymerisation of p-divinylbenzene initiated by potassium persulfate. It was observed that polymerisation rate and conversion increased with the increase of temperature. (Choi et al., 2008) This can be attributed to the efficiency in initiator decomposition at high temperature. Another factor is interfacial structure of droplets which may affect the entry rate of radical decomposed from hydrophilic initiator. If the interfacial structure is rigid, the entry rate of radicals into droplet may be reduced

due to this barrier, thus affecting the reaction rate adversely.(Gan et al., 1992, Mosca et al., 2013)

2.5 Miniemulsion stabilised by silica nanoparticles and its polymerisation process

Currently, a variety of inorganic particles including silica, Laponite clay, zinc oxide, titania have been employed as Pickering emulsifiers to stable surfactant-free system or to prepare hybrid nanoparticles. Compared with surfactant, Pickering emulsifier has many advantages such as strong interfacial stability, resistance to foam, reproducible property, low toxicity, and low cost. Hence Pickering emulsifiers have wild application prospect in the fields of cosmetic, food, pharmacy, petroleum, and effluent treatment. However, in polymerisation process, it is necessary to effectively bind solid particles to polymeric core to keep the system stable. The use of an auxiliary co-monomer can promote the adsorption of solid particles due to their interaction.

In the following review, the adsorption of nanoparticles on oil water phase, effect of silica nanoparticles on droplet size and stability of miniemulsion, interaction between auxiliary co-monomer and silica nanoparticle during polymerisation are introduced. The possibility of ILs acting the same as an auxiliary co-monomer is also discussed.

2.5.1 Adsorption of nanoparticles on oil water interface

Solid particles are normally dispersible in the continuous phase and can collect at the liquid-liquid interface as a steric/electrostatic barrier to prevent the collision of droplets and stabilise emulsion. The wetting property of the solid particles has great

influence on the stability of emulsion. Three phase contact angle is a useful parameter to represent the wetting property, and can be calculated by the following equation:

$$\cos \theta_{ow} = \frac{\gamma_{so} - \gamma_{sw}}{\gamma_{ow}} \quad \text{Eq.2.15}$$

where θ_{ow} is the three phase contact angle, γ_{so} is the interfacial tension between solid particle and oil phase, γ_{sw} is the interfacial tension between solid particle and water phase, γ_{ow} is the interfacial tension between oil phase and water phase (Binks and Clint, 2002). In general, hydrophilic particles with θ_{ow} less than 90° , for example silica or metal oxides, can stabilise o/w emulsion. While hydrophobic particles with θ_{ow} more than 90° , such as carbon, can stabilise w/o emulsion (Binks, 2002). The scheme is shown in Fig.2.23. In contrast to surfactants which adsorb and desorb dynamically on the surface of droplets, the adsorption of solid particles are frequently viewed as irreversible. This means once solid particles attach to the surface of droplets, they may not easily desorb as surfactants. This irreversible adsorption has been explained by Binks (Binks, 2002). After supposing that the particles are small enough that their gravity can be neglected, the energy E for removing the particles from the interface can be expressed as:

$$E = \pi r^2 \gamma_{ow} (1 \pm \cos \theta_{ow})^2 \quad \text{Eq.2.16}$$

where r is the radius of particle; γ_{ow} is the interfacial tension between two phases; θ_{ow} is the three phase contact angle; $-$ represents particle moves into water phase; $+$ represents particle moves into oil phase. According to Eq.2.16, with a proper θ_{ow} , the energy required for the particles to desorb into water phase is orders of magnitude larger than the thermal energy (kT), thus the adsorption is normally irreversible. For example, by measured three phase contact angle of magnetite particles (2~6 nm)

between water and 3-methacryloxypropyl trimethoxysilane (TPM) and interfacial tension between water and TPM, Sacanna *et al.* calculated the desorption energy of magnetite particles with a value of 20~200 kT. (Sacanna et al., 2007)

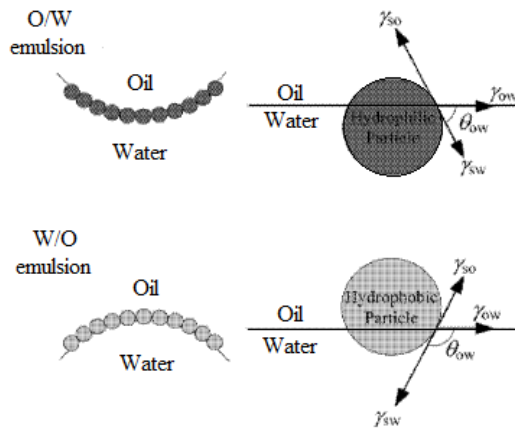


Fig.2.23 Scheme of three phase contact angle

2.5.2 Effect of silica nanoparticle on droplet size and stability of miniemulsion

Silica nanoparticle is chosen as Pickering emulsifier for this research. The process of preparing miniemulsion stabilised by silica nanoparticles is the same as miniemulsion stabilised by surfactant. Factors affecting droplet size and stability of miniemulsion stabilised by surfactant can be reference for miniemulsion stabilised by silica nanoparticles. The effect of silica nanoparticle is focused here.

The droplet size of emulsion/miniemulsion decreases with the increase of silica nanoparticle concentration then tends to be stable. Maryam Kargar *et al.* studied Pickering emulsions stabilised by modified starch (MS). (Kargar et al., 2012) When concentration of MS (wt/wt) increased from 0.1 % to 1 %, droplet size dramatically decreased from 14.5 μm to 5.2 μm . However, further increasing concentration of MS to 2.5 %, droplet size fluctuated at 5.1 μm . K. K öhler *et al.* also found that droplet

size was nearly constant after silica nanoparticle, a Pickering emulsifier, reached a certain value. (Köhler et al., 2010)

The stability of miniemulsion/emulsion is influenced by three phase contact angle of silica nanoparticles as described in 2.5.1. Three phase contact angle of silica nanoparticles can be adjusted to a proper value by surface modification, thus enhancing the stability of emulsion.(Binks and Lumsdon, 2000b) Polarity of oil phase also affects the three phase contact angle, thus deciding the type of emulsion. High polar oil can only form W/O emulsion, while non-polar oil can only form O/W emulsion.(Binks and Lumsdon, 2000a) Surface charge of nanoparticle, represented by zeta potential, also influences the stability. Nanoparticles at their isoelectric point could perform better as Pickering emulsifier due to the weaker electrostatic repulsion among nanoparticles adsorbed on the surface of droplets, thus achieving good emulsification results. (Köhler et al., 2010) The surface charge can be adjusted by the pH of water phase and electrolyte concentration in water phase. (Köhler et al., 2010, P. Binks and O. Lumsdon, 1999)

2.5.3 Interaction between auxiliary co-monomer and silica nanoparticle during polymerisation

The effective binding between silica nano-particles and polymeric core is essential to keep the system stable. However, the interaction between silica nanoparticles and polymers are normally insufficient to ensure the stability during polymerisation process. The use of an auxiliary comonomer which has strong interaction with solid particles is a solution for both Pickering emulsion polymerisation and Pickering miniemulsion polymerisation.

2.5.3.1 Pickering emulsion polymerisation

Percy *et al.* successfully prepared vinyl polymer-silica nanocomposites in a surfactant-free system with the assist of an auxiliary comonomer, 4-vinylpyridine (4-VP).(Percy et al., 2000) In the absence of 4-VP, the interaction between silica and polymer particles (PMMA and PS) turned out to be insufficient, leading to instability during the nanocomposite formation process. While adding 4-VP to a certain amount, stable vinyl polymer-silica nanocomposites can be formed. This is due to the strong acid-base interaction between hydroxyl groups of silica and nitrogen atoms of 4-VP, which benefits the absorption of silica on the surface of polymer particles. Another similar auxiliary comonomer, 2-vinylpyridine (2-VP), was also attempted. But it was less effective, probably due to its less basic property and steric constraints.

Chen *et al.* then attempted a new auxiliary comonomer, 1-vinylimidazole (1-VID) to prepare PMMA-silica nanocomposites.(Chen et al., 2004) Similar to 4-VP, the strong acid-base interaction between hydroxyl groups of silica and nitrogen atoms of 1-VID played a key role in the absorption of silica on the surface of particles, thus the content of silica attached to PMMA-silica nanocomposites was directly affected by the amount of 1-VID added in oil phase. Fig.2.24 shows the reaction scheme for the formation of PMMA-silica nanoparticles in the present of 1-VID and in the absence of 1-VID. The average particle sizes were influenced by the content of silica, and could range from 120 nm to 350 nm. Yin *et al.* attempted another monomer styrene, and prepared asymmetric PS-silica nanocomposites in the present of 1-VID.(Yin et al., 2011)

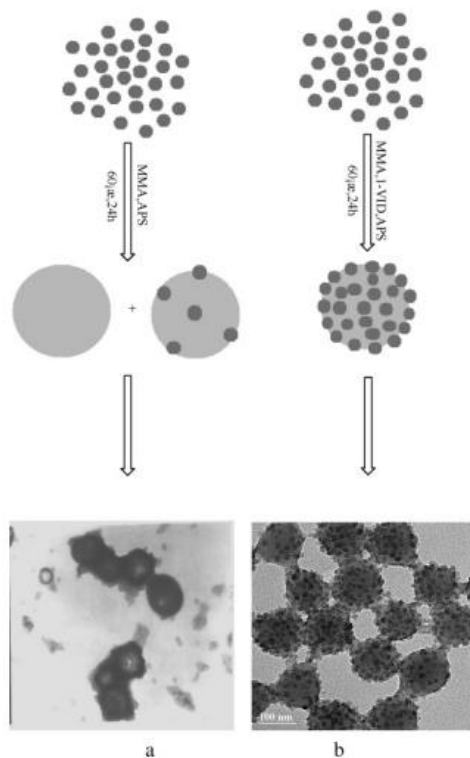


Fig.2.24 Reaction scheme for the formation of PMMA-silica nanoparticles (Chen et al., 2004)

To extend the potential auxiliary comonomer, Chen *et al.* then introduced a commercially available cationic monomer, 2-(methacryloyl)ethyltrimethylammonium chloride (MTC) to prepare PMMA-silica nanocomposites.(Chen et al., 2005) Narrow distributed nanocomposites in a size ranging from 180 nm to 600 nm can be achieved. Different from acid-base interaction, silica was adsorbed onto polymer particles by the strong electrostatic interaction between negatively charged silica and positively charged MTC. Due to the strong electrostatic interaction, the amount of MTC for stabilising dispersion was much less compared with 4-VP and 1-DIV. The same research group further changed the continuous phase from water to water/acetone mixture.(Yuhong et al., 2009) Due to the adding of acetone, the dielectric constant of continuous phase became lower, leading to the increase in electrostatic repulsion between particles. Hence, smaller particles could be achieved as less coagulative nucleation happened. The solid content of product can be as high as 25 wt%.

In order to reduce the cost, Zhang *et al.* used acrylonitrile (AN) as an economical auxiliary comonomer to synthesise PS-silica nanocomposites in isopropyl alcohol (IPA)/water medium.(Zhang et al., 2007) The stability of dispersion system increased as the increase of AN concentration. The authors claimed there was interaction between AN and silica that benefited the connection between silica and polymer nanoparticles. But the detail explanation of the interaction was not mentioned.

2.5.3.2 Pickering miniemulsion polymerisation

Tiarks *et al.* first prepared raspberry-like copolymer-silica nanocomposites by Pickering miniemulsion polymerisation. The acid-base interaction between the auxiliary comonomer, 4-VP and silica was crucial for the stability of system. The size of nanocomposites could be adjusted from 120 nm to 220 nm by controlling the content of silica and 4-VP. (Tiarks et al., 2001b)

Up to now, the silica mentioned above is negatively charged. Schrade *et al.* novelly introduced alumina-coated cationic silica as the Pickering emulsifier, and prepared positively charged, raspberry-like nanocomposites by Pickering miniemulsion polymerisation.(Schrade et al., 2011) The auxiliary comonomers used to enhance the interaction between cationic silica and droplet/particles were acrylic acid (AA), methacrylic acid (MAA), and acrylamide (AAM).

Fortuna et al. prepared PS-silica nanocomposites in the absence of any auxiliary comonomer. The surface charge of silica was reduced by adjusting the PH of the system, for example 3.5.(Fortuna et al., 2009) The silica attachment on the surface of droplets/polymer particles was improved, due to the decrease of electrostatic repulsion between silica nanoparticles.

2.5.4 The possibility of ILs acting as an auxiliary co-monomer

From the review in the part of 2.5.3, the auxiliary comonomers used includes 4-VP, 2-VP, 1-VID, MTC, AN, AA, MAA, and AAM.

It is notable that the structure of C_8mimPF_6 (The ILs chosen for this study) has some similarity to 1-VID shown in Fig.2.25. Both of them have an imidazole ring. This means C_8mimPF_6 can be a potential component acting the same as auxiliary comonomer, 1-VID. In fact, a strong interaction between imidazole based ILs and silica nano-particles via hydrogen bond and Van der Waals' force can be formed. (Liu et al., 2010, Lei et al., 2010) This interaction may enhance the adsorption of silica nanoparticles on the surface of polymeric core, thus keeps the dispersion stable during polymerisation.

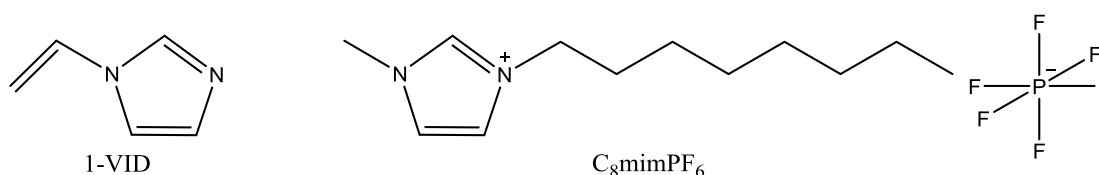


Fig.2.25 Structure of 1-VID and C_8mimPF_6

However, C_8mimPF_6 cannot participate in Pickering emulsion polymerisation due to its lack of carbon-carbon bonds. It may function if applied in Pickering miniemulsion polymerisation. C_8mimPF_6 dissolved in droplets may absorb silica on the surface of droplets/polymer particles by hydrogen bond and Van der Waals' force, thus enhance the stability of the system during polymerisation.

Chapter 3 Factors on initial droplet size and stability of miniemulsion

3.1 Introduction

Miniemulsion polymerisation is selected as the method to encapsulate C_8mimPF_6 inside particles for the preparation of latex coating containing C_8mimPF_6 . Achieving stable miniemulsion is a crucial step for further polymerisation. Two kinds of emulsifiers will be chosen for stabilising miniemulsion: conventional anionic surfactant, and a Pickering emulsifier, *i.e.* silica nanoparticle. Silica nanoparticle, as an alternative to conventional surfactant, can overcome the lacks in gloss and water resistance of film caused by surfactant residual (Schrade et al., 2013). For miniemulsion stabilised by surfactant, various factors including energy input, surfactant type, surfactant concentration, C_8mimPF_6 concentration, and temperature on initial droplet size and stability of miniemulsion were investigated. As to miniemulsion stabilised by silica nanoparticle, systematically studying various factors, including energy input, pH of water phase, silica nanoparticle concentration, C_8mimPF_6 concentration, and temperature on initial droplet size and stability of miniemulsion would be carried out.

3.2 Materials and methods

3.2.1 Materials

Methyl methacrylate (MMA, CP), sodium dodecyl sulfate (SDS, CP), sodium dodecyl sulfonate (SDSO, CP), and sodium dodecyl benzene sulfonate (SDBS, AR) were purchased from Sinopharm Chemical Reagent Co., Ltd. NS-30 (20 nm silica

nanoparticle, pH = 9.5, 30 wt%) was supplied as dispersion of silica nanoparticle by Yuda Chemical Co. Hexadecane (HD, 98%) was from Aladdin Industrial Inc. 1-octyl-3-methylimidazolium hexafluorophosphate (C_8mimPF_6 , 99%) was supplied by Shanghai Cheng Jie Chemical Co.. The density of C_8mimPF_6 is 1.18 g/cm^3 at $20 \text{ }^\circ\text{C}$. Ultra-pure water with a resistivity of $18.2 \text{ M}\Omega\cdot\text{cm}^{-1}$ was used in all experiments.

3.2.2 Preparation of miniemulsion

Fig.3.1 describes the general procedure for the preparation of miniemulsion. The specific procedure for miniemulsion stabilised by surfactant and silica nanoparticle will be shown in 3.2.2.1 and 3.2.2.2, respectively.

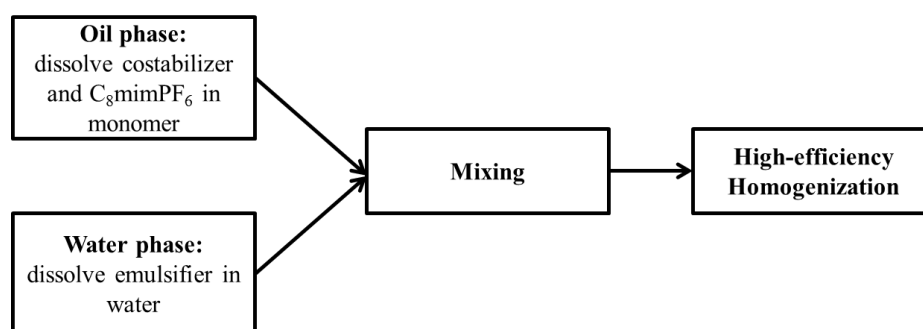


Fig.3.1 Procedure for the preparation of miniemulsion.

3.2.2.1 Miniemulsion stabilised by surfactant

Oil phase was prepared by dissolving 5 wt% HD, different weight percentage of C_8mimPF_6 into MMA while keeping the total weight of oil phase constant. Both HD and C_8mimPF_6 were infinitely miscible in MMA. A homogeneous oil phase was obtained after gently stirring. The contents of MMA, HD, and C_8mimPF_6 in oil phase are shown in Table.3.1.

Table.3.1 Formula of oil phases

Sample code	Components in oil phase (wt% based on oil phase)		
	MMA	HD	C ₈ mimPF ₆
O-1	95	5	0
O-2	94.9	5	0.1
O-3	94.5	5	0.5
O-4	94	5	1
O-5	90	5	5
O-6	85	5	10
O-7	80	5	15
O-8	75	5	20
O-9	65	5	30

Water phase was prepared by dissolving a given amount of surfactant in ultra-pure water. The type and concentration of surfactant in water phase is showed in Table.3.2.

Table.3.2 Formula of water phases containing surfactant

Sample code	Type of surfactant	Amount (mM)
W-sur-1	SDS	30
W-sur-2	SDBS	30
W-sur-3	SDSO	30
W-sur-4	SDSO	10
W-sur-5	SDSO	20
W-sur-6	SDSO	40
W-sur-7	SDSO	50

To prepare miniemulsion stabilised by surfactant, sonicator (Xinzhi Scientz II) was chosen as the homogeniser as shown in Fig.3.2. Because the solid content of conventional latex is normally no less than 30 wt%,(Ai et al., 2010) to meet the requirement of minimum solid content, the ratio between oil and water phase was set as 3 to 7. In this case, 15 mL oil was added into 35 mL water phase in a 100 ml plastic container. The mixture was kept at 40 °C to ensure the dissolution of surfactants

(SDSO, SDS, SDBS) in water phase. Ultrasound probe was then placed in the middle of the container and kept at one centimeter below the surface of the mixture as shown in Fig.3.3. The output power of sonicator was set as 57~133 W. After homogenising the mixture for 1~8 minute in a state of 1 second on and 1 second off, miniemulsion was obtained.



Fig.3.2 Image of a sonicator (Xinzhi Scientz II)

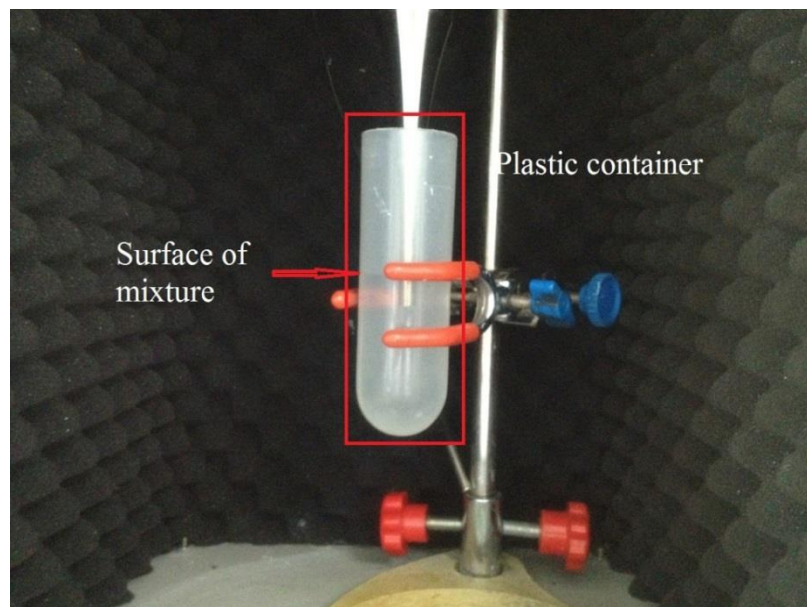


Fig.3.3 Position of plastic container and ultrasound probe

3.2.2.2 Miniemulsion stabilised by silica nanoparticle

The formula of oil phase for miniemulsion stabilised by silica nanoparticle was the same as the one for miniemulsion stabilised by surfactant.

Water phase was prepared by dissolving silica sol, NS-30 (a dispersion of 20 nm silica nanoparticle with a 30 wt% solid content) into ultra-pure water to the target concentration (gram of silica nanoparticle per litre of water phase, or mass concentration); and the pH was adjusted using 0.1 mol/L aqueous NaOH or HCl solution at the same time. Table.3.3 shows the formula of water phases containing silica nanoparticle.

Table.3.3 Formula of water phases containing silica nanoparticle

Sample code	Concentration of silica nanoparticle		pH
	g/l	wt%	
W-sil-1	10	1.0	3
W-sil-2	30	3.0	3
W-sil-3	50	4.9	3
W-sil-4	70	6.8	3
W-sil-5	90	8.6	3
W-sil-6	50	4.9	5
W-sil-7	50	4.9	7
W-sil-8	50	4.9	9
W-sil-9	50	4.9	11

High speed disperser (IKA T25) shown in Fig.3.4 was chosen in place of sonicator to prepare miniemulsion stabilised by silica nanoparticles, as miniemulsion homogenised by sonicator was too viscous to form uniform mixture. High speed disperser has a rotor-stator structure (stator/rotor (\emptyset): 18/12.7 mm, gap between rotor and stator: 0.3 mm) as shown in Fig.3.5. As the rotor rotates, it leads to the circulation

that draws the fluid in and out of the rotor-stator field, thus contributing to uniform mixture. In order to meet the minimum requirement for the solid content of latex, 30 wt%, the ratio between oil and water phase was fixed as 3 to 7. In this situation, 30 mL oil phase was added into 70 mL water phase in a 250 ml baker. The mixture was kept at 40 °C. Rotor was then placed in the middle of the baker and kept the tip of the rotor one centimetre above the bottom of the baker as shown in Fig.3.6. The stirring speed of high speed disperser ranged from 8000 rpm to 20000 rpm. After homogenising the mixture for 8 minute, a stable miniemulsion was formed.



Fig.3.4 Image of a high speed disperser (IKA T25)

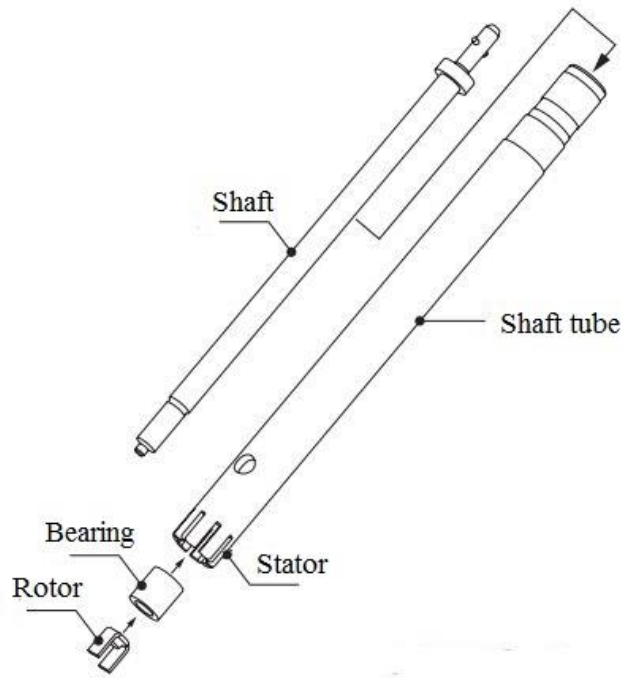


Fig.3.5 Illustration of stator/rotor structure

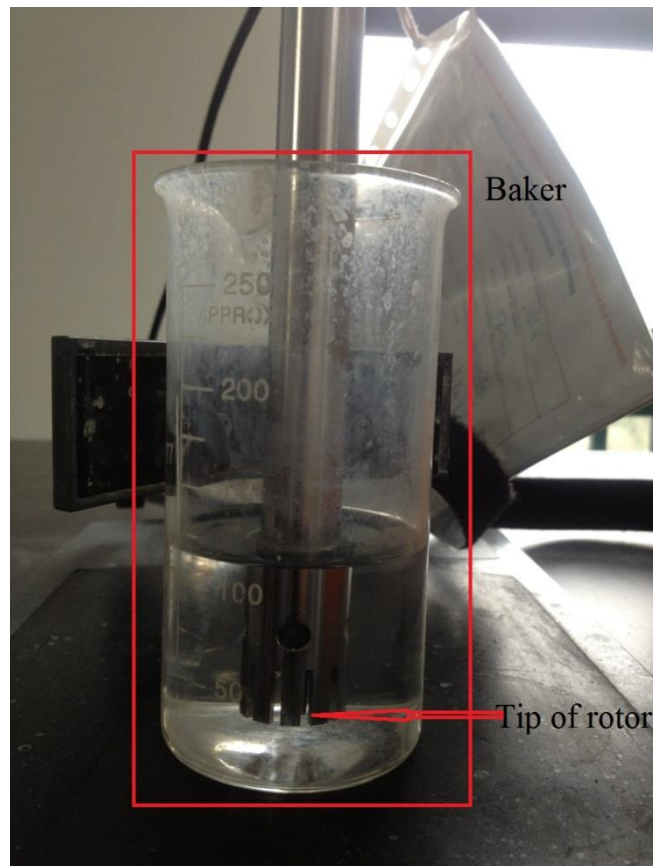


Fig.3.6 Position of baker and tip of rotor

3.2.3 Characterisation of miniemulsion

3.2.3.1 Droplet size measurement

The droplet size and size distribution of miniemulsion with different aging times were measured using the laser diffraction method (Mastersizer 3000, Malvern Inc). This technique has been widely accepted as a tool to evaluate droplet size (Zhang et al., 2012, Winkelmann and Schuchmann, 2011). The measuring steps are as followed. The sample was diluted with water solution to meet the requirement of obscuration. For miniemulsion stabilised by surfactant, the diluted solution was water saturated with surfactant (used in the miniemulsion preparation) and monomer to prevent coalescence during sample measurement (Meliana et al., 2011). While for miniemulsion stabilised by silica nanoparticle, water saturated with monomer was used as the dilute solution for miniemulsion. No increase in droplet size could be detected with the increase of measurement time. This meant silica nanoparticle would not easily desorb from surface of droplet, leading to the coalescence. All measurements were repeated for three times.

3.2.3.2 Stability of miniemulsion during storage

3.2.3.2.1 Direct observation

To evaluate the macroscopic stability of miniemulsion, 22 mL miniemulsion was sealed in a cylindrical glass bottle (\varnothing : 28 mm, H: 45 mm), and stored at 20 °C. At this volume, there was enough space between the top of miniemulsion and the bottle cap, so the change of miniemulsion could be observed completely though the transparent glass bottle. Two kinds of destabilisation phenomena might occur during storage: creaming on the top layer; sediment at the bottom layer. As shown in Fig.3.7,

the bottle was placed upside down to measure the height of sediment. The height of creaming was difficult to measure due to its irregular shape.

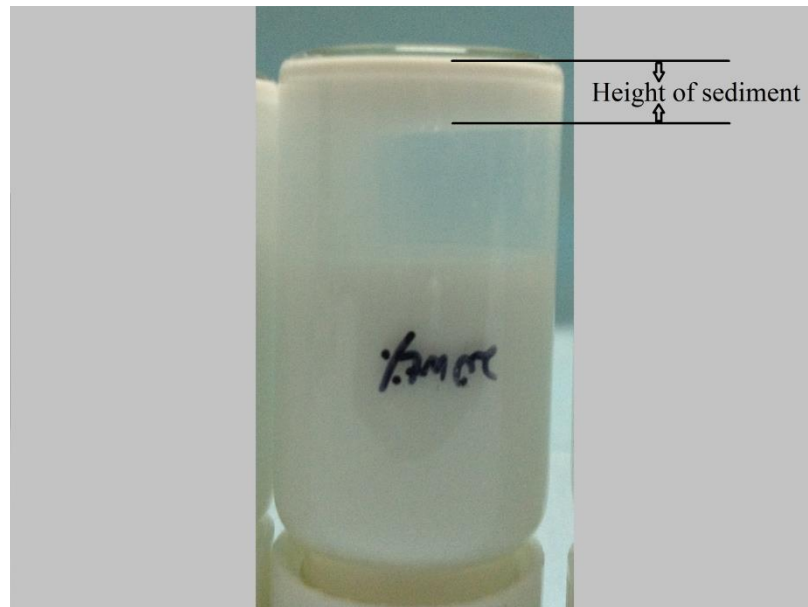


Fig.3.7 Image of a bottle placed upside down in order to measure the height of sediment.

3.2.3.2.2 Centrifugation

Centrifugation was a method to accelerate the process of stability testing (Casey, 2009, Jumaa and Müller, 2002). Destabilisation may occur within hours rather than days of storage. To shorten observation time, stability of miniemulsion was determined by centrifugation at 5000 rpm for 2 hours (TDZ5-WS, Xiangyi Instruments). Miniemulsion was then separated into two layers. The top layer was oil phase, and the bottom layer was miniemulsion phase. The oil phase was removed by pipette and weighted. All measurements were repeated for three times.

3.2.3.3 Viscosity measurement

Viscosities of water phases and oil phase were measured using the rotational Rheometer with cone-and-plate system (Kinexus Pro+, Malvern Inc). The diameter of the cone was 60 mm and the cone angle was 1° . Measurement was conducted with the

shear rate ranging from 10 s^{-1} to 1000 s^{-1} at 40°C . The viscosity was insensitive to the change of shear rate, so the final viscosity was the average value of viscosities with different shear rate.

Viscosities of miniemulsions were measured using the same rotational rheometer with the plate-and-plate system which was used for solid in liquid dispersion. The upper plate had a diameter of 40 mm, and the gap between upper and lower plates was 1.0 mm. Measurement was conducted with the shear rate ranging from 0.1 s^{-1} to 1000 s^{-1} at 20°C , the storage temperature.

3.2.3.4 Interfacial tension measurement

The interfacial tension between the oil phase and water phase was measured using the Du Nouy ring method (BZY-2 tensiometer, Hengping Instruments). The measurement was carried out at 40°C . All measurements were repeated three times.

3.2.3.5 Zeta potential measurement

Zeta potentials of the miniemulsion were measured using the trace laser Doppler electrophoresis method (ZetasizerNano ZS, Malvern Inc) at 20°C . Miniemulsion stabilised by surfactant was injected into high concentration sample cell without dilution. Miniemulsion stabilised by silica nanoparticle was diluted ten times by water before injected into a disposable sample cell. Because pH has a great influence on zeta potential, the diluted ones had the same pH as the original one. All measurements were repeated three times.

3.3 Results and discussion

3.3.1 Miniemulsion stabilised by surfactant

Due to droplet nucleation mechanism, particles are directly “copied” from droplets during miniemulsion polymerisation, thus initial droplet size directly decides final particle size in latex. As particle size in turn influences the film formation process and film property (Jensen and Morgan, 1991, Eckersley and Helmer, 1997), it is necessary to understand factors on initial droplet size of miniemulsion in order to produce latex with controllable particle size. Stability of miniemulsion during storage would further affect stability of miniemulsion during polymerisation (Asua, 2002), so it would be helpful to explain stability during polymerisation after having a better understanding of stability of miniemulsion during storage.

In this section, the effects of energy input, surfactant concentration, and C_8mimPF_6 concentration on initial droplet size, and the effect of surfactant type, C_8mimPF_6 concentration, and temperature on stability of miniemulsion were investigated.

3.3.1.1 Factors affecting initial droplet size of miniemulsion

3.3.1.1.1 Effect of energy input on initial droplet size

The initial droplet size of miniemulsion is determined by both droplet breakup and droplet coalescence. In terms of droplet breakup, the driving force is disruptive energy which is supplied by homogeniser. In the study of factors affecting initial droplet size of miniemulsion, energy input of homogeniser was first focused. Sonicator was chosen as the homogeniser. To study the effect of energy input, the formulas of oil and water phases were fixed. The amount of coalescing agent added in

latex coating is 0~10 wt% based on solid content.(Toussaint et al., 1997, Lahtinen et al., 2003, Raja et al., 2010) In order to have a better performance as a coalescing agent, C₈mimPF₆ concentration in oil phase was fixed as 10 wt% (O-6) for all the studies, except for the study of effect of C₈mimPF₆ concentration. Water phase contained 30 mM SDSO (W-sur-3).

Fig.3.8 shows the initial droplet size of miniemulsion as a function of input duration with different input powers ranging from 57 W to 133 W. It is found that, at a fixed input duration, an increase in input power, from 57 W to 95 W, results in an apparent decline on droplet size of miniemulsion. Further increasing input power up to 133 W, has less influence on droplet size. It can be seen that miniemulsion with smaller droplet size can be achieved with higher input power. However, upon a certain input power, further increase in input power has less effect on reduction of droplet size. This is because, although further increase upon a certain input power may accelerate breakup of droplet, coalescence caused by excessive cavitation phenomena may also become dominant, which may hinder further decrease in droplet size (Canselier et al., 2002). On the other hand, when input power is fixed, *e.g.* 95 W, with an increase in input duration, *i.e.* from 1 min to 6 min, droplet size sharply decreases from 384.3 nm to 235.3 nm. Continuing to increase input duration up to 8 min, trend of decline on droplet size becomes unapparent, slight from 235.3 nm to 231.6 nm. It can be seen that upon a certain input duration, further increase in input duration has less effect on reduction of droplet size.

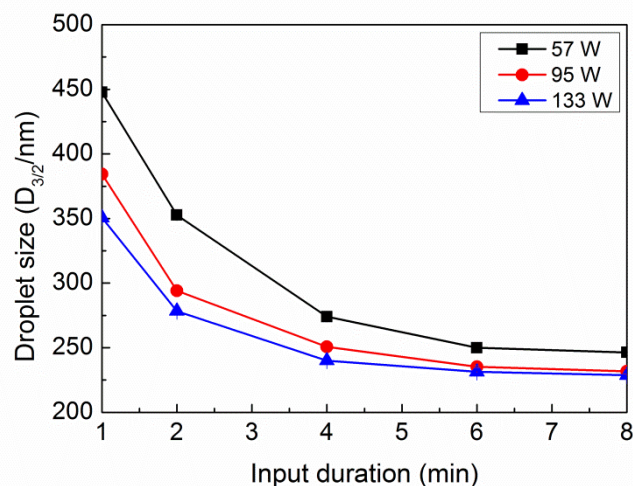


Fig.3.8 Initial droplet size of miniemulsion as a function of input duration with different input powers ranging from 57 W to 133 W.

Based on above results, the operation condition of sonicator for preparing miniemulsion is to set an input power of 95 W with an input duration of 6 min. This is because, for all input power ranges, reduction on droplet size is less apparent ones input duration is higher than 6 min. To make use energy efficiently, input duration is set as 6 min. At an input duration of 6 min, upon 95 W, a further increase in input power has a less effect on reduction of droplet size. So an input power with 95 W is chosen. Such operation condition will be employed in the following study.

3.3.1.1.2 Effect of surfactant concentration on initial droplet size

Surfactant plays a key role on droplet breakup and prevention coalescence during homogenisation, thus initial droplet size is directly decided by concentration of surfactant. In order to evaluate the role of surfactant on initial droplet size of miniemulsion, SDSO was chosen as the target surfactant (miniemulsion stabilised by SDSO was more stable than other two surfactants, SDS and SDSO as discussed in 3.3.1.2.1), and water phases containing different concentrations of SDSO ranging from 10 mM (W-sur-4), 20 mM (W-sur-5), 30 mM (W-sur-3), 40 mM (W-sur-6) to

50 mM (W-sur-7) were prepared. Concentration of C_8mimPF_6 in oil phase was fixed as 10 wt% (O-6). The reason why 10 wt% was chosen was explained in 3.3.1.1.1. Miniemulsion was prepared by sonicator with an input power of 95 W for 6 min.

Fig.3.9 shows the variation of droplet sizes as a function of surfactant concentration for miniemulsions. The droplet size decreases sharply with the increase of surfactant concentration in the lower concentration up to 30 mM. Further increase of surfactant concentration from 30 mM to 50 mM, the change of droplet size becomes less pronounced. Similar observation was reported by Abismaïl et al. when studied the relationship between droplet size and surfactant concentration at the 130 W output power of sonicator (Abismaïl et al., 1999).

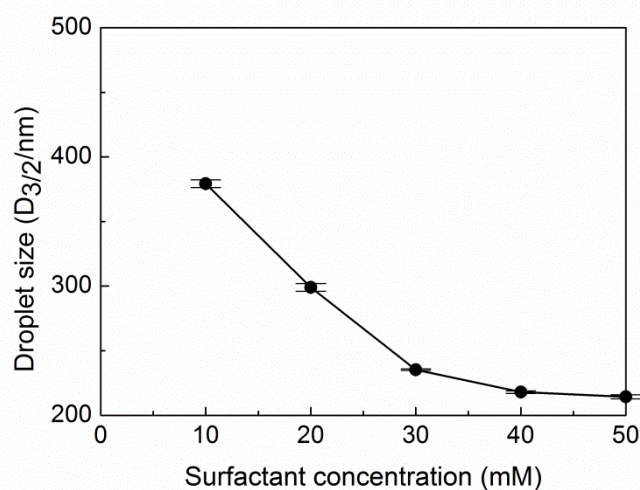


Fig.3.9 Variation of droplet sizes as a function of surfactant concentration for miniemulsions containing 10 wt% C_8mimPF_6 stabilised with SDSO

In order to identify the reason causing different changing rates on droplet size reduction when increasing SDSO concentration, the interfacial tension for different oil water composition was investigated. Results are shown in Fig.3.10. It is found that the interfacial tension decreases sharply with an increase in surfactant concentration from 0 to 10 mM, and further increase SDSO concentration to 30 mM, results in a

slow reduction on interfacial tension. The interfacial tension becomes more stable when the SDSO concentration is above 30 mM. Such observation indicates the change of surface adsorption of surfactant hence surface activity on the interface during the miniemulsion droplet formation process. Below 30 mM, adsorption of SDSO on the oil/water interface did not form a saturated monolayer. Thus when more SDSO were added, they continually adsorbed on the interface result in sharp reduction on the interfacial tension initially. Above 30 mM, a saturated adsorption of SDSO on the interface was obtained. This meant no further surface activity change occur thus the interfacial tension remained stable.

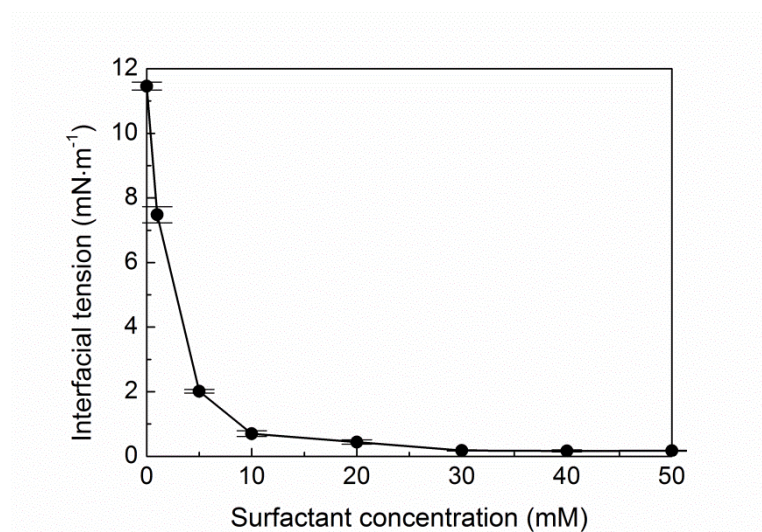


Fig.3.10 Variation of interfacial tension as a function of surfactant concentration

Based on the above observation, it is clear that that initial droplet size was directly affected by the concentration of surfactant (SDSO) during ultrasonic homogenisation process. In the initial droplet formation process, the droplets were disrupted and coalesced before reaching a dynamic steady state. Landfester et al. reported that within a certain range of surfactant concentrations, the droplet size in steady state was determined by the surfactant concentration because smaller droplets

created by disruption could only be stable if excess surfactant was left for stabilisation, otherwise they would coalesce to form bigger one (Landfester et al., 1999a). Low surfactant concentration would lead to the incompletely covered interface, thus more surfactants were required to prevent smaller droplets from coalescence (Hecht et al., 2011). These may explain the sharp decline on droplet size shown in Fig.3.9.

3.3.1.1.3 Effect of C_8mimPF_6 concentration on initial droplet size

In order to evaluate the role of C_8mimPF_6 in the miniemulsion formulation, the initial droplet sizes for miniemulsions containing different C_8mimPF_6 concentrations were investigated. The same surfactant SDSO with fixed concentration in water phase 30 mM (W-sur-3) was chosen. The oil phase contained different concentrations of C_8mimPF_6 ranging from 0 wt% (O-1), 0.1 wt% (O-2), 0.5 wt% (O-3), 1 wt% (O-4), 5 wt% (O-5), 10 wt% (O-6), 15 wt% (O-7), 20 wt% (O-8) to 30 wt% (O-9). Miniemulsion was prepared by sonicator with an input power of 95 W for 6 min.

Fig.3.11 shows variation of droplet sizes as a function of C_8mimPF_6 concentration for miniemulsions stabilised with SDSO. It is interesting to note that at lower concentration of C_8mimPF_6 , i.e. between 0 and 1 wt%, there are sharp decline on droplets size of the miniemulsions, then droplet size trends to be stable until 5 wt%, whilst beyond this point, droplet size of the miniemulsion tended to increase as the concentration of C_8mimPF_6 increased. Currently, with a fixed SDSO concentration 30 mM, the effect of C_8mimPF_6 concentration on initial droplet size is considered. At other SDSO concentration, e.g. 20 mM, 40 mM, variation of droplet sizes as a function of C_8mimPF_6 concentration should also be measured. This would be done in further work.

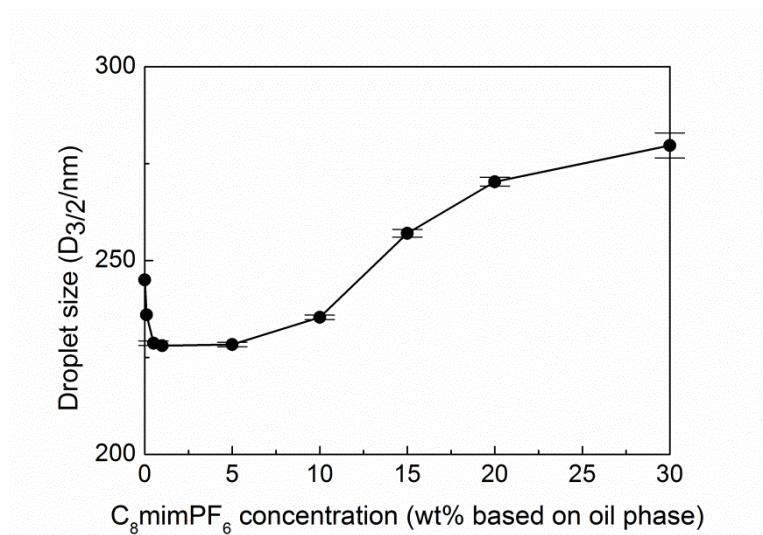


Fig.3.11 Variation of droplet sizes as a function of C_8mimPF_6 concentration for miniemulsions stabilised with SDSO

The initial droplet size of miniemulsion is determined by combined effect of droplet breakup and droplet coalescence. For droplet breakup, the prerequisite is that the disruptive energy should overcome the surface energy controlled by interfacial tension and viscoelastic energy controlled by the viscosity of dispersed phase (Asua, 2014). We try to explain the effect of C_8mimPF_6 on initial droplet size of miniemulsion from the following two aspects: viscosity and interfacial tension.

From the open literature, it has been reported that increase of the viscosity of oil phase (dispersed phase) may affect miniemulsion droplet size. This is depends on the viscosity ratio between dispersed phase and continuous phase. Nazarzadeh and Sajjadi studied the viscosity effects of dispersed phase (silicon oil) on droplet size of miniemulsion prepared by ultrasound (Nazarzadeh and Sajjadi, 2010). They found that the average droplet size sharply decreased as the increase of dispersed/continuous phase ratio, reached a minimum when the viscosity ratio was around 1.0, and then remained constant, followed by a significant increase at viscosity ratio beyond 10.

In this study, the viscosity of C_8mimPF_6 is 1052 mPa·s at 20°C (Tomida et al., 2007b), and that of MMA is 0.5311 mPa·s at 30°C (Vadamalar et al., 2008). The viscosity of water phase is 0.839 mPa·s at 40 °C. The effect of C_8mimPF_6 on viscosity of oil phase cannot be ignored. Fig.3.12 shows the variation of viscosity ratio between oil phase and water phase as a function of C_8mimPF_6 concentration in oil phase. The viscosity ratio increases as the increase of C_8mimPF_6 concentration in oil phase and ranges from 0.7 to 2.5. This is well below the critical increasing point (i.e. 10) being observed by Nazarzadeh and Sajjadi (Nazarzadeh and Sajjadi, 2010), which means the increase of droplet size between 10 wt% and 30 wt% of C_8mimPF_6 may not due to the increase of viscosity. Compared with silicon oil, C_8mimPF_6 can ionize in solution, results in variation of surface charger, which in turn may affect interfacial activity; hence droplet size. These factors may be more important and will be evaluated further in the following section.

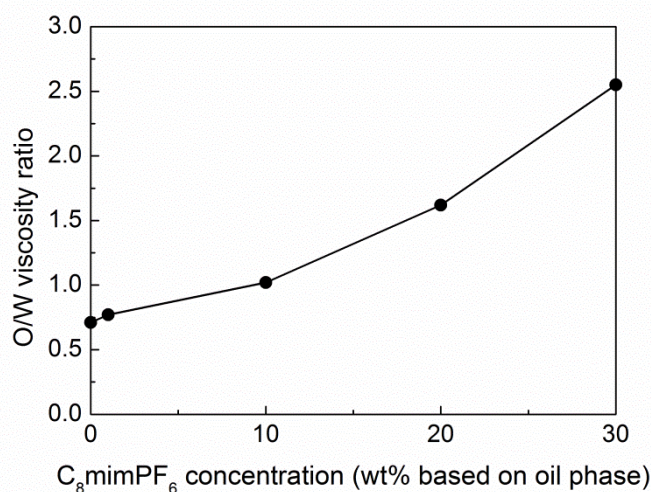


Fig.3.12 Variation of viscosity ratio between oil phase and water phase as a function of C_8mimPF_6 concentration

Interfacial tensions between oil and water at different concentrations of C_8mimPF_6 in oil phase were measured. Fig.3.13 shows interfacial tensions for

different concentrations of SDSO in water phase as a function of C_8mimPF_6 concentration in the oil phase ranging from 0 wt%, 0.1 wt%, 0.5 wt%, 1 wt%, 10 wt% to 20 wt%. The changes of interfacial tensions for different concentrations of SDSO in water phase, i.e. 0 mM, 0.1 mM, and 30 mM, are compared. It is interesting to note that in the absence of surfactant SDSO in water phase, the interfacial tension decreases sharply from $14.82 \text{ mN}\cdot\text{m}^{-1}$ to $11.46 \text{ mN}\cdot\text{m}^{-1}$ as the concentration of C_8mimPF_6 increases up to 10 wt%. Similar trends are found for the water phase containing 0.1 mM SDSO and 30 mM SDSO. Especially for water phase containing 30mM SDSO, the interfacial tension changed from $3.94 \text{ mN}\cdot\text{m}^{-1}$ to $0.31 \text{ mN}\cdot\text{m}^{-1}$ when concentration of C_8mimPF_6 increased from 0 wt% to 1 wt%. The sharp decrease in interfacial tension explained the reduction of droplet size at 1 wt% compared to 0 wt% C_8mimPF_6 showed in Fig.3.11.

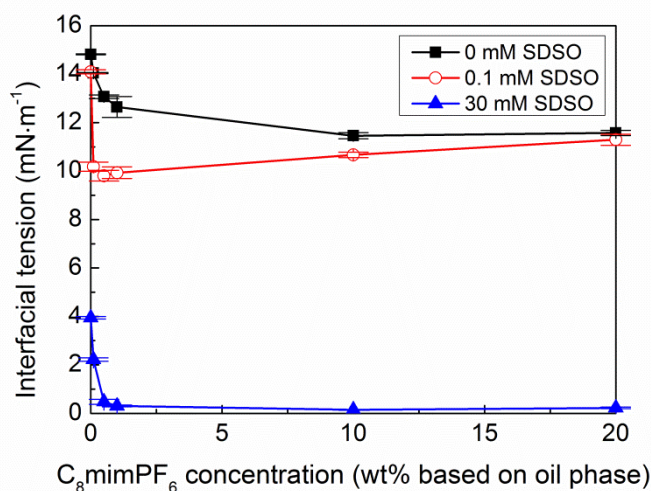


Fig.3.13 Variation of interfacial tensions as a function of C_8mimPF_6 concentration at 0, 0.1, 30 mM SDSO in water phase

To some extent, C_8mimPF_6 might act as surfactant, hence when bringing oil phase and water phase into contacting point, the C_8mimPF_6 molecules might accumulate at the interface between water phase and oil phase, thus reduce the

interfacial tension. The adsorption process might continue until $C_8\text{mimPF}_6$ adsorbed on the interface form a saturated monolayer, then no more reduction on interfacial tension in the excess of $C_8\text{mimPF}_6$. From Fig.3.13, such critical point occurs circa 1 wt% of $C_8\text{mimPF}_6$. A similar phenomenon has been observed by Hezave et al. who studied the effect of 1-dodecyl-3-methylimidazolium chloride ($C_{12}\text{mimCl}$) on the interfacial tension between water and crude oil phase.(Hezave et al., 2013) However, unlike what we have studied, $C_{12}\text{mimCl}$ is hydrophilic and dissolves in the water phase. The interfacial tension decreased from $39.98 \text{ mN}\cdot\text{m}^{-1}$ to $6.84 \text{ mN}\cdot\text{m}^{-1}$ when $C_{12}\text{mimCl}$ concentration increased from 0 ppm to 5000 ppm. Fitchett et al. studied the change of interfacial tension between water phase and pure RTILs phase for different type of RTILs, i.e. 1-octyl-3-methylimidazolium bis(perfluoromethylsulfonyl)imide ($C_8\text{mimBMSI}$) and 1-dodecyl-3-methylimidazolium bis(perfluoromethylsulfonyl)imide ($C_{12}\text{mimBMSI}$).(Fitchett et al., 2005) They found that the interfacial tension reduced from $11.7\text{mN}\cdot\text{m}^{-1}$ to $10.4 \text{ mN}\cdot\text{m}^{-1}$ when RTILs changed from $C_8\text{mimBMSI}$ into $C_{12}\text{mimBMSI}$. This suggested the dependence of interfacial tension on the cation chain length. The results reported in literatures, together with our result, indicate that cations of RTILs may have certain surface activity function. Such interfacial activity for oil and water can be enhanced as carbon chain length increases.

Fig.3.13 also shows that in the absence of $C_8\text{mimPF}_6$, as SDSO concentration increases from 0 mM to 0.1 mM, there is a limited change on the interfacial tension, e.g. decreases slightly from $14.82 \text{ mN}\cdot\text{m}^{-1}$ to $14.09 \text{ mN}\cdot\text{m}^{-1}$. However, adding just 0.1 wt% $C_8\text{mimPF}_6$ in the oil phase, the interfacial tension is dramatically reduced from $14.04 \text{ mN}\cdot\text{m}^{-1}$ to $10.18 \text{ mN}\cdot\text{m}^{-1}$ as the surfactant concentration increases from 0 mM to 0.1 mM. This suggested that there is strong interaction between SDSO and $C_8\text{mimPF}_6$ which further reduced their interfacial tension. The main reason might be

attributed into two aspects. Firstly, because the imidazolium moiety of C_8mimPF_6 cation and the sulfonic acid moiety of SDSO anion are hydrophilic, the carbon chains in both C_8mimPF_6 cation and SDSO anion are hydrophobic, both cations of C_8mimPF_6 and anions of SDSO accumulated at the interface, with hydrophilic moieties towards the aqueous side and carbon chains towards oil side hence stabilised the interface between oil and water phase. Secondly, there might be an electrostatic attraction between the positively charged imidazolium moiety in C_8mimPF_6 cations and the negatively charged sulfonic acid moiety in SDSO anions, which could result in a tighter space alignment at the interface to further stabilise the interface. These two joined effects contribute to the significant decrease in the interfacial tension when the concentration of SDSO in water phase increases from 0 to 0.1 mM in the presence of C_8mimPF_6 . Similar synergistic effect between anionic surfactants and imidazolium cations of C_8mimPF_6 has been reported in vesicle and micelles formation. (Yuan et al., 2010, Pal and Chaudhary, 2013)

The strong interaction between C_8mimPF_6 and surfactant SDSO mentioned above only occurred at lower concentration of C_8mimPF_6 . For a fixed concentration of SDSO (30 mM), an increase of C_8mimPF_6 concentration from 0.5 wt% to 20 wt% causes almost no change on interfacial tension. While at 0.1 mM concentration of SDSO, the interfacial tension even increases. This might be explained by the phenomenon that micelles composed of surfactant and C_4mimPF_6 in water phase might form and grow when hydrophobic C_4mimPF_6 dissolved in water phase. (Behera and Pandey, 2007) In our case, because C_8mimPF_6 partially dissolved in water ($2.26 \text{ g}\cdot\text{L}^{-1}$ at $25 \text{ }^\circ\text{C}$), (Fortunato et al., 2004) as the concentration of C_8mimPF_6 in oil phase increases, thus more C_8mimPF_6 could be dissolved into water phase. In this case, part of C_8min^+ cations might interact with SDSO anions being adsorbed on the oil/water

interface. As a result, the SDSO may be desorbed from oil/water interface to participate in the formation of micelles in water phase, to increase the interfacial tension. In order to confirm this hypothesis, further investigations are needed.

3.3.1.2 Factors affecting stability of miniemulsion

3.3.1.2.1 Effect of surfactant type on stability

The choice of surfactant has great influence on making a stable miniemulsion. A useful parameter to determine the suitability of surfactant is the Hydrophile-lipophile balance (HLB) value proposed by Griffin.(Griffin, 1949) If the HLB value of the surfactant used fits the HLB value of the required oil phase, the produced droplets with the surfactant would be stable. In colloidal science, HLB values ranging from 8 to 18 would favor the formation of O/W emulsion.(Berg, 2010) In this study, two types of anionic surfactants with the HLB values in the range for O/W emulsion were chosen: SDSO (HLB=12.3 obtained by calculation) and SDBS (HLB=10.6).(Housaindokht and Nakhaei Pour, 2012) A widely used anionic surfactant, SDS, was also chosen even though its HLB value is 40, which is out of the normal range for O/W emulsion.(Housaindokht and Nakhaei Pour, 2012) The surfactant concentration in water phase was kept at 30 mM (W-sur-1, W-sur-2, W-sur-3) and the oil phase contained 10 wt% C₈mimPF₆, 85 wt% MMA and 5 wt% HD (O-6).

It is known that the instability of droplets in miniemulsion is mainly caused by coalescence and Ostwald-ripening.(Schork et al., 2005) Coalescence is the process that two droplets collide with each other to form one bigger droplet. Ostwald-ripening is the process that monomers diffuse from smaller droplets to larger ones due to the higher chemical potential of smaller ones. Both cases lead to an increase in droplets

size, and ultimately macro-phase separation into oil phase occurs due to the gravitational force. The instability process will be accelerated via centrifugation. Thus the oil phase may be separated within hours rather than days or weeks of storage.(Casey, 2009) Centrifugation method was employed to investigate the instability of miniemulsion. The amount of oil phase appearing on the top layer is a good indication for the tendency of instability. The larger the oil phase weight, the more instable the miniemulsion will be.

Table.3.4 shows the influence of surfactant types on oil phase weight of miniemulsions after centrifugation at different concentrations (0 wt%, 10 wt% and 20 wt%) of C_8mimPF_6 . Without C_8mimPF_6 , SDBS has the least oil phase weight whilst in the presence of C_8mimPF_6 ; SDSO has the least oil phase weight compared with other two miniemulsions stabilised by SDS or SDBS. Since our formula developed is aiming to use RTILs to reduce glass transition temperature, T_g , which is one of the key properties in coating products. It is clear SDSO, which offers better performance on stability in the presence of RTILs would be a more suitable surfactant among the three surfactants.

It is interesting to note that 10 wt% C_8mimPF_6 has the lowest oil phase compared with other two (0 wt% C_8mimPF_6 , 20 wt% C_8mimPF_6) in the stabilisation of SDSO. It will be explained in the following content. In this study, Ostwald-ripening was well prevented by co-stabiliser, HD, thus coalescence was the main reason leading to the increase in droplet size.(Kong et al., 2015) Because the interfacial tension of 0 wt% C_8mimPF_6 ($3.94 \text{ mN}\cdot\text{m}^{-1}$) was much higher than 10 wt% C_8mimPF_6 ($0.15 \text{ mN}\cdot\text{m}^{-1}$), such a reduction on interfacial tension represented the additional adsorption of surfactant on the surface of droplet, and hence preventing

droplet from coalescence. In this case, droplets in 10 wt% C₈mimPF₆ miniemulsion were less likely to collide into bigger ones which would lead to appearance of oil phase due to the vertical movement of bigger droplets. This explained why the miniemulsion with 10 wt% concentration of C₈mimPF₆ had less oil phase than the 0 wt% miniemulsion. As for 20 wt% C₈mimPF₆, though its interfacial tension (0.22 mN·m⁻¹) was close to 10 wt% C₈mimPF₆, the absolute zeta potential of 20 wt% C₈mimPF₆ (13.8 mV) was much smaller than 10 wt% C₈mimPF₆ (32.3 mV). When the absolute zeta potential is low, it means the repulsion between droplets cannot prevent collide, hence the droplets in dispersion will coalesce into bigger one. The increase in droplet size of 20 wt% C₈mimPF₆ aggravated the vertical movement of droplets, leading to the appearance of oil phase.

Table.3.4 Mass ratio of separated oil phase with miniemulsion containing different concentrations of C₈mimPF₆ and surfactants

Surfactant type	Mass ratio of separated oil phase with miniemulsion (%)		
	0 wt% C ₈ mimPF ₆	10 wt% C ₈ mimPF ₆	20 wt% C ₈ mimPF ₆
SDBS	0.11±0.03	4.24±0.12	10.71±0.31
SDSO	1.69±0.09	0.66±0.12	1.11±0.09
SDS	0.87±0.11	5.34±0.15	6.85±0.10

The instability of miniemulsion was also studied by measuring the average mean droplet size, D_{3/2} at different storage time for various miniemulsions for fixed concentration of C₈mimPF₆ (10 wt%). Fig.3.14 shows variation of droplet sizes as a function of time for miniemulsions stabilised with different surfactants upon aging at 20 °C. Droplet size of miniemulsion in the stabilisation of SDS increases at a rapid rate, especially after 72 h storage. The miniemulsion stabilised by SDBS increases slightly from the initial 308 nm to 364 nm after 288 h, while the miniemulsion stabilised by SDSO, the increase of droplet size is minimum from initial 235 nm to

272 nm after 288 h. The increase of droplet size with aging time gives an intuitive judgment of instability of miniemulsion. Based on Fig.3.14, the stabilities of miniemulsions from high to low were ranked as: miniemulsion SDSO>miniemulsion SDBS>miniemulsion SDS. The result shows consistency with the result of centrifugation (Table.3.4). The miniemulsion containing SDSO gave smaller droplet size with better stability. Thus SDSO was identified as the most suitable surfactant for stabilising oil phase containing C₈mimPF₆.

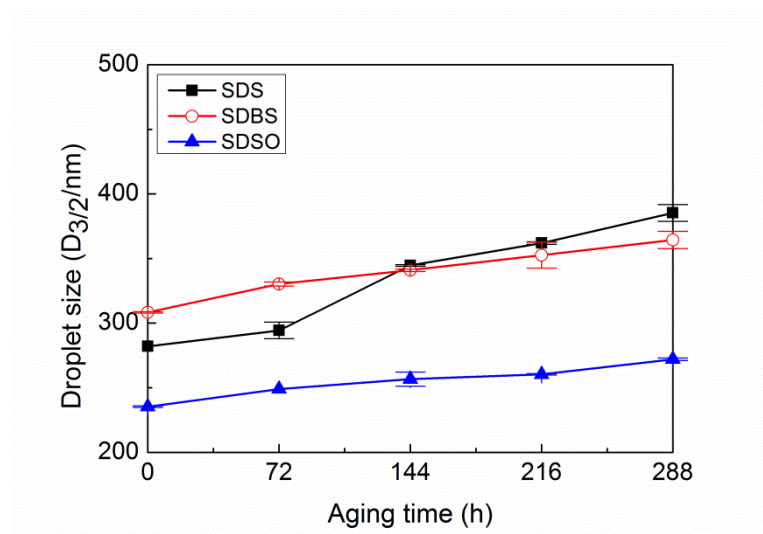


Fig.3.14 Variation of droplet sizes as a function of time for miniemulsions containing 10 wt% C₈mimPF₆ stabilised with different surfactants upon aging at 20°C

In this work, to prevent Ostwald-ripening in a relatively short time, a common type of co-stabiliser, HD was added in oil phase. Assuming Ostwald-ripening did occur, by making an initial calculation on the Ostwald-ripening rate based on Lifshitz-Slyozov-Wagner (LSW) theory:

$$w = \frac{d(d_m^3)}{d(t)} = \frac{8D\sigma CV_m}{9RT} \quad \text{Eq.3.1}$$

where w is the Ostwald-ripening rate for single component species (cm³·s⁻¹), d_m is the average oil droplet diameter (cm), t is the storage time (s), D is the diffusion

coefficient of oil molecules in water ($\text{cm}^2\cdot\text{s}^{-1}$), σ is the interfacial tension at the oil-water interface ($\text{mN}\cdot\text{m}^{-1}$), C is the water solubility of the bulk oil (mLmL^{-1}), V_m is the molar volume of oil ($\text{cm}^3\cdot\text{mol}^{-1}$), T is the absolute temperature (K), and R is the gas constant. (Tauer, 2005) In the absence of HD, the Ostwald-ripening rate of MMA, w , was estimated as $3.97\cdot 10^{-14} \text{ cm}^3\cdot\text{s}^{-1}$. (Tauer, 2005) Rearrange Eq.3.1, the diameter of droplet size at time t may be expressed as:

$$d_m(t) = \sqrt[3]{wt + (d_m(0))^3} \quad \text{Eq.3.2}$$

, taking the initial droplet size $d_m(0)$ as 235.3 nm which was the initial size of miniemulsion containing SDSO shown in Fig.3.14. The new droplet size after 1 minute $d_m(60)$ could be estimated as 1338 nm. This is about 5 times larger than the one obtained after 12 days storage in our measurement shown in Fig.3.14. Clearly, Ostwald-ripening rate theory does not fit our experimental results which further proved that presence of HD did prevent the Ostwald-ripening. Thus the increase in droplet size of miniemulsions obtained in this work may be mainly caused by coalescence as the droplet size increased.

3.3.1.2.2 Effect of $C_8\text{mimPF}_6$ concentration on stability

In order to evaluate the role of $C_8\text{mimPF}_6$ on stability of miniemulsion during storage, oil phase containing different concentrations of $C_8\text{mimPF}_6$ ranging from 0 wt% (O-1), 1 wt% (O-4), 5 wt% (O-5), 10 wt% (O-6), 20 wt% (O-8) to 30 wt% (O-9) based on oil phase were prepared, and surfactant SDSO with fixed concentration in water phase 30 mM (W-sur-3) was chosen. After homogenisation by sonicator with an input power of 95 W for 6 min, miniemulsions were stored at 20 °C for 288 h. Results were listed in Table.3.5.

Table.3.5 Droplet sizes of miniemulsions containing different concentrations of C₈mimPF₆ before and after 288 h storage

C ₈ mimPF ₆ (wt%)	Initial droplet size (nm)	Droplet size after storage (nm)	Increase rate of droplet size (%)	Creaming	Sedimentation
0	245	268	9.4	No	No
1	228	233	2.2		
5	228	236	3.5		
10	235	272	15.7		
20	270	325	20.4		
30	280	411	46.8		

It was observed that all miniemulsions were visually stable, without creaming or sedimentation occurred after 288 h storage. Creaming or sedimentation is normally induced by gravity force. According to Stoke's law, migration rate of droplets induced by gravity force is in proportion to the square of droplet diameter. For miniemulsion with nanoscale droplet sizes, the migration rate of droplets could be less apparent, hence inhibiting creaming or sedimentation. (Bazylińska et al., 2014)

Even though miniemulsions were visually stable, after 288 hours storage, droplet sizes (shown in table.3.5) were found being increased, especially at concentration of C₈mimPF₆ above 10 wt%. The rate of increase on droplet size became more pronounced up to 46.8% compared to the lower one 2.2% obtained at 1 wt% of C₈mimPF₆. Such an increase in droplet sizes might be attributed to the effect of coalescence and Ostwald ripening, which could lead to the instability of miniemulsion. It is interesting to note, such instability of miniemulsion seemed independent of initial droplet size. Table.3.5 showed that the initial droplet size for miniemulsion at 10 wt% C₈mimPF₆ was 235 nm, which was smaller than the one obtained at 0 wt% C₈mimPF₆, 245 nm. The rates of increase in droplet size for miniemulsion at 10 wt% C₈mimPF₆ was faster, 272 nm, while for miniemulsion at 0

wt% C_8mimPF_6 , the droplet size after storage was 268 nm. Such unusual change on droplet size in the presence of C_8mimPF_6 might be due to the interaction between C_8mimPF_6 and SDSO at droplet interface. The underneath mechanism were explained in the following session. To have a full picture on stability of droplet during 288 h storage time, droplet sizes of miniemulsions containing different concentrations of C_8mimPF_6 were continually measured at 72, 144, 216 and 288 hours. Results were shown in Fig.3.15.

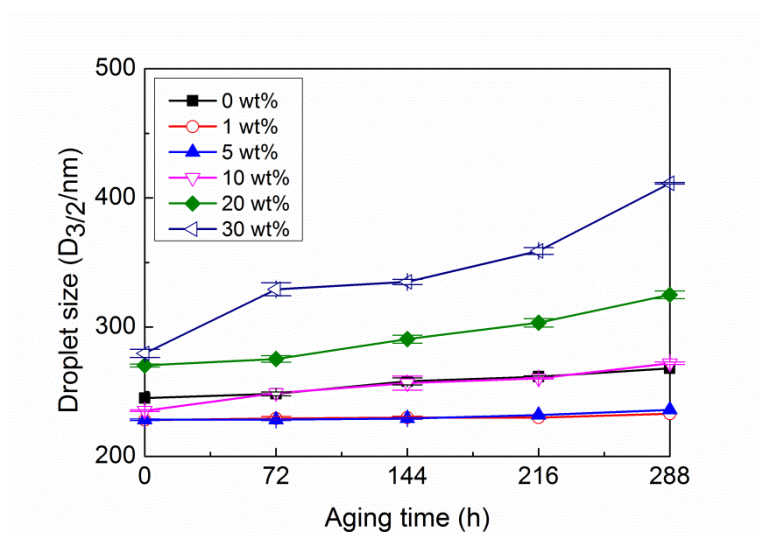


Fig.3.15 Variation of droplet sizes as a function of time for miniemulsions containing different C_8mimPF_6 concentrations at 20°C

It was found that the increase of droplets for miniemulsions containing 10 wt%, 20 wt%, and 30 wt% C_8mimPF_6 were much rapid compared with those containing 0 wt%, 1 wt%, and 5 wt% C_8mimPF_6 . This suggested that above certain concentration of C_8mimPF_6 , *e.g.* at 10 wt%, more C_8mimPF_6 in oil phase had a negative effect on the stability of miniemulsion.

To have a better understand of miniemulsions at initial stage and after 288 h storage, droplet size distributions at 0 h and 288 h storage for miniemulsions containing 0 wt%, 1 wt%, 5 wt%, 10 wt%, 20 wt%, and 30 wt% of C_8mimPF_6 are

illustrated (Fig.3.16). It is found, for miniemulsion without C_8mimPF_6 , the droplet distribution peak moves towards larger size slightly. No obvious changes on distributions could be detected for miniemulsions with concentrations of C_8mimPF_6 at 1 wt% and 5wt% after 288 h storage. However, further increase the of C_8mimPF_6 , droplet distribution exhibits bimodal distributions with larger size appearing after 288 h storage. The results are consistent with the mean droplet size measured at the same concentration ranges of C_8mimPF_6 shown in Fig.3.15. Clearly, above a critical concentration, *e.g.* at 10 wt%, further increase in C_8mimPF_6 concentration accelerated the movement of droplets towards larger size, indicating the instability of miniemulsion.

The instability of miniemulsion at higher concentration of C_8mimPF_6 might be due to two factors: coalescence and Ostwald ripening. Based on our previous study, Ostwald ripening could be well inhibited in the presence of co-stabiliser, HD (Kong et al., 2015). Thus the increase of droplet size observed in Fig.3.15 might be attributed to the coalescence effect. Coalescence could take place into two processes: collision of droplets and drainage of the liquid between the droplets to form one large droplets (Asua, 2002). Collision was mainly due to Brownian motion and van der Waals force (Bazylińska et al., 2014). If droplets were stabilised by ionic surfactants, the induced electrostatic repulsion due to oriented adsorption of the ionic surfactants at oil/water interface could prevent the collision of droplets (DOANE et al., 2011). Thus the coalescence rate during storage of miniemulsions was strongly dependent on interfacial activity between water and oil phase (Berg, 2010).

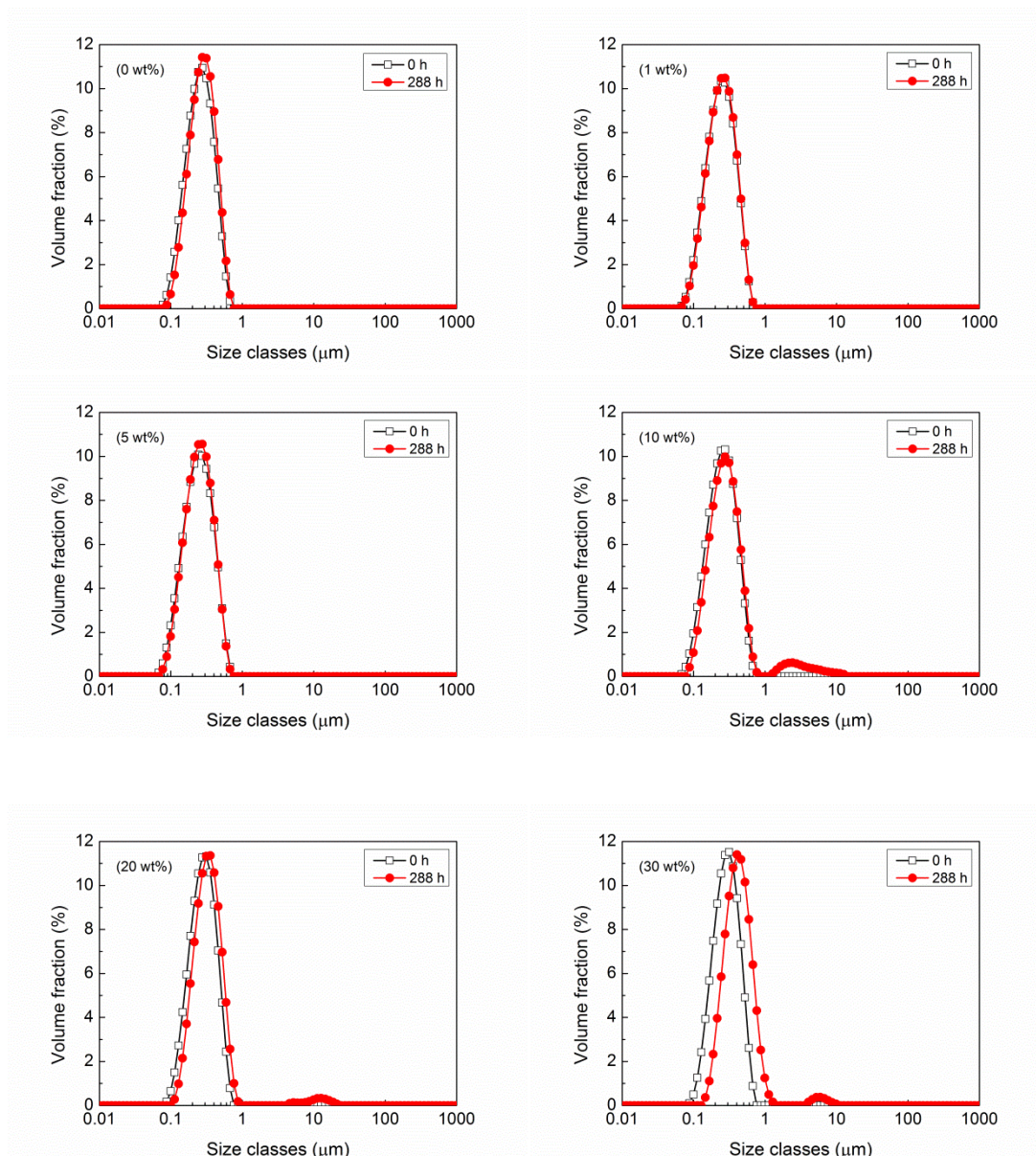


Fig.3.16 Droplet size distribution at 0 h and 288 h aging time for miniemulsions containing different concentrations of C_8mimPF_6 .

The interfacial activity could be characterised by measuring interfacial tensions between water phase and oil phase containing different concentrations of C_8mimPF_6 . Result of interfacial tension was shown in Fig.3.13. It can be seen that the interfacial tension decreased significantly from $3.94 \text{ mN}\cdot\text{m}^{-1}$ to $0.31 \text{ mN}\cdot\text{m}^{-1}$ with the concentration of C_8mimPF_6 increased from 0 wt% to 1 wt%. Such a reduction on interfacial tension confirmed the adsorption of surfactant on the surface of droplet,

and hence preventing droplet from coalescence. This partially explained why miniemulsion with 1 wt% concentration of C_8mimPF_6 had better stability during storage than 0 wt% miniemulsion as Fig.3.15 showed. However, further increase in the concentration of C_8mimPF_6 , *i.e.* above 10 wt%, interfacial tension became independent of change of the concentration of C_8mimPF_6 though at the same range of concentration of C_8mimPF_6 , the increase of droplet size became more pronounced indicating the instability of droplets. This suggested that interfacial tension was no longer a suitable property for characterising the interfacial activity in miniemulsion we studied. Consider the conductivity of C_8mimPF_6 , surface charge could be a more sensible parameter for evaluating interfacial activity of the system we studied.

The surface charge could be evaluated using zeta potential, which is a measure for the degree of electrostatic repulsion between adjacent droplets/particles. The larger the zeta potential, the higher the electrostatic expulsion, hence results in more stable droplets. Thus the stability of colloidal dispersion being electrically charged can be related to its zeta potential. Positive or negative zeta potential indicating the dispersion is positively charged or negatively charged. Thus the absolute zeta potential would matter the stability. When the absolute zeta potential is low, it means the repulsion between droplets cannot prevent collide, hence the droplets in dispersion will coalesce and flocculate. The droplets with higher zeta potential indicate that the electric repulsions between droplets are stronger hence can effectively prevent coalescence. Normally, when the absolute zeta potential is higher than 30 mV, droplets in dispersion are in a stable state.(Sonavane et al., 2008)

With the above theory as a guideline, a series of measurements on zeta potential was carried out for miniemulsions prepared at different concentrations of C_8mimPF_6 ,

ranging from 0 wt%, 0.1 wt%, 0.5 wt%, 1 wt%, 5 wt%, 10 wt%, 15 wt%, 20 wt%, and 30 wt%. Results are shown in Fig.3.17. Negative zeta potentials are observed for all the miniemulsions which suggested that droplets are negatively charged. The absolute zeta potential increases from 35.6 mV to 45.8 mV with an increase of C_8mimPF_6 concentration from 0 wt% to 1 wt%. The absolute zeta potential then decreases from 45.8 mV to 7.8 mV as further increasing the C_8mimPF_6 concentration up to 30 wt%. This result is quite different to the tendency on interfacial tension, which is almost unchanged above 1 wt% C_8mimPF_6 shown in Fig.3.13. For miniemulsions containing C_8mimPF_6 at 0 wt% and 10 wt%, the values are all larger than 30 mV. This indicates that the droplet sizes were relatively stable in this region. For miniemulsions containing C_8mimPF_6 at 20 wt%, and 30 wt%, the absolute zeta potential are less than 30 mV, which indicating that droplets were unstable in this region. Such observations are consistent with the droplet stability results in shown in Fig.3.15, which further suggest that variation of surface charge on interface O/W may be the main reason causing the instability of droplet at higher concentration of C_8mimPF_6 . In this case, the static interfacial tension value will not be suitable on reflecting interfacial activity.

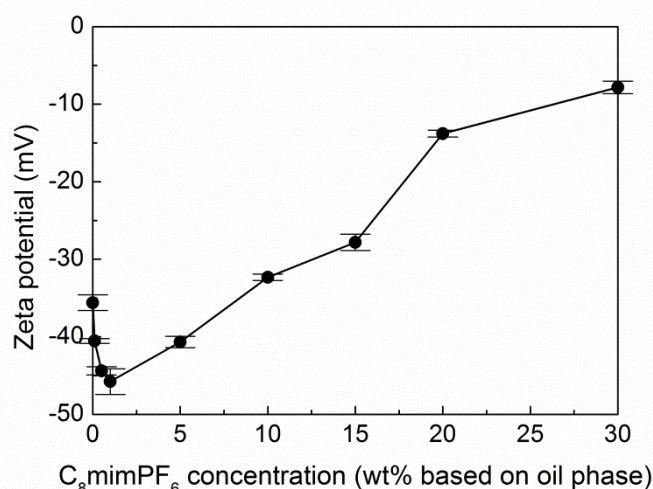


Fig.3.17 Variation of zeta potentials of droplet sizes as a function of C_8mimPF_6 concentration

The unique zeta potential behaviour mentioned above might be best explained by Chaumont et al. who studied the interface between water and C_8mimPF_6 by a molecular dynamics simulation.(Chaumont et al., 2005) According to the simulation result, PF_6^- anions were more hydrophilic as compared with C_8mim^+ cations, hence more PF_6^- anions dispersed in the water phase than C_8mim^+ cations. Thus a small excess of C_8mim^+ cations was kept in the C_8mimPF_6 phase. C_8mim^+ cations might accumulate at the interface and were ordered with their imidazolium moiety towards the water phase and carbon chain towards oil phase. The excessive C_8mim^+ cations accumulated at the O/W interface caused the interface being positively charged. This positively charged interface was experimentally proven by Fitchett et al. who found that the surface charge at the $C_{10}mimBMSI$ /water interface were positive and had value up to $27 \mu C \cdot cm^{-2}$.(Fitchett et al., 2005) Based on the points mentioned above, we can deduce that in this study, in the presence of C_8mimPF_6 , the droplets would be positively charged due to adsorption of excessive C_8mim^+ cations on the droplet interface regardless the existence of surfactants. On the other hand, in the presence of SDSO anion in the water phase, the droplet would be negatively charged due to the adsorption of the SDSO anion on the interface. As Fig.3.17 shows that in the absence of C_8mimPF_6 , it is no surprise that a large negative zeta potential has been found. As compared with droplets of 0 wt% C_8mimPF_6 , when adding a small amount of C_8mimPF_6 , more SDSO were adsorbed on the interface due to tightened space alignment at interface, as explained in the early section. Thus the interface became more negatively charged causing an increase on the absolute zeta potential. Such interface charge would continuously increase until the adsorption of SDSO at interface was saturated. The point at 1 wt% C_8mimPF_6 (Fig.3.13) is a good example. Above this saturation point, as a further increase in C_8mimPF_6 concentration, e.g. 10

wt%, 20 wt% and 30 wt%, no more SDSO would adsorb on the interface, but the amount of C_8mimPF_6 dissolved in water phase might increase, hence more excessive C_8mim^+ cations would be kept in the oil phase as mentioned above and adsorbed on water/oil interface to neutralize the negative interface charge, thus decreased the absolute zeta potential. A similar phenomenon that C_8mimPF_6 affected the zeta potential of micelles has also been reported by Rai et al. (Rai et al., 2010) They found that the solubility of C_4mimPF_6 has been enhanced due to the micelles of SDBS in water phase and the absolute zeta potential of negatively charged micelles decreased as the increase of C_4mimPF_6 concentration in water phase. They claimed that such change on zeta potential was caused by the interaction of anionic surfactant with C_4mim^+ cations.

3.3.1.2.3 Effect of temperature on stability

In order to evaluate the role of temperature, oil phase containing 10 wt% C_8mimPF_6 (O-6) was prepared, and surfactant SDSO with fixed concentration in water phase 30 mM (W-sur-3) was chosen. After homogenisation, miniemulsion was stored at different temperature ranging from 30 °C to 60 °C for 240 min.

Fig.3.18 shows variation of droplet sizes as a function of storage time for miniemulsion containing 10 wt% C_8mimPF_6 at different temperatures. Because phase separation took place within 30 min when stored at 60 °C, only variation of droplet sizes at 30 °C, 40 °C, and 50 °C are shown in Fig.3.18. It is observed that the size of droplet in miniemulsion increased by 40% after being stored at 50 °C for 240 min, whilst at 40 °C and 30 °C, there was little change on droplet size. A sharp increase in size at 50°C was probably attributed to the high frequency of droplet/particle

movement at 50 °C, hence the opportunity of droplet/particle collision would increase which induced droplet/particle coalescence.

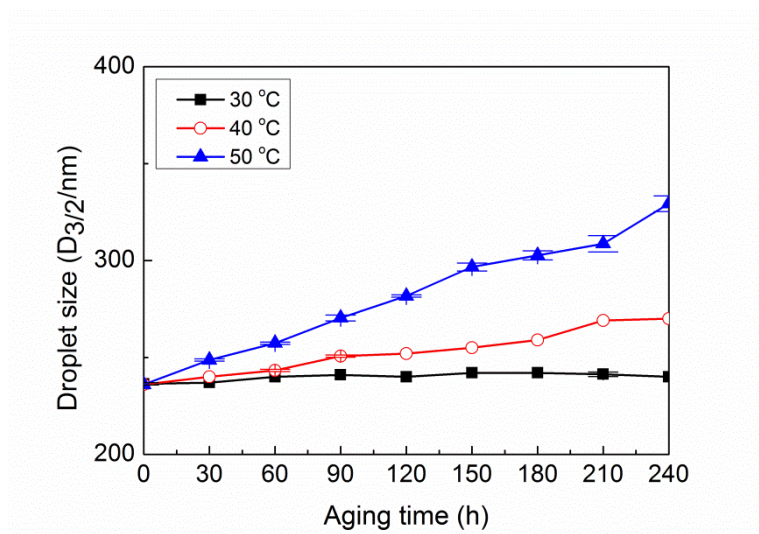


Fig.3.18 Variation of droplet sizes as a function of storage time for miniemulsion containing 10 wt% C₈mimPF₆ at different temperatures.

3.3.2 Miniemulsion stabilised by silica nanoparticles

In order to overcome the lacks in gloss and water resistance of film caused by surfactant residual, silica nanoparticle, as an alternative to conventional surfactant, was employed to stabilise miniemulsion containing C₈mimPF₆. The effects of energy input, pH of water phase, silica nanoparticle concentration, and C₈mimPF₆ concentration on initial droplet size, and the effects of pH of water phase, C₈mimPF₆ concentration, and temperature on stability of miniemulsion were investigated.

3.3.2.1 Factors affecting initial droplet size of miniemulsion

3.3.2.1.1 Effect of energy input on initial droplet size

In order to evaluate the effect of energy input on initial droplet size, the formula for preparing miniemulsion was fixed. In this formula, oil phase contained 10 wt%

C₈mimPF₆ (O-6), and water phase contained 50 g/l silica nanoparticle with a pH of 3 (W-sil-3). High speed disperser was chosen as the homogeniser. Two factors related to energy input, stirring speed and input duration, were studied.

Fig.3.19 shows the initial droplet size of miniemulsion as a function of input duration with different stirring speed ranging from 16000 rpm to 24000 rpm. At a fixed input duration, with the increase in stirring speed, *i.e.* from 16000 rpm to 20000 rpm, there is a sharp decline on droplet size of the miniemulsion. Continuing increase stirring speed up to 24000 rpm, trend of decline on droplet size becomes unapparent. On the other hand, when the input power is fixed, *e.g.* 20000 rpm, with the increase in input duration, *i.e.* from 1 min to 8 min, there is a sharp decline on droplet size of the miniemulsion, from 644 nm to 436 nm. Continuing increase input duration up to 10 min, the trend of decline on droplet size becomes negligible. It can be seen that upon a certain input duration, further increase in input duration has less effect on reduction of droplet size.

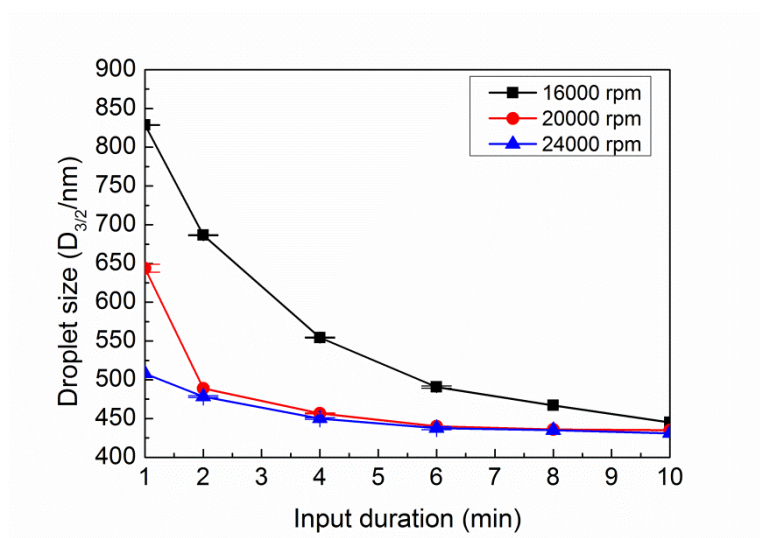


Fig.3.19 Initial droplet size of miniemulsion as a function of input duration with different stirring speed ranging from 16000 rpm to 24000 rpm.

Based on above results, the operation condition of high speed disperser for preparing miniemulsion is to set an input power of 20000 rpm with an input duration of 8 min. Such operation condition will be employed in the following study.

3.3.2.1.2 Effect of pH of water phase on initial droplet size

The pH of water phase would directly affect surface charge (zeta potential) of silica nanoparticle dispersed in it, which in turn has an influence on emulsifying effect of silica nanoparticle. In order to study the effect of pH of water phase, water phases containing 50 g/l silica nanoparticles with pH ranging from 3 (W-sil-3), 5 (W-sil-6), 7 (W-sil-7), 9 (W-sil-8) to 11 (W-sil-9) were prepared. Oil phase contained 10 wt% C₈mimPF₆, 85 wt% MMA and 5 wt% HD (O-6). The reason why 10 wt% was chosen was explained in 3.3.1.1.1. Miniemulsions were prepared by high speed disperser at 20000 rpm for 8 min.

Fig.3.20 shows variation in droplet sizes as a function of pH of water phase for miniemulsions stabilised with silica nanoparticles. It is found that the droplet size increases from 436 nm to 865 nm with the increase of pH from 3 to 7. Then there is a sharp increase in the droplet size from 865 nm to 3156 nm when pH continually increases to 11. It can be seen that the pH of water phase directly affected the initial droplet size of miniemulsion, and smaller size can be achieved at lower pH, *e.g.* 3.

The variation of initial droplet size of miniemulsion as a function of pH value of water phase maybe due to the fact that changing pH value would cause the change of zeta potential of silica nanoparticles dispersed in water phase. The difference in zeta potential of silica nanoparticles may affect their absorption on the surface of droplet, which in turn affected droplet size of miniemulsion. In order to prove this hypothesis, zeta potential of silica nanoparticles dispersed in water phase with different pH values

were determined. The result is shown in Fig.3.21. It is found that zeta potential of silica nanoparticles sharply decreased from -2.0 mV to -31.6 mV with the increase of pH from 3 to 7. Then this trend would fade down, with a slight decrease from -31.6 mV to 38.8 mV, as the pH of water phase continually increases to 11. When the pH of water phase is equal to 3, zeta potential value is found close to 0.

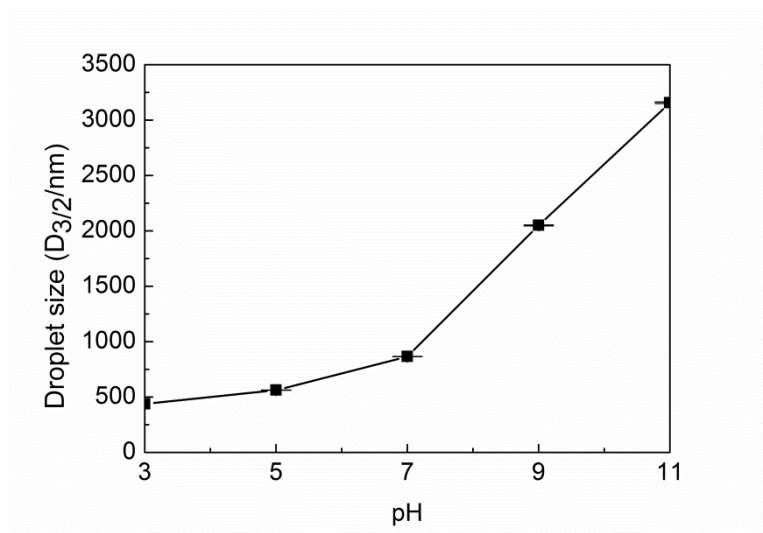


Fig.3.20 Variation in droplet sizes as a function of water phase pH for miniemulsions stabilised with silica nanoparticles

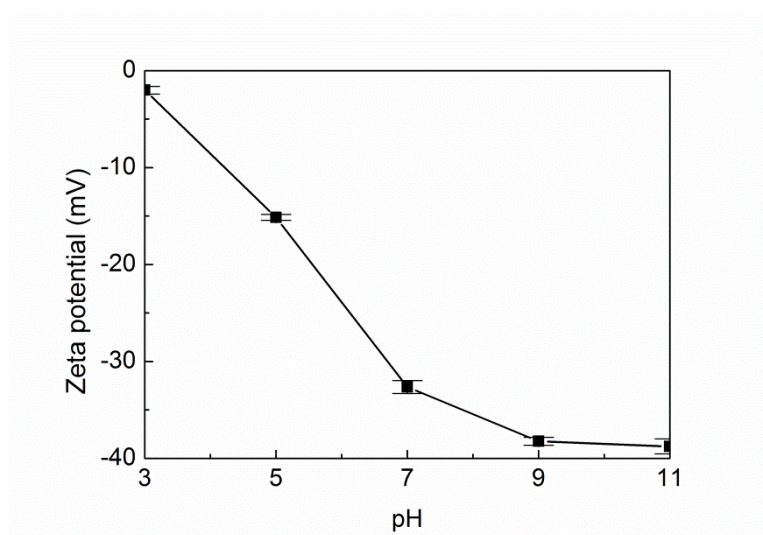


Fig.3.21 Variation in zeta potential of silica nanoparticles in water phase as a function of pH of water phase

The minimum zeta potential was found to be at pH equal to 3 means, the electrostatic repulsion between silica nanoparticles adsorbed on the surface of droplets was at minimum. This indicated that the adsorption of silica nanoparticles became easier due to the weak electrostatic repulsion. In this case, when large droplets were broken into smaller ones, silica nanoparticles might be easier to be adsorbed on the newly formed droplet surface, preventing the re-coalescence of smaller droplets. This may be the main reason that smaller droplets were obtained at pH=3 as compared to the one at other higher pH value. Similar observations were also reported by Köhler *et.al* who employed silica nanoparticle as Pickering emulsifier to stabilise corn oil in water emulsion. (Köhler et al., 2010)

3.3.2.1.3 Effect of silica nanoparticle concentration on initial droplet size

The concentration of emulsifier, *i.e.* silica nanoparticle, is another important parameter to determine the droplet size of miniemulsion. In order to study this effect, pH of water phase was maintained at 3, and concentration of silica nanoparticles in water phase was ranged from 10 g/l (W-sil-1), 30 g/l (W-sil-2), 50 g/l (W-sil-3), 70 g/l (W-sil-4) to 90 g/l (W-sil-5). Oil phase contained 10 wt% C₈mimPF₆, 85 wt% MMA and 5 wt% HD (O-6). Miniemulsions were prepared by high speed disperser at 20000 rpm for 8 min.

Fig.3.22 shows variation in droplet sizes as a function of silica nanoparticle concentration for miniemulsions containing 10 wt% C₈mimPF₆. It has been found that droplet size decreases sharply from 2000 nm to 490 nm with the increase in silica nanoparticle concentration from 10 g/l up to 50 g/l. Further increase in silica nanoparticle concentration from 50 g/l to 90 g/l would result in very little change in the droplet size. Such result was also observed by Maryam Kargar *et al.* who made

Pickering emulsions by a high speed disperser (Silver-son L4RT) in the stabilisation of modified starch (MS) (Kargar et al., 2012). When the concentration of MS (wt%) increased from 0.1% to 1%, droplet size dramatically decreased from 14 μm to 5 μm . However, droplet size fluctuated at 5 μm when the concentration of MS increased further to 2.5 %. Köhler *et al.* also found that, after homogenised by a high pressure homogeniser, the droplet size became independent of silica nanoparticle concentration once the concentration became sufficiently high.(Köhler et al., 2010) The independency of droplet size at higher Pickering emulsifier concentration was probably due to the dynamic equilibrium between maximum breakage of droplets obtained at a given energy input and the coalescence of droplets when excessive emulsifier was present.

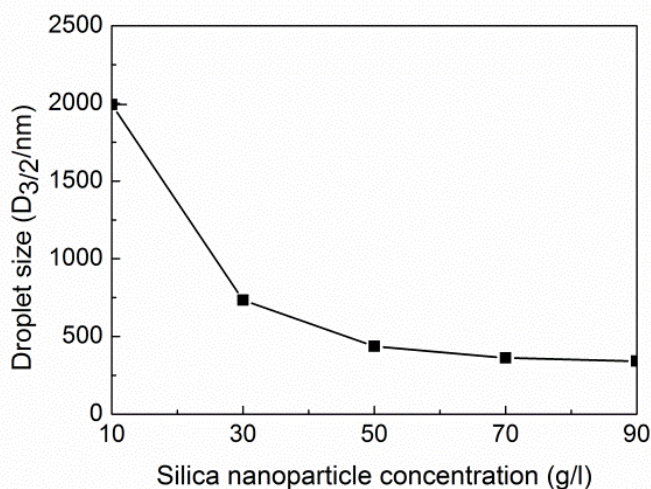


Fig.3.22 Variation in droplet sizes as a function of silica nanoparticle concentration for miniemulsions containing 10 wt% C_8mimPF_6 .

3.3.2.1.4 Effect of C_8mimPF_6 concentration on initial droplet size

Since early work indicated that C_8mimPF_6 concentration had a strong influence on the droplet size of miniemulsion when sodium dodecyl sulfonate (SDSO) was used as a surfactant, it would be helpful to evaluate such C_8mimPF_6 concentration effect on

droplets stabilised by silica particles. The pH of water phase was maintained at 3, and concentration of silica nanoparticles in water phase was fixed at 50 g/l (W-sil-3). Different concentrations of C_8mimPF_6 in oil phase ranged ranging from 0 wt% (O-1), 1 wt% (O-4), 5 wt% (O-5), 10 wt% (O-6), 20 wt% (O-8), to 30 wt% (O-9) were evaluated. Miniemulsions were prepared by high speed disperser at 20000 rpm for 8 min.

Fig.3.23 shows variation in droplet sizes as a function of C_8mimPF_6 concentration for miniemulsions stabilised by silica nanoparticles. It has been found that at lower concentration of C_8mimPF_6 , *i.e.* between 0 and 1 wt%, there is a sharp decline in the droplet size of miniemulsions, followed by an increase in the droplet size as the concentration of C_8mimPF_6 increases to 5wt%. It is interesting to note that beyond this point, droplet size of the miniemulsion became independent with further increase in the concentration of C_8mimPF_6 . Currently, silica nanoparticle concentration was fixed as 50 g/L. Studies on other silica nanoparticle concentrations, *e.g.* 30 g/L, 70 g/L should be carried out. This would be mentioned in further work.

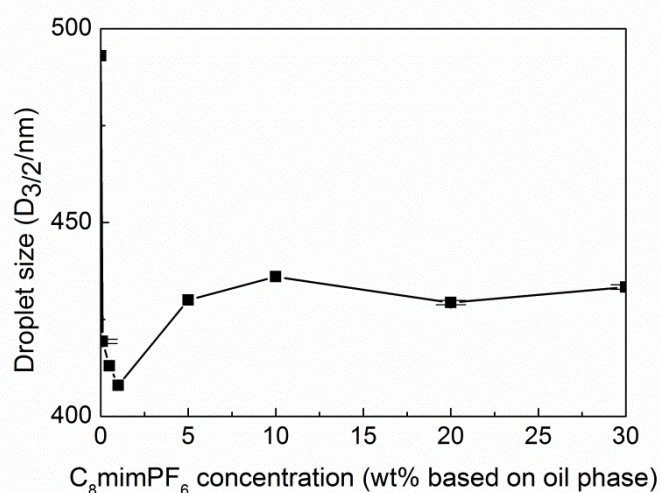


Fig.3.23 Variation in droplet sizes as a function of C_8mimPF_6 concentration for miniemulsions stabilised by silica nanoparticle

By the comparison between miniemulsion stabilised by surfactant and by silica nanoparticle, it can be seen that at lower concentration of C_8mimPF_6 , *i.e.* between 0 and 1 wt%, there are sharp declines on droplet size of miniemulsions, no matter surfactant or silica nanoparticle are used. Then the trends become different with the continuing increase in C_8mimPF_6 concentration. For miniemulsion stabilised by surfactant, droplet size trends to be stable until 5 wt%, whilst beyond this point, droplet size of the miniemulsion tended to increase as the concentration of C_8mimPF_6 increased. While for miniemulsion stabilised by silica nanoparticle, droplet size tends to increase until 5wt%; beyond this point, droplet size of the miniemulsion fluctuates at 430 nm. The same as miniemulsion stabilised by surfactant, we try to explain the trend of droplet size as a function of C_8mimPF_6 concentration from the following two aspects: oil/water phase viscosity ratio and interfacial tension.

The viscosity ratio between oil phase and water phase was calculated and plotted against the relevant C_8mimPF_6 concentration in oil phase as shown in Fig.3.24. It is observed that the viscosity ratio increases from 0.88 to 3.16 as the C_8mimPF_6 concentration increases from 0 to 30 wt%. The viscosity ratio is around 1 when C_8mimPF_6 concentration is 1 wt%, where the smallest droplet size was achieved. From the open literature, it was reported that in a simple shear field, with lower interfacial tension for oil and water phase, maximum energy transfer may be achieved at an oil/ water viscosity ratio around 1.(Nazarzadeh and Sajjadi, 2010, Karam and Bellinger, 1968). Thus the maximum efficiency in energy transfer maybe achieved at 1 wt% C_8mimPF_6 concentration resulting in a smaller droplet size. This is consistent to the one we have observed in miniemulsion stabilised by surfactant. However the continue increase on viscosity ratio above 1 wt% C_8mimPF_6 concentration is clearly inconsistent with the variation of droplet size at the same

liquid system. This suggests that viscosity is not the main parameter affecting the droplet size.

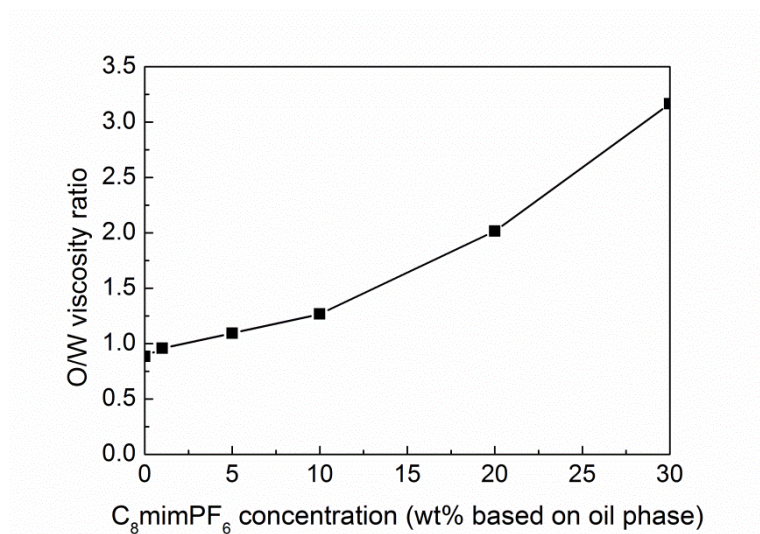


Fig.3.24 Variation in the viscosity ratio between oil phase and water phase as a function of $C_8\text{mimPF}_6$ concentration.

The interfacial property may be more important. The interfacial tensions between oil phases containing different concentrations of $C_8\text{mimPF}_6$ and water phases were measured. $C_8\text{mimPF}_6$ concentration in oil phase ranged from 0 wt%, 0.1 wt%, 0.5 wt%, 1wt%, 10 wt% to 20 wt%, and two different concentrations of silica nanoparticles in water phase, i.e. 0 g/l, and 50 g/l, are compared. The result is shown in Fig.3.25. It is interesting to note that in the absence of silica nanoparticles in water phase, interfacial tension decreases sharply from $14.82 \text{ mN}\cdot\text{m}^{-1}$ to $12.64 \text{ mN}\cdot\text{m}^{-1}$ with the increase of $C_8\text{mimPF}_6$ concentration from 0 to 1 wt%. Similar trends are found for water phase containing 50 g/l silica nanoparticle. Especially, for water phase containing 50 g/l silica nanoparticle, interfacial tension changes from $14.09 \text{ mN}\cdot\text{m}^{-1}$ to $11.88 \text{ mN}\cdot\text{m}^{-1}$ when the $C_8\text{mimPF}_6$ concentration increases from 0 wt% to 1 wt%. This explains the reduction of droplet size at 1 wt% compared to 0 wt% $C_8\text{mimPF}_6$ shown in Fig.3.23.

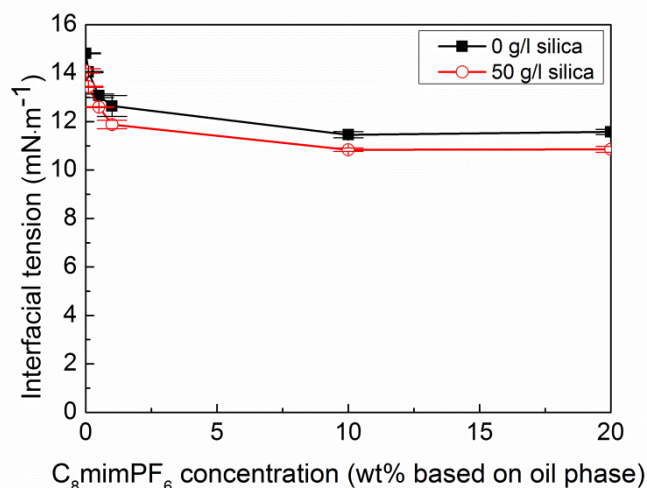


Fig.3.25 Variation in the interfacial tensions as a function of C₈mimPF₆ concentration at 0, 50 g/l silica nanoparticles in water phase.

To sum up, the sharp decline on droplet size of miniemulsion between 0 and 1 wt% C₈mimPF₆ obtained in Fig.3.23 may attribute to the combination of viscosity and interfacial tension due to the change of concentration of C₈mimPF₆. However, the effect of C₈mimPF₆ on droplet size at a higher C₈mimPF₆ concentration, *e.g.* above 5 wt% becoming less sensitive which cannot be explained clearly, and a further future study shall be carried out.

It is interesting to note that C₈mimPF₆ could reduce the oil/water interfacial tension from the result of Fig.3.25. The reason why C₈mimPF₆ had a certain surface activity function was due to its cation with a hydrophilic imidazolium moiety and a hydrophobic carbon chain, which has been explained in the study of miniemulsion stabilised by surfactant (in the part of 3.3.1.1.3). However, the interaction between C₈mimPF₆ and silica nanoparticle was different from surfactant. For example, from the interfacial tension result between surfactant (SDSO) and C₈mimPF₆, in the absence of C₈mimPF₆, as SDSO concentration in water phase increased from 0 mM to 0.1 mM, there was a limited change in interfacial tension, which decreased slightly

from $14.82 \text{ mN}\cdot\text{m}^{-1}$ to $14.09 \text{ mN}\cdot\text{m}^{-1}$. After adding only 0.1 wt% C_8mimPF_6 in oil phase, interfacial tension dramatically reduced from $14.04 \text{ mN}\cdot\text{m}^{-1}$ to $10.18 \text{ mN}\cdot\text{m}^{-1}$. While for silica nanoparticle, as silica nanoparticle concentration in water phase increased from 0 g/l to 50 g/l, interfacial tension decreased slightly from $14.82 \text{ mN}\cdot\text{m}^{-1}$ to $14.04 \text{ mN}\cdot\text{m}^{-1}$. After adding 0.1 wt% C_8mimPF_6 in oil phase, the decrease in interfacial tension was not apparent, reducing from $14.04 \text{ mN}\cdot\text{m}^{-1}$ to $13.44 \text{ mN}\cdot\text{m}^{-1}$. Because silica nanoparticle did not have a structure the same as SDSO which contains a hydrophilic moiety connected with a hydrophobic carbon chain, the jointed effects mentioned in SDSO were less to happen.

3.3.2.2 Factors affecting stability of miniemulsion

3.3.2.2.1 Effect of pH of water phase on stability

The pH of water phase directly affects surface charge (zeta potential) of silica nanoparticle dispersed in it. The surface charge has an influence on the absorption of silica nanoparticle on the surface of droplet, which directly decides the stability of droplet. In order to study such effect of pH of water phase, water phases containing 50 g/l silica nanoparticles with pH ranging from 3 (W-sil-3), 5 (W-sil-6), 7 (W-sil-7), 9 (W-sil-8) to 11 (W-sil-9) were prepared. Oil phase contained 10 wt% C_8mimPF_6 , 85 wt% MMA and 5 wt% HD (O-6). Miniemulsion was prepared by homogenising oil/water phase mixture *via* high speed disperser at 20000 rpm for 8 min.

Miniemulsions prepared at high pH were viscose and lack of fluidity. In order to gain further understanding of fluidity and stability of the miniemulsion, which is a key parameter for coating products, viscosity as a function of shear rate was evaluated. The result is shown in Fig.3.26. It can be seen that viscosities decrease remarkably with the increase of shear rate for miniemulsions prepared under pH=5, 7,

9, and 11. While such decrease is less remarkable for pH=3. Normally, decreasing in viscosity with the increase of shear rate is referred as a shear thinning behaviour.(Yilmaz, 2014) This shear thinning behaviour indicated that the aggregation of particles occurred, and the decrease of viscosity at higher shear rates indicated the breaking of aggregation into primary particles. (Wittmar et al., 2012) A near Newtonian behavior of miniemulsion found at pH=3 means less aggregation hence more stable miniemulsion was achieved. Thus water phase with a pH of 3 was chosen for the following experiment.

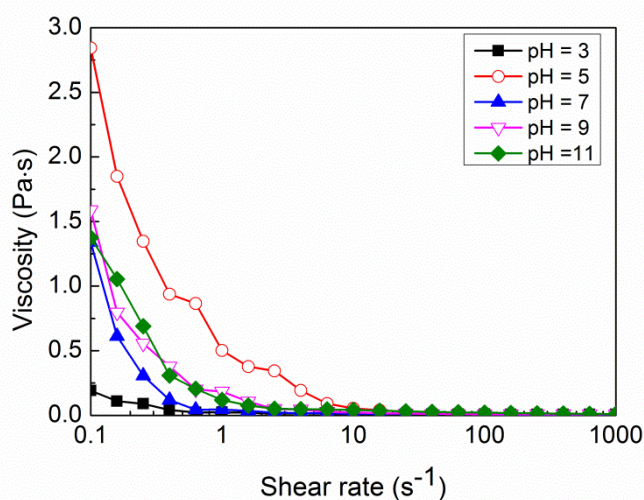


Fig.3.26 Variation of viscosity as a function of shear rate for miniemulsions prepared under different pH of water phase

From the result of Fig.3.21, when pH was 3, the absolute zeta potential of silica nanoparticles was around 0. Electrostatic repulsion between silica nanoparticles adsorbed on the surface of droplets was low. Adsorption became easier on account of weak electrostatic repulsion, thus more silica nanoparticles could be adsorbed on the surface of droplets. The close-packed silica nanoparticle may act as an obstacle among droplets, thus preventing collide between droplets. So, due to the adsorption of silica nanoparticles, static repulsion between droplets was enhanced.

3.3.2.2.2 Effect of C_8mimPF_6 concentration on stability

The storage stability of miniemulsions containing different concentrations of C_8mimPF_6 was studied by preparing miniemulsions with the same formula and energy input mentioned in 3.3.1.2.4, a formula and energy input used to study effect of C_8mimPF_6 concentration on initial droplet size. The method to study stability here is the same as the one used to study stability of miniemulsion stabilised by surfactant. First, miniemulsion would be stored and observed whether it was visually stable, that is to say, without creaming or sedimentation. If miniemulsion was visually stable, change of droplet size as a function of storage time would be measured.

According to the method mentioned above, a certain amount of miniemulsion was sealed in a cylindrical glass bottles and observed with different aging time at 20 °C. The result is summarised in Table.3.6. It can be seen that creaming at the top of sample (Fig.3.27) occurred for miniemulsion containing 0 wt%, 1 wt% and 5 wt% C_8mimPF_6 , Sediment at the bottom of sample (Fig.3.27) was detected for miniemulsions containing 10 wt%, 20 wt%, and 30 wt% C_8mimPF_6 at the same time.

Table.3.6 Stability of miniemulsions containing different C_8mimPF_6 concentrations with different aging time. (-: stabilisation; *: creaming; \: sedimentation)

Aging time (h)	The phenomenon of Reversible change					
	0 wt% C_8mimPF_6	1 wt% C_8mimPF_6	5 wt% C_8mimPF_6	10 wt% C_8mimPF_6	20 wt% C_8mimPF_6	30 wt% C_8mimPF_6
0	-	-	-	-	-	-
72	*	-	-	\	\	\
144	*	*	*	\	\	\
216	*	*	*	\	\	\
288	*	*	*	\	\	\

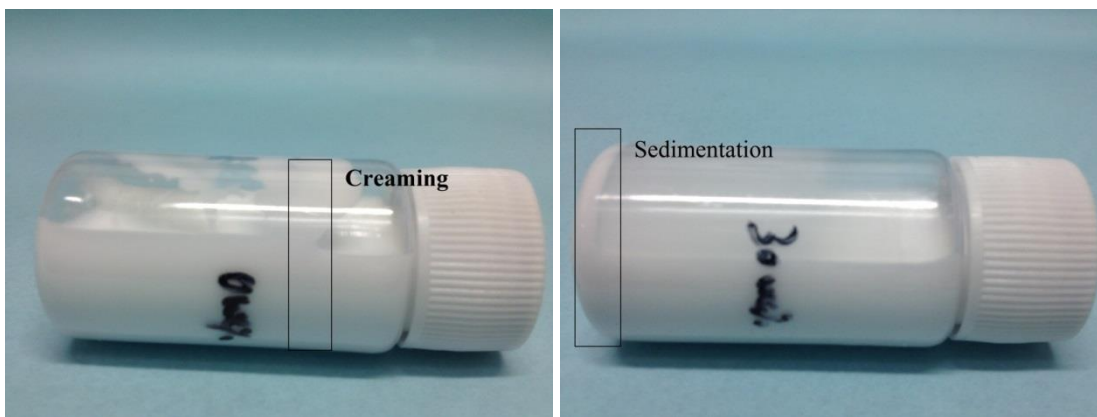


Fig.3.27 A typical image of creaming and sedimentation (the cylindrical glass bottle is held horizontally to see the creaming at the top of sample or the sediment at the bottom of sample)

Creaming was difficult to be quantified due to its irregular shape as shown in Fig.3.27. However, sediment can be further quantified, by measuring the height of sediment. Fig.3.28 shows variation in the height ratio of sediment to initial miniemulsion as a function of aging time for miniemulsions containing 10 wt%, 20 wt%, and 30 wt% C_8mimPF_6 . It is found that the sedimentation rate increases with the aging time from 0 h to 288 h for all miniemulsions. The height of sediment for 10 wt% C_8mimPF_6 miniemulsion was much less as compared with 20 wt% and 30 wt% C_8mimPF_6 for all aging time.

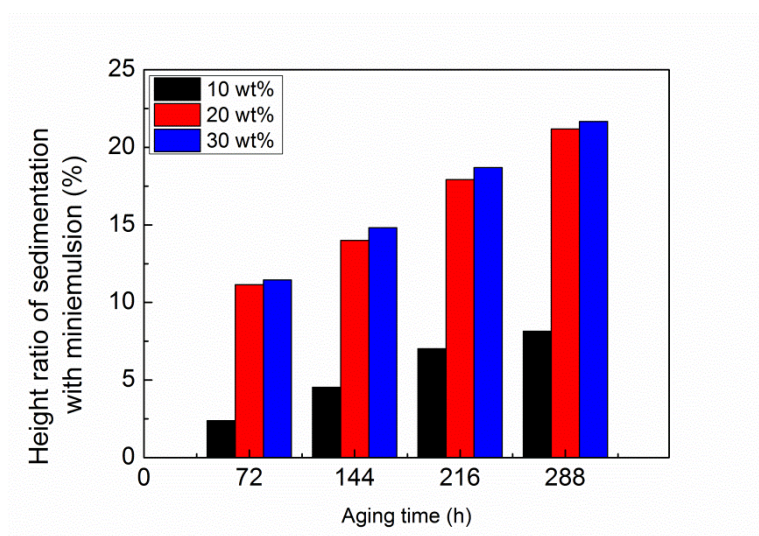


Fig.3.28 Variation in height ratio of sediment with miniemulsion as a function of aging time for miniemulsions containing 10 wt%, 20 wt%, and 30 wt% C_8mimPF_6 .

Creaming or sedimentation is caused by the vertical migration of droplets, which follows the Stoke's law.(Abismaïl et al., 1999) According to the Stoke's law, if the density of droplet is higher than the water phase, sedimentation occurs. Conversely, creaming occurs. The degree of creaming or sedimentation is proportional to density difference between droplet and water phases. To confirm such effect caused by the density difference, density of oil phase containing different concentrations of C₈mimPF₆ and water phase containing different concentrations of silica nanoparticles are measured at 20 °C, and result is shown in Table.3.7.

Table.3.7 Density of oil phase containing different concentrations of C₈mimPF₆ and water phase containing different concentrations of silica nanoparticles at 20 °C

Oil phase	Density (g/cm ³)	Water phase	Density (g/cm ³)
0 wt% C ₈ mimPF ₆	0.928	0 g/L silica	0.997
1 wt% C ₈ mimPF ₆	0.93	10 g/L silica	1.002
5 wt% C ₈ mimPF ₆	0.94	30 g/L silica	1.013
10 wt% C ₈ mimPF ₆	0.953	50 g/L silica	1.025
20 wt% C ₈ mimPF ₆	0.979	70 g/L silica	1.037
30 wt% C ₈ mimPF ₆	1.007	90 g/L silica	1.050

Due to the adsorption of silica nanoparticles, density of droplets would be larger than original oil phase. This explained why sedimentation still occurred even though densities of oil phase containing 10 wt%, 20 wt%, 30 wt% C₈mimPF₆ were less than water phase containing 50 g/l silica nanoparticles. From the result of Table.3.7, density of oil phase increases with the increase of C₈mimPF₆, especially, this increase becomes more apparent when C₈mimPF₆ concentration ranges from 10 wt% to 30 wt%. 10 wt% was a critical point. Below such concentration, density of droplet may be less than that of water phase, leading to the creaming. While upon such concentration, density of droplet became higher than that of water phase, and this was the reason why sedimentation occurred. With the increase in C₈mimPF₆ concentration

from 10 wt% to 30 wt%, density difference between droplet and water phase becomes larger, leading to the aggravation in sedimentation rate shown in Fig.3.28.

To further evaluate the effect of surface charge of droplet on stability of droplet, systematic investigation on zeta potential of miniemulsions prepared with a pH of 3 at different concentrations of C_8mimPF_6 , ranging from 0 wt%, 0.1 wt%, 0.5 wt%, 1 wt%, 5 wt%, 10 wt%, 20 wt%, and 30 wt% was undertaken. Results are shown in Fig.3.29. Negative zeta potentials are observed for miniemulsions containing 0 wt% and 0.1 wt% C_8mimPF_6 , which suggests that droplets are negatively charged in the presence of silica nanoparticles. Then zeta potential becomes positive with further increase in C_8mimPF_6 concentration. A sharp increase in zeta potential from -1.69 mV to 4.63 mV with an increase of C_8mimPF_6 concentration from 0 wt% to 1 wt, followed by a slow increase on zeta potential from 4.63 mV to 9.12 mV with an increase in C_8mimPF_6 concentration from 1 wt% to 5 wt%. The zeta potential curve is levelled off as further increasing the C_8mimPF_6 concentration up to 30 wt%.

It can be seen that the absolute zeta potentials of all miniemulsions are much less than 30 mV, a point upon which dispersion system would be more stable. (Sonavane et al., 2008) In this case, droplets may collide with each other more frequently, leading to coalescing into a larger one, or aggregating into cluster. Droplet or cluster with larger size would migrate vertically with a faster rate, and finally led to the appearance of creaming and sedimentation as shown in Table.3.7.

It is not surprising to note that, in the absence of C_8mimPF_6 , the zeta potential of droplet is negative. At fixed pH value of water phase (pH = 3), the only factor that affected the charge of droplet was silica nanoparticles adsorbed on the surface of droplet. As Fig.3.21 shows, the zeta potential of silica nanoparticles is equal to -2.01

mV, which is close to that value of droplet, -1.69 mV shown in Fig.3.29. This means the charge of droplet was mainly contributed by silica nanoparticles.

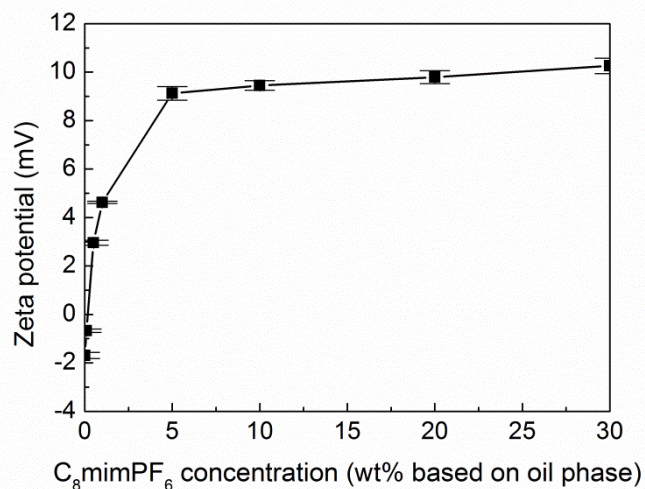


Fig.3.29 Variation in the zeta potentials of droplet sizes as a function of C₈mimPF₆ concentration.

However, in the presence of C₈mimPF₆, zeta potential moves towards positive with the increase of C₈mimPF₆. This movement can be detected even at 0.1 wt% C₈mimPF₆. The unique zeta potential behaviour mentioned above might be best explained by Chaumont et al. who studied the interface between water and C₈mimPF₆ by a molecular dynamics simulation.(Chaumont et al., 2005) According to the simulation result, PF₆⁻ anions were more hydrophilic as compared with C₈mim⁺ cations, hence more PF₆⁻ anions dispersed in the water phase than C₈mim⁺ cations. Thus a small excess of C₈mim⁺ cations was kept in the C₈mimPF₆ phase. C₈mim⁺ cations might accumulate at the interface and were ordered with their imidazolium moiety towards the water phase and carbon chain towards oil phase. The excessive C₈mim⁺ cations accumulated at the O/W interface caused the interface being positively charged. This was consistent with the experimental work reported by Fitchett et al. who found that the surface charges at the C₁₀mimBMSI/water interfaces

were positive and had value up to $27 \mu\text{C}\cdot\text{cm}^{-2}$. (Fitchett et al., 2005) It is clear that the presence of C_8mimPF_6 , with excessive C_8mim^+ cations on the droplet interface would neutralize the negative charged silica nanoparticles, leading to a less negative charged droplet, e.g. 0.1 wt% C_8mimPF_6 . As a further increase in C_8mimPF_6 concentration, e.g. from 0.1 wt% and 30 wt%, the amount of C_8mimPF_6 dissolved in water phase might increase, hence more excessive C_8mim^+ cations would be kept in the oil phase as mentioned above and adsorbed on water/oil interface. Some of C_8mim^+ may be consumed to neutralize the negative charged of silica nanoparticles; the remaining would make the droplet positive charged, leading to an increase on surface charge.

3.3.2.2.3 Effect of temperature on stability

In order to evaluate the role of temperature, pH of water phase was maintained at 3, and concentration of silica nanoparticles in water phase was fixed at 50 g/l (W-sil-3). Oil phase containing 10 wt% C_8mimPF_6 (O-6) was prepared. After homogenising oil/water phase mixture by high speed disperser at 20000 rpm for 8 min, miniemulsion was obtained and stored at different temperature ranging from 30 °C to 60 °C for 4.0 h. Variation of droplet sizes as a function of storage time for miniemulsion containing 10 wt% C_8mimPF_6 at different temperatures is shown in Fig.3.30.

It is observed that the size of droplet in miniemulsion increased by 67.6% after being stored at 60 °C for 4 hours, and 52.6% at 50 °C for the same aging time. Whilst at 40 °C and 30 °C, there was little change on droplet size. The sharp increases in size at 50°C, 60 °C were probably attributed to the high frequency of droplet/particle movement at high temperature, hence the opportunity of droplet/particle collision would increase which induced droplet/particle coalescence. This indicates that the

mini-emulsion is more unstable at higher temperature. This instability caused by temperature was also reported by Asua (Asua, 2002).

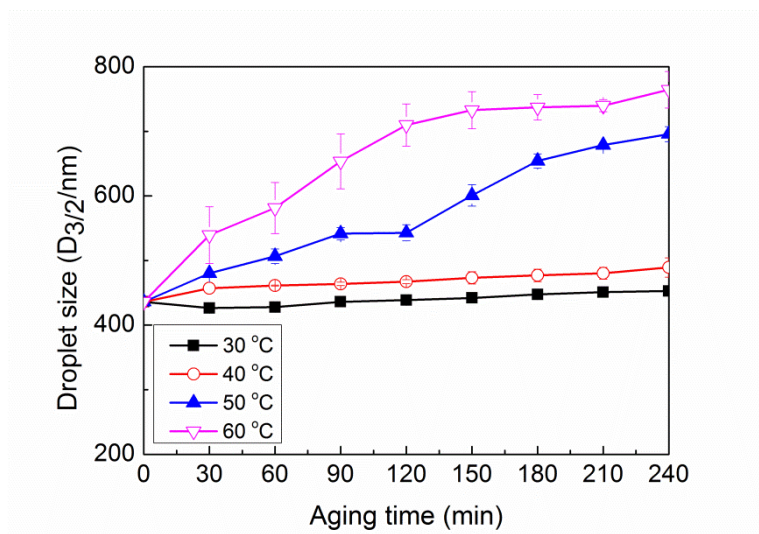


Fig.3.30 Variation of droplet sizes as a function of storage time for miniemulsion containing 10 wt% C_8mimPF_6 at different temperatures.

3.4 Conclusion

In the stabilisation of surfactant (SDSO) or Pickering emulsifier (silica nanoparticle), miniemulsion containing C_8mimPF_6 was prepared. Factors affecting initial droplet size and stability of miniemulsion were systematically investigated.

For miniemulsion stabilised by surfactant, results were summarised as follows.

With an increase in energy input, *e.g.* input power and input duration, there is a sharp decline on initial droplet size; but a further increase in energy input has less effect on droplet size reduction. When fixing 10 wt% C_8mimPF_6 , initial droplet size sharply decreased as SDSO concentration increased up to 30 mM, and then tended to be stable. When fixing 30 mM SDSO, within 1wt% C_8mimPF_6 concentration, the initial droplet size decreased with the addition of C_8mimPF_6 , and then trended to level off until 5 wt% C_8mimPF_6 , followed by an increase in initial droplet size up to 30 wt%

C₈mimPF₆. This trend in initial droplet size was partly due to the effect of C₈mimPF₆ concentration on viscosity of oil phase and interfacial tension. Especially, a sharp decrease in O/W interfacial tension at low C₈mimPF₆ concentration indicated the synergistic effects between anionic surfactant and imidazolium cations.

SDSO was chosen from three surfactants with different HLB values based on their performance regarding the stability of miniemulsion. When fixing 30 mM SDSO, above 10 wt% C₈mimPF₆, adding more C₈mimPF₆ to the oil phase weakens the droplet stability remarkably. The existence of C₈mimPF₆ in droplets had great influence on zeta potential of droplets that affected the stability of miniemulsion. Because the absolute zeta potentials were less than 30 mV for miniemulsions containing 20 wt%, 30 wt% C₈mimPF₆, they were unstable during long time storage. The dispersion of the anions of C₈mimPF₆ towards water were faster than the cations of C₈mimPF₆, hence more cations were kept in droplets. The cations neutralized negatively charged surfactant, causing the decrease in the absolute zeta potential when C₈mimPF₆ concentration was above 5 wt%. Increase in droplet size became apparent at high temperature, e.g. 50 °C, probably attributed to the high frequency of droplet/particle movement at high temperature.

For miniemulsion stabilised by silica nanoparticle, results were summarised as follows.

Initial droplet size decreases sharply with an increase in energy input, e.g. stirring speed and input duration; but such effect fades down with a further increase in energy input. Suitable pH of water phase, with a value of 3, was chosen as smallest droplet size could be achieved. At this pH, silica nanoparticles were around its isoelectric point, benefiting the reduction in droplet size. When 10 wt% C₈mimPF₆

was added, initial droplet size sharply decreased as the silica nanoparticle concentration increased up to 50 g/l, and then further increase in silica nanoparticle concentration had limited effect on reduction of droplet size. When fixing 50 g/l silica nanoparticles, within 1wt% C₈mimPF₆ concentration, the initial droplet size decreased with the addition of C₈mimPF₆, and then tended to increase until 5 wt% C₈mimPF₆, followed by fluctuation around 430 nm up to 30 wt% C₈mimPF₆. Such trend in initial droplet size was partly due to the combined effects of C₈mimPF₆ on viscosity of oil phase and interfacial tension.

A stable miniemulsion with less aggregation could be achieved when prepared under water phase with a pH of 3. At this pH, where silica nanoparticles were around its isoelectric point, more silica nanoparticles could be crowded on the surface of droplets on account of weak electrostatic repulsion among them, benefiting the enhancement in stability. When fixing 50 g/l silica nanoparticles, instability of miniemulsion during storage could be detected for all C₈mimPF₆ concentrations. Creaming occurred at 0~5 wt%, and sedimentation occurred at 10~30 wt% C₈mimPF₆ concentrations, depending on the density difference between droplet and water phase. Due to the weak electrostatic repulsion between droplets, droplets may coalesce or aggregate into larger ones, leading to faster vertical migration, causing the appearance of creaming or sedimentation. Increase in droplet size became apparent at high temperature, e.g. 50 °C and 60 °C, probably attributed to the high frequency of droplet/particle movement at high temperature.

Chapter 4 Factors on polymer yield and stability of miniemulsion polymerisation

4.1 Introduction

In previous chapter, miniemulsions containing C_8mimPF_6 in the stabilisation of surfactant and silica nanoparticles were prepared. Factors affecting initial droplet size and stability of miniemulsion were systematically investigated. In this chapter, the following step, miniemulsion polymerisation was focused. Two kinds of initiators, hydrophobic 2, 2-azobis (isobutyronitrile) (AIBN), and hydrophilic hydrogen peroxide/ascorbic acid (H_2O_2/AAC) were used to initiate the polymerisation. For miniemulsion stabilised by surfactant, factors including initiator type, initiator concentration, temperature, and C_8mimPF_6 concentration on yield of polymer and stability of miniemulsion during polymerisation were studied. For miniemulsion stabilised by silica nanoparticle, factors including initiator type, temperature, pH of water phase and C_8mimPF_6 concentration on yield of polymer and stability of miniemulsion during polymerisation were investigated.

4.2 Materials and methods

4.2.1 Materials

Methyl methacrylate (MMA, CP) was purchased from Sinopharm Chemical Reagent Co., Ltd and purified by vacuum distillation to remove inhibitor. 2, 2-azobis (isobutyronitrile) (AIBN, 97%) was purchased from Aladdin Industrial Inc and recrystallized by ethanol. L-Ascorbic acid (AAC, AR), hydrogen peroxide (H_2O_2 , AR), and sodium dodecyl sulfonate (SDSO, CP) were purchased from Sinopharm

Chemical Reagent Co., Ltd. Hexadecane (HD, 98%) was from Aladdin Industrial Inc. 1-octyl-3-methylimidazolium hexafluorophosphate (C_8mimPF_6 , 99%) was supplied by Shanghai Cheng Jie Chemical Co., Ltd. NS-30 (20 nm silica nanoparticle, pH = 9.5, 30 wt%) was supplied as silica sol by Yuda Chemical Co. Ultra-pure water with a resistivity of $18.2 M\Omega \cdot cm^{-1}$ was used in all experiments.

4.2.2 Preparation of miniemulsion

4.2.2.1 Miniemulsion stabilised by surfactant

Oil phase contained 5 wt% HD, the remaining 95 wt% containing C_8mimPF_6 and MMA. Both HD and C_8mimPF_6 were infinitely miscible in MMA. A homogeneous oil phase was obtained after gently stirring. Especially, if hydrophobic AIBN was used for polymerisation, a certain mole of this initiator would be dissolved in oil phase. The contents of components in oil phase are shown in Table.4.1

Table.4.1 Formula of oil phase

Sample code	Components in oil phase (wt% based on oil phase)			Initiator (mol% based on MMA)
	MMA	HD	C_8mimPF_6	AIBN
O-1	95	5	0	0
O-4	94	5	1	0
O-5	90	5	5	0
O-6	85	5	10	0
O-8	75	5	20	0
O-9	65	5	30	0
O-10	95	5	0	1.0
O-11	94	5	1	1.0
O-12	90	5	5	1.0
O-13	85	5	10	1.0
O-14	75	5	20	1.0
O-15	65	5	30	1.0
O-16	85	5	10	0.1
O-17	85	5	10	0.5
O-18	85	5	10	2.0

Water phase was prepared by dissolving a given amount of surfactant in ultra-pure water. The type and concentration of surfactant in water phase is showed in Table.4.2.

Table.4.2 Formula of water phases containing surfactant

Abbreviation	Type of surfactant	Amount (mM)
W-sur-3	SDSO	30

Oil in water miniemulsion (O/W) was prepared with a volume ratio of oil to water phase equal to 3 to 7. Oil phase was added into water phase in a 100 ml plastic container. The total volume of the mixture was 50 mL and kept at 40 °C. Sonicator (Xinzhi Scientz II) was chosen as the homogeniser. Position the Ultrasound probe Sonicator in the middle of the container and kept at one centimeter below the surface of the mixture. The output power of sonicator was set as 95 W. After homogenising the mixture for 6 minute in a state of 1 second on and 1 second off, miniemulsion was obtained.

4.2.2.2 Miniemulsion stabilised by silica nanoparticle

The formula of oil phase and preparing process for miniemulsion stabilised by silica nanoparticle was the same as the one for miniemulsion stabilised by surfactant.

Water phase was prepared by dissolving silica sol, NS-30 into ultra-pure water to the target concentration (gram of silica nanoparticle per litre of water phase); and the pH was adjusted to the required value using 0.1 mol/L aqueous NaOH or HCl solution at the same time. Table.4.3 shows the formula of water phases containing silica nanoparticle.

Table.4.3 Formula of water phases containing silica nanoparticle

Abbreviation	Amount (g/l)	pH
W-sil-3	50	3
W-sil-6	50	5
W-sil-7	50	7
W-sil-8	50	9
W-sil-9	50	11

Oil in water miniemulsion (O/W) was prepared with a volume ratio of oil to water phase equal to 3 to 7. Oil phase was added into water phase in a 250 ml baker. The total volume of the mixture sample was 100 mL and kept at 40 °C. High speed disperser (IKA T25) was chosen as the homogeniser. Rotor of high speed disperser was in the middle of the baker and then placed the tip of the rotor one centimeter below the surface of the mixture. The stirring speed of high speed disperser was set as 20000 rpm. After homogenising the mixture for 8 minute, a stable miniemulsion was formed.

4.2.3 Miniemulsion polymerisation

4.2.3.1 Miniemulsion stabilised by surfactant

The miniemulsion polymerisation was carried out in a four-necked flask equipped with a stirrer, a reflux condenser, a thermometer, and a nitrogen inlet. The flask was immersed in a water bath for controlling reaction temperature. 150 mL miniemulsion was loaded into the flask, and was gently stirred with nitrogen bubbling for about 1.5 h to remove oxygen in the flask. Then the temperature of water bath was set to reaction temperature. The method of adding the initiator depended on the type of initiator. When H₂O₂/AAc was used, the H₂O₂/AAc solution with molar ratio of H₂O₂ to AAc equal to 1 to 1.3 as initiator was injected into the miniemulsion directly

after the desired reaction temperature was reached, and then the polymerisation reaction was started. Table.4.4 shows the formula of H₂O₂/AAc initiator solution. When AIBN was used as an initiator, because AIBN could not be added into the miniemulsion directly due to its hydrophobicity, it was dissolved in oil phase before the preparation of the miniemulsion, and then the reaction temperature was adjusted to the desired temperature to start the polymerisation. The reaction process was under nitrogen protection.

Table.4.4 Formula of H₂O₂/AAc initiator solution

Sample code	H ₂ O (5mL)	Initiator (mol% based on MMA)	
		H ₂ O ₂	AAc
I-1	5	0.1	0.13
I-2	5	0.5	0.65
I-3	5	1.0	1.3
I-4	5	2.0	2.6

4.2.3.2 Miniemulsion stabilised by silica nanoparticle

The formula of H₂O₂/AAc initiator solution and polymerisation process for miniemulsion stabilised by silica nanoparticle was the same as the one for miniemulsion stabilised by surfactant.

4.2.4 Characterisation

4.2.4.1 Determination of yield of polymer

The commonly used methods to determine the yield of polymer is gravimetric method and gas chromatograph. For gravimetric method, the yield of polymer can be calculated by measuring polymer solid after evaporating water, residual monomer and any other volatile components. Gas chromatograph can accurately detect trace of

residual monomer in liquid sample; the yield of polymer can be calculated accordingly. Because latex contains solid polymer which may deposit on the GC system, a pre-treatment is need before gas chromatograph analysis. The pre-treatment includes solvent extraction method, thermal desorption technique, and full evaporation headspace gas chromatograph technique.(Chai et al., 2004) Other methods, like Fourier transform inferred spectroscopy and Raman spectroscopy have been employed as a on-line monitoring method to detect the conversion of monomer.(Chatzi et al., 1997, Pianelli et al., 1999)

In this study, the yield of polymer was determined gravimetrically. The product was sampled at regular intervals during reaction, and stored in refrigerator to terminate the reaction. After evaporating the monomer under ventilated condition and storing in oven at 120 °C for 4 h, polymer (PMMA), C₈mimPF₆, and emulsifier (SDSO or silica nanoparticle) remained in the solid product. From the results in Fig.5.7 and Fig.5.18, no new no new characteristic peaks were formed for particles containing C₈mimPF₆, compared with pure PMMA and pure C₈mimPF₆. This implies no chemical reaction occurred between C₈mimPF₆ and PMMA, so the content of PMMA can be obtained by subtracting the content of C₈mimPF₆, and emulsifier from the solid product. The yield of polymer was calculated as follows.

According to original formula of miniemulsion, the weight percent of components could be calculated, which was a% for MMA, b% for C₈mimPF₆, c% for HD, d% for water, e% for emulsifier, and f% for initiator. A sample weighted M₁ g was taken during reaction. After baking the sample to a constant weight, only PMMA, C₈mimPF₆, and emulsifier left, and its weight was recorded as M₂. The weight of PMMA can be calculated as: $M_{\text{PMMA}} = M_2 - 0.01b \cdot M_1 - 0.01e \cdot M_1$. The weight of

original MMA can be calculated as: $M_{\text{MMA}} = 0.01a \cdot M_1$. So the yield of polymer can be expressed as follows: $Y = \frac{M_2 - 0.01b \cdot M_1 - 0.01e \cdot M_1}{0.01a \cdot M_1} \times 100\%$.

4.2.4.2 Droplet/particle size measurement

The droplet/particle sizes and size distributions of miniemulsion at different reaction times were measured using the laser diffraction method (Mastersizer 3000, Malvern Inc). This technique has been widely accepted as a tool to evaluate droplet/particle size. (Zhang et al., 2012, Winkelmann and Schuchmann, 2011, Wang et al., 2014) For miniemulsion stabilised by surfactant, the sample was diluted with a water solution to meet the requirement of obscuration. The diluted water solution was saturated with SDSO and monomers to prevent coalescence during sample measurement. (Meliana et al., 2011) While for miniemulsion stabilised by silica nanoparticle, water saturated with monomer was used to as the dilute solution for miniemulsion. All measurements were repeated three times.

4.2.4.3. Viscosity measurement

The viscosities of latexes after polymerisation were measured using the rotational rheometer with the plate-and-plate system. The upper plate had a diameter of 40 mm, and the gap between upper and lower plates was 1.0 mm. Measurement was conducted with the shear rate ranging from 0.1 s^{-1} to 1000 s^{-1} at $20 \text{ }^\circ\text{C}$, the storage temperature.

4.2.4.4. Morphology observation

The morphologies of particles after polymerisation were studied by a field emission scanning electron microscope (SEM) (Σ IGMA/VP, Carl Zeiss Microscopy

Ltd.) at an accelerating voltage of 3 kV. Samples for SEM analysis were prepared as follows. The original latexes were diluted with water to 0.5 wt%. Droplets of diluted latexes were dropped onto the surface of aluminum foil, followed by drying in air. The aluminum foil used here was stuck with object tables whose other side was stuck to the objective table by conductive adhesive tape, followed by drying in air.

4.3 Results and discussion

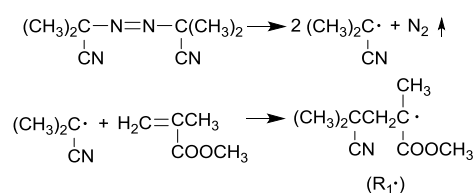
4.3.1 Miniemulsion stabilised by surfactant

In this section, the various factors, including the initiator type, initiator concentration, temperature, and C₈mimPF₆ concentration on yield of polymer as well as stability of miniemulsion during polymerisation are discussed. The reaction schemes for free radical polymerisation of MMA initiated by AIBN and H₂O₂/AAc are illustrated below.

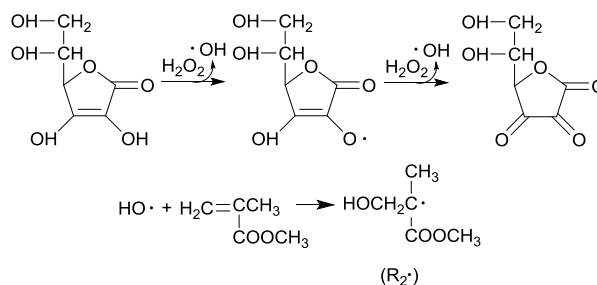
In free radical polymerisation, the first step is the generation of free radical via the decomposition of initiators, followed by the chain propagation, chain termination or chain transfer.(Flory, 1953)

Radical generation: Generation of radicals from AIBN and H₂O₂/AAc are shown as follows.(Flory, 1953, Kitagawa and Tokiwa, 2006)

AIBN:

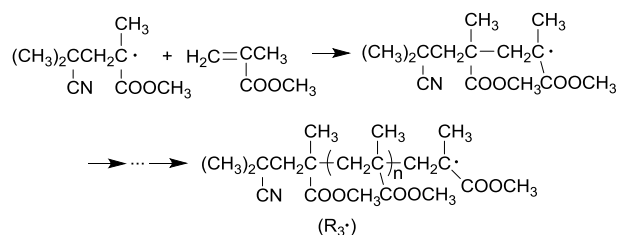


H₂O₂/AAc:

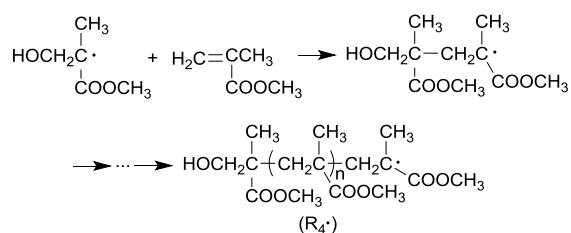


Chain propagation: Addition reactions between monomer radicals (R₁· or R₂·) and MMA form new radicals. The newly formed radical continues to react with MMA, forming a long chain radical. This is a strong exothermal reaction with low activation energy.

AIBN:

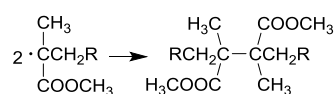


H₂O₂/AAc:

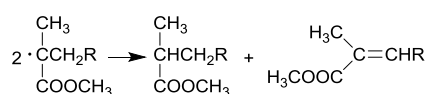


Chain termination: Highly active long chain radicals (R₃· or R₄·) cannot exist stably, and are likely to terminate with other radicals. This bi-radical termination contains coupling termination and disproportionation termination. The long chain radical can be expressed in a more general form given below.

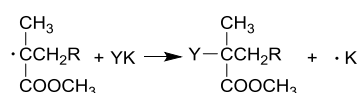
Coupling termination means single electrons from two radicals bond with each other by covalent bond.



Disproportionation termination is a process in which one radical captures a hydrogen atom or other atom of another radical to terminate both two radicals.



Chain transfer: Long chain radicals may capture one atom from a monomer, initiator, solvent, and macromolecule which is expressed as YK in the following scheme, and transfers one electron to the molecules losing one atom. The new radical, $\cdot\text{K}$, forms and continues chain propagation.



4.3.1.1 Factors affecting yield of polymer during miniemulsion polymerisation

4.3.1.1.1 Effect of temperature on yield of polymer

In order to study the effects of temperature, a miniemulsion containing 10 wt% C_8mimPF_6 (based on oil phase) was prepared, and initiated by 1.0 mol% AIBN at temperatures ranging from 30 °C to 50 °C. Above 55 °C phase separation occurred.

Fig.4.1 shows the yield of polymer as a function of reaction time for the miniemulsion containing 10 wt% C_8mimPF_6 at different temperatures initiated by AIBN. It is observed that 50 °C results in the highest final yield of polymer (95.1 %) and the shortest reaction time (60 min), whilst at 40 °C, a sharp increase in yield of

polymer is also observed within 60 min, followed by a slow increase until 150 min with a final yield of polymer at 89.5 % being achieved. From Fig.4.1, it is also noted that at 30 °C, nearly no reaction occurs. The change in reaction rate observed in Fig.4.1 was mainly caused by the difference in decomposition rate of initiator which is strongly dependent on temperature. For AIBN, it was reported in open literature that its half-life time was 80 min at 80 °C,(Perrier et al., 2005) while this time expanded to 37 h if temperature reduced to 55 °C.(Svec and Frechet, 1995) Clearly, higher temperature promoted higher efficiency in radical generation from the decomposition of AIBN, and such effective temperature ranged between 50 °C and 90 °C.(Balke and Hamielec, 1973, Jia et al., 1999, Yamamoto, 2013) It is not surprising that no reaction takes place at 30 °C, as such low temperatures may cause inefficiency in radical generation, leading to the lack of radicals for further polymerisation. However, it is unexpected to observe a high final yield of polymer at 40 °C, which is below the efficient decomposition temperature of AIBN. This was probably attributed to the presence of C₈mimPF₆, and would be discussed in the following section.

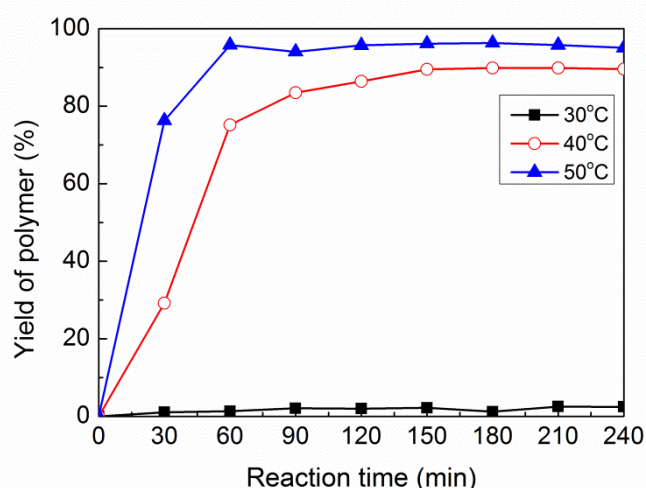


Fig.4.1 Yield of polymer as a function of reaction time for miniemulsion containing 10 wt% C₈mimPF₆ at different temperatures initiated by AIBN.

A similar temperature effect is also observed with polymerisation initiated by H₂O₂/AAc shown in Fig.4.2. Higher reaction rate is achieved at higher temperature 50 °C compared to the lower temperature of 30 °C, though the final yield of polymer for all conditions is approximately 100.0%. It is interesting to note that by replacing AIBN with H₂O₂/AAc, polymerisation could be completely carried out at 30 °C. This is because activation energy of redox initiator (40 ~ 80 KJ·mol⁻¹) is much lower than bond dissociation energy required for thermal decomposition initiator (125 ~ 160 KJ·mol⁻¹). This allows radicals of redox initiator could be generated under milder conditions.(Sarac, 1999) In this case, temperatures for initiating polymerisation by H₂O₂/AAc can be as low as 25 °C.(Kitagawa and Tokiwa, 2006) Also, polymerisation can occur even at 20 °C, which further indicates the potential effect of C₈mimPF₆ on the reaction process.

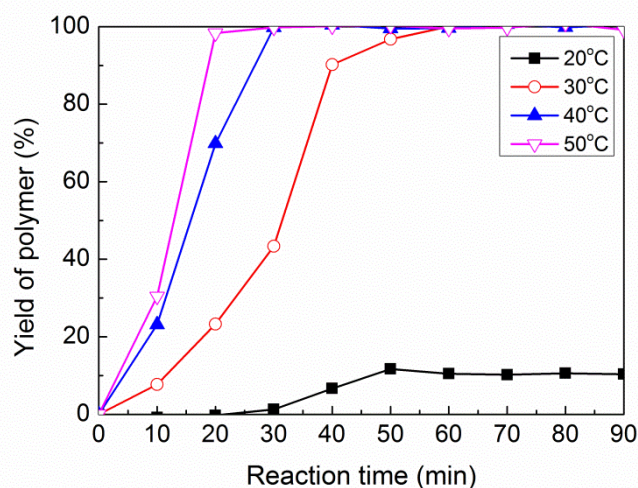


Fig.4.2 Yield of polymer as a function of reaction time for miniemulsion containing 10 wt% C₈mimPF₆ at different temperatures initiated by H₂O₂/AAc.

4.3.1.1.2 Effect of initiator concentration on yield of polymer

To study the effects of initiator concentrations, miniemulsion containing 10 wt% C₈mimPF₆ (based on oil phase) were prepared, and initiated by different

concentrations of AIBN at 40 °C. From the open literature, the dosage of AIBN to initiate emulsion/mini-emulsion polymerisation of MMA ranged from 0.03 mol% to 2.4 mol% (based on MMA). (López-Martínez et al., 2007, Tiarks et al., 2001a, Cheung and Gaddam, 2000, Hong et al., 2009) Taking above dosage as reference, the amount of AIBN used in this study varied from 0.1 mol% to 2 mol% (based on monomer). The final yield of polymer initiated by AIBN with different concentrations is shown in Table.4.5. It has been found that the final yield of polymer increases whilst reaction time becomes shorter with the increase of AIBN concentration from 0.1 mol% to 1.0 mol%. Further increases in AIBN concentration to 2.0 mol% had very little effect on the final yield of polymer.

Table.4.5 Final yield of polymer in miniemulsion containing 10 wt% C₈mimPF₆ initiated by different concentrations of AIBN at 40 °C

AIBN concentration (mol%)	Final yield (%)	Reaction time (min)
0.1	29.1	240
0.5	78.9	180
1.0	89.5	150
2.0	90.2	150

Another hydrophilic initiator, H₂O₂/AAc, was also used to study such effects, under the same C₈mimPF₆ concentration and temperature. The final yield of polymer initiated by different concentrations of H₂O₂/AAc is shown in Table.4.6. When H₂O₂ concentration is 0.1 mol%, no reaction takes place. At such low concentrations, the hydroxyl radicals generated might be wasted by oxygen surviving in water phase before reacting with monomers. Generally, oxygen is an inhibitor that can capture radicals. In this study, it might react with AAc and produce superoxide. Such superoxide could effectively scavenge hydroxyl radicals. (Kitagawa and Tokiwa,

2006) At low H₂O₂ concentration, hydroxyl radicals generated from H₂O₂ might run out completely due to this effective scavenger, thus no reaction occurred. As H₂O₂ concentration increases from 0.5 mol% to 2 mol%, there is a higher final yield of polymer, i.e. 100% yield is achieved. It is also observed that the reaction rate is sensitive to the concentration of initiator being used. Increase in the concentrations of H₂O₂ from 0.5 mol% to 1 mol% results in a shorter reaction time at the same yield of polymer, 100%. However, such reduction in reaction time due to the increase of initiator concentration could be diminished once the concentration of initiator reaches a certain value, e.g. 1 mol%. The results are consistent with the observation found by AIBN. This indicates that 1.0 mol% could be the optimised concentration to achieve a high final yield of polymer with shorter reaction time.

Table.4.6 Final yield of polymer in miniemulsion containing 10 wt% C₈mimPF₆ initiated by different concentrations of H₂O₂/AAc at 40 °C

H ₂ O ₂ concentration (mol%)	Final yield (%)	Reaction time (min)
0.1	0.0	90
0.5	100.0	50
1.0	100.0	30
2.0	100.0	30

4.3.1.1.3 Effect of C₈mimPF₆ concentration on yield of polymer

Following the observation of temperature effect in the presence of C₈mimPF₆, it is necessary to investigate different concentrations of C₈mimPF₆ ranging from 0 wt% to 30 wt% on miniemulsion polymerisation initiated by 1.0 mol% AIBN at 40 °C to gain a better understanding of the role of C₈mimPF₆ in miniemulsion polymerisation.

From Fig.4.3, it can be observed that in the absence of C₈mimPF₆, no reaction occurs. However, by adding as little as 1 wt% of C₈mimPF₆ can trigger the reaction

with final yield of polymer equal to 83.1%. Different concentrations of C_8mimPF_6 would show very different trends on the final yield of polymer, in which 83.1% yield was achieved for 1 wt% C_8mimPF_6 in 240 min, as compared to 89.5% yield with 10 wt% C_8mimPF_6 in 150 min. The reaction rate increases with the increase of C_8mimPF_6 concentration up to 10 wt%, however, a further increase in C_8mimPF_6 results in a reduction on reaction rate though the final yield are similar, which is around 89.0%.

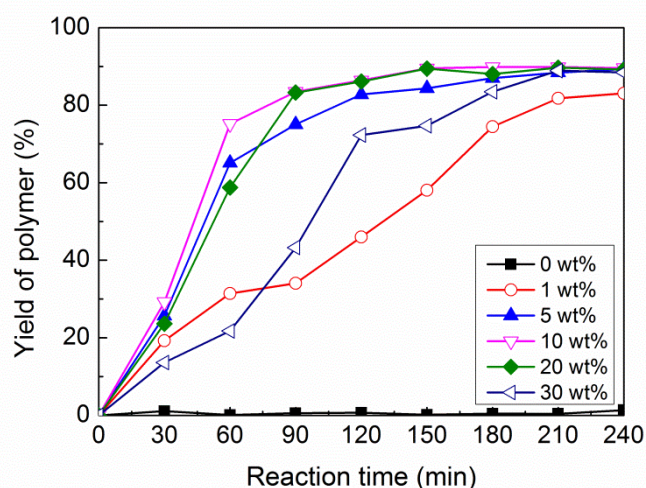


Fig.4.3 Yield of polymer as a function of reaction time for miniemulsions containing different C_8mimPF_6 concentrations initiated by AIBN.

The marked increase in reaction rate in the presence of 1 wt% C_8mimPF_6 might be attributed to two reasons: 1), AIBN could not be decomposed at such low temperatures, e.g. 40 °C, leading to the difficulty in reaction for 0 wt% C_8mimPF_6 . While in the presence of C_8mimPF_6 , this decomposition was enhanced; 2), C_8mimPF_6 may efficiently accelerate chain propagation rate, as well as reduce the termination rate of free radical polymerisation which was observed by another RTIL with similar structure, C_4mimPF_6 .(Harrisson et al., 2002, Harrisson et al., 2003)

In order to explore whether the decomposition of AIBN would occur at 40 °C, the polymerisation of 0 wt% C₈mimPF₆ was expanded to 72 h. A final yield of polymer with a value of more than 80% was achieved after 72 h. This implied that radicals could be generated by the decomposition of AIBN even at 40 °C, and caused the chain propagation. On the other hand, Thurecht *et al.* studied the decomposition of AIBN in 1-butyl-3-methylimidazolium hexafluorophosphate (C₄mimPF₆) and found that the rate constant of decomposition was similar to that recorded in organic solvents such as toluene and xylene.(Thurecht *et al.*, 2008) This indicates that the increase in reaction rate observed in Fig.4.3 in the presence of C₈mimPF₆ might not be attributed to its enhancement on decomposition of AIBN, instead, it might be due to other processes of free radical polymerisation, *e.g.* chain propagation, and chain termination at a lower temperature, *e.g.* 40 °C. Exact details are yet to be uncovered. Based on the open literature, *e.g.* Thurecht *et al.* reported that when polymerisation of MMA in 1-ethyl-3-methylimidazolium ethyl sulphate (C₂mimEtSO₄) was initiated by AIBN, parts of monomers were separated into extremely small domains by the barrier of C₂mimEtSO₄ domain, radical could be protected in C₂mimEtSO₄ domain. There was a partition between radical protected in C₂mimEtSO₄ domains and radical formed in monomer, thus chain termination could be well prevented.(Thurecht *et al.*, 2008) This could fit for our case, when radicals generated from AIBN were much less at 40 °C, the protection of radicals from chain termination might be more important. Thus more radicals may coexist under the protection of C₈mimPF₆. In addition, RTILs could accelerate the rate on chain propagation.^{16, 17} The radical protection together with acceleration of chain propagation in the present of C₈mimPF₆ might contribute to the large increase on reaction rate for a system containing only 1 wt% C₈mimPF₆.

In order to further determine the mechanism for C₈mimPF₆ effect in polymerisation reaction, some basic kinetics theories for miniemulsion polymerisation are worth considering. In miniemulsion polymerisation, its process can be divided into two stages. At stage I, droplets transform into particles through droplet nucleation. The efficiency of droplet nucleation is normally very high. However, micellar nucleation and homogenisation nucleation may still occur. At stage II, the effect of micellar nucleation and homogenisation nucleation fades down, thus the number of particles in aqueous phase would remain constant. Monomers stored in particles are continuously consumed with the progress of polymerisation process. Assuming the number of particles per unit volume of aqueous phase remains constant during polymerisation, polymerisation rate at stage II can be expressed as Eq.4.1:(Bechthold and Landfester, 2000)

$$R_p = \frac{k_p [M] \bar{n} N}{N_A} \quad \text{Eq.4.1}$$

where R_p is the rate of polymerisation; k_p is the chain propagation rate constant; [M] is the monomer concentration in droplet/particle; \bar{n} is the average effective radical number per droplet/particle; N is the number of droplet/particle per unit volume of aqueous phase in miniemulsion; N_A is Avogadro's number.

From Eq.4.1, as N_A is a constant, the polymerisation rate, R_p, is directly proportional to k_p, [M], \bar{n} and N. The impact of C₈mimPF₆ on the individual terms could be explicated in more details.

For example, even by adding 1 wt% of C₈mimPF₆, in the system may drastically increase chain propagation rate (k_p). It may also cause a reduction in the rate of the chain termination resulting in more radicals coexisting in droplet/particle form, hence

the number of radicals in droplets/particles, \bar{n} , would increase. The number of droplet/particle per unit volume of aqueous phase, N , which is inversely proportional to the droplet/particle size would also increase because of much smaller droplet size produced by 1 wt% of C_8mimPF_6 shown in Fig.4.15. With almost the same monomer concentration in droplets/particles $[M]$, it is not surprised to observe a significant increase in reaction rate in the presence of 1 wt% C_8mimPF_6

As C_8mimPF_6 concentrations increase, other factors may also come into play. For example in the case of a miniemulsion containing above 20 wt% C_8mimPF_6 , the volume of oil phase is fixed so the concentration of monomer, $[M]$ may be reduced. Likewise, the concentration of initiator (AIBN or H_2O_2/AAC), which had the same proportion as monomer being used, could be reduced significantly leading to a reduction in the rate of radical formation and hence the number of radical in particles, \bar{n} could be decreased. The impact of C_8mimPF_6 on the polymerisation reaction rate may be a combined effect of k_p , $[M]$, \bar{n} and N . At the moment, we cannot fully quantify the term, k_p and \bar{n} , however, considering the change of k_p would not be significant when we increased the concentration of C_8mimPF_6 from 1 wt% to 30 wt%, we could assume they are constant. The change of \bar{n} has similar effect as the change of $[M]$. Thus the polymerisation rate, R_p could be related with monomer concentration $[M]$ and the number of particle, N , expressed as Eq.4.2:

$$R_p \propto [M] \cdot N \quad \text{Eq.4.2}$$

where $[M]$ can be calculated using the initial concentration of MMA added in the oil phase, and N can be calculated from Eq.4.3.

$$N = \frac{V_{oil}}{\frac{4}{3}\pi r^3 V_{water}} \quad \text{Eq.4.3}$$

Since the oil phase volume, V_{oil} and the aqueous phase volume, V_{water} are fixed, the number of particles, N , is inversely proportional to the particle/droplet radius, r , (taken from 30 minutes, when the droplet/particle size become constant).

Based on Eq.4.2, that the variation of the dimensional group of $[M] \cdot N$ would reflect the change of R_p . Plotting $[M] \cdot N$ as function of C_8mimPF_6 concentration, results are shown in Fig.4.4.

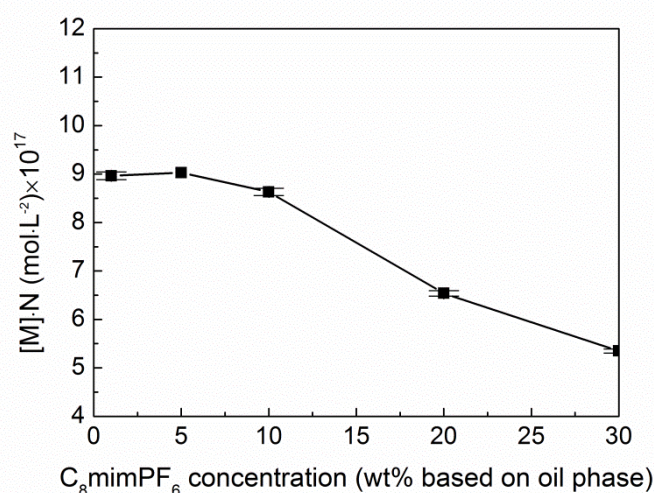


Fig.4.4 Dimensional Group $[M] \cdot N$ as a function of C_8mimPF_6 concentration for miniemulsions initiated by AIBN

It has been observed that the dimensional group $[M] \cdot N$ at 1 wt% of C_8mimPF_6 is equal to $9 \times 10^{-17} mol \cdot L^{-2}$ which is a much higher level and reaches the peak at 5 wt% of C_8mimPF_6 followed by a sharp decline as the concentration of C_8mimPF_6 increased from 10 wt% to 30 wt%. This trend implied that the polymerisation rate, R_p , would change in the similar manner and this is consistent with the reaction rate reduction at a similar liquid condition as observed in Fig.4.3.

To extend our understanding of the impact of C_8mimPF_6 on reaction rates, the hydrophilic type initiator, H_2O_2/AAC , (a mixture of 1.0 mol% H_2O_2 and 1.3 mol%

AAc based on monomer), was used to replace AIBN with other conditions kept the same. The yields of polymer during miniemulsion polymerisation at different concentrations of C_8mimPF_6 ranging from 0 wt% to 30 wt% were evaluated. Results are shown in Fig.4.5. A 100% yield of polymer is achieved at all C_8mimPF_6 concentration ranges being studied. The time taken to complete the reaction is increased from 20 min to 50 min as the concentration of C_8mimPF_6 increases from 0 to 30 wt %. The overall reaction rate is ranked according to the C_8mimPF_6 concentrations as follows: 0 wt%, 1 wt% > 5 wt%, 10 wt% > 20 wt%, 30 wt%.

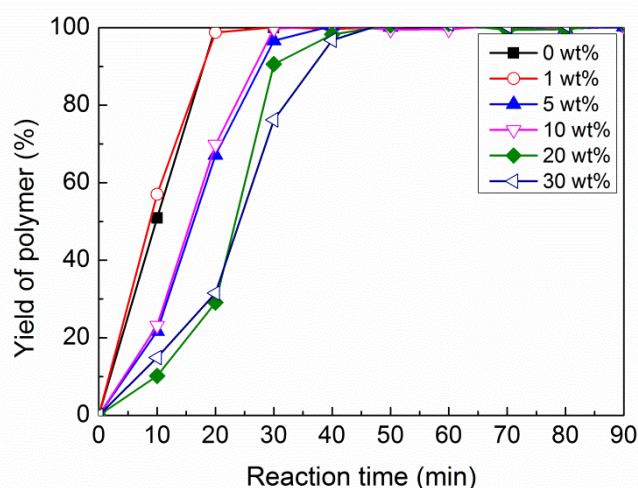


Fig.4.5 Yield of polymer as a function of reaction time for miniemulsions containing different C_8mimPF_6 concentrations initiated by H_2O_2/AAc .

Fig.4.5 exhibits very different effects of C_8mimPF_6 on the reaction rate of miniemulsions polymerisation as compared to the one with hydrophobic AIBN as an initiator. By comparison, reaction rates between 0 wt% C_8mimPF_6 and 1 wt% C_8mimPF_6 (Fig.4.5) showed no apparent increases. The different effects in the presence of 1 wt% C_8mimPF_6 might be attributed to the fact that H_2O_2/AAc is hydrophilic, miniemulsion polymerisation can only occur when radicals generated in aqueous phase transport to the reactant site, MMA, which is present in oil phase.

Hence mass transfer of radicals between dispersed phase and continuous phase may play a more important role during reaction process.(Chern, 2006) The number of radicals available for reaction in the droplet/particles for H₂O₂/AAc system might be determined by the entry of radicals from water phase. In other words, the interfacial barrier or resistance which is related to the interfacial structure between water phase and droplet/particle could play a key role in the radicals transfer process. Research result in chapter 3 with similar liquid formula suggested that by adding 1 wt% of C₈mimPF₆ in MMA oil phase caused a marked reduction in oil/water interfacial tension, from 3.94 mN·m⁻¹ to 0.31 mN·m⁻¹ (shown in Table.4.7) which was attributed to the synergistic effect between C₈mim⁺ cation and SDSO anion, and hence resulted in a tighter interfacial space alignment.(Kong et al., 2015)

Table.4.7 Interfacial tensions between water phase and oil phase containing different concentrations of C₈mimPF₆ at 40 °C

C ₈ mimPF ₆ (wt%)	Interfacial tension (mN·m ⁻¹)
0	3.94
1	0.31
5	0.21
10	0.15
20	0.22
30	/

It has been reported in open literature that the tighter interfacial structure may reduce the entry rate of radicals into droplets.(Gan et al., 1992, Mosca et al., 2013, Cao et al., 2008) Thus it would be expected that the number of radicals in droplets/particles, \bar{n} , would be reduced. Such negative effects could cancel the other positive kinetic effects, such as radical chain propagation and chain termination rate. This could be the main reason why the presence of 1 wt% of C₈mimPF₆ in miniemulsion polymerisation initiated by AIBN exhibited a positive effect on the reaction rate whilst no apparent effect on reaction rate was detected for H₂O₂/AAc.

For polymerisation with concentrations of C_8mimPF_6 higher than 1 wt%, the variation of interfacial tension are insignificant, thus the difference on interfacial resistance for radical transportation may be treated as constant. With similar assumptions for k_p and \bar{n} , as mentioned in Fig.4.4 discussion, we may use dimensional group $[M] \cdot N$ to evaluate the variation of reaction rate with different C_8mimPF_6 concentrations from 1 wt% to 30 wt% shown in Fig.4.6. There is a sharp decline on $[M] \cdot N$ at C_8mimPF_6 concentrations ranging from 1 wt% to 5 wt% and 10 wt to 20 wt% whilst the changes in between of the curves are rather flat. This trend appears to be in agreement with the variation of reaction rate in the same system. This confirms the mixed effect of C_8mimPF_6 on reaction rate with different initiator.

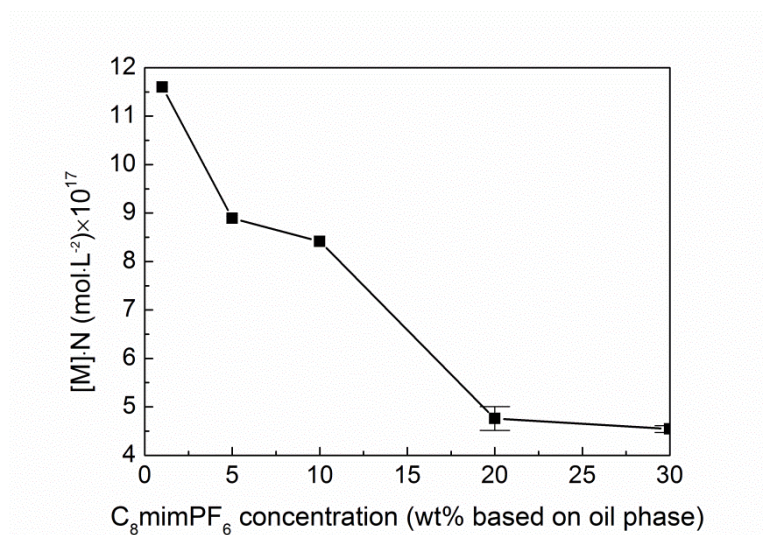


Fig.4.6 Dimensional group $[M] \cdot N$ as a function of C_8mimPF_6 concentration for miniemulsions initiated by H_2O_2/AAC

4.3.1.2 Factors affecting stability of miniemulsion during polymerisation

4.3.1.2.1 Effect of temperature on stability

To illustrate the reaction mechanism at different temperature, the formula of miniemulsion and polymerisation conditions were the same as the ones when we studied the effect of temperature on kinetics of miniemulsion polymerisation.

Fig.4.7 illustrates the variation of droplet/particle sizes for miniemulsion initiated by $\text{H}_2\text{O}_2/\text{AAc}$ at different temperatures. A marked reduction on droplet/particle size is observed soon after reaction took place, *e.g.* 10 min for 30 to 50 °C, 40 min for 20 °C. As the reaction progresses, the change of droplet/particle size behaves differently. *E.g.* at 20 °C, 30 °C and 40 °C, droplet/particle size remains unchanged. While at 50 °C, a sharp increase in droplet/particle size is found after 20 min, then the droplet/particle size remains unchanged until the reaction is completed. This suggests that in addition to the properties of C_8mimPF_6 , which affected initial droplet size of miniemulsion, the final particle size of latex would depend on both process conditions such as temperature and the reaction mechanism.

A sharp increase in size at 50°C was probably attributed to the high frequency of droplet/particle movement at 50 °C, hence the opportunity of droplet/particle collision would increase which induced droplet/particle coalescence. Similar observations have been also found for miniemulsion initiated by AIBN (Fig.4.9), which shows the strong dependency of droplet size on temperature. This indicates that the miniemulsion is more unstable at higher temperature, *e.g.* 50 °C. Such instability caused by temperature can even be observed without polymerisation. This result was shown in Fig.3.18 in chapter 3. It is observed that the size of droplet in miniemulsion increased by 40% after being stored at 50 °C for 4 hours, whilst at 40 °C and 30 °C, there was little change on droplet size.

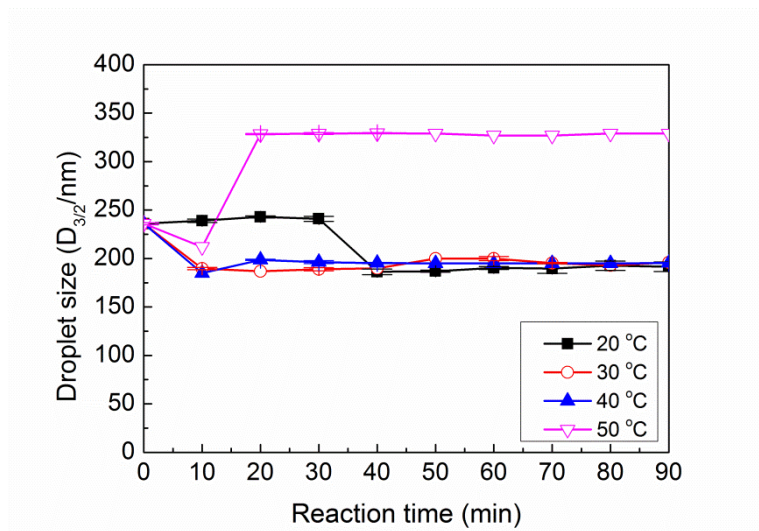


Fig.4.7 Variation of droplet/particle sizes as a function of reaction time for miniemulsion containing 10 wt% C₈mimPF₆ at different temperatures initiated by H₂O₂/AAc.

The reduction in droplet size after the initial reaction period shown in Fig.4.7 was probably attributed to the homogeneous nucleation or micellar nucleation mechanism.(Chern and Liou, 1999b, Schork et al., 2005, Asua, 2002) For homogeneous nucleation, primary particles are generated in the aqueous phase via the chain propagation of the radicals with monomers dissolved in water. They are stabilised by the surfactant dissolved in water or released from droplet surface. As to micellar nucleation, polymerisation takes place in micellar and forms primary particles. In both micellar and homogeneous cases, smaller size of particles would be quickly generated. When the number of such smaller latex particles increases significantly, the mean droplet/particle size is expected to be reduced. The droplet size distribution results showed in Fig.4.8 also demonstrated the shift on the peak of droplet size distribution towards smaller size.

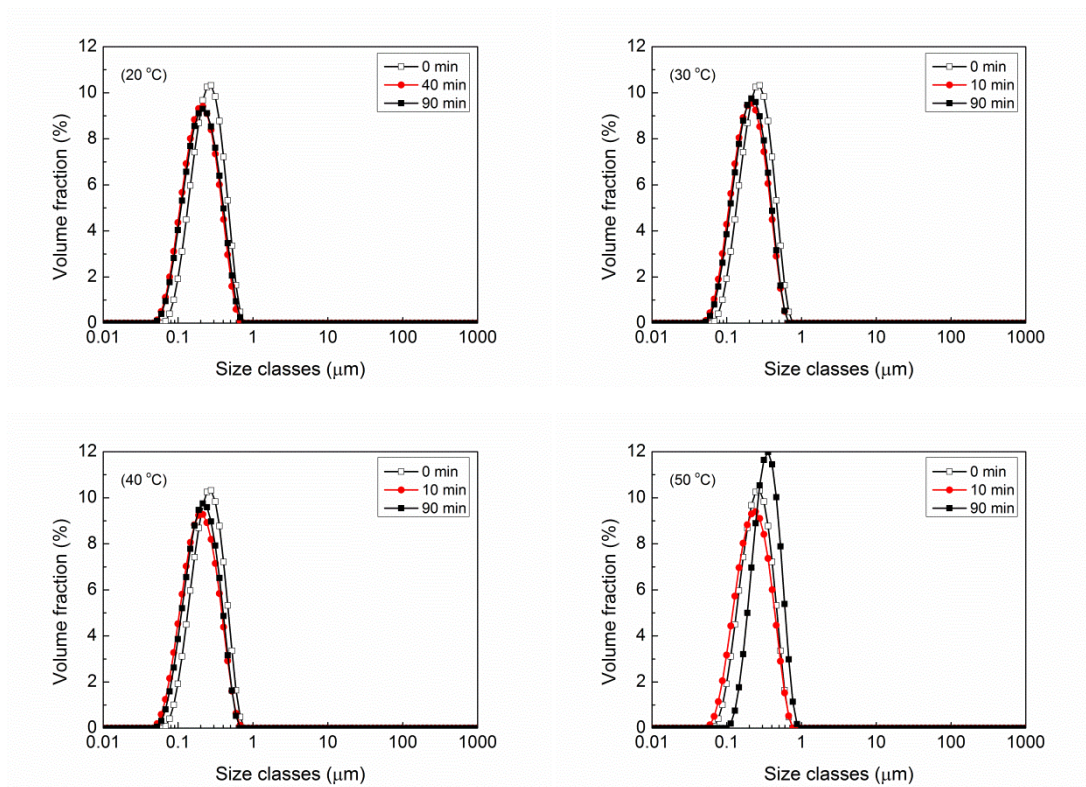


Fig.4.8 Droplet/particle size distribution at different reaction time for miniemulsion containing 10wt% C₈mimPF₆ at different temperatures initiated by H₂O₂/AAc.

For hydrophilic initiators, this is not surprising. As for micellar or homogeneous nucleation, both initiation and chain propagation requires radicals presented in water phase and this could be easily achieved for hydrophilic initiator, such as H₂O₂/AAc. Similar inferences could also be made about miniemulsion polymerisation of styrene initiated by hydrophilic initiator sodium persulfate (Chern and Liou, 1999b).

In order to evaluate the effect of nucleation mechanism on droplet/particle size, H₂O₂/AAc was replaced by the hydrophobic initiator, AIBN. The investigation on the droplet/particle size as a function of reaction time at similar temperature ranging from 30 °C to 50 °C under similar miniemulsion formula was conducted. Results are illustrated in Fig.4.9. A small reduction on droplet/particle size was observed for both 50 °C and 40 °C at initial 30 min. As the reaction progresses further, the droplet/particle size at 40°C remains unchanged, while the droplet/particle size at 50

°C increases sharply, then remains constant after 60 min until reaction is terminated. For miniemulsions at 30°C, the droplet/particle size remains unchanged though all the process may be attributed to the fact that nearly no reaction occurs.

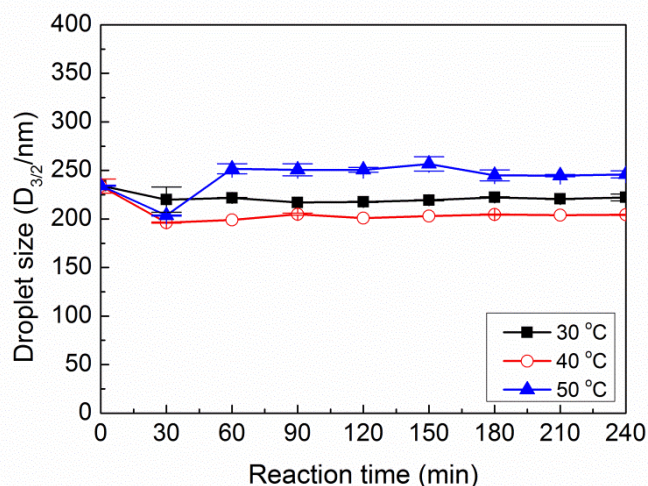


Fig.4.9 Variation of droplet/particle sizes as a function of reaction time for miniemulsion containing 10wt% C₈mimPF₆ at different temperatures initiated by AIBN.

Fig.4.10 shows the droplet/particle size distribution for miniemulsions containing 10 wt% C₈mimPF₆ at different temperatures initiated by AIBN. It is found that for the reaction temperature at 50 °C, after 240 min reaction, a more multi-modal distribution appears, whilst at 30 °C and 40 °C, only unimodal appears throughout the reaction. Some larger droplets/particles appear ranging from a few μm to 100 μm, results in an increase in mean droplet/particle size observed in Fig.4.9, though the peak distribution remained almost unchanged since the reaction started. This is a clear indication of an early stage of coalescence of droplets/particles. Compared with Fig.4.9, it might be postulated that such multi-modal distribution due to the coalescence of droplets might occur at 60 min after the reaction and be kept constant until the end of reaction. This implies that, in addition to the influence of the reaction, the final latex particle size could be affected by the coalescence of droplet/particle

induced by the temperature effect. The results appear to be consistent with ones observed in Fig.4.7, where $\text{H}_2\text{O}_2/\text{AAc}$ is used as the initiator.

By observing the main peaks at different reaction temperatures shown in Fig.4.10, it exhibits that both size range and distribution peak are almost identical, which indicates different nucleation mechanisms compared to $\text{H}_2\text{O}_2/\text{AAc}$. This suggests that droplet nucleation could play a key role for AIBN. This is not surprising since AIBN is hydrophobic. It would be expected that decomposition of AIBN to produce radicals should take place easily in oil phase, where the monomer, MMA was presented. Thus it would favour droplet nucleation, where initiation and chain propagation would occur in oil droplets. The final particles of latex would be copied from the oil droplets till termination of reaction. Thus particle size remained constant.

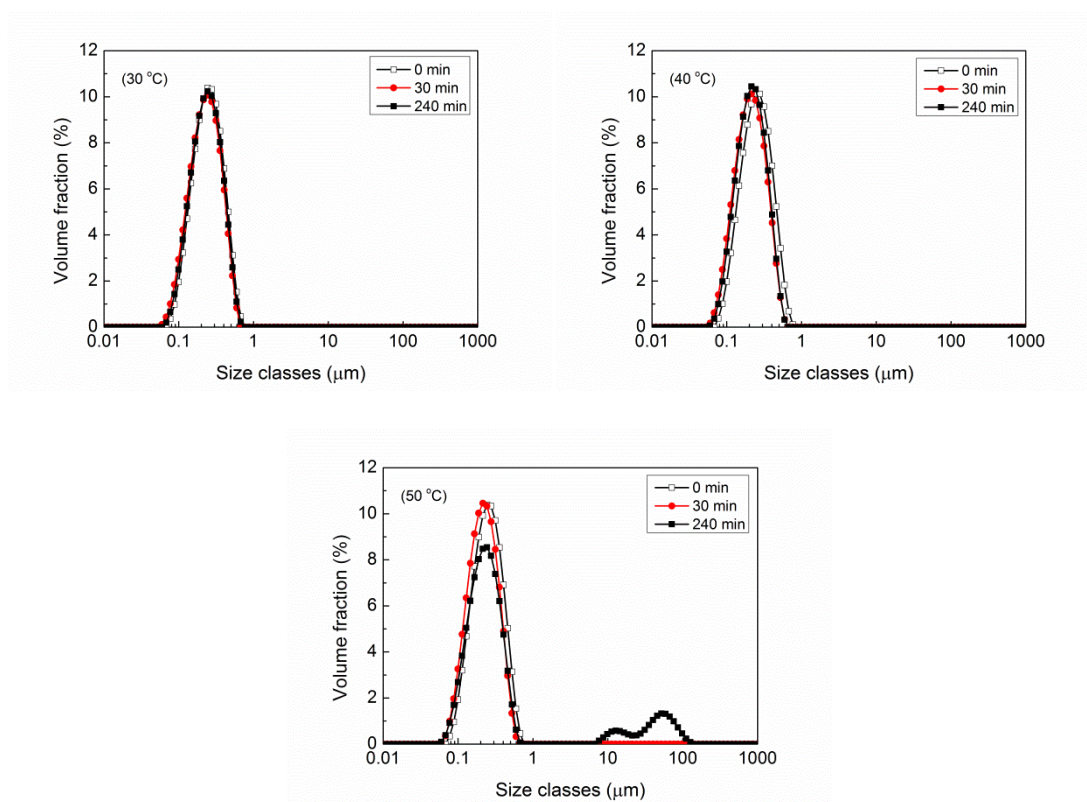


Fig.4.10 Droplet/particle size distribution at different reaction time for miniemulsion containing 10wt% C_8mimPF_6 at different temperatures initiated by AIBN.

On the other hand, the small reduction in mean droplet size for polymerisation initiated by AIBN, suggests that it is possible that the micelle or homogeneous nucleation also occurred simultaneously. Possible explanations could be that the free radicals necessary for micellar or homogeneous nucleation were generated from the small fraction of hydrophobic initiator dissolved in water phase.(Chern and Liou, 1999c, Mørk and Makame, 1997) Another source could be radicals desorbed from the droplet/particle and resided in water phase, as the solubility of radical decomposed from AIBN in water phase would increase significantly. It has been observed that isobutyroni-trile which has the same structure as radicals generated from AIBN but in its molecular state is far more hydrophilic as compared with AIBN.(Shang and Shan, 2012) Thus it is possible that radicals generated from AIBN may diffuse quickly from droplets into aqueous phase after reaction started and they became the source of radicals for micellar or homogeneous nucleation.

4.3.1.2.2 Effect of initiator concentration on stability

To illustrate the mechanism for the initiator concentration effect, the formula of miniemulsion and polymerisation conditions were the same as the ones when we studied the effect of initiator concentration on kinetics of miniemulsion polymerisation.

Fig.4.11 shows the droplet size as a function of reaction time for miniemulsion containing 10wt% C_8mimPF_6 at different H_2O_2/AAC concentrations. The trends of decrease are observed for 2.0 mol%, 1.0 mol%, and 0.5 mol% at initial 30 min, indicating the micellar or homogeneous nucleation as described in section 4.3.2.1.1. The degree of decrease for 2.0 mol% was less compared with the other two, and this

will be explained in Fig.4.12. Because nearly no reaction happened for 0.1 mol% H_2O_2 , the droplet size remains stable all the process.

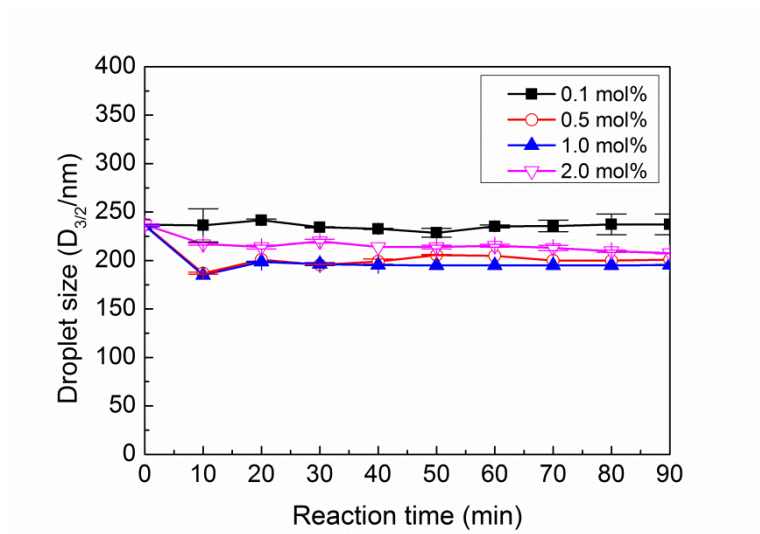


Fig.4.11 Variation of droplet size as a function of reaction time for miniemulsion containing 10wt% C_8mimPF_6 at different H_2O_2/Aa concentrations.

Fig.4.12 shows the droplet size distribution at different reaction time for miniemulsion containing 10wt% C_8mimPF_6 at different H_2O_2/Aa concentrations. Droplet size distribution moves towards smaller size after the initiation of reaction for 2.0 mol%, 1.0 mol%, and 0.5 mol% at initial 30 min. In the case of 2.0 mol%, a second peak in the range of 1 μm to 10 μm appears, indicating the aggregation of droplets. This peak slows down the trend of decrease mentioned in Fig.4.11. As reaction continues, droplet size distribution does not change obviously till the end of reaction for 1.0 mol%, and 0.5 mol%. But for 2.0 mol%, the second peak becomes broader, representing the aggravation of aggregation. Because nearly no reaction happened for 0.1 mol%, the droplet size distribution remains the same all the process.

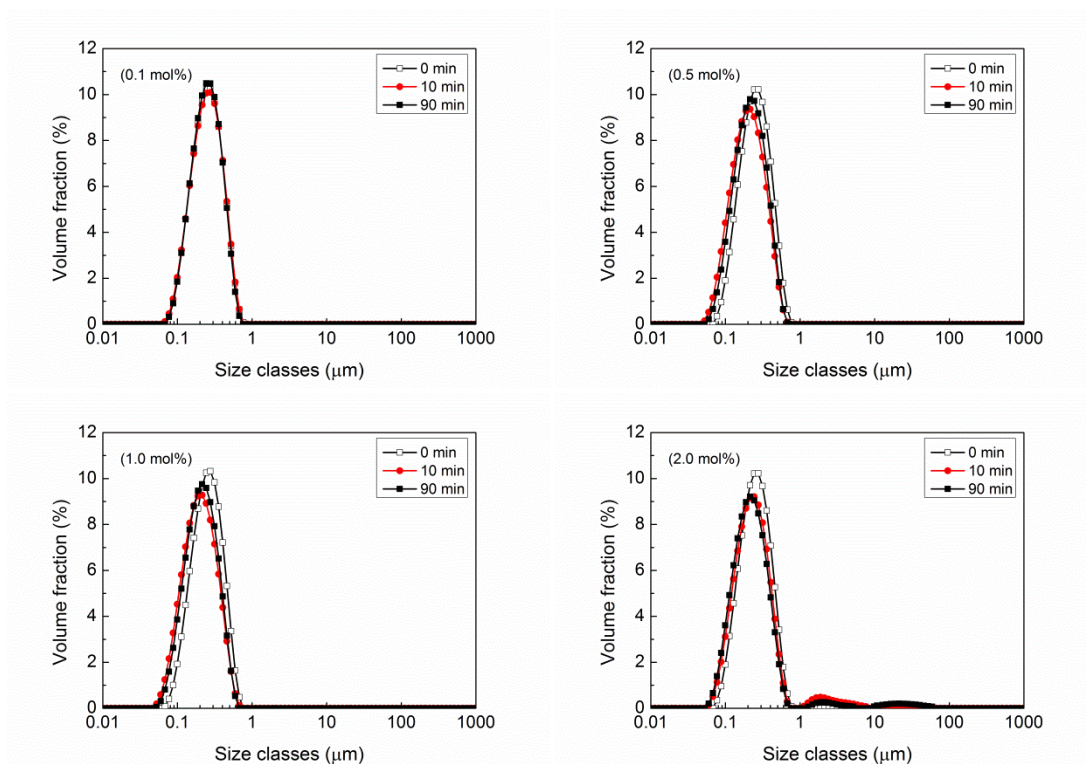


Fig.4.12 Droplet size distribution at different reaction time for miniemulsion containing 10wt% C_8mimPF_6 at different H_2O_2/AAC concentrations.

Fig.4.13 shows the droplet size as a function of reaction time for miniemulsion containing 10wt% C_8mimPF_6 concentration at different AIBN concentration. The trends of decrease are observed for all concentrations, indicating the micellar or homogeneous nucleation as described in section 4.3.2.1.1. In the following reaction, the droplet size of 1.0, 0.5, and 0.1 mol% remains stable, while the size of 2.0 mol% increases where it is accompanied by remarkable droplet coalescence.

Fig.4.14 shows the droplet size distribution at different reaction time for miniemulsion containing 10wt% C_8mimPF_6 at different AIBN concentrations. Droplet size distribution moves towards smaller size after the initiation of reaction for all concentrations at initial 30 min. As reaction continues, droplet size distribution does not change obviously till the end of reaction for 1.0 mol%, 0.5 mol%, and 0.1 mol%.

But for 2.0 mol%, a second peak in the range of 10 μm to 1000 μm appears, indicating the aggregation of droplets.

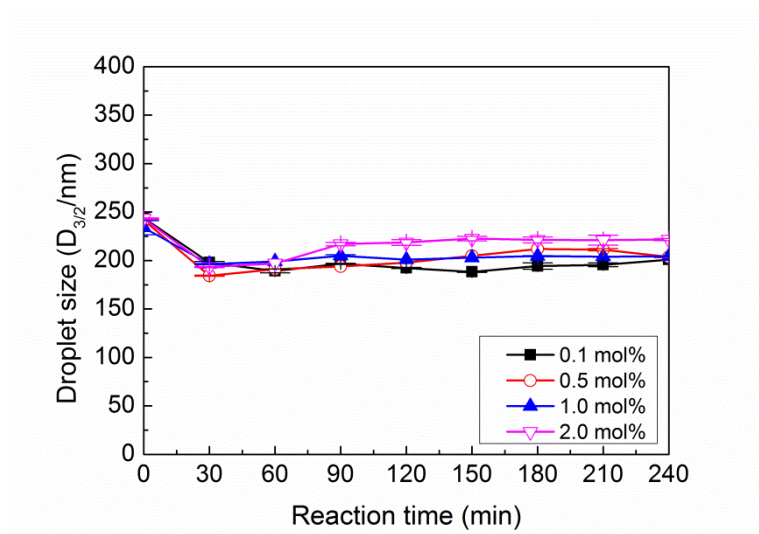


Fig.4.13 Variation of droplet size as a function of reaction time for miniemulsion containing 10wt% C_8mimPF_6 at different AIBN concentrations.

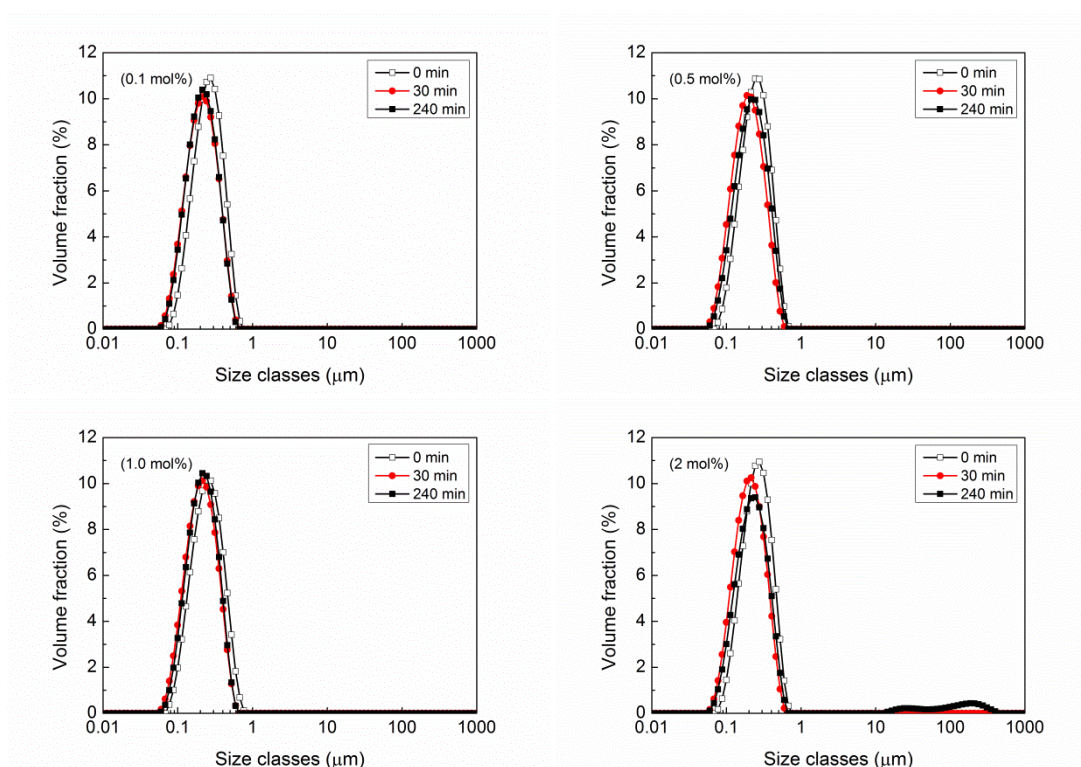


Fig.4.14 Droplet size distribution at different reaction time for miniemulsion containing 10wt% C_8mimPF_6 at different AIBN concentrations

4.3.1.2.3 Effect of C_8mimPF_6 concentration on stability

In order to investigate the underlying mechanism for the C_8mimPF_6 effect on droplet/particle size of miniemulsion during polymerisation, experiments were conducted using the same formula of miniemulsion and polymerisation conditions as the experiments investigating the effect of C_8mimPF_6 on the yield of polymer.

Fig.4.15 shows the variation of droplet/particle sizes as a function of reaction time for miniemulsions containing different C_8mimPF_6 concentrations initiated by AIBN. The reduction in droplet/particle size for miniemulsions containing 1, 5, 10, 20, 30 wt% of C_8mimPF_6 after the initial 30 min of starting reaction is observed. This may be attributed to micellar or homogeneous nucleation as described in section 4.3.2.1.1. With the progression of the reaction, the droplet/particle size for the miniemulsions containing 1 wt%, 5 wt%, and 10 wt% C_8mimPF_6 remains unchanged. This suggests that the droplet nucleation is a more dominating factor to influence the droplet/particle size, which is consistent to the one observed in section 4.3.2.1.1. Such observations are very different to those without reactions, in which the change of C_8mimPF_6 concentration would cause remarkable differences in the rate of increase of droplet size during storage. Details about this work were reported in our early work (Kong et al., 2015). Fig.4.15 shows that the droplet/particle size increases significantly for miniemulsions with 20 wt% and 30 wt% C_8mimPF_6 , as the reaction progresses. It is worth mentioning that with the increase of storage time (where no reaction took place), the droplet size of miniemulsions containing higher concentrations of C_8mimPF_6 also increased to a similar magnitude as mentioned in 3.3.1.2.3. This indicates that although the droplet nucleation appeared to be

dominating, the final particle size of latex was strongly influenced by the droplet/particle size at the early stage of reaction and the storage stability.

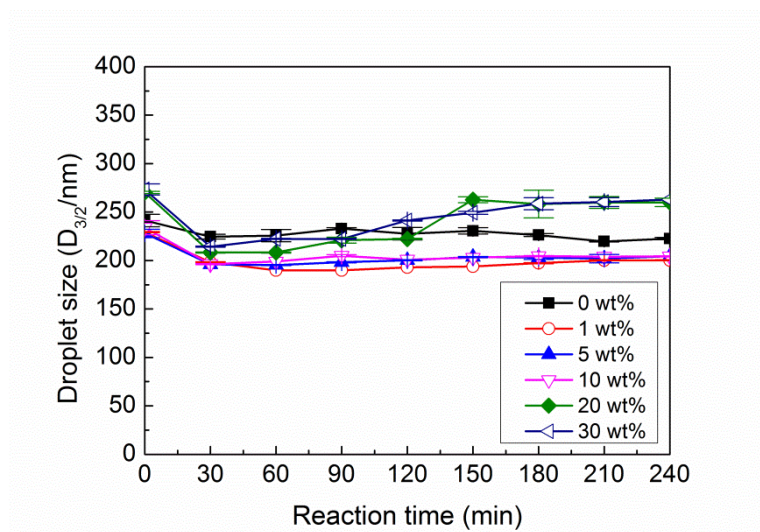


Fig.4.15 Variation of droplet/particle sizes as a function of reaction time for miniemulsions containing different C_8mimPF_6 concentrations initiated by AIBN.

Fig.4.16 shows the variation of droplet/particle sizes as a function of reaction time for miniemulsions containing different C_8mimPF_6 concentrations initiated by H_2O_2/AAC . The decreasing trends are observed for all C_8mimPF_6 concentrations for the initial 10 min, which confirm the occurrence of micellar or homogeneous nucleation during reaction. As the reaction progresses, the droplet/particle size for miniemulsions containing different concentrations of C_8mimPF_6 ranging from 0 to 20 wt% remains constant, while at 30 wt% concentration of C_8mimPF_6 , droplet/particle size increases significantly due to droplet coalescence. This confirms the dependency of intrinsic storage stability of miniemulsion on final particle size of latex, which was supported by the system where AIBN was used as initiator.

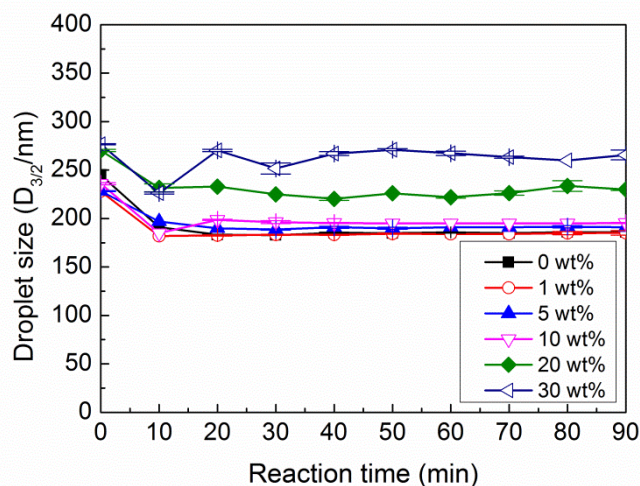


Fig.4.16 Variation of droplet/particle sizes as a function of reaction time for miniemulsions containing different C₈mimPF₆ concentrations initiated by H₂O₂/AAc.

4.3.2 Miniemulsion stabilised by silica nanoparticle

In order to overcome the lacks in gloss and water resistance of film caused by surfactant residual, silica nanoparticle, as an alternative to conventional surfactant, was employed to stabilise miniemulsion containing C₈mimPF₆. The effects of initiator type, temperature, pH of water phase, and C₈mimPF₆ concentration on yield of polymer as well as stability of miniemulsion during polymerisation were investigated.

4.3.2.1 Factors affecting yield of polymer during miniemulsion polymerisation

4.3.2.1.1 Effect of initiator type on yield of polymer

Two types of initiators, hydrophobic AIBN, and hydrophilic H₂O₂/AAc were used to initiate the polymerisation. Based on our previous study, in the stabilisation of surfactant, sodium dodecyl sulfonate (SDSO), reaction rate of miniemulsion containing C₈mimPF₆ was strongly depended on the type of initiator used, due to the difference in site where radicals generated. To study effect of initiator type on Pickering miniemulsion polymerisation, a miniemulsion containing 10 wt%

C_8mimPF_6 stabilised by 50 g/l silica nanoparticles (pH = 3) was prepared and initiated by 1.0 mol% AIBN and 1.0 mol% H_2O_2/Ac at 40 °C. For AIBN, it was dissolved in oil phase before the preparation of miniemulsion, while in terms of H_2O_2/Ac , polymerisation was initiated by injecting its water solution in miniemulsion.

Fig.4.17 shows the yield of polymer as a function of reaction time for miniemulsion containing 10 wt% C_8mimPF_6 stabilised by silica nanoparticles in the initiation of AIBN and H_2O_2/Ac at 40 °C. It is observed that when stabilised by silica nanoparticles, AIBN results in a higher final yield of polymer (86.0%). The yield of polymer is in a gentle increase at initial 5 h, followed by a sharp increase in the coming 2.5h, and then fades down at the end of polymerisation, 7.5 h. Whilst for H_2O_2/Ac , a sharp increase in yield of polymer is observed within 30 min, then no further polymerisation takes place until the end with a value of 28.1% in final yield of polymer.

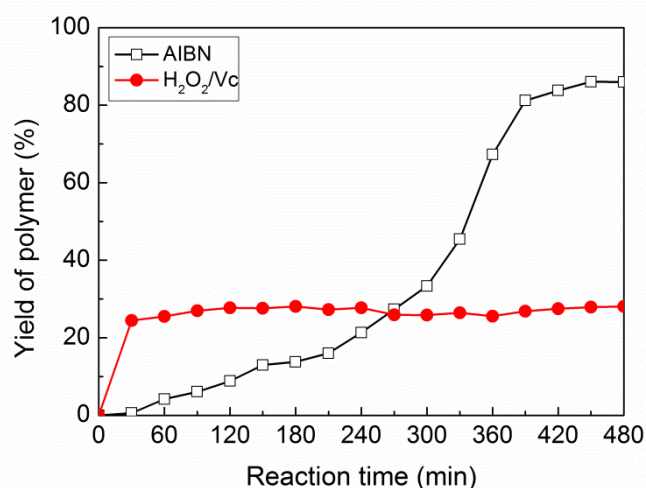


Fig.4.17 Yield of polymer as a function of reaction time for miniemulsion containing 10 wt% C_8mimPF_6 stabilised by silica nanoparticles in the initiation of AIBN and H_2O_2/Ac at 40 °C.

It is interesting to note that, when initiated by H_2O_2/Ac , miniemulsion stabilised by SDSO has a much higher final yield (100%) as shown in Fig.4.2,

compared with the one stabilised by silica nanoparticles (28.1%). This difference in yield of polymer might be attributed to the fact that miniemulsion polymerisation is a heterogeneous reaction, hence mass transfer of radicals between oil phase and water phase shall be considered. For hydrophilic H_2O_2/AAC , radicals were generated in water phase, and they can only initiate the polymerisation after entering the oil droplet. Interfacial structure between water phase and droplet directly affected the entry of radicals. When stabilised by silica nanoparticles, these solid particles accumulated at the droplet-water interface might be in a tighter spatial arrangement. It was confirmed by the observation of polymer particle, the product of miniemulsion shown in Fig.5.17. It can be seen from SEM image that the surface of polymer particle was covered with closely packed solid particles in a diameter around 20 nm. The tighter interfacial structure may strongly reduce the entry rate of radicals into droplet, (Gan et al., 1992, Mosca et al., 2013, Cao et al., 2008) resulting in lower final yield of polymer, i.e. 28.1%. Such inefficiency in yield of polymer caused by a hydrophilic initiator, potassium persulfate (KPS), was also reported by Zhou *et al.* when studied polymerisation of Pickering emulsion stabilised by silica nanoparticle.(Zhou et al., 2013) The inefficiency could be ascribed to the obstacle to mass transfer caused by the “densely packed” silica nanoparticles on the surface of droplets. While in the stabilisation of SDSO, radicals generated in water phase may still have access to droplets. Otherwise, such high final yield of polymer could not be achieved.

4.3.2.1.2 Effect of temperature on yield of polymer

In order to study the effects of temperature, a miniemulsion containing 10 wt% C_8mimPF_6 in the stabilisation of 50 g/l silica nanoparticles (pH = 3) was prepared,

and initiated by 1.0 mol% AIBN at temperatures ranging from 30 °C to 60 °C. The product was visually stable at all temperatures, which meant no phase separation, sedimentation, and coagulation was detected during polymerisation.

Fig.4.18 shows the yield of polymer as a function of reaction time for the miniemulsion containing 10 wt% C_8mimPF_6 at different temperatures initiated by AIBN.

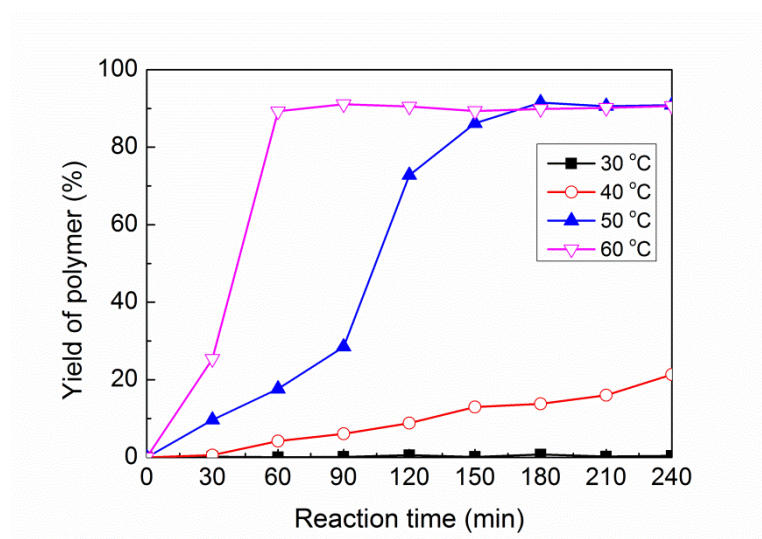


Fig.4.18 Yield of polymer as a function of reaction time for miniemulsion containing 10 wt% C_8mimPF_6 at different temperatures initiated by AIBN.

It is observed that 60 °C results in a high final yield of polymer (91.1 %) and the shortest reaction time (1 h). Whilst at 50 °C, a gentle increase in yield of polymer is observed within 1.5 h, followed by a sharp increase in the coming 1.0h, and then polymerisation ends at 3 h with a final yield of 91.4%. At 40 °C, polymerisation still continues at the end of 4 h in a slow reaction rate, and fades down at 8 h with a final yield of 86.0% shown in Fig.4.17. From Fig.4.18, it is also noted that at 30 °C, nearly no reaction occurs. The change in reaction rate observed in Fig.4.18 was mainly caused by the difference in decomposition rate of initiator at different temperature which was explained in 4.3.1.1.1. The high final yield (86.0%) achieved at 40 °C,

which was below the efficient decomposition temperature of AIBN, again confirmed the enhancement in chain propagation rate and the reduction in termination rate of free radical polymerisation caused by C_8mimPF_6 as discussed in 4.3.1.1.3.

4.3.2.1.3 Effect of pH of water phase on yield of polymer

In order to study effects of pH of water phase, water phases containing 50 g/l silica nanoparticles with different pH (3, 5, 7, 9, and 11) were prepared. Oil phase contained 10 wt% C_8mimPF_6 , 85 wt% MMA and 5 wt% HD. Miniemulsion was prepared by homogenising oil phase with water phase, and initiated by 1.0 mol% AIBN at 60 °C. When pH of water phase was 9 and 11, phase separation occurred soon after initiation, and final product was in a state of blocks. While at a pH of 7 and 5, no phase separation was detected, however, miniemulsion became viscous during polymerisation. Final product was lack of fluidity. Stable product could only be achieved at pH=3. More detail discussion about pH of water phase on stability of miniemulsion will be carried out in 4.3.2.1.3.

Fig.4.19 shows the yield of polymer as a function of reaction time for the miniemulsion containing 10 wt% C_8mimPF_6 at different pH of water phase. It is observed that the reaction times for all pH were similar, 1 h. However, the final yield of polymer was different. PH of 5 has the highest final yield with a value of 96.1%, followed by pH of 3 (91.1%), and lowest was pH of 7 with a value of 81.7%. Because phase separation occurred at the beginning of polymerisation for pH of 9 and 11, they are not shown in Fig.4.19.

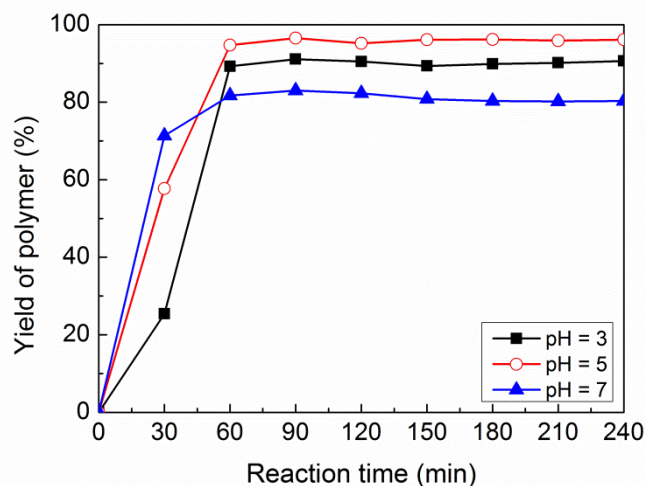


Fig.4.19 Yield of polymer as a function of reaction time for the miniemulsion containing 10 wt% C_8mimPF_6 at different pH of water phase.

4.3.2.1.4 Effect of C_8mimPF_6 concentration on yield of polymer

To study effect of C_8mimPF_6 concentration, oil phases containing different concentrations of C_8mimPF_6 ranging from 0 wt% to 30 wt% were prepared. Water phase contained 50 g/l silica with a pH of 3. Miniemulsion was prepared by homogenising oil phase with water phase, and initiated by 1.0 mol% AIBN at 60 °C. When C_8mimPF_6 concentrations was 0 wt%, 1 wt% and 5 wt%, miniemulsion became viscous during polymerisation, and final product was lack of fluidity. Stable product could be achieved at 10 wt%, 20 wt% and 30 wt% C_8mimPF_6 . More detail discussion about C_8mimPF_6 concentration on stability of miniemulsion will be carried out in 4.3.2.1.3.

Fig.4.20 shows the yield of polymer as a function of reaction time for miniemulsions containing different C_8mimPF_6 . It is observed that miniemulsions containing 0 wt% and 1 wt% C_8mimPF_6 have a longer reaction time, 1.5 h, with a final yield of 84.5% for 0 wt% C_8mimPF_6 and 83.0% for 1 wt% C_8mimPF_6 . Reaction time reduces to 1 h for miniemulsions containing 5 wt%, 10 wt%, 20 wt%, and 30

wt% C_8mimPF_6 . Their final yields are similar in values, which are 87.3% for 5 wt% C_8mimPF_6 , 89.2% for 10 wt% C_8mimPF_6 , 95.0% for 20 wt% C_8mimPF_6 , and 91.6% for 30 wt% C_8mimPF_6 .

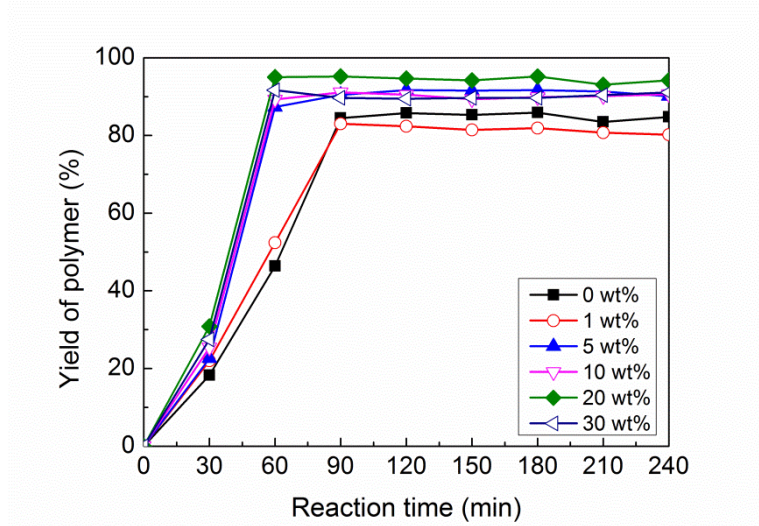


Fig.4.20 Yield of polymer as a function of reaction time for miniemulsion containing different C_8mimPF_6

4.3.2.2 Factors affecting stability of miniemulsion during polymerisation

4.3.2.2.1 Effect of temperature on stability

To illustrate the mechanism for the temperature effect, the formula of miniemulsion and polymerisation conditions were the same as the ones when we studied the effect of temperature on yield of polymer of miniemulsion polymerisation.

Although miniemulsion was visually stable during polymerisation, in a microscope, droplets/particles could be bridged together, (Musyanovych et al., 2007) leading to the increase in droplet/particle size. Droplet/particle sizes at different reaction time were also measured to monitor the stability of miniemulsion. Fig.4.21 illustrates variation of droplet/particle sizes as a function of reaction time for miniemulsion containing 10 wt% C_8mimPF_6 at different temperatures initiated by

AIBN. For 60 °C, 50 °C, 40 °C, an increase in droplet/particle size is accompanied with polymerisation. Such increase stops at a time when no further polymerisation takes place, *e.g.* 1.0 h for 60 °C with a size of 1102 nm, 3.0 h for 50 °C with a size of 1200 nm, and 7.5 h for 40 °C with a size of 1197 nm. For miniemulsion at 30°C, the droplet/particle size remains unchanged though all the process attributed to the fact that nearly no reaction occurs.

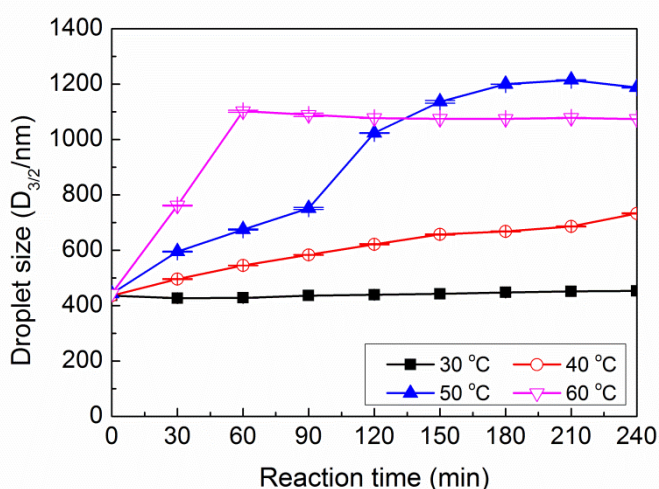


Fig.4.21 Variation of droplet/particle sizes as a function of reaction time for miniemulsion containing 10 wt% C₈mimPF₆ at different temperatures initiated by AIBN.

It is interesting to note that, miniemulsion stabilised by silica nanoparticle performed different stability compared with the one stabilised by surfactant, depending on the polymerisation temperature. At 40 °C, final particle size of miniemulsion stabilised by silica nanoparticle was 1197 nm, almost 2.7 times larger than original droplet size, 436 nm. While for miniemulsion stabilised by SDSO, final particle size was 205 nm, nearly the same as original droplet size, 234 nm. It can be seen that miniemulsion stabilised by silica nanoparticles had a worse stability than the one stabilised by SDSO when polymerised 40 °C. Such worse stability was probably not due to increase in temperature, *i.e.* from room temperature to 40 °C. Because from

the result of Fig.3.22, which shows variation of droplet sizes as a function of storage time for miniemulsion in the absence of initiator, there is little change on droplet size when stored at 40 °C. That means at this temperature, droplet/particle movement was not frequent enough, leading to droplet/particles coalescence. A possible reason for the instability was due to the incompatibility between silica nanoparticles and polymer core when monomer transfers into polymer, which is a common challenge for silica nanoparticle as a Pickering emulsifier.(Schrade et al., 2013) So with the conduct of polymerisation, silica nanoparticles may desorb from droplet/particles due to this incompatibility, leading to more frequent coalescence.

At 60 °C, final particle size of miniemulsion stabilised by silica nanoparticle was 1102 nm, 2.5 times larger than original droplet size, 436 nm. While for miniemulsion stabilised by SDSO, phase separation occurred. Miniemulsion stabilised by SDSO had a worse stability than the one stabilised by silica nanoparticle. Such worse stability was probably due to high polymerisation temperature. At this temperature, even in the absence of initiator, phase separation took place within 30 min (shown in 3.3.1.2.3). This means electrostatic repulsion between droplets attributed by SDSO cannot effectively prevent droplet/particle collision due to high frequency of droplet/particle movement at such high temperature, thus leading to coalescence and phase separation, finally. However, for miniemulsion stabilised by silica nanoparticle, even though droplet/particle suffer from coalescence due to desorption of silica nanoparticle and high temperature, silica nanoparticle closely packed at surface of droplet/particle may act as a barrier that can prevent coalescence between droplet/particle. Such steric repulsion seems more effective in keeping droplet/particle stable at higher temperature.

4.3.2.2.2 Effect of pH of water phase on stability

In order to investigate the effect of C_8mimPF_6 on stability of miniemulsion during polymerisation, experiments were conducting using the same formula of miniemulsion and polymerisation conditions as the ones when we studied the effect of pH of water phase on yield of polymer during miniemulsion polymerisation. The pH of water phase ranged from 3, 5, 7, and 9 to 11.

Fig.4.22 illustrates variation of droplet/particle sizes as a function of reaction time for miniemulsion containing 10wt% C_8mimPF_6 at different pH of water phase. When pH is 7, droplet/particle size sharply increases and peaks at 4660 nm after reaction started about 0.5 h. At the same time, miniemulsion became extremely viscous. Droplet/particle size then reduces continuously to 2650 nm at 1 h, the time polymerisation completes. A small reduction in droplet/particle size to 2000 nm at 1.5 h then occurs though the result on yield of latex shown in Fig.4.19 indicates no further reaction takes place. While for pH of 5 and 3, droplet/particle size gently increases until the end of polymerisation, 1 h, then remains relatively stable.

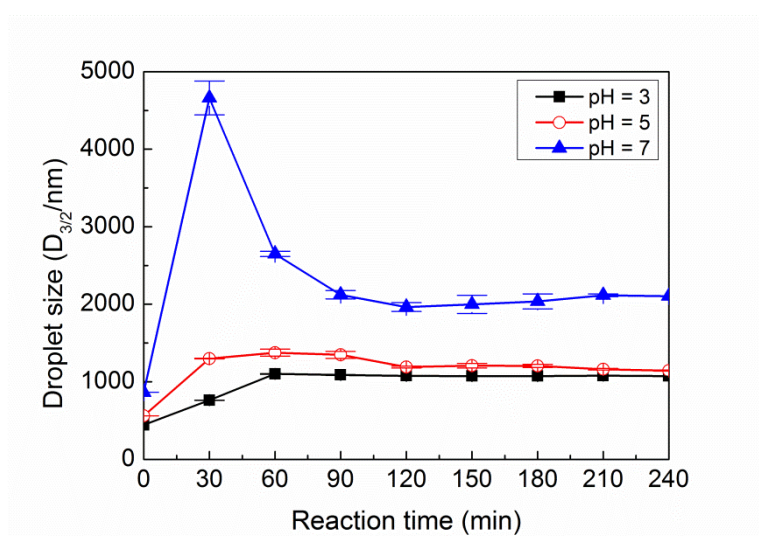


Fig.4.22 Variation of droplet/particle sizes as a function of reaction time for miniemulsion containing 10wt% C_8mimPF_6 at different pH of water phase.

Morphologies of products after polymerisation were observed by SEM to study effect of pH of water phase on stability of final product. The results are shown in Fig.4.23.

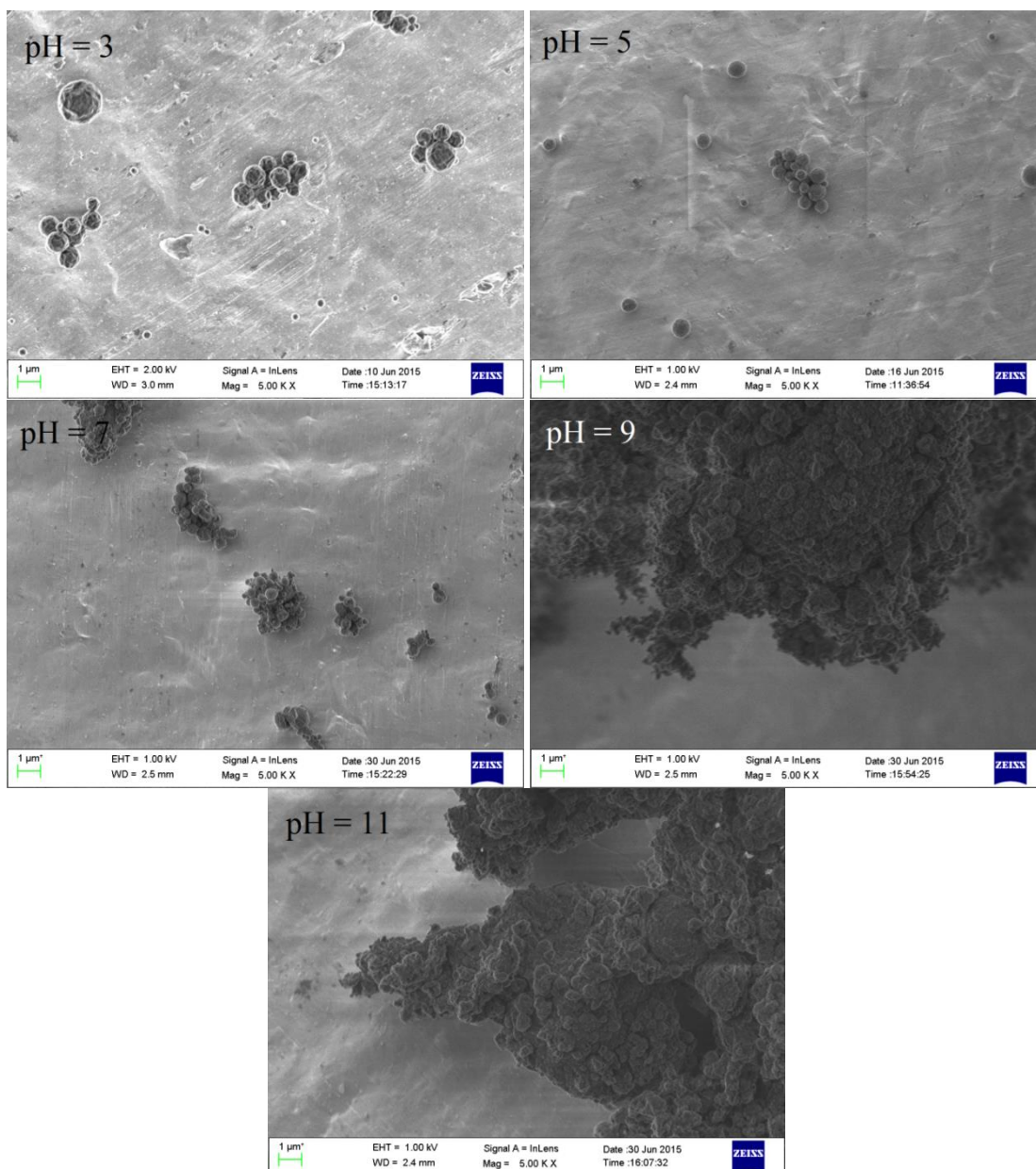


Fig.4.23 Morphologies of products after polymerisation at different of pH of water phase

At low pH, *e.g.* 3 and 5, particles are in spherical shapes. Some particles separate individually, and some particles aggregate into clusters. This aggregation might be the reason causing the increase in droplet/particle size during

polymerisation. At a pH of 7, most particles aggregate into bigger clusters, and the spherical shape of particle can be detected on the outer layer of cluster. While for pH of 9 and 11, only large irregular shape of aggregated blocks with a size larger than micron level can be detected. The spherical shape of particle cannot be detected on the outer layer of blocks. This indicates that phase separation occurred before the formation of particles; otherwise spherical shapes would be kept, and could be detected on the outer layer of blocks or single particle. By the comparison of products obtained at different pH, it can be seen that stable product could be achieved in acid environment. Once the water phase becomes basic, the particles produced would become unstable.

Products prepared at a pH of 5 and 7 were viscose, especially 7 which was lack of fluidity. In order to detect rheological property of products, variation of viscosities as a function of shear rate for products prepared under different pH of water phase were measured. The result is shown in Fig.4.24. It can be seen that viscosities decrease remarkably with the increase of shear rate for products prepared under pH = 5, and 7. For example, viscosity of pH = 7 is 10.42 Pa·s at 0.1 s^{-1} , and this value sharply decreases to 0.020 Pa·s when shear rate increases to 1000 s^{-1} . Normally, decreasing in viscosity with the increase of shear rate is refereed as a shear thinning behaviour.(Yilmaz, 2014) This shear thinning behavior suggested the presence of aggregation, thus the decrease of viscosity at higher shear rates indicated the breaking of aggregation into primary particles.(Wittmar et al., 2012) While such decrease is less remarkable for pH = 3. The value of viscosity is 0.093 Pa·s at 0.1 s^{-1} , and decreases to 0.003 Pa·s as the increase of shear rate up to 1000 s^{-1} . It can be seen that aggregation for pH = 3 was much less apparent.

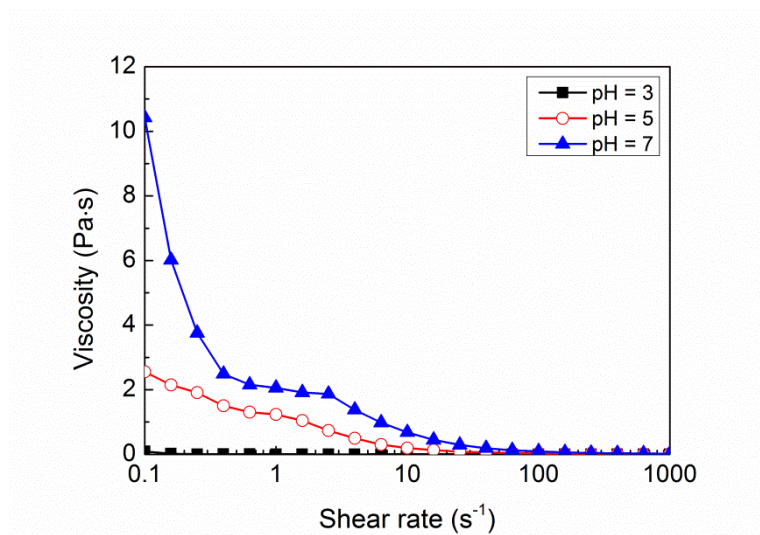


Fig.4.24 Variation of viscosities as a function of shear rate for products prepared under different water phase pH

To sum up the above results, pH of water phase strongly affected droplet/particle size during polymerisation as well as stability of product which was confirmed by corresponding morphologies of product, and rheological property of product. The change in pH of water phase may affect absolute zeta potential of silica nanoparticle, thus in turn leading to the difference in stability of miniemulsion during polymerisation. From the result of Fig.3.22, zeta potential of silica nanoparticles sharply decreased from -2.0 mV to -31.6 mV with the increase of pH from 3 to 7. Then this trend fades down, with a slight decrease from -31.6 mV to -38.8 mV, as the pH of water phase continually increases to 11. Especially, zeta potential was close to 0, the isoelectric point, when pH of water phase was 3. Around the isoelectric point, *i.e.* pH = 3, electrostatic repulsion between silica nanoparticles adsorbed on the surface of droplets was low. That means the surface of droplets could accommodate more silica nanoparticles due to the weak electrostatic repulsion. As more silica nanoparticles was close-packed on the surface of droplet/particles, static repulsion between droplet/particles was enhanced, which could efficiently prevent aggregation.

This might be the main reason for a stable product being achieved at pH = 3. With the increase in pH, electrostatic repulsion between silica nanoparticles adsorbed on the surface of droplets became high, thus the surface of droplet could hold less silica nanoparticles. Due to the lack of silica nanoparticles on the surface of droplet/particles, static repulsion between droplet/particles was reduced. So aggregation between droplet/particles, and even phase separation were easier to happen. Fig.4.25 shows polymerisation process of miniemulsion at difference pH of water phase, and illustrates the difference in stability due to the change in pH. Fortuna *et al.* also adjusted the pH of system to 3.5, in order to reduce the surface charge of silica nanoparticles when preparing silica nanoparticles armored polystyrene particles by Pickering miniemulsion polymerisation.(Fortuna et al., 2009)

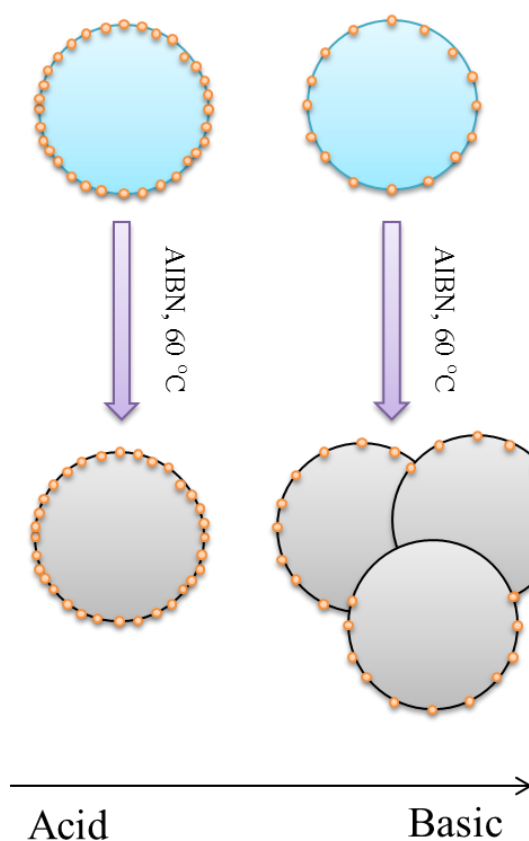


Fig.4.25 Polymerisation process of miniemulsion at difference pH of water phase

4.3.2.2.3 Effect of C_8mimPF_6 concentration on stability

In order to investigate the underlying mechanism for the C_8mimPF_6 effect on stability of miniemulsion during polymerisation, experiments were conducting using the same formula of miniemulsion and polymerisation conditions as the ones when we studied the effect of C_8mimPF_6 concentration on yield of polymer during miniemulsion polymerisation.

Fig.4.26 illustrates variation of droplet/particle sizes as a function of reaction time for miniemulsions containing different concentrations of C_8mimPF_6 . An increase in droplet/particle size is accompanied with polymerisation for all C_8mimPF_6 concentrations. Such increase stops at a time when no further polymerisation takes place, e.g. 1.5 h for 0 wt% and 1 wt% C_8mimPF_6 , and 1 h for 5 wt%, 10 wt%, 20 wt%, and 30 wt% C_8mimPF_6 . The final particle sizes for 0 wt%, 1 wt%, and 5 wt% C_8mimPF_6 are larger, with a value of 1271 nm, 1221 nm, and 1172 nm, respectively. While the sizes for 10 wt%, 20 wt%, and 30 wt% C_8mimPF_6 are smaller, with a value of 1074 nm, 997 nm, and 974 nm, respectively.

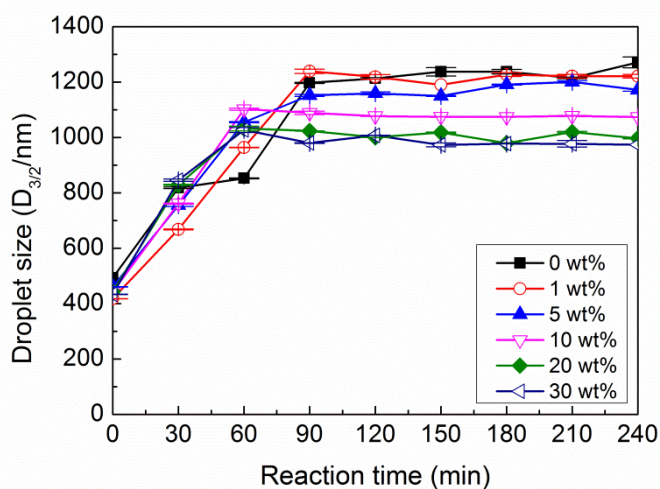


Fig.4.26 Variation of droplet/particle sizes as a function of reaction time for miniemulsions containing different C_8mimPF_6

Morphologies of products after polymerisation were observed by SEM to study effect of C_8mimPF_6 concentration on stability of final product. The results are shown in Fig.4.27. Particles in spherical shapes can be detected for all products. Some particles exist apart, and some particles aggregate into clusters. The aggregation is more apparent for 0 wt%, 1 wt% and 5 wt% C_8mimPF_6 , which might be the reason causing the increase in droplet/particle size during polymerisation.

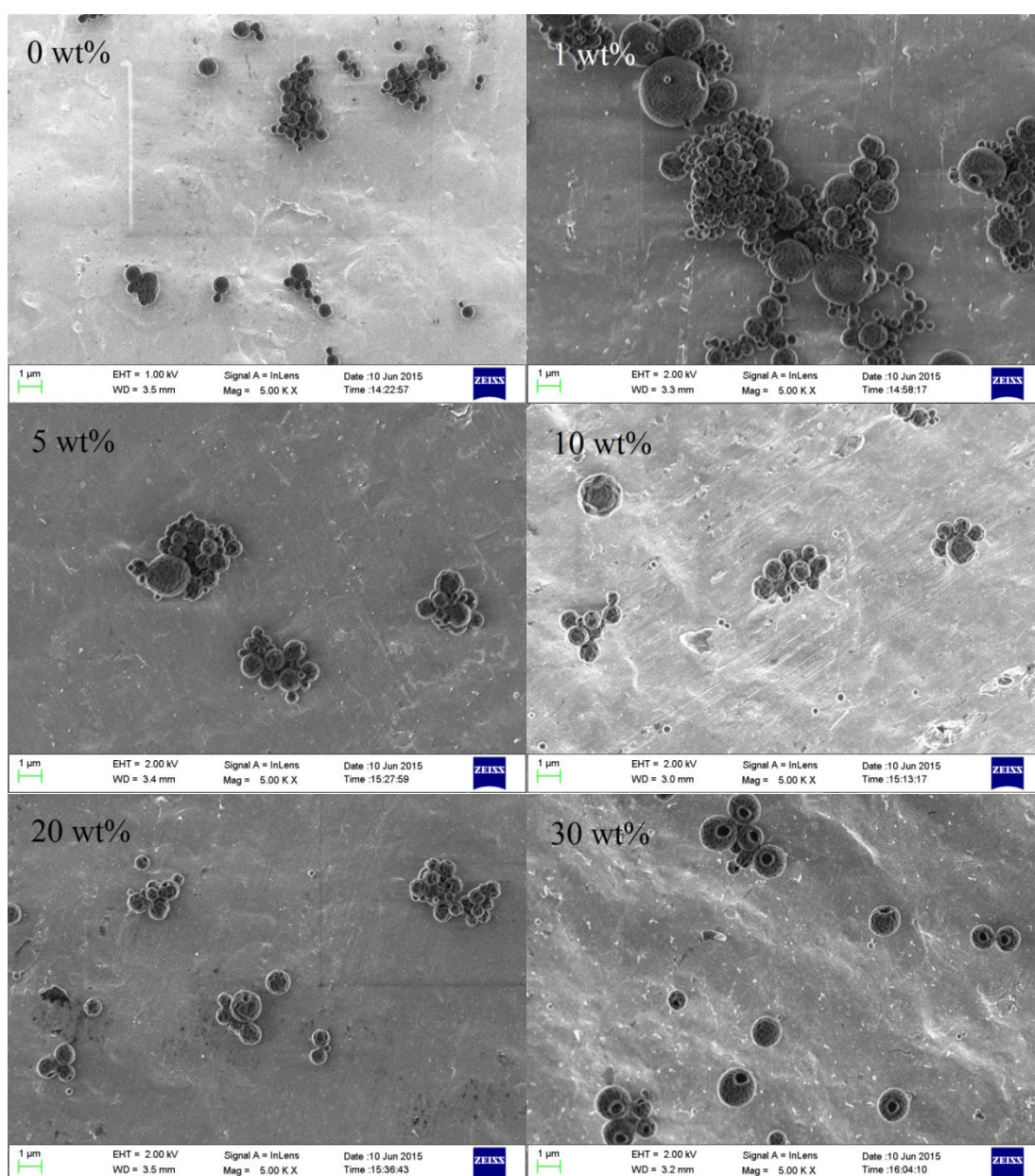


Fig.4.27 Morphologies of products after polymerisation

Droplet/particle size distribution at different reaction time for miniemulsion containing different concentrations of C_8mimPF_6 was measured to further reveal effect of C_8mimPF_6 concentration on stability of miniemulsion before and after polymerisation. The result is shown in Fig.4.28.

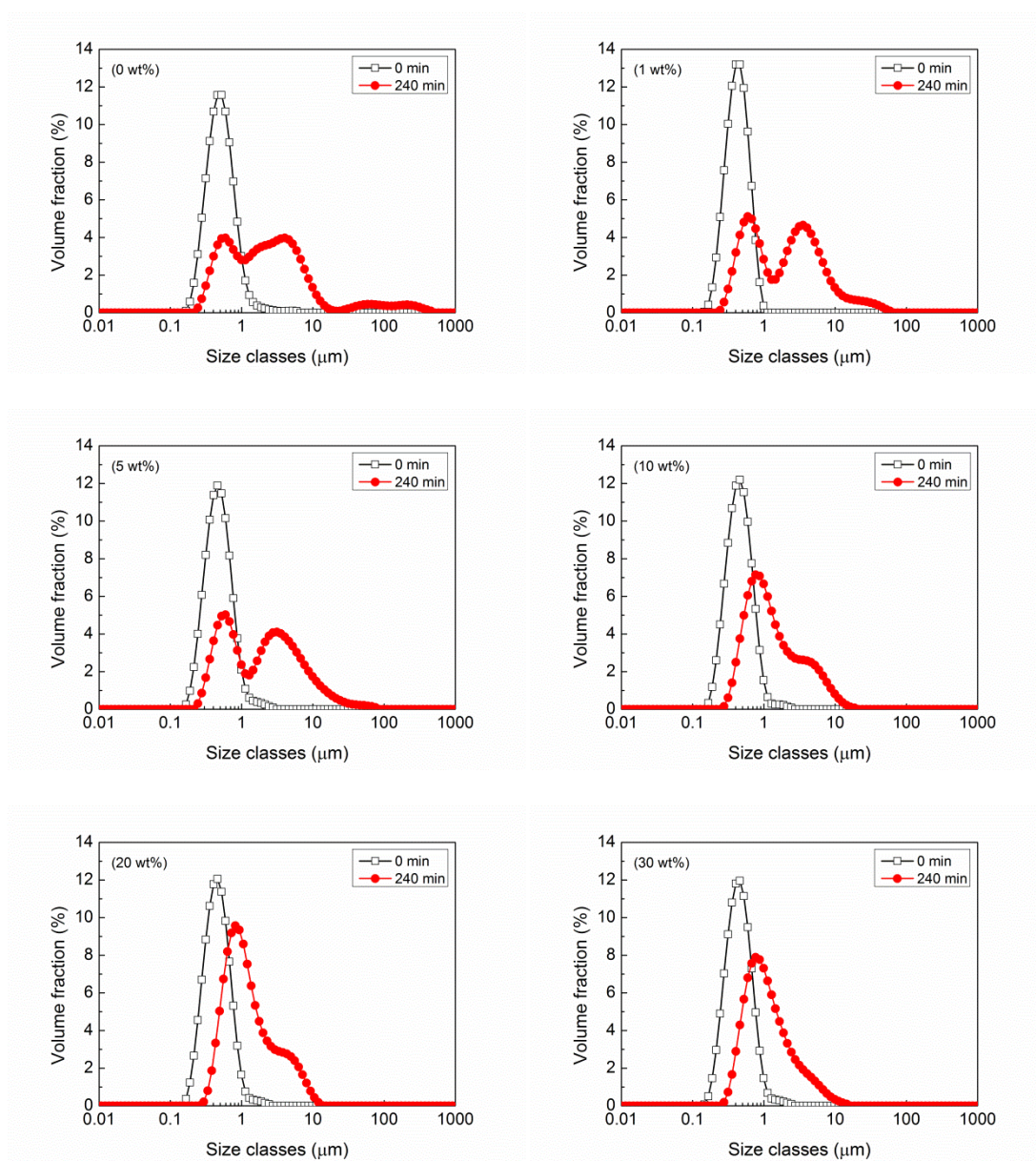


Fig.4.28 Droplet/particle size distribution at different reaction time for miniemulsion containing different C_8mimPF_6 .

The droplet size distributions for all miniemulsions before polymerisation are unimodal with a size ranging from 0.1 μm to 1 μm. After polymerisation, particle size

distributions for all products move towards larger size, and become broader. Especially, bimodal distributions can be detected for 0 wt%, 1 wt%, 5 wt% C_8mimPF_6 . The emerging second peak ranges from 1 μm to 10 μm , and occupies more than half the area of total peak area. Such peak represents the cluster of aggregated particles shown in Fig.4.27. And the clusters are in large quantity, as the area of second peak makes up a considerable percent of total peak area. Also, some extremely large clusters in the range of 10 μm to 100 μm can be detected, but in small quantity. While for 10 wt%, 20 wt%, 30 wt% C_8mimPF_6 , the second peak ranging from 1 μm to 10 μm is less apparent, and has much smaller area which means less particles aggregated into clusters. Extremely large clusters are not found for these products. It can be seen that the presence of C_8mimPF_6 , upon a certain concentration, e.g. 10 wt%, can efficiently prevent the aggregation of droplet/particle during polymerisation, and achieve products with smaller particle size.

It is interesting to note that products with larger particle size, e.g. 0 wt%, 1 wt%, and 5 wt% C_8mimPF_6 , were also viscous as shown in Fig.4.29. To compare such difference, rheological property of products would be detected.

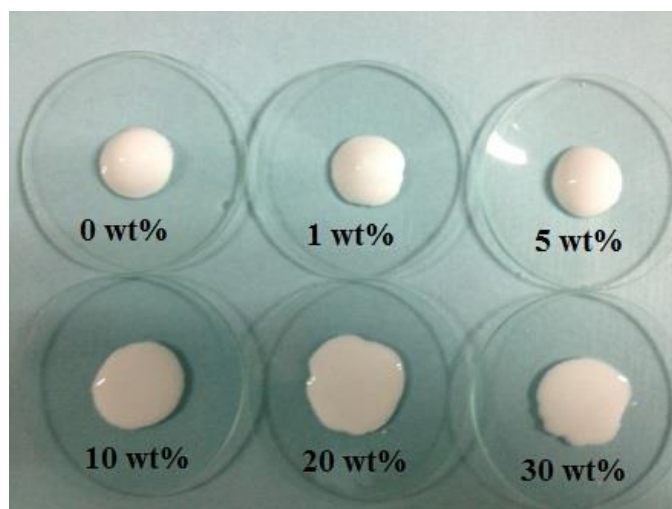


Fig.4.29 Images of products after polymerisation

In order to detect rheological property of products, variation of viscosities as a function of shear rate for products obtained at different C_8mimPF_6 concentrations was measured. Fig.4.30 shows variation of viscosities as a function of shear rate for products prepared under different C_8mimPF_6 concentrations. It can be seen that viscosities decrease remarkably with the increase of shear rate for products prepared under 0 wt%, 1wt%, and 5 wt% C_8mimPF_6 . For example, viscosity of 0 wt% C_8mimPF_6 is 35.92 Pa·s at 0.1 s^{-1} , and this value sharply decreases to 0.024 Pa·s when shear rate increases to 1000 s^{-1} . The decrease in viscosity exhibits a strong shear thinning behaviour, suggesting the presence of aggregation.(Yilmaz, 2014, Wittmar et al., 2012) However, such decrease is less remarkable for 10 wt%, 20 wt%, and 30 wt% C_8mimPF_6 . The rheological result, together with the result of droplet/particle size distribution, suggests that the present of C_8mimPF_6 could efficiently prevent aggregation of droplet/particle during polymerisation, and this effect played a better role at high concentrations of C_8mimPF_6 , e.g. 10 wt%.

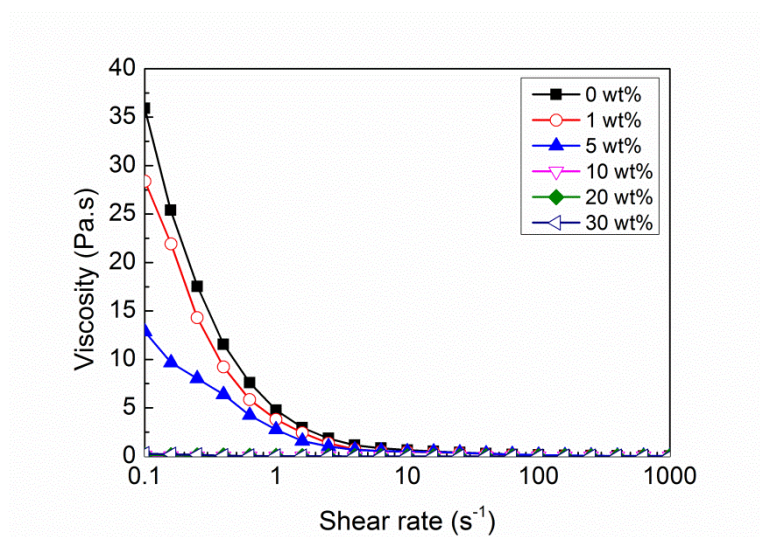


Fig.4.30 Variation of viscosities as a function of shear rate for products prepared under different C_8mimPF_6 concentrations.

The enhancement on stability due to the presence of C_8mimPF_6 was probably attributed to the strong interaction between C_8mimPF_6 and silica nanoparticles. Such interaction has already been reported between some imidazolium-based RTILs and silica nanoparticles. Liu *et al.* immobilised 1-ethyl-3-methylimidazolium hexafluorophosphate (C_2mimPF_6) onto the surface of silica nanoparticles by grinding C_2mimPF_6 /silica nanoparticle mixture in methanol, followed by removing methanol in vacuum. It was found that immobilised C_2mimPF_6 (35 wt%) have lower melting points (T_m) than bulk C_2mimPF_6 . The reduction in T_m was mainly caused by the decrease in the mobility of C_2mimPF_6 cations, due to the strong Van der Waals interactions between immobilised C_2mimPF_6 and silica nanoparticles. On the other hand, the FTIR peak of hydroxyl groups of silica nanoparticles downshifted from 3441 cm^{-1} to 3400 cm^{-1} . This shift indicated the formation of hydrogen bonds between hydroxyl groups of silanols and the F atom of PF_6^- anion. Furthermore, a remarkable change in Raman peak intensity occurred after C_2mimPF_6 was immobilised onto the surface of silica nanoparticles, indicating the strong interaction between them. (Liu *et al.*, 2010) Lei *et al.* synthesised an imidazolium-based RTIL with double bond anion, 1-methylimidazolium methacrylate (MimMa) and used it to modify the styrene butadiene rubber (SBR)/silica composites. The shift of functional group of MimMa detected by FTIR spectra and the difference of the absorption peak of Si detected by XPS proved the interaction between silica and MimMa. (Lei *et al.*, 2010)

As C_8mimPF_6 has an imidazolium-based cation and an anion containing F atom, also taking hydroxyl groups on the surface of silica nanoparticles in to consideration, it is reasonable to confirm the interaction between C_8mimPF_6 and silica nanoparticles. This interaction was essential to keep the miniemulsion stable during polymerisation. When monomers were transforming into polymers, silica nanoparticles may desorb

from the surface of droplet/particles due to their incompatibility with polymer core. Droplet/particles were lack of coverage due to this desorption, and became easier to aggregate. While in the presence of C_8mimPF_6 upon a certain value, e.g. 10 wt% C_8mimPF_6 , the binding between silica nanoparticles and droplet/particles could be effectively enhanced due to the interaction between C_8mimPF_6 stored in droplet/particles and silica nanoparticles.

4.4 Conclusion

A new latex containing C_8mimPF_6 , in the stabilisation of surfactant or silica nanoparticle has been developed for low VOCs latex coatings. This was achieved by encapsulating C_8mimPF_6 inside particles via miniemulsion polymerisation. Two types of initiators, hydrophobic AIBN and hydrophilic H_2O_2/AAC were chosen as target initiator. Systematic investigations on various factors on kinetics of miniemulsion polymerisation and stability of miniemulsion during polymerisation were carried out.

For miniemulsion stabilised by surfactant, results were summarised as follows.

It has been found that the kinetics of miniemulsion polymerisation strongly depended on temperature, C_8mimPF_6 concentration and type of initiator being used. Higher temperatures resulted in higher reaction rates regardless of any initiator being used. For AIBN, the presence of C_8mimPF_6 , reaction efficiency improved significantly at concentrations as low as 1 wt% C_8mimPF_6 . A much higher final yield of polymer could also be found at 40 °C which was beyond the normal effective decomposition temperature range of AIBN (50 °C to 90 °C). The effect of RTILs can be attributed to the faster chain propagation rate, slower chain termination rate caused by radical protection function of RTILs. At high concentrations of C_8mimPF_6 , e.g. 20

wt% and 30 wt%, combination effects such as monomer concentration in droplet/particle, the average radical number per droplet/particle, and number of droplet/particle in miniemulsion all decreased with the increase of C_8mimPF_6 concentration which counter acted against the positive effect of C_8mimPF_6 on reaction rate, leading to the decrease in overall reaction rate.

For polymerisation initiated by hydrophilic H_2O_2/AAC , a different behavior in terms of reaction rate was observed as compared to systems where AIBN was used. The presence of C_8mimPF_6 had a negative effect on reaction rates as compared to the systems without C_8mimPF_6 though the final yields of polymer were similar. It appears that the higher the concentration of C_8mimPF_6 in droplet, the slower the reaction progress. We postulated that for polymerisation of MMA, when the hydrophilic initiator was used, because particle formation was subject to generation of radicals, transportation of radicals from water phase to droplet where monomer was present. Thus the overall reaction rate not only depended on the generation of radicals from decomposition of initiator, but also the transfer of radicals from water phase to the reaction site of MMA, which was in droplet form. Such transfer could be the limiting step for the overall reaction. In this case, the presence of C_8mimPF_6 , especially at lower concentration, could result in much tighter space alignment at the oil/water interface caused by the synergistic effect between C_8mim^+ cation and SDSO anion. The tighter interfacial structure would increase the transfer resistance for radicals entering to droplet, thus significantly slowing down the entry rate of radicals into droplet. In this case, reaction rate depended on effective transfer of radicals from water phase to droplet.

The simultaneous measurement on droplet/particle size during polymerisation provided extra evidence on the effect of temperature, initiator concentration and C₈mimPF₆ concentration and reaction mechanism, which associated with the change of droplet/particle size during reaction. It can be concluded that the final particle size of latex strongly depended on reaction mechanism, temperature, initiator concentration and C₈mimPF₆ concentration. Higher temperature (50 °C), higher initiator concentration (2 mol%) and higher C₈mimPF₆ concentrations (20 wt% and 30 wt%) promoted droplets coalescence causing increase in particle size of latex regardless of the type of initiator used. At lower temperatures (40 °C) and lower concentrations of C₈mimPF₆, where more stable droplets could be provided, the particle size of latex tended to be influenced by the reaction mechanism, *e.g.* when homogeneous or micelle nucleation was important during polymerisation initiated by hydrophilic initiator, H₂O₂/AAc, a marked reduction in droplet/particle size compared to the initial droplet size could be obtained whilst for reaction initiated by hydrophobic AIBN, the droplet/particle size reduction could be minimum due to different mechanism, *i.e.* droplet nucleation took place more frequently for hydrophobic initiator.

For miniemulsion stabilised by silica nanoparticle, results were summarised as follows.

It has been found that a higher final yield of polymer could be achieved by AIBN, a hydrophobic initiator, compared with hydrophilic H₂O₂/AAc. The inefficiency of H₂O₂/AAc was ascribed to the obstacle caused by the “densely packed” silica nanoparticles on the surface of droplets which prevented the entry of radicals from water phase into droplets. Compared with 40 °C, reaction temperature at

60 °C gave a higher final yield. As to pH of water phase, pH of 5 has the highest final yield with a value of 96.1%, followed by pH of 3 (91.1%), and lowest was pH of 7 with a value of 81.7%. Changing of concentrations of C₈mimPF₆ ranging from 0 to 30 wt% had only small effect on product yield, varying from 85wt% to 91 wt%.

Among temperatures ranging from 40 °C to 60 °C, 60 °C was with a product in smaller particle size. PH of water phase directly affected the stability of product, and a stable product could only be achieved at pH = 3. At this pH, silica nanoparticles were around its isoelectric point, leading to the decrease in electrostatic repulsion between silica nanoparticles adsorbed on the surface of droplets. More silica nanoparticles could be crowded on the surface of droplet/particles, which could efficiently prevent aggregation. The change of concentrations of C₈mimPF₆ ranging from 0 to 30 wt%, had more impact on product stability, *e.g.* only above 10 wt% C₈mimPF₆, stable products could be achieved. The enhancement on stability was due to the strong interaction between C₈mimPF₆ and silica nanoparticles via hydrogen bond and Van der Waals' force.

Chapter 5 Characterisation of latex containing C₈mimPF₆

5.1 Introduction

In previous chapter, polymerisation of miniemulsions containing C₈mimPF₆ in the stabilisation of surfactant and silica nanoparticles was carried out. Factors affecting yield of polymer and stability of miniemulsion during polymerisation were systematically investigated. In this chapter, we are going to focus on the characterisation of the latexes, which are the products after polymerisation. The properties to be evaluated included effect of C₈mimPF₆ concentration on stability of latex, glass transition temperature of polymer and deformation of particle, thermal stability of film, and mechanical property of film. Latexes stabilised by surfactant, and latexes stabilised by silica nanoparticle would be discussed separately.

5.2 Materials and methods

5.2.1 Materials

Methyl methacrylate (MMA, CP) was purchased from Sinopharm Chemical Reagent Co., Ltd and purified by vacuum distillation to remove inhibitor. 2, 2-azobis (isobutyronitrile) (AIBN, 97%) was purchased from Aladdin Industrial Inc and recrystallized by ethanol. L-Ascorbic acid (AAc, AR), hydrogen peroxide (H₂O₂, AR), and sodium dodecyl sulfonate (SDSO, CP) were purchased from Sinopharm Chemical Reagent Co., Ltd. Hexadecane (HD, 98%) was from Aladdin Industrial Inc. 1-octyl-3-methylimidazolium hexafluorophosphate (C₈mimPF₆, 99%) was supplied by Shanghai Cheng Jie Chemical Co., Ltd. NS-30 (20 nm silica nanoparticle, pH =

9.5, 30 wt%) was supplied as silica sol by Yuda Chemical Co. Ultra-pure water with a resistivity of 18.2 MΩ·cm⁻¹ was used in all experiments.

5.2.2 Preparation of miniemulsion

5.2.2.1 Miniemulsion stabilised by surfactant

Oil phase contained 5 wt% HD, the remaining 95 wt% containing C₈mimPF₆ and MMA. Both HD and C₈mimPF₆ were infinitely miscible in MMA. A homogeneous oil phase was obtained after gently stirring. The contents of MMA, HD, and C₈mimPF₆ in oil phase are shown in Table.5.1.

Table.5.1 Formula of oil phases

Sample code	Amount (wt% based on total weight of oil phase)		
	MMA	HD	C ₈ mimPF ₆
O-1	95	5	0
O-4	94	5	1
O-5	90	5	5
O-6	85	5	10
O-8	75	5	20
O-9	65	5	30

Water phase was prepared by dissolving a given amount of surfactant in ultra-pure water. The type and concentration of surfactant in water phase is showed in Table.5.2.

Table.5.2 Formula of water phases containing surfactant

Abbreviation	Type of surfactant	Amount (mM)
W-sur-3	SDSO	30

Oil in water miniemulsion (O/W) was prepared with a volume ratio of oil to water phase equal to 3 to 7. Oil phase was added into water phase in a 100 ml plastic container. The total volume of the mixture was 50 mL and kept at 40 °C. Sonicator (Xinzhi Scientz II) was chosen as the homogeniser. Position the Ultrasound probe Sonicator in the middle of the container and kept at one centimeter below the surface of the mixture. The output power of sonicator was set as 95 W. After homogenising the mixture for 6 minute in a state of 1 second on and 1 second off, miniemulsion was obtained.

5.2.2.2 Miniemulsion stabilised by silica nanoparticle

Oil phase contained 5 wt% HD, the remaining 95 wt% containing C₈mimPF₆ and MMA. Both HD and C₈mimPF₆ were infinitely miscible in MMA. A homogeneous oil phase was obtained after gently stirring. A certain mole of AIBN was then dissolved in oil phase. The contents of MMA, HD, and C₈mimPF₆ in oil phase and amount of AIBN added are shown in Table.5.3.

Table.5.3 Formula of oil phase

Sample code	Components in oil phase (wt% based on oil phase)			Initiator (mol% based on MMA)
	MMA	HD	C ₈ mimPF ₆	AIBN
O-10	95	5	0	1.0
O-11	94	5	1	1.0
O-12	90	5	5	1.0
O-13	85	5	10	1.0
O-14	75	5	20	1.0
O-15	65	5	30	1.0

Water phase was prepared by dissolving silica sol, NS-30 into ultra-pure water to the target concentration (gram of silica nanoparticle per litre of water phase); and

the pH was adjusted to 3 using 0.1 mol/L HCl solution at the same time. Table.5.4 shows the formula of water phases containing silica nanoparticle.

Table.5.4 Formula of water phases containing silica nanoparticle

Abbreviation	Amount (g/l)	pH
W-sil-3	50	3

Oil in water miniemulsion (O/W) was prepared with a volume ratio of oil to water phase equal to 3 to 7. Oil phase was added into water phase in a 250 ml baker. The total volume of the mixture sample was 100 mL and kept at 40 °C. High speed disperser (IKA T25) was chosen as the homogeniser. Rotor of high speed disperser was in the middle of the baker and then placed the tip of the rotor one centimeter above the bottom of the baker. The stirring speed of high speed disperser was set as 20000 rpm. After homogenising the mixture for 8 minute, a stable miniemulsion was formed.

5.2.3 Miniemulsion polymerisation

5.2.3.1 Miniemulsion stabilised by surfactant

The miniemulsion polymerisation was carried out in a four-necked flask equipped with a stirrer, a reflux condenser, a thermometer, and a nitrogen inlet. The flask was immersed in a water bath for controlling reaction temperature. 150 mL miniemulsion was loaded into the flask, and was gently stirred with nitrogen bubbling for about 1.5 h to remove oxygen in the flask. Then the temperature of water bath was set to 40 °C, the reaction temperature. H₂O₂/AAc was selected as the initiator. H₂O₂/AAc solution with molar ratio of H₂O₂ to AAc equal to 1 to 1.3 was injected into the miniemulsion directly after the desired reaction temperature was reached, and

then the polymerisation reaction was started. Table.5.5 shows the formula of H₂O₂/AAc initiator solution.

Table.5.5 Formula of H₂O₂/Ac initiator solution

Sample code	H ₂ O (5mL)	Initiator (mol% based on MMA)	
		H ₂ O ₂	AAc
I-3	5	1.0	1.3

5.2.3.2 Miniemulsion stabilised by silica nanoparticle

The miniemulsion polymerisation was carried out in a four-necked flask equipped with a stirrer, a reflux condenser, a thermometer, and a nitrogen inlet. The flask was immersed in a water bath for controlling reaction temperature. 150 mL miniemulsion was loaded into the flask, and was gently stirred with nitrogen bubbling for about 1.5 h to remove oxygen in the flask. AIBN was used as the initiator. AIBN was dissolved in oil phase before the preparation of the miniemulsion, and then the reaction temperature was adjusted to the 60 °C to start the polymerisation. The reaction process was under nitrogen protection.

5.2.4 Characterisation

5.2.4.1 Stability of latex

5.2.4.1.1 Direct observation

For latexes stabilised by silica nanoparticle, 22 mL latex was sealed in a cylindrical glass bottle (Ø: 28 mm, H: 45 mm) to observe whether destabilisation occurred during storage at 20 °C. Two kinds of destabilisation phenomena might occur during storage: creaming on the top layer; sediment at the bottom layer. The

bottle was placed upside down to measure the height of sediment. The height of creaming was difficult to measure due to its irregular shape.

5.2.4.1.2 Particle size measurement

For latexes stabilised by surfactant, no apparent creaming or sedimentation was detected. In order to observe instability of latexes, particle sizes and distributions of latexes with different aging time were measured using the laser diffraction method (Mastersizer 3000, Malvern Inc). This technique has been widely accepted as a tool to evaluate particle size.(Zhang et al., 2012, Winkelmann and Schuchmann, 2011, Wang et al., 2014) The sample was diluted with water solution to meet the requirement of obscuration. The diluted water solution saturated with SDSO was used to prevent coalescence during sample measurement.(Meliana et al., 2011) All measurements were repeated for three times.

5.2.4.2 Zeta potential measurement

The zeta potentials of latexes were measured using the trace laser dopper electrophoresis method (ZetasizerNano ZS, Malvern Inc) at 20°C. The original latexes were diluted with water to 0.5 wt%.(Ni et al., 2006) Since pH has a great influence on zeta potential, the diluted latexes had the same pH as the original one.(Singh et al., 2014) All measurements were repeated for three times.

5.2.4.3 Glass transition temperature measurement

The glass transition temperature (T_g) of particles was detected by differential scanning calorimetry (DSC) (SII-DSC 6220, Seiko Instruments Inc). Particles for DSC analysis were prepared the same way as described in spectroscopic analyses, and sealed in aluminium pans with a weight of circa. 10 mg. The measurement was

carried out within temperature ranged from 25 °C to 140 °C at a heating rate of 10 °C/min under nitrogen. The T_g was taken as the start-point of the heat capacity increment according to the DSC curve segment representing glass-to-rubber transition.

5.2.4.4 Spectroscopic analyses

The Fourier Transform Infrared (FTIR) spectra of particles were obtained using FTIR spectrophotometer (Nicolet iS10, Thermo Fisher Scientific Inc) over the wave number in the range from 4000 to 400 cm^{-1} . Particles for FTIR spectra were precipitated from latex by adding 10 wt% sodium chloride (NaCl), and separated by centrifugation at 10000 rpm for 20 min, then re-dispersed by water. After repeating purification process mentioned above for three times, the particles were stored in vacuum oven at 40°C over night to remove water. 20 mg particles were mixed with 280mg potassium bromide (KBr), grinded, and pressed into pellet for spectroscopic analyses.

5.2.4.5 Morphology observation

The morphology of particles was observed by a transmission electron microscope (TEM) (Hitachi H7650, Hitachi Ltd.) at an accelerating voltage of 80 kV. Samples for TEM analysis were prepared by dropping droplets of latex which was diluted 50 times by water on the surface of copper grid coated with carbon, followed by drying in air.

The deformation degree of particles under different storage temperature was studied by a field emission scanning electron microscope (SEM) (SIGMA/VP, Carl Zeiss Microscopy Ltd.) at an accelerating voltage of 3 kV. Samples for SEM analysis

were prepared as follows. The original latexes were diluted with water to 0.5 wt%. Droplets of diluted latexes were dropped onto the surface of aluminium foil, followed by drying in air. The aluminium foil used here was stuck to the object tables using a conductive adhesive tape,. After storing objective tables containing particles under different temperature (120 °C, 100 °C, 80 °C, 60 °C) for 2 h, gold was deposited on the particles by the high vacuum sputter coater (EM SCD500, Leica Microsystems GmbH) for follow-up SEM observation.

5.2.4.6 Molecular weight and distribution measurement

Molecular weight and distribution was determined by gel permeation chromatograph (GPC) (GL-2000, waters Inc). Polymers for GPC measurement were prepared by dissolving particles which was obtained as described in spectroscopic analyses in tetrahydrofuran (THF). GPC experiment was carried out at 30 °C in THF solution with PMMA as standard (flow rate: 1.0 mL/min; columns: PLgel 20um Mixed-A, PLgel 20um Mixed-C, and PLgel 20um Mixed-E).

5.2.4.7 Mechanical property analysis

The mechanical property of film was analysed by tensile test (TCS-2000, GoTech Testing Machines Inc). Films for tensile test were prepared as follows: 2 g of latex was poured into rectangular ceramic crucible (70mm × 15mm × 15mm), then stored in oven at 120°C for 2 h. For latexes stabilised by surfactant, films formed by latexes containing 0, 1, 5 wt% C₈mimPF₆ cracked, while latexes containing 10, 20, 30 wt% C₈mimPF₆ formed crack free films. Subsequently, films of 10, 20, 30 wt% C₈mimPF₆ were cut into films in a size of 40.0mm × 5.5mm × 1.0~0.8mm. The films were fixed into the universal testing machine for tensile testing at a crosshead speed

of 1.5 mm/min. For latexes stabilised by silica nanoparticle, films formed by latexes containing 0, 1, 5, 10, 20, 30 wt% C₈mimPF₆ cracked.

5.2.4.8 Thermogravimetric analysis

The thermogravimetric (TG) analysis of the film was carried out using a simultaneous thermal analyser (STA 449 F3 Jupiter, Netzsch Inc). Films for TG analysis were prepared the same way as described in mechanical property analyses, and placed in open alumina pans with an approximate weight of 10 mg. The measurement was carried out from 25 °C to 550 °C at a heating rate of 10 °C/min under nitrogen.

5.3 Results and discussion

5.3.1 Latexes stabilised by surfactant

In this section, the effects of C₈mimPF₆ concentration on stability of latex during storage, glass transition temperature of polymer and deformation of particle, mechanical property of film, and thermal property of film were investigated.

5.3.1.1 Effect of C₈mimPF₆ concentration on stability of latex during storage

As latex may go through a certain period of time between preparation and application, its stability during storage would need to be considered. During storage, particles in latex may contact and collide with each other due to Brownian motion. When the electrostatic or steric repulsion are weak and cannot obstruct the attractive force between particles, particles may stick to each other and form aggregation, followed by flocculation and coagulation.(Ohshima, 2012) Due to the formation of aggregation, the average size of particles would move towards a larger

size.(Kobayashi et al., 2005) By the detection of variations in size, the instability of latex can be intuitively represented. On the other hand, due to the vertical movement of aggregated particles by gravitational effect, creaming or sedimentation could be detected visually.(Kobayashi et al., 2005, Abismaïl et al., 1999)

Latexes containing different concentrations of C_8mimPF_6 were stored at 20 °C for 576 h. No apparent creaming or sedimentation was detected during storage. This indicated that vertical movement of particles were not apparent. However, aggregation of particles may still occur. In order to establish any instability, particle sizes of latexes were continually measured at 144, 288, 432, 576 hours, and the results are shown in Fig.5.1. It is observed that the change in the particle sizes of 0 wt%, 1 wt%, 5 wt%, 10 wt%, 20 wt% and 30 wt% C_8mimPF_6 from initial conditions are very different. The particle sizes of 0 wt%, 1 wt%, 5 wt%, 10 wt%, 20 wt% and 30 wt% C_8mimPF_6 increase from initial size at 186 nm, 189 nm, 192 nm, 200 nm, 228 nm and 264 nm to final size at 189 nm, 189 nm, 196 nm, 218 nm, 273 nm and 335 nm, respectively, after 288 h storage. The particle size would remain unchanged during 576 h storage for latex containing lower a concentration of C_8mimPF_6 , *i.e.* below 5wt%. The increasing rate of particle size for 10 wt%, 20 wt% and 30 wt% are much pronounced, which are 9.0%, 19.7% and 26.9%, respectively. These tendencies suggest that in the presence of C_8mimPF_6 at a lower concentrations, *i.e.* less than 10 wt%, better stability can be obtained. Above certain concentration, *e.g.* at and above 10 wt%, adding C_8mimPF_6 would cause instability of the latex. It is interesting to note that high concentrations of C_8mimPF_6 , *e.g.* above 10 wt%, in oil phase also had a negative effect on the stability of miniemulsion, leading to the remarkable increase in particle size during storage, as discussed in 3.3.1.2.2. Therefore, the addition of

C_8mimPF_6 in oil phase at a certain concentration, *e.g.* 10 wt% and above may weaken the stability of miniemulsions as well as latexes after polymerisation.

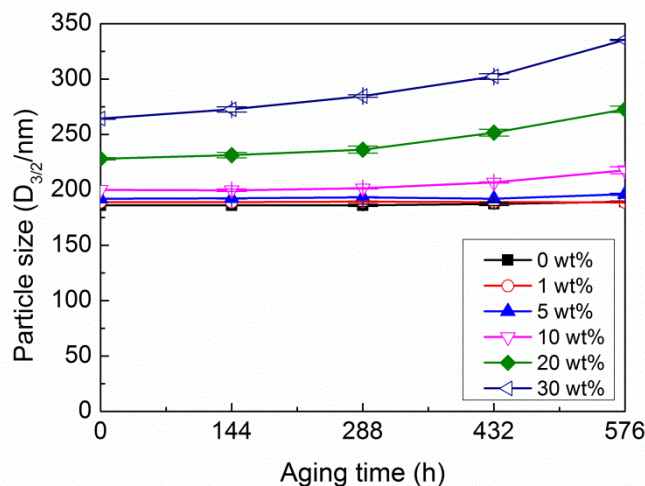


Fig.5.1 Variation in the particle sizes as a function of time for latexes containing different C_8mimPF_6 concentrations at 20°C

In order to gain further insight on the variation of particles size for latexes at different concentrations of C_8mimPF_6 , further investigation of factor such as particle size distribution was carried out. Fig.5.2 demonstrates the particle size distributions at 0 h and 576 h of aging time for latexes containing different concentrations of C_8mimPF_6 . There are no obvious changes in the main peaks of particles between 0 wt% and 5 wt% C_8mimPF_6 concentrations after 576 h of storage time. However, as the concentration of C_8mimPF_6 increases, *e.g.* 20 wt% and 30 wt%, the bimodal of particle distribution emerges though the main peak of particle distribution is similar after 576 h storage. The increase in the area of second peak is significant, indicating the strong aggregation of particles occurs during storage. The results explain why particle size increased significantly for latex containing C_8mimPF_6 concentration more than 20 wt% as shown in Fig.5.1. Evidently, above a critical concentration, *i.e.* 10 wt% C_8mimPF_6 , latexes become unstable and may aggregate easier.

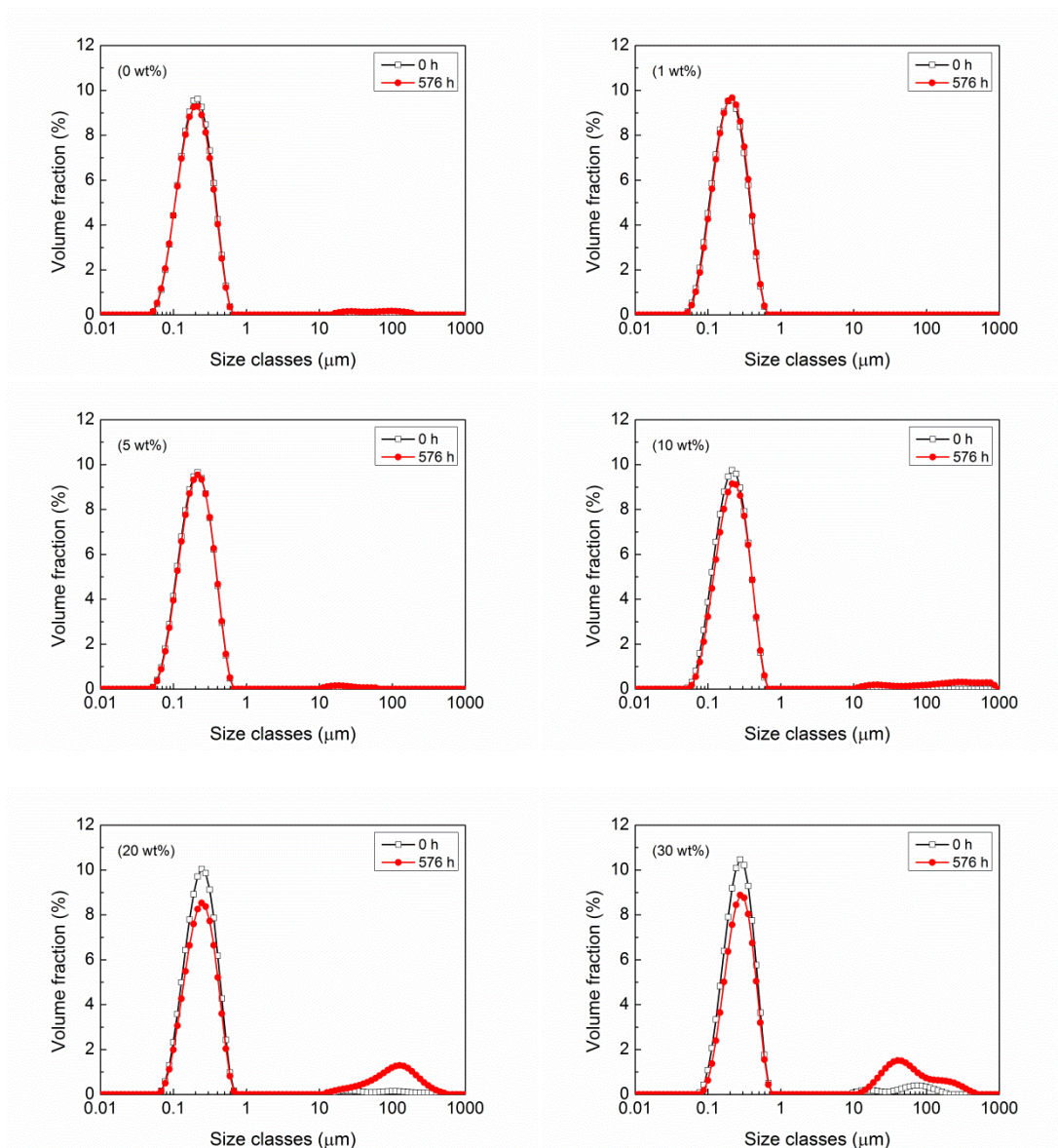


Fig.5.2 Particle size distribution at 0 h and 576 h of aging time for latexes containing different concentrations of C_8mimPF_6 .

Considering anionic surfactant was used in this study, the stability of latex could be influenced by the electrostatic repulsion between adjacent particles. It has been reported that the electrostatic repulsion played a key role on the stability of latex in the presence of anionic surfactant.(Ohshima, 2012) The degree of electrostatic repulsion between particles in a dispersion system can be indicated by zeta potential. With a higher zeta potential, there is higher electrostatic expulsion, hence resulting in more stable particles. Positive or negative zeta potentials indicate whether the

dispersion is positively charged or negatively charged. Thus, the absolute zeta potential would be a measure of the stability of latex. Particles with higher zeta potential indicate that the electric repulsions between particles are stronger and hence can effectively prevent aggregation. Normally, when the absolute zeta potential is higher than 30 mV, particles in a dispersion are in a stable state.(Sonavane et al., 2008)

With the above theories as guidelines, a series of measurements of the zeta potential were carried out for latexes at all concentrations of C_8mimPF_6 , and the results are shown in Fig.5.3. Negative zeta potential values are observed for all the latexes, which suggest that particles are negatively charged. The absolute zeta potential increases from 40.7 mV to 50.8 mV with an increase of C_8mimPF_6 concentration from 0 wt% to 1 wt%, and the absolute zeta potential then decreases from 50.8 mV to 21.0 mV with a further increase in the C_8mimPF_6 concentration up to 30 wt%. For latexes containing C_8mimPF_6 with less than 10 wt%, the absolute zeta potentials are higher than 30 mV. This indicates that the particle sizes were relatively stable in this region. For latexes containing C_8mimPF_6 above 20 wt%, the absolute zeta potential are less than 30 mV, which indicates that particles were unstable in this region. Such observations are consistent with the latex stability results shown in Fig.5.1 and Fig.5.2. Such results also imply that surface charge hence electric repulsion between particles plays a dominating role on the stability of latex.

The unique zeta potential behaviour mentioned above was explained by our previous study about miniemulsion containing C_8mimPF_6 shown in 3.3.1.2.2. It might be attributed to the enhanced absorption between cations of C_8mimPF_6 and anions of SDSO, and the hydrophilicity of PF_6^- anions as compared with C_8mim^+ cations.

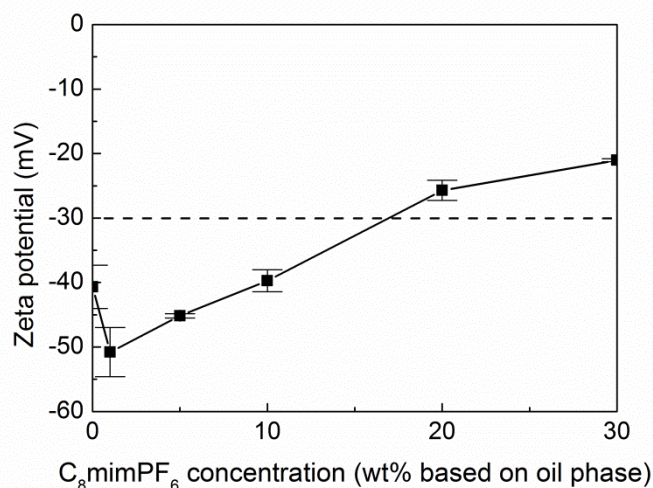


Fig.5.3 Variation in the zeta potentials of latexes as a function of $C_8\text{mimPF}_6$ concentration

5.3.1.2 Effect of $C_8\text{mimPF}_6$ concentration on T_g of polymer and particle deformation

The film formation process is a transformation process from wet particle dispersion into dry continuous film. This process is normally divided into three stages: 1), particle drying and close-packing; 2), particle deformation; 3), particle inter-diffusion.(Keddie and Routh, 2010) Coalescing agents mainly have impact on stage 2 and stage 3, which may enhance the deformation from close-packing particles into a dodecahedral structure as well as the diffusion of molecular chain through the boundary of deformed particle into another particle.(Raja et al., 2012, Keddie and Routh, 2010) Coalescing agent can effectively decrease T_g of polymer, thus enhancing the deformation and inter-diffusion of particles. In order to study the effect of $C_8\text{mimPF}_6$ concentration on the film formation process, T_g of polymer and the deformation images of particles under different storage temperature were measured.

Fig.5.4 illustrates T_g of polymer containing different $C_8\text{mimPF}_6$ concentrations. In the absence of $C_8\text{mimPF}_6$, T_g is 120 °C which is approximately the same to pure

PMMA reported by other authors. (Scott et al., 2002, Scott et al., 2003) Adding 1 wt% C_8mimPF_6 into latex, resulting smaller reduction on T_g value from 120 °C into 119.2 °C. A significant reduction on T_g is found for latex containing C_8mimPF_6 concentration above 10 wt%. For example, with 30 wt% C_8mimPF_6 , T_g drops to 54.5 °C. The effect on reducing T_g of PMMA has also been observed for other types of RTILs, including 1-butyl-3-methylimidazolium hexafluorophosphate (C_4mimPF_6), 1-hexyl-3-methylimidazolium hexafluorophosphate (C_6mimPF_6), and 1-ethyl-3-methylimidazolium bis(trifluoromethylsulfonyl)imide ($C_2mimTFSI$). (Scott et al., 2002, Scott et al., 2003, Mok et al., 2011) The efficiency in reducing T_g of PMMA is due to their low T_g (-76 °C for C_4mimPF_6 , -78 °C for C_6mimPF_6 , -92 °C for $C_2mimTFSI$) and compatibility with PMMA. As C_8mimPF_6 has a T_g as low as -82 °C, and is also compatible with PMMA, (Harris et al., 2007, Perrier et al., 2002) C_8mimPF_6 is comparable to other RTILs mentioned above in reducing T_g . For example, with 30 wt% content, T_g of PMMA can be decreased to 54.5 °C when plasticised by C_8mimPF_6 which is slight lower than the value of C_4mimPF_6 , around 60.0 °C. In summary, C_8mimPF_6 can reduce the T_g of PMMA, acting as a plasticiser.

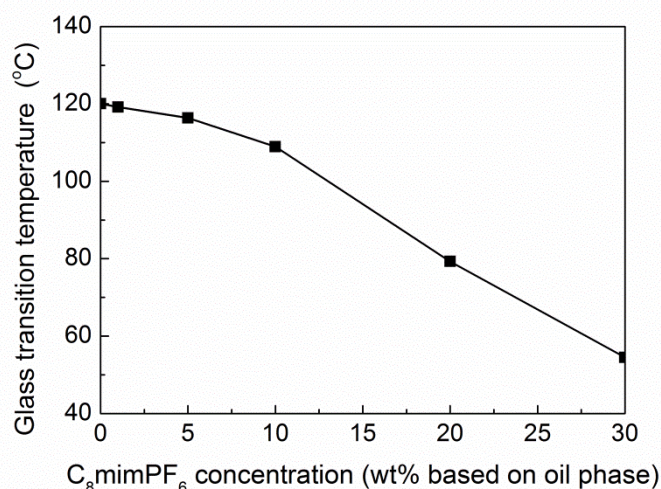
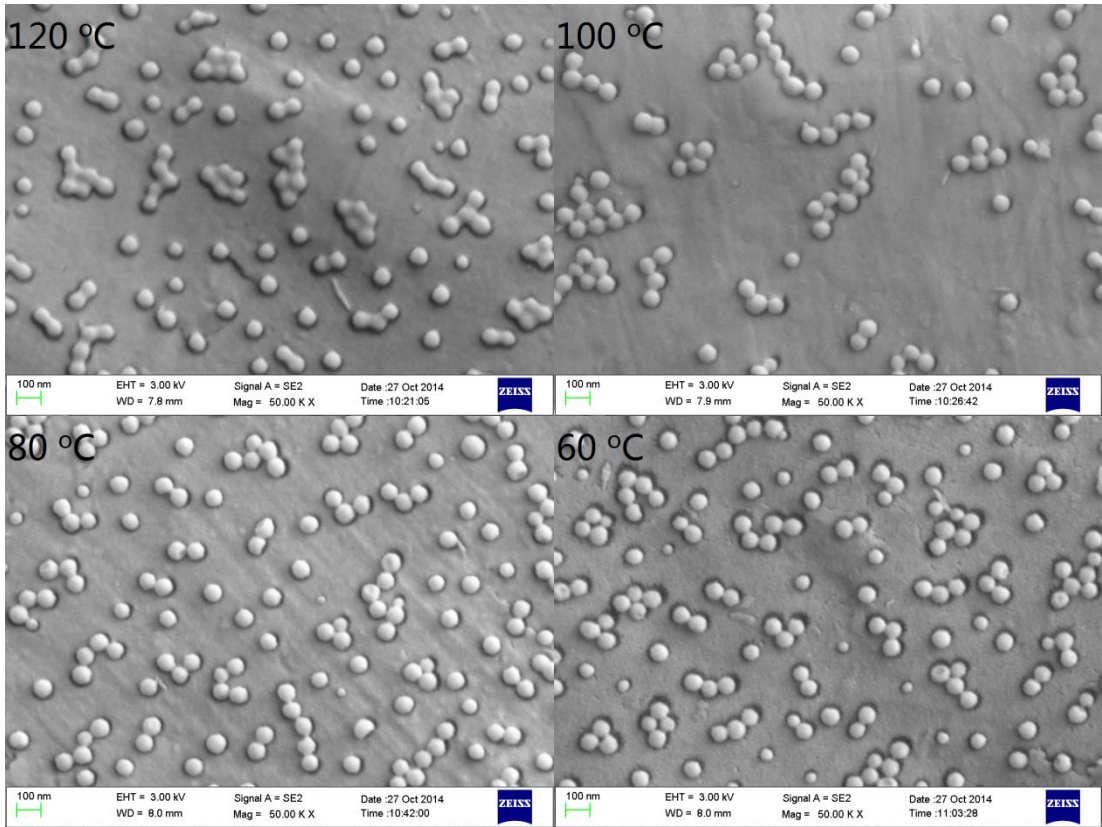


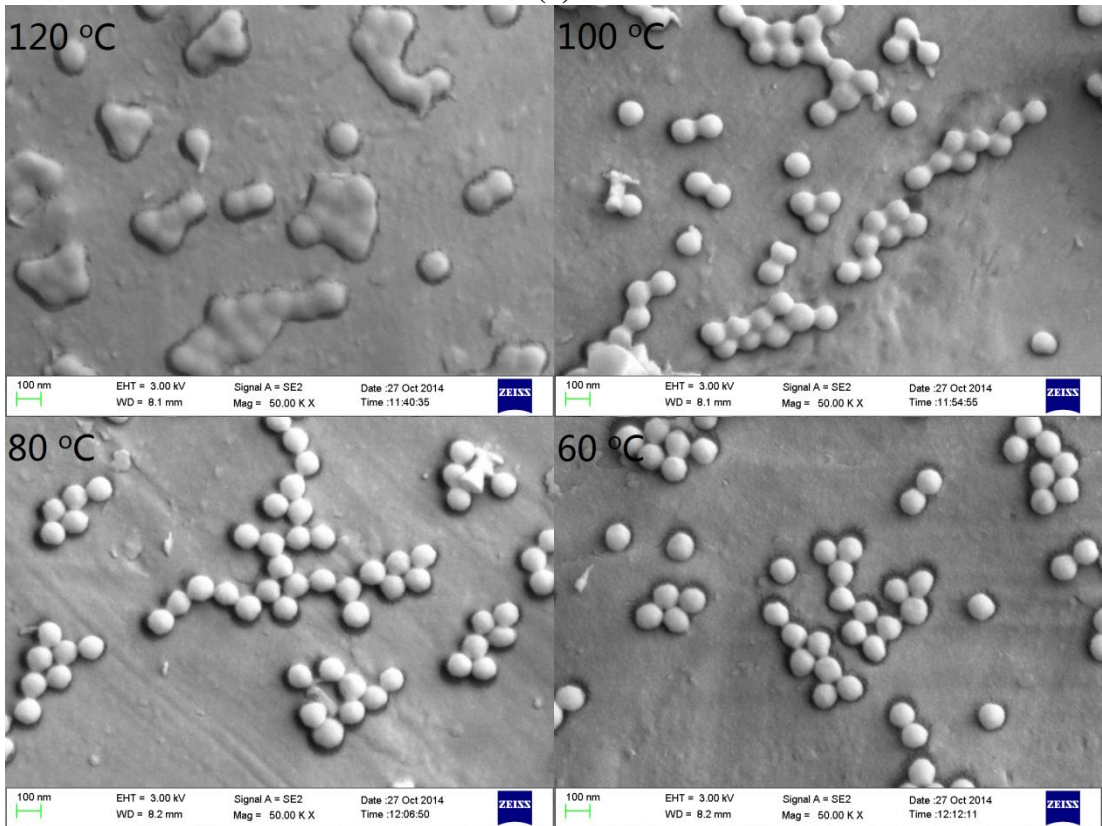
Fig.5.4 Glass transition temperature of particles containing different C_8mimPF_6 concentrations.

In order to investigate the effect of C_8mimPF_6 on the deformation of particles, particles were laid on the surface of aluminium foil, and stored under different temperatures for 2 h, sequentially observed by SEM. A more specific procedure was shown in 5.2.4.5. Fig.5.5 shows the deformation of particles containing C_8mimPF_6 with different concentrations under different storage temperature for 2 h. Fig.5.5 (a) represents 0 wt% C_8mimPF_6 . At 120 °C, the spherical shape of particles is still present, but the boundary between particles becomes less distinct. This meant that the deformation of particles was carried out at this temperature. While at 100 °C, 80 °C, and 60 °C, the boundaries between particles are still distinguishable, indicating the limited deformation. Fig.5.5 (b) represents the 10 wt% C_8mimPF_6 , and the temperature that the boundary between particles becomes less distinct decreased to 100 °C, whereas such temperature would decrease to 80 °C and 60 °C for 20 wt% and 30wt% C_8mimPF_6 , respectively as shown in Figures 5 (c) and 5(d).

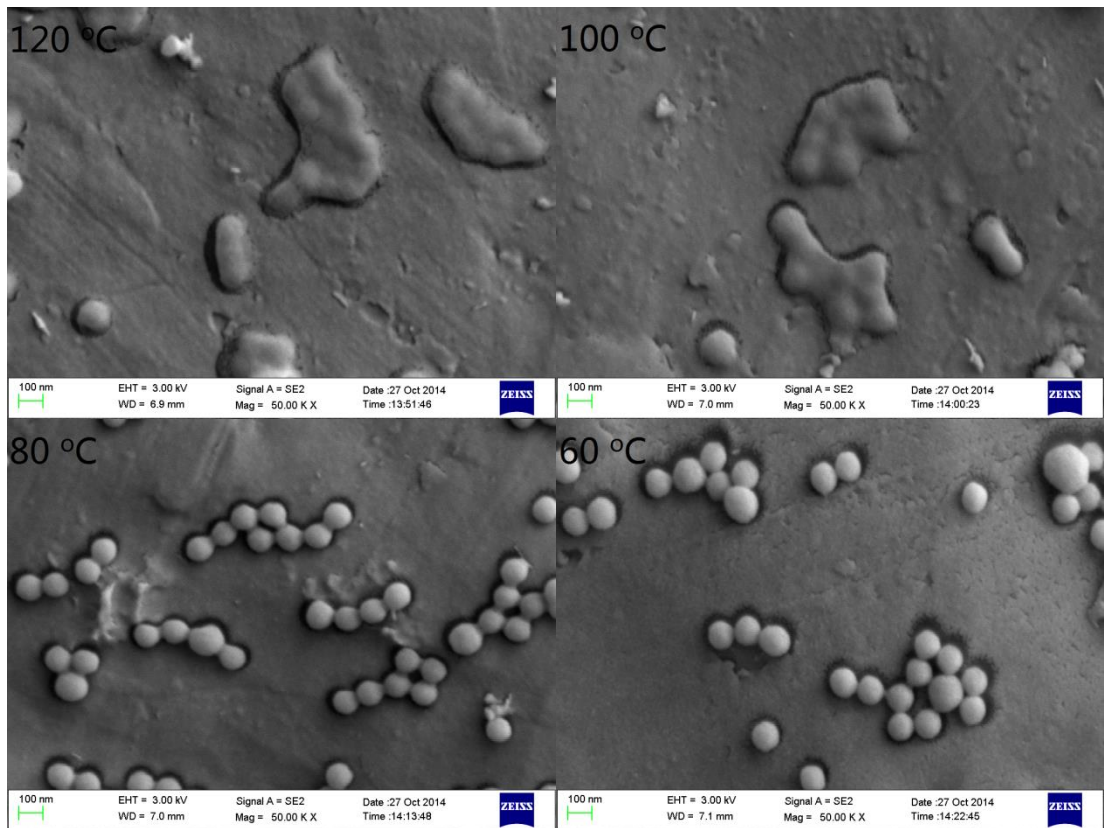
It can be concluded from Fig.5.5 (a) to Fig.5.5 (d) that deformation becomes pronounced as the content of C_8mimPF_6 increased under the same baking temperature. At 120 °C, the upper limit of the baking temperature is taken as an instance to compare deformation degree of particles with different C_8mimPF_6 concentrations. For 0 wt% C_8mimPF_6 , the boundary between particles becomes less distinct at this temperature. While for 10 wt%, 20 wt%, and 30 wt%, the discrete particles would become a continuous block, and the spherical shape as well as the boundary between particles would disappear. This means that the deformation, sometimes inter-diffusion of particles was carried out remarkably. As for 60 °C, the lower limit of the baking temperature, the boundary between particles is still distinguishable for 0 wt%, 10 wt%, and 20 wt% C_8mimPF_6 . Whilst for 30 wt% C_8mimPF_6 , the boundary between particles becomes less distinct, indicating an apparent deformation.



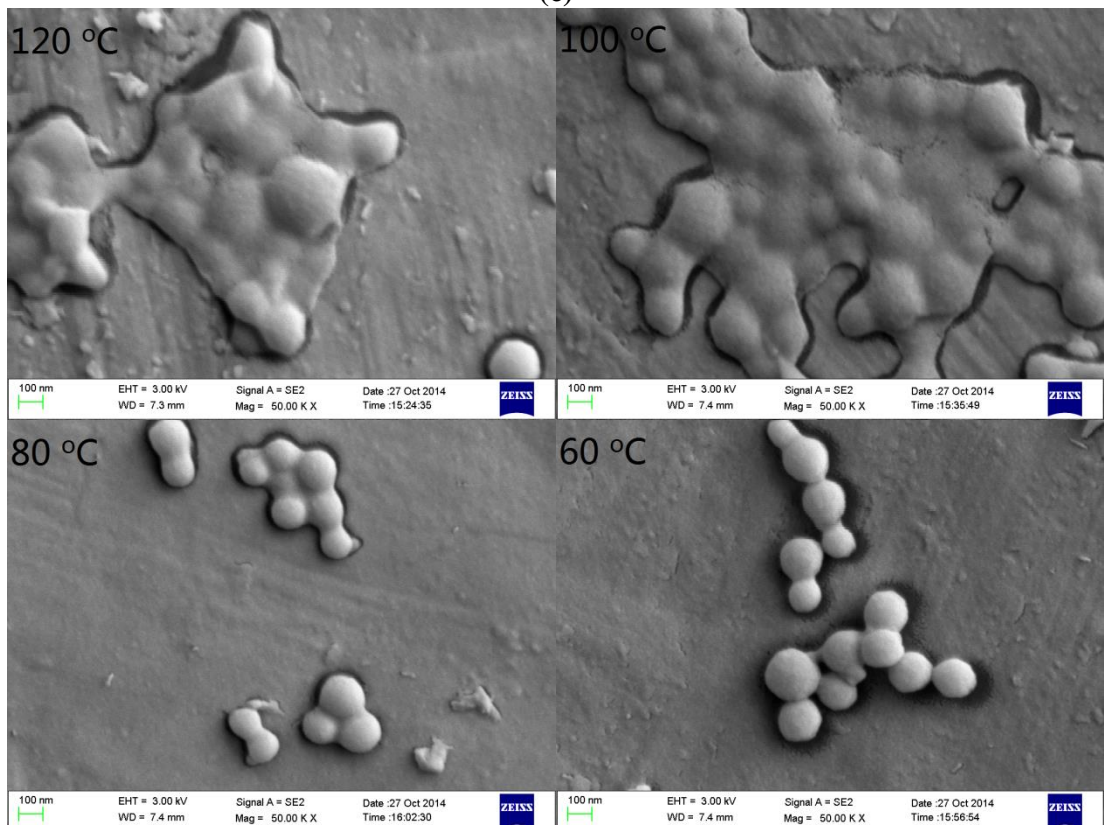
(a)



(b)



(c)



(d)

Fig.5.5 Deformation of particles containing different C_8mimPF_6 under different storage temperature for 2 h. (a) 0 wt% C_8mimPF_6 ; (b) 10 wt% C_8mimPF_6 ; (c) 20 wt% C_8mimPF_6 ; (d) 30 wt% C_8mimPF_6 .

In summary, C₈mimPF₆ could effectively reduce the T_g of polymer and enhance deformation of particles, thus it is a suitable coalescing agent for film formation.

Considering homogeneous products (no oil droplets are detected on the top or at the bottom) and low solubility of C₈mimPF₆ (2.26 g L⁻¹ at 25°C), the sole place that C₈mimPF₆ remained is inside particles due to the droplet nucleation, indicating that C₈mimPF₆ was successfully encapsulated inside particles. It is interesting to study the existence form of C₈mimPF₆ inside particles, as it may reveal why C₈mimPF₆ could effectively reduce T_g of polymer and enhance deformation of particles.

Firstly, we try to investigate whether C₈mimPF₆ exists as a micro-molecule that permeates into the space between polymers or incorporates in a polymer during polymerisation. To achieve this goal, particles were separated from dispersing system for FTIR spectroscopic analysis.

Fig.5.6 shows the FTIR spectra of pure C₈mimPF₆ and PMMA. In the FTIR spectra of pure C₈mimPF₆, peaks at 3173 cm⁻¹, 2958 cm⁻¹, 2930 cm⁻¹, 2859 cm⁻¹, 1576 cm⁻¹, 1469 cm⁻¹ for C₈mim⁺ are observed and assigned as C-H stretching vibration of aromatic ring, asymmetric C-H stretching vibration of CH₃ group, C-H stretching vibration of alkyl group, symmetric C-H stretching vibration of CH₂ group, framework vibration of alkyl group, C-H stretching vibration of alkyl group, respectively; peaks at 837 cm⁻¹, 558 cm⁻¹ for PF₆⁻ are assigned as P-F stretching vibration, bending vibration, respectively. (Iimori et al., 2007, Sun et al., 2007, Okada et al., 2012, Peng et al., 2013, Aroca et al., 2000) For PMMA, peaks at 2951 cm⁻¹, 1724 cm⁻¹, 1435 cm⁻¹, 1148 cm⁻¹ are observed and referred to as asymmetric C-H stretching vibration of CH₃ group, C=O stretching vibration, CH₃ stretching vibration, -O-CH₃ stretching vibration, respectively. (Ramesh et al., 2007) It can be seen that

peaks at 1724 cm^{-1} , 1148 cm^{-1} are specific to PMMA without overlapping peaks of C_8mimPF_6 . It is the same for C_8mimPF_6 peaks at 3173 cm^{-1} , 837 cm^{-1} , and 558 cm^{-1} .

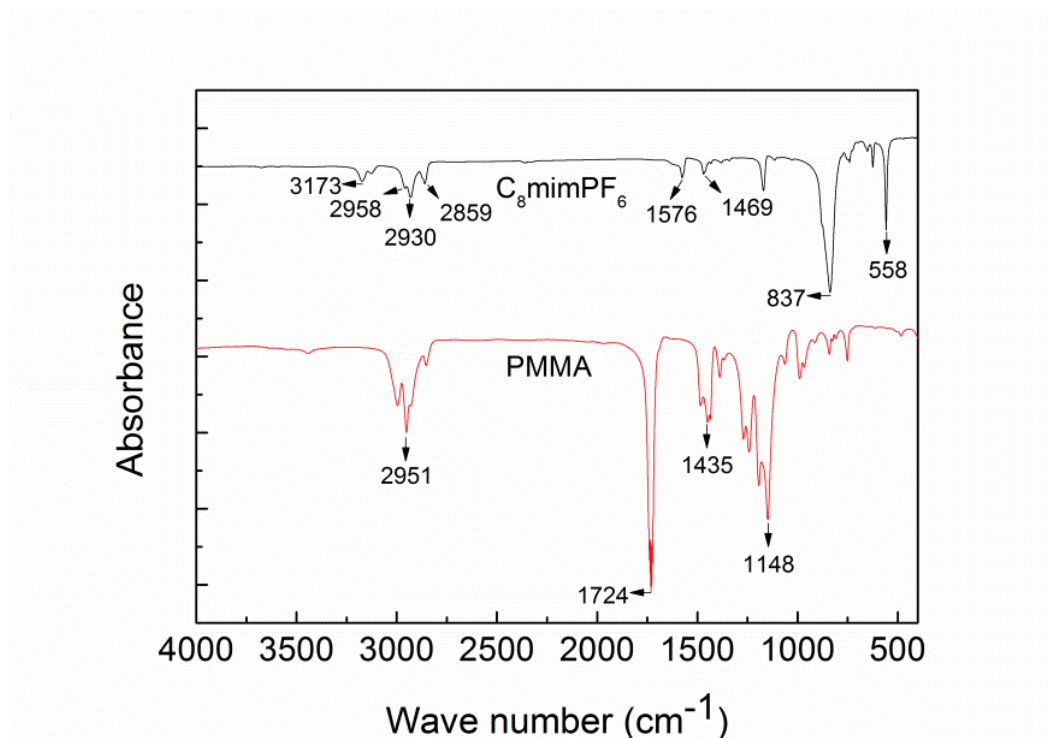


Fig.5.6 FTIR spectra for C_8mimPF_6 and PMMA.

Fig.5.7 shows the FTIR spectra for particles containing 0 wt%, 10 wt%, 20 wt%, 30 wt% C_8mimPF_6 as well as pure C_8mimPF_6 . The characteristic peaks of C_8mimPF_6 , *i.e.* 3173 cm^{-1} , 837 cm^{-1} , and 558 cm^{-1} , are all observed in FTIR spectra of particles containing 10 wt%, 20 wt%, 30 wt% C_8mimPF_6 . This confirms the encapsulation of C_8mimPF_6 inside PMMA particles. In addition, no new characteristic peaks were formed for particles containing 10 wt%, 20 wt%, 30 wt% C_8mimPF_6 , compared with pure PMMA (0 wt% C_8mimPF_6) and pure C_8mimPF_6 . This implies that no chemical reaction occurred between PMMA chains and C_8mimPF_6 during free radical polymerisation. For free radical polymerisation, chain propagation occurs between radicals and monomers containing carbon-carbon double chain, *e.g.* MMA in this study. However, there is no carbon-carbon double chain exists in C_8mimPF_6 ,

making it difficult to participate in free radical polymerisation. Hence, it is likely that C_8mimPF_6 was still in a state of micro-molecule, permeating into the space between polymers. Such plasticiser in a state of micro-molecule is called external plasticiser.

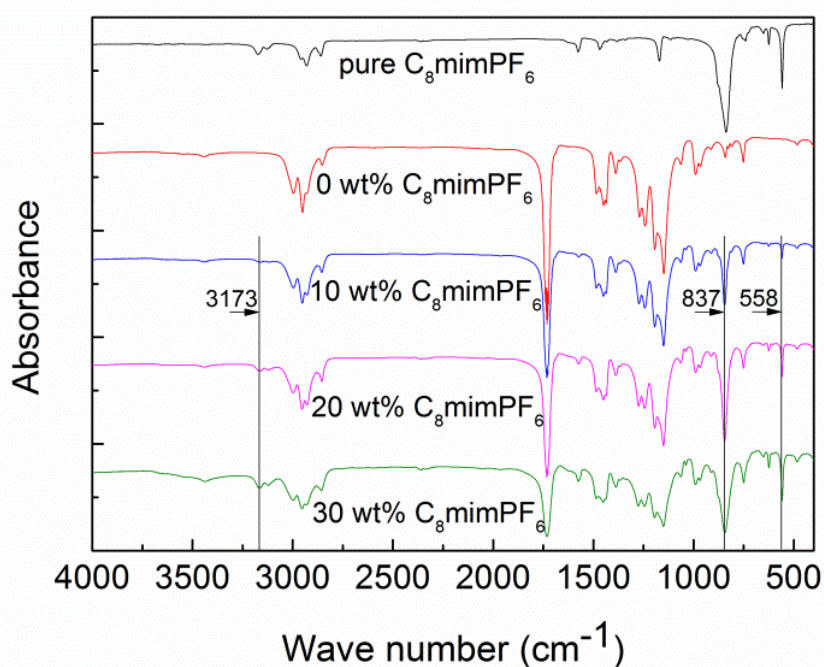


Fig.5.7 FTIR spectra for particles containing different C_8mimPF_6 concentrations and pure C_8mimPF_6 .

The reason why an external plasticiser can efficiently reduce T_g of polymer can be explained by the free volume theory.(Wypych, 2004) Free volume is used to describe free space between molecules caused by the motion of chain ends, side chains, and main chain. Such motion fades down with the decrease of temperature, leading to the decrease in free volume. Especially, when temperature reduces to T_g , a critical point that polymer changes from a non-crystalline, glass-like state to a rubbery state, molecules become densely packed with negligible internal mobility, and free volume decreases into a minimum value. When external plasticiser permeates into the space between polymers, the number of end groups, the number of side chains, and

the chance for main chain movement all increase, leading to the increase in free volume of polymer system. That is to say, further temperature can be decreased when free volume reaches its minimum value. Thus T_g of polymer can be reduced due to the external plasticiser.(Wypych, 2004) Specific to this study, the reduction in T_g of PMMA was due to the presence of C_8mimPF_6 acting as an external plasticiser.

Subsequently, we aim to investigate the compatibility between C_8mimPF_6 and PMMA within the particle. This compatibility is essential for an external plasticiser. If some parts of external plasticiser permeate into the space between polymers and other form a separated phase due to the limited compatibility, only the permeating parts play the plasticising function.(Wypych, 2004) As coalescing agent is a kind of plasticiser, its compatibility with polymer is essential for particle deformation. For example, if a coalescing agent was added into latex coating by dissolving in water phase, it should have moderate water miscibility. Such miscibility not only ensures its solubility in water phase, but also makes it possible to swell the shell of particles, and then soften the core of particles by penetration during film formation.(Raja et al., 2012)

Specific to this study, C_8mimPF_6 was encapsulated inside particles by the miniemulsion polymerisation. C_8mimPF_6 might be separated from PMMA as a core-shell structure or compatible with PMMA as a homogeneous particle as shown in Fig.5.8. If a core-shell structure occurs, only the permeating C_8mimPF_6 in shell plays the function of coalescing agent. In this case, a considerable amount of C_8mimPF_6 would be wasted in core.

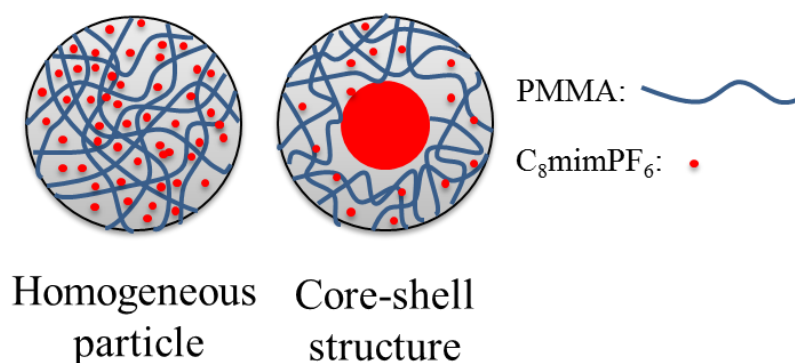


Fig.5.8 Illustration of a homogeneous particle and a particle with a core-shell structure

In order to reveal whether the core-shell structure occurred in PMMA/C₈mimPF₆ particles, TEM images of particles containing different C₈mimPF₆ concentrations were taken. If a core-shell structure exists, there will be an aberration between the shell composed of polymer and core composed of hydrophobe from the TEM image of particle. (Cardoso et al., 2013, Romio et al., 2009b) Results are shown in Fig.5.9 where no core-shell structures are observed for sample at all C₈mimPF₆ concentrations range, indicating C₈mimPF₆ was not separated from PMMA forming a new phase during polymerisation reaction. It is likely, that during miniemulsion polymerisation, PMMA continuously formed and occupied the shell of droplet, while C₈mimPF₆ also existed in the shell due to its compatibility with PMMA rather than concentrated into the core of droplet. After the reaction, the whole droplet became a solid particle with the existence of C₈mimPF₆ throughout the particle.

This compatibility between PMMA and C₈mimPF₆ was favourable for C₈mimPF₆ as a coalescing agent. If PMMA concentrated as shell phase and C₈mimPF₆ concentrated as core phase, the space between polymer would be lack of permeated C₈mimPF₆ as illustrated in Fig.5.8, leading to the ineffectiveness in plasticising. In this case, the diffusion of polymer between particles which is essential for the deformation and coalescence of particles are less possible to be carried out.

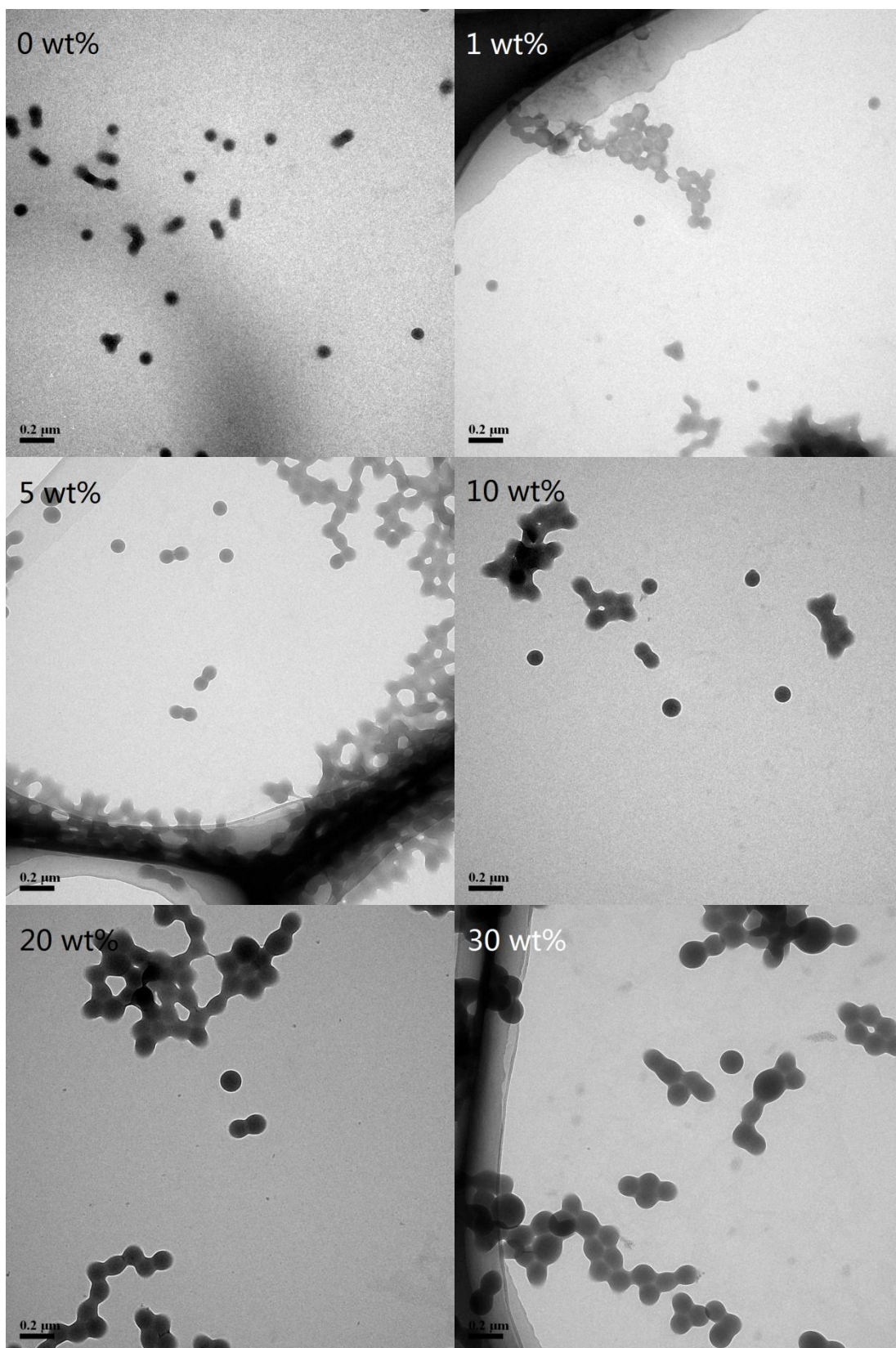


Fig.5.9 TEM images of particles containing different C_8mimPF_6 concentrations

5.3.1.3 Effect of C₈mimPF₆ concentration on molecular weight and distribution

Table.5.6 shows number-average molecular weight and polydispersity of polymers prepared from polymerisation of miniemulsions containing different C₈mimPF₆ concentrations.

Table.5.6 Number-average molecular weight and polydispersity of polymers prepared from polymerisation of miniemulsions containing different C₈mimPF₆ concentrations.

C ₈ mimPF ₆ concentration (wt%)	Number-average molecular weight (g/mol)	Polydispersity
0	347171	3.10
1	364640	2.97
5	241407	3.94
10	237953	3.41
20	216036	3.16
30	178894	3.18

It can be seen that the number-average molecular weight slightly increases from 347171 g/mol to 364640 g/mol when C₈mimPF₆ concentration increases from 0 wt% to 1 wt%. The number-average molecular weight then continuously decreases with a further increase in C₈mimPF₆ concentration to 30 wt%. In addition, the polydispersities are relatively high, ranging from 2.97 to 3.94.

Molecular weight distributions of polymers prepared from polymerisation of miniemulsions containing different C₈mimPF₆ concentrations are shown in Fig.5.10. It can be seen that distributions are relatively broad for all C₈mimPF₆ concentrations. The molecular weight distributions shift to lower molecular weights when the concentration of C₈mimPF₆ increases from 1 wt% to 30 wt%.

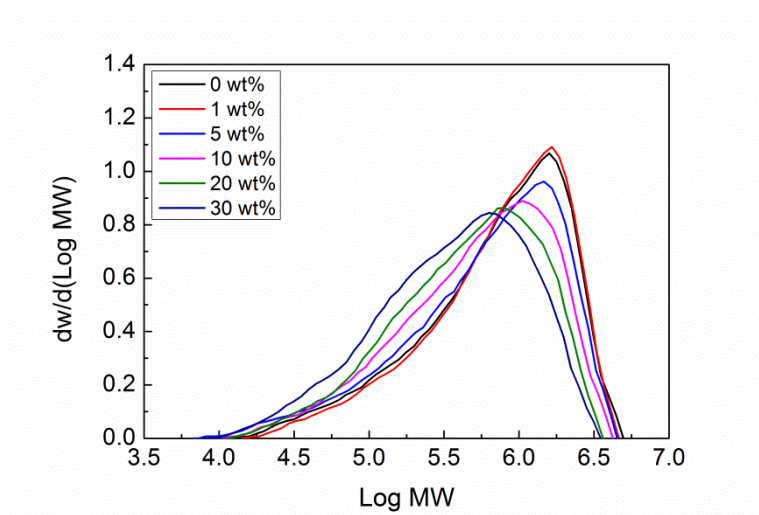


Fig.5.10 Molecular weight distributions of polymers prepared from polymerisation of miniemulsions containing different C_8mimPF_6 concentrations.

5.3.1.4 Effect of C_8mimPF_6 concentration on mechanical properties of film

Based on our previous study, C_8mimPF_6 can effectively reduce T_g of polymer and enhance deformation of particles at lower temperatures, acting as an external plasticiser. Such plasticising effect may still play a role after film formation, mainly affecting the mechanical properties of film, as C_8mimPF_6 remains in film due to its non-volatility. In order to investigate the effect of C_8mimPF_6 concentration on the mechanical property of the final film, latexes were baked at 120 °C within 2 h for film formation. The films formed by latexes containing 0, 1, 5 wt% cracked, while latexes containing 10, 20, 30 wt% C_8mimPF_6 could form continuous films. Their mechanical properties, including stress–strain curves and Young’s modulus, were studied according to these cases.

Fig.5.11 shows stress-strain curves for films formed from latexes containing different C_8mimPF_6 concentrations. Stress-strain curves were obtained by tensile test as described in 5.2.4.6. Film in cuboid shape was fixed into the universal testing machine, and then crosshead would stretch the film by moving at a speed of 1.5

mm/min. When the film was fractured into two pieces, crosshead would stop moving. From the result of Fig.5.11, for film of 30 wt% C_8mimPF_6 , stress increases with the increase of strain, and then a turning point appears at the stress-strain curve, at which stress reaches a maximum value. This point is called yield point. Over the yield point, a further increase in strain leads to a decrease in stress, followed by the fracture of film. Because the fracture occurs after the yield point, such fracture is called ductile fracture. Strain at the point of fracture is called the elongation at break, which is 21.5% for film of 30 wt% C_8mimPF_6 . For 10 wt% and 20 wt% C_8mimPF_6 , stress increases with the increase of strain, and then fracture of film occurs before the yield point. Such fracture is called brittle fracture. The elongation at break is 1.5 % for 10 wt% C_8mimPF_6 and 6.4 % for 20 wt% C_8mimPF_6 .

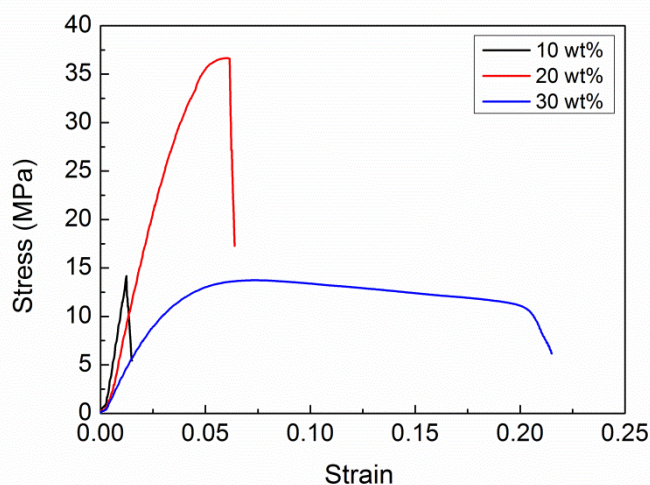


Fig.5.11 Stress–strain curves of films formed from latexes containing different C_8mimPF_6 concentrations

By the comparison between films formed from latexes containing different C_8mimPF_6 , it can be seen that elongation at break of the film was significantly enhanced upon the adding of C_8mimPF_6 . Such effect has been reported when studied

the composite of single-walled carbon nanotube/C₄mimTFSI and the composite of polyvinyl chloride (PVC)/C₄mimPF₆.(Oh et al., 2013, Hou and Wang, 2011)

Another difference is the fracture of 30 wt% C₈mimPF₆ is ductile fracture, while that of 10 wt% and 20 wt% is brittle fracture. Such difference in fracture is also shown in stress–strain curves of glassy polymer at different temperatures. From the illustration in Fig.5.12, when the temperature is far lower than the T_g of polymer, brittle fracture occurs, and a slight increase in temperature leads to ductile fracture. When the temperature is close to T_g, after the yield point, stress remains constant or slightly increases with the increase in strain, and then the increase in stress becomes apparent until it fractures. At a temperature higher than T_g, in the absence of the yield point, with a remarkable increase in strain, the increase in stress is not apparent, and then stress increases remarkably before the fracture occurs. From a microcosmic aspect, when the temperature is lower than T_g, the deformation of glassy polymer after the yield point is mainly due to molecule chain movement. That is to say, in the presence of external force, densely packed molecule chains begin to move, and the stretch of molecule chain leads to the deformation of polymer. In some cases, when the temperature is far lower than T_g, fracture occurs before the molecule chain movement, which is known as brittle fracture. At a temperature higher than T_g, molecule chains have internal mobility, and may stretch easily under external force. Such stretch causes molecule orientation, leading to an enhancement in tensile strength. So stress increases apparently, until the fracture. In this study, test was carried out at 20 °C, which was far lower than the T_g of polymers containing 10 wt% and 20 wt% C₈mimPF₆ (108.9 °C for 10 wt% C₈mimPF₆, 79.3 °C for 20 wt% C₈mimPF₆), so brittle fracture occurred for these two samples. While T_g of polymer containing 30 wt% C₈mimPF₆ (54.5 °C) was close to test temperature compared with

former two, molecule chain movement may occur before fracture, thus ductile fracture took place.

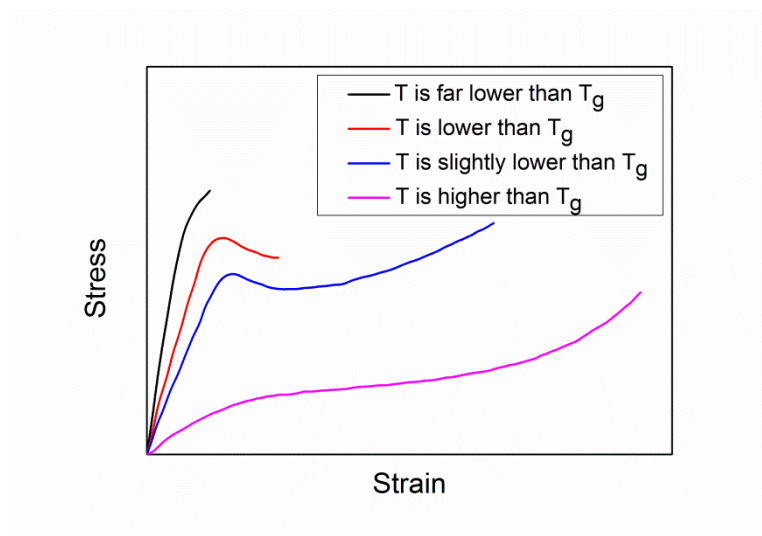


Fig.5.12 stress–strain curves of glassy polymer at different temperatures

Fig.5.13 shows Young's modulus of films formed from latexes containing different C_8mimPF_6 concentrations. The Young's modulus decreases from 1517.0 MPa to 390.7 MPa as the concentration of C_8mimPF_6 concentration increases from 10 wt% to 30 wt%. Such a phenomenon has also been reported when studied the mechanical properties of composite of (PVC)/ C_4mimPF_6 .(Hou and Wang, 2011) They found that Young's modulus of PVC decreased from 3755 MPa to 3024 MPa after adding 10 wt% C_4mimPF_6 . These changes in mechanical properties were mainly attributed to the function of RTILs as an external plasticiser. Polymers were swollen due to existence of RTILs in polymers, hence promoting the mobility of chain segments, leading to a softer material being produced. (Oh et al., 2013) In this case, the polymer became more flexible, had higher elongation, but lower Young's modulus.

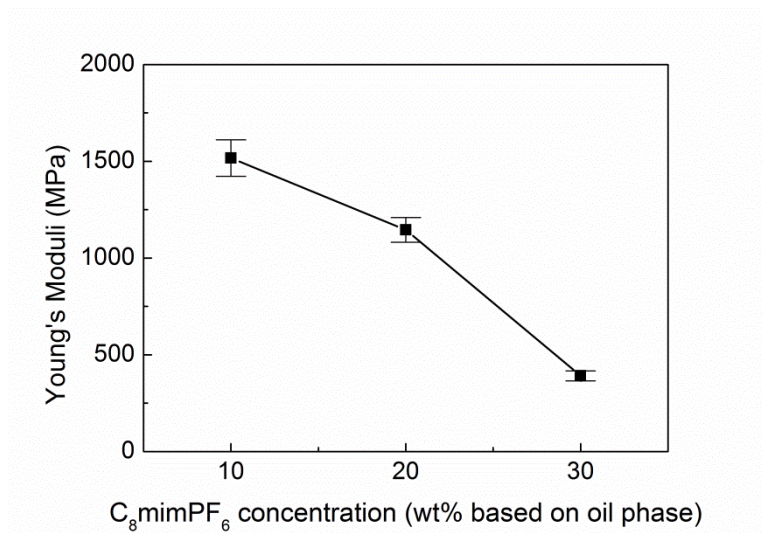


Fig.5.13 Young's modulus of films formed latexes containing different C_8mimPF_6 concentrations

5.3.1.5 Effect of C_8mimPF_6 concentration on thermal properties of film

C_8mimPF_6 shows high thermal stability over a wide range of temperatures, as the decomposition happened at a temperature as high as 400 °C (Fig.5.14). The film may have a better thermal stability to resist fire hazard in the present of C_8mimPF_6 . In order to reveal the resistance of films towards high temperatures, the thermogravimetric (TG) analysis of films was carried out. The measurement was carried out from 25 °C to 550 °C at a heating rate of 10 °C/min under nitrogen. Fig.5.14 shows the TG curves for films formed from latexes containing different C_8mimPF_6 concentrations. The onset of the weight loss for film without C_8mimPF_6 is the same as films containing C_8mimPF_6 . However, as the temperature increased, especially from 350 °C to 450 °C, the weight loss of film without C_8mimPF_6 is much more remarkable as compared with the one containing C_8mimPF_6 at the same temperature, though the weight loss is not sensible to the change of concentration of C_8mimPF_6 from 10 wt% to 30 wt% in the film. This confirmed the benefit of adding C_8mimPF_6 to improve the thermal stability of film. Similar observations have been

reported when studied the composite of networked PMMA/C₂mimTFSI by Susan *et al.* and was attributed to the thermal stability of C₂mimTFSI. (Susan et al., 2005b)

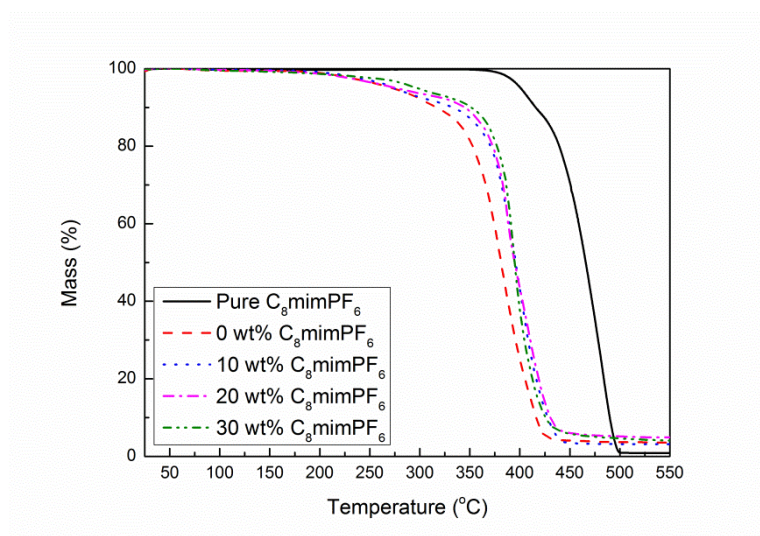


Fig.5.14 TG curves for films formed from latexes containing different C₈mimPF₆ concentrations.

5.3.2 Latexes stabilised by silica nanoparticle

In this section, the effects of C₈mimPF₆ concentration on stability of latex, glass transition temperature of polymer and deformation of particle, and thermal property of film were investigated.

5.3.2.1 Effect of C₈mimPF₆ concentration on stability of latex

During storage, due to the Brownian motion, particles in latex may contact and collide with each other, then form aggregation, followed by flocculation and coagulation, thus the instability of latex becomes remarkable.(Ohshima, 2012) On the other hand, vertical movement caused by gravity may aggravate as particles aggregate into larger ones, leading to the creaming or sedimentation.(Kobayashi et al., 2005, Abismaïl et al., 1999)

In order to investigate the stability of latexes containing different C₈mimPF₆ concentrations, a certain amount of latexes were sealed in a cylindrical glass bottles at 20 °C, and regularly observed. The result is summarised in Table.5.7. It can be seen that the initial latexes containing 0, 1, 5 wt% C₈mimPF₆ are viscous, subsequently these latexes turn into a state of coagulation as the storage continues. For latexes containing 10, 20, 30 wt% C₈mimPF₆, they are initially stable when first prepared. However sedimentations are detected at 144 hours and form a layer of sediment as time continues.

Table.5.7 Stability of latexes containing different C₈mimPF₆ concentrations with different aging time. (-: stabilisation; +: thickness; *: coagulation; \: sedimentations)

Aging time (h)	Stability of latexes					
	0 wt% C ₈ mimPF ₆	1 wt% C ₈ mimPF ₆	5 wt% C ₈ mimPF ₆	10 wt% C ₈ mimPF ₆	20 wt% C ₈ mimPF ₆	30 wt% C ₈ mimPF ₆
0	-	-	-	-	-	-
144	*	*	*	\	\	\
288	*	*	*	\	\	\
432	*	*	*	\	\	\
576	*	*	*	\	\	\

To have a quantitative comparison, the height of sediment was measured. Variation in height ratio of sediment to initial height of latex as a function of aging time for latexes containing 10 wt%, 20 wt%, and 30 wt% C₈mimPF₆ is shown in Fig.5.15. The height of sediment for latex containing 10 wt% C₈mimPF₆ is relatively less compared with 20 wt% and 30 wt% C₈mimPF₆ at initial storage time up to 288 h. An increase in the height of sediment with the aging time was observed for all latexes sample up to 432 h. Such change is eased and the height was kept constant as further increasing the aging time from 432 h to 576 h.

Based on this result, we have decided to choose concentration of C_8mimPF_6 at above 10 wt% and ensure the properties characterisation was taken within 24 h, so that the results observed are not due to the instability of miniemulsion

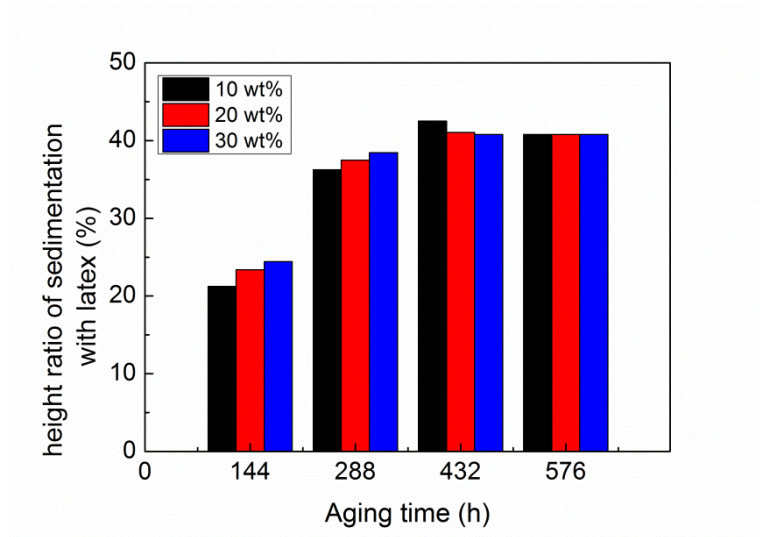


Fig.5.15 Variation in height ratio of sediment with latexes as a function of aging time for latexes containing 10 wt%, 20 wt%, and 30 wt% C_8mimPF_6 .

5.3.2.2 Effect of C_8mimPF_6 concentration on T_g of polymer and particle deformation

From the result of latex stabilised by surfactant, C_8mimPF_6 could effectively reduce T_g of polymer and enhance deformation of particle, acting as a coalescing agent. In order to study whether C_8mimPF_6 has the same function for latex stabilised by silica nanoparticle, T_g of polymer and the deformation images of particles under different storage temperature were measured.

Fig.5.16 illustrates T_g of polymer containing different C_8mimPF_6 concentrations. In the absence of C_8mimPF_6 , T_g is 110.0 °C which is slightly lower than the T_g of pure PMMA (120 °C) reported by other authors. (Scott et al., 2002, Scott et al., 2003) After adding solely 1 wt% C_8mimPF_6 , the T_g decreases 1.0 °C to 109.0 °C. The effect of C_8mimPF_6 on reducing T_g is obvious even under the

circumstance of low concentration. The T_g continuously decreases with the increase of C_8mimPF_6 and drops to 65.1 °C with 30 wt% C_8mimPF_6 .

Such effect has been observed for different RTILs species, including 1-butyl-3-methylimidazolium hexafluorophosphate (C_4mimPF_6), 1-hexyl-3-methylimidazolium hexafluorophosphate (C_6mimPF_6), and 1-ethyl-3-methylimidazolium bis(trifluoromethylsulfonyl)imide ($C_2mimTFSI$). (Scott et al., 2002, Scott et al., 2003, Mok et al., 2011) All these RTILs have similar characteristics with low T_g (-76 °C for C_4mimPF_6 , -78 °C for C_6mimPF_6 , -92 °C for $C_2mimTFSI$) and compatibility of polymer. It is also the same for C_8mimPF_6 . In conclusion, C_8mimPF_6 can effectively reduce the T_g of PMMA, thus acting as a plasticiser.

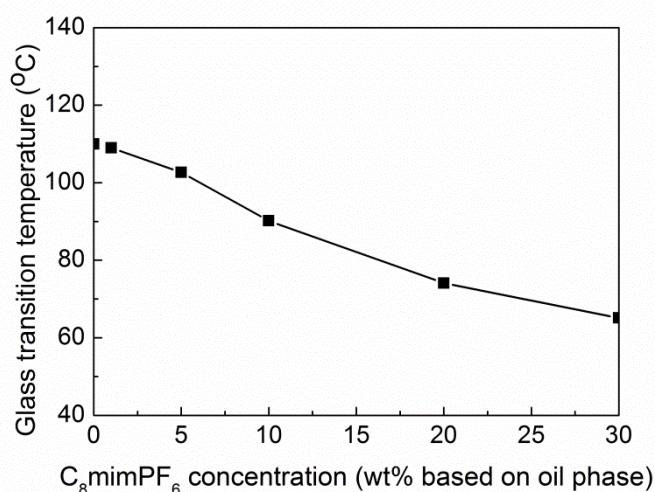
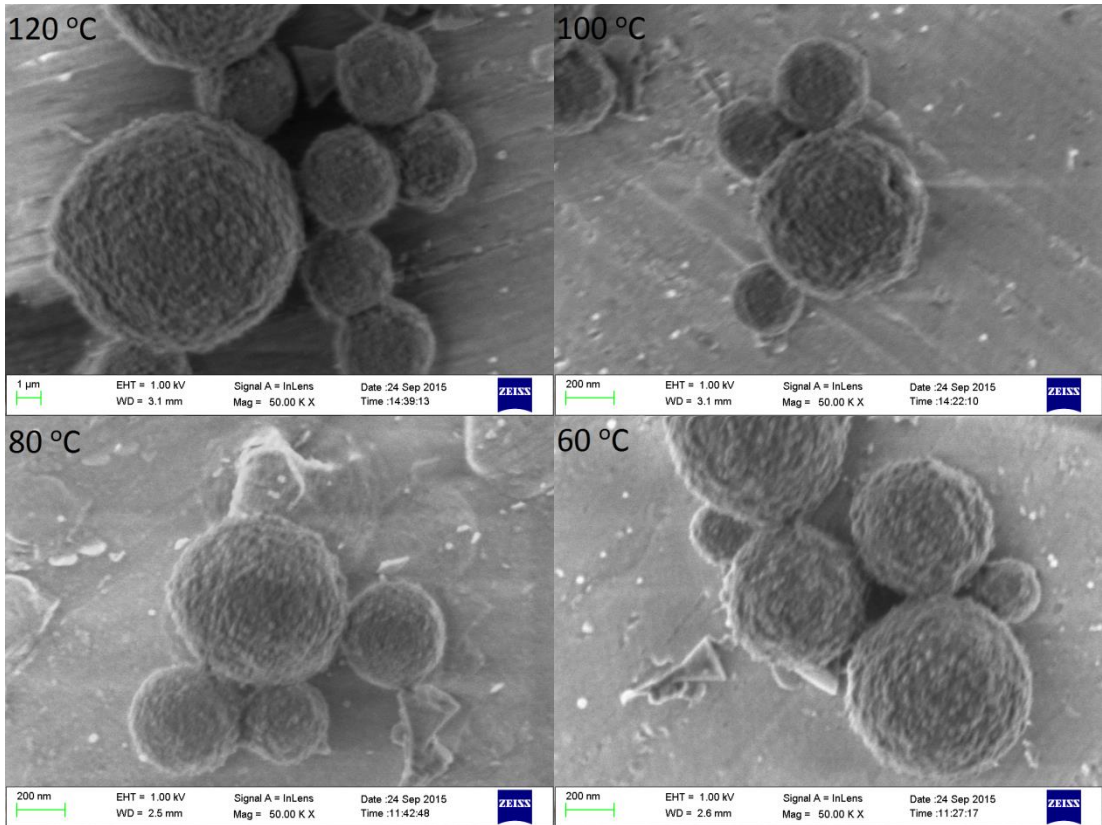
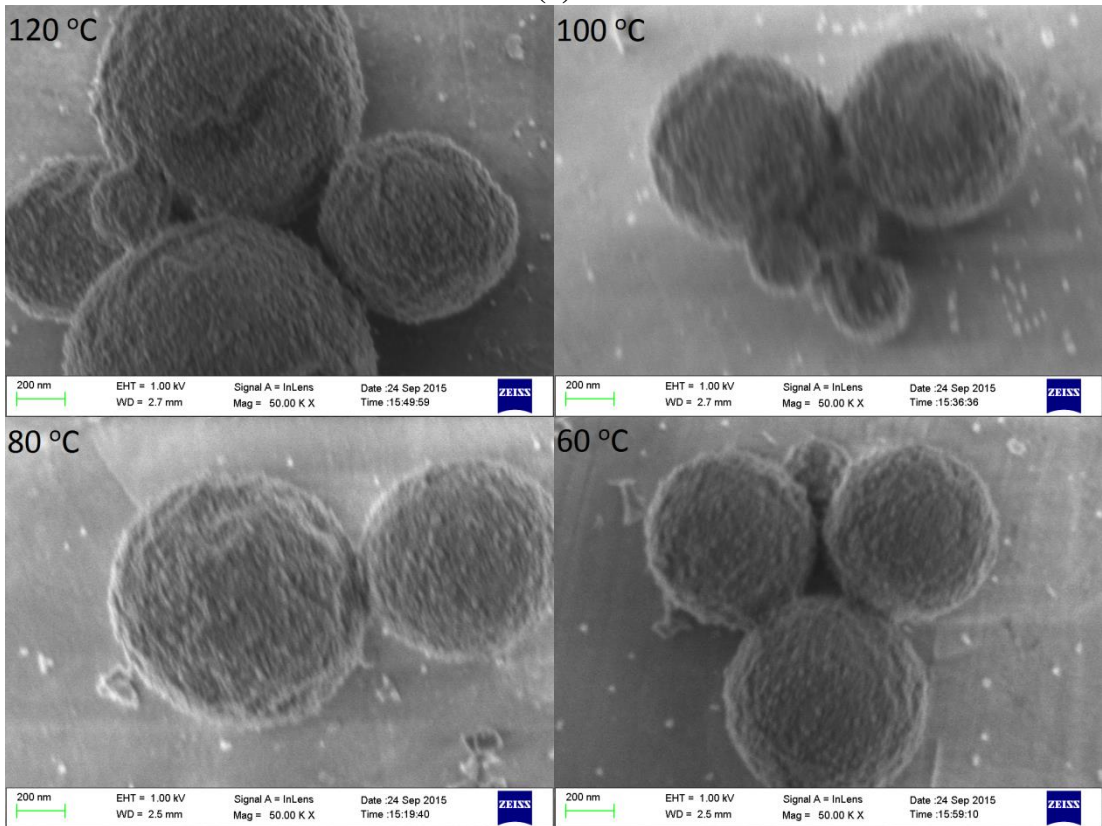


Fig.5.16 Glass transition temperature of particles containing different C_8mimPF_6 concentrations.

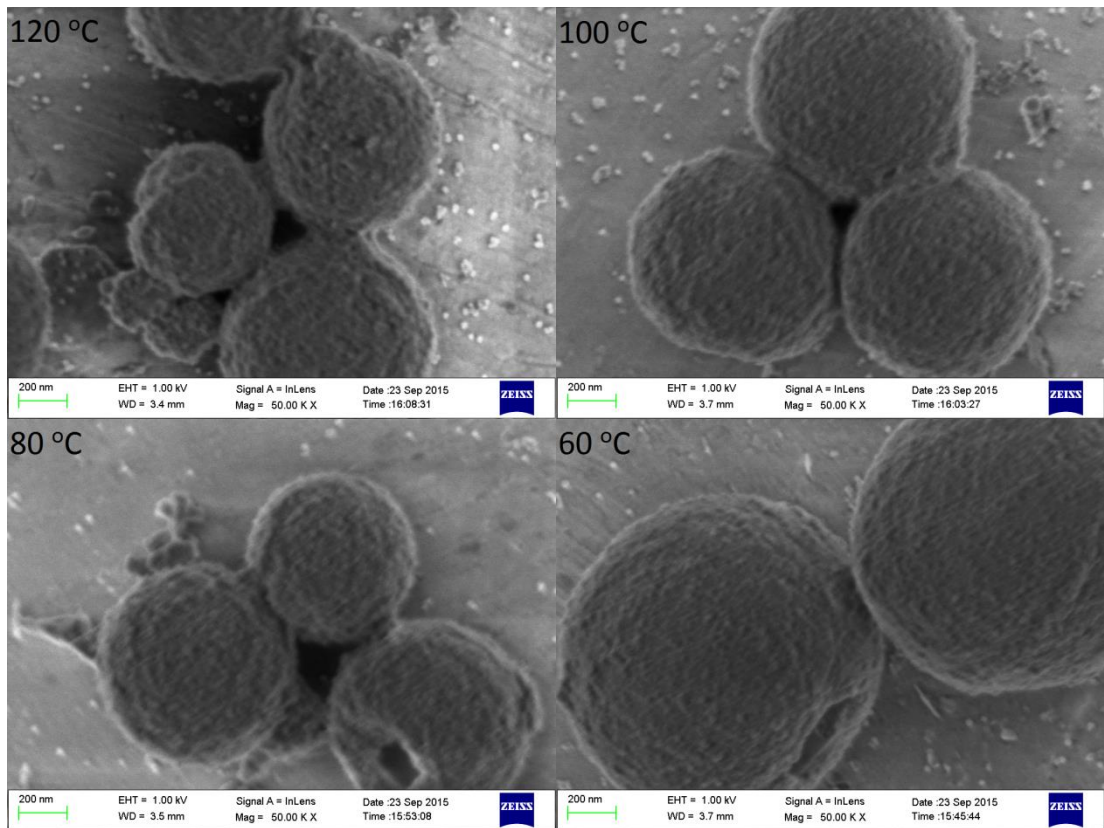
In order to investigate the effect of C_8mimPF_6 on the deformation of particles, particles were laid on the surface of aluminium foil, and stored under different temperatures for 2 h, sequentially observed by SEM. Fig.5.17 shows the deformation of particles containing C_8mimPF_6 with different concentrations under different storage temperature for 2 h.



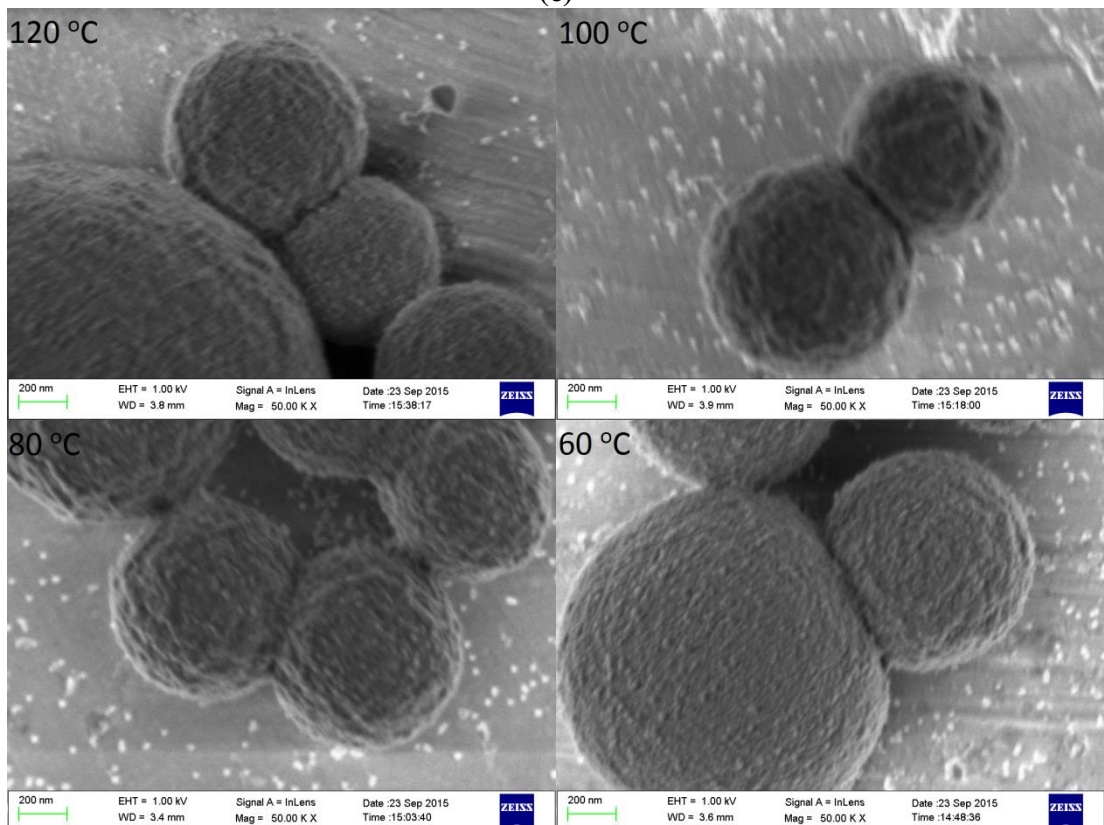
(a)



(b)



(c)



(d)

Fig.5.17 Deformation of particles containing different C_8mimPF_6 under different storage temperatures for 2 h. (a) 0 wt% C_8mimPF_6 ; (b) 10 wt% C_8mimPF_6 ; (c) 20 wt% C_8mimPF_6 ; (d) 30 wt% C_8mimPF_6 .

It can be seen that, at low C_8mimPF_6 concentration, *e.g.* 0 wt%, 10 wt%, the deformation of particles is not apparent. Even stored at 120 °C, the spherical shapes of particles present, and the boundaries between particles are distinguishable. At higher C_8mimPF_6 concentration, *e.g.* 20 wt%, the spherical shapes of particles are kept. However, adjacent particles start to coalesce, and the boundaries between particles become less distinct, especially at high temperature, *e.g.* 120 °C, and 100 °C. As C_8mimPF_6 concentration continually increase to 30 wt%, coalescence between adjacent particles become remarkable at all baking temperature, and shapes of particles turn into an intermediate state between sphere and hemisphere.

The deformation of particles stabilised by silica nanoparticles is different from that of particles stabilised by surfactant, SDSO. When particles were stabilised by SDSO, taking 120 °C, the upper limit baking temperature, for example, the boundary between particles became less distinct at 0 wt% C_8mimPF_6 , and discrete particles become a continuous block with the disappearance of the boundary between particles at 10 wt%, 20 wt%, and 30 wt%. While for particles stabilised by silica nanoparticles, at 120 °C, the spherical shapes of particles are kept or partially kept and the transformation from discrete particles to a continuous block is not detected for all C_8mimPF_6 concentrations. It can be seen that particles stabilised by silica nanoparticles are less likely to deform and coalesce compared with those stabilised by SDSO, probably due to the existence of silica nanoparticles.

The phenomenon that C_8mimPF_6 could effectively reduce the T_g of polymer but deformation of particles was limited can be explained as followings in the microcosmic aspects.

The reason why C_8mimPF_6 could effectively reduce the T_g of polymer here study has already been explained in 5.3.1.2. The homogeneous product indicated the successful encapsulation of C_8mimPF_6 . From the result of Fig.5.18, characteristic peaks of PMMA (1724 cm^{-1} , 1148 cm^{-1}) and C_8mimPF_6 (3173 cm^{-1} , 837 cm^{-1} , and 558 cm^{-1}) are all observed in FTIR spectra of 10 wt%, 20 wt%, 30 wt% C_8mimPF_6 , and no new characteristic peaks are formed for particles containing 10 wt%, 20 wt%, 30 wt% C_8mimPF_6 . This result indicates C_8mimPF_6 was still in a state of micro-molecule dispersed inside particles, acting as an external plasticiser. Due to the function as an external plasticiser, C_8mimPF_6 can effectively decreases T_g of polymer

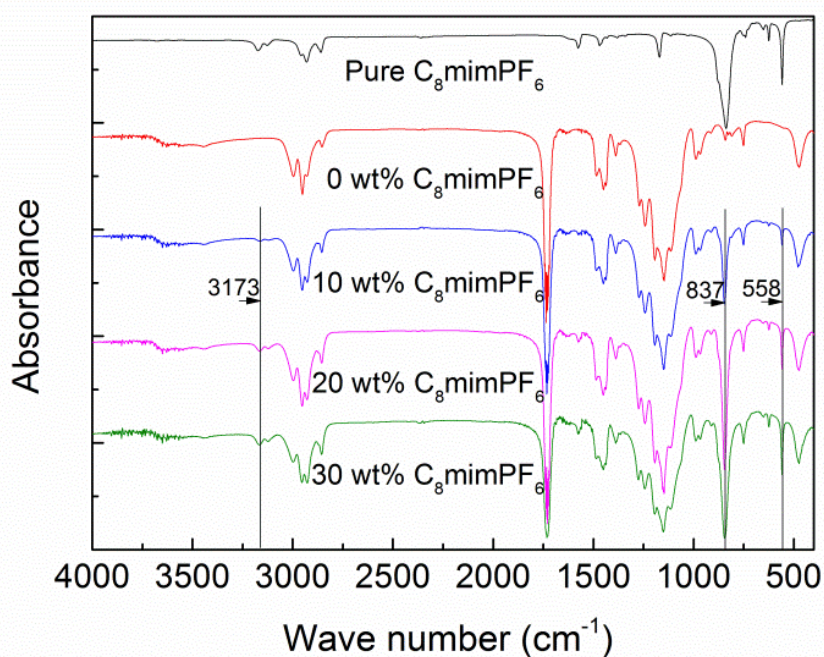


Fig.5.18 FTIR spectra for particles containing different C_8mimPF_6 concentrations and pure C_8mimPF_6 .

From the result of Fig.5.17, particles stabilised by silica nanoparticles are less likely to deform and coalesce compared with those stabilised by SDSO. Compared with particles stabilised by SDSO, the surface of particles stabilised by silica nanoparticles is rough, which was probably caused by the aggregation of silica

nanoparticles on the surface. These silica nanoparticles may inhibit the deformation and coalescence of particles.

In order to have a better observation of these surfaces, particles for TEM analysis were prepared as follows: latex was diluted 50 times by water and dropped on the surface of copper grid coated with carbon, followed by drying in air. Then TEM images of particles containing different C_8mimPF_6 concentrations with a magnification of 300 K were taken. Results are shown in Fig.5.19.

It can be seen that the surfaces of particles containing 0 wt%, 1 wt%, 5 wt%, 10 wt%, 20 wt% and 30 wt% C_8mimPF_6 are all rough. Their surfaces are fully covered by spheres in a diameter of 20 nm. Since silica nanoparticles used in this study are in a range of 20 nm, it was acceptable to draw the conclusion that these spheres are silica nanoparticles. So silica nanoparticles are tightly covered on the surface of particles, leading to the roughness in surface.

When polymers are transformed from a state of particles into a state of continuous film, the diffusion of polymer through the boundary of deformed particle into another particle is essential.(Raja et al., 2012, Keddie and Routh, 2010) However, when particles were fully covered by silica nanoparticles, these solid particles may become obstacles for the diffusion. In this case, the movement of polymers inside particles still occurred, but the diffusion of polymers between different particles was less likely to happen due to obstacles on the surface of particles. This might be the reason why particles stabilised by silica nanoparticles had a limitation in deformation and coalescence.

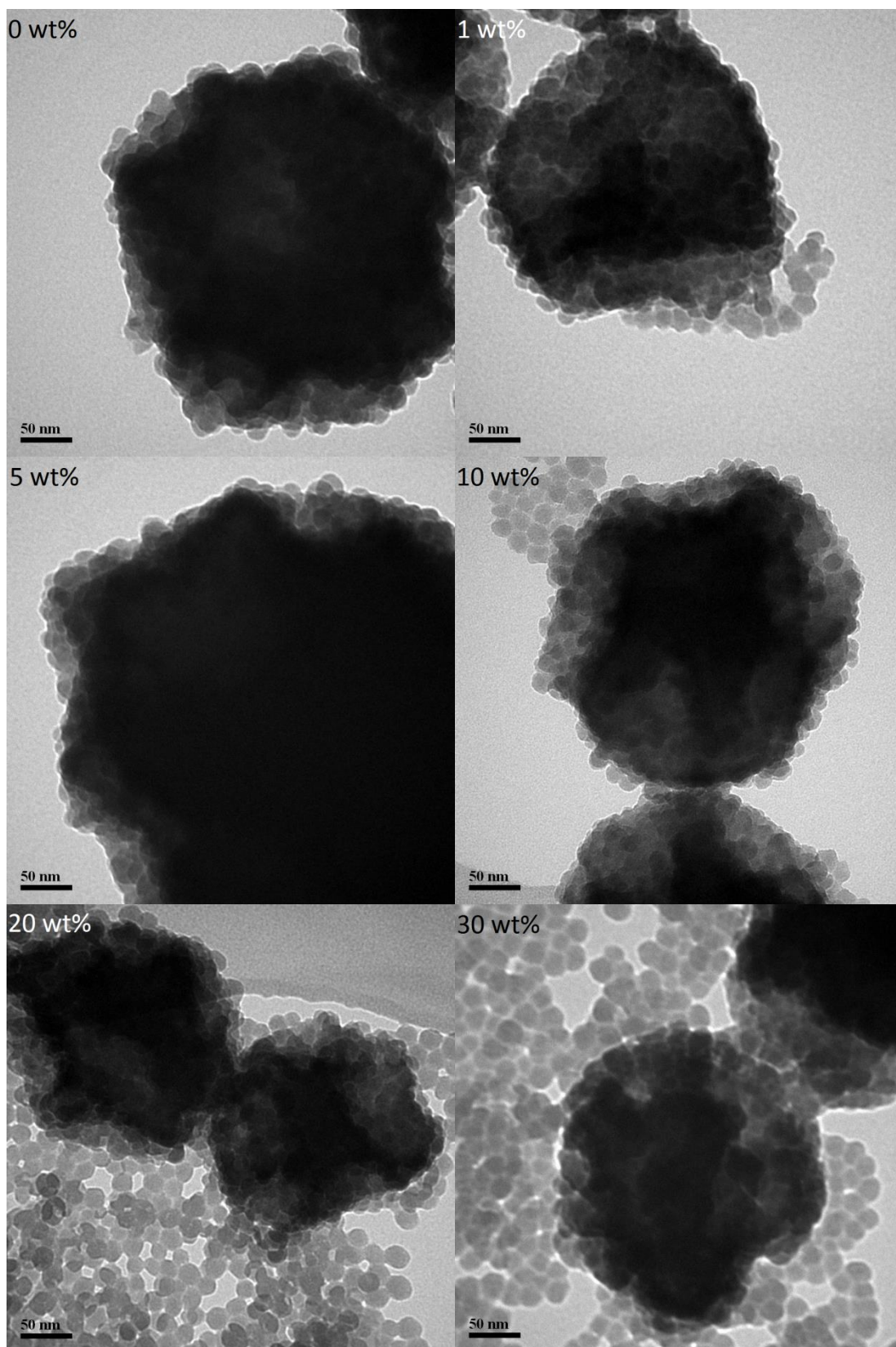


Fig.5.19 TEM images of particles containing different C_8mimPF_6 concentrations

5.3.2.3 Effect of C₈mimPF₆ concentration on molecular weight and distribution

The number-average molecular weight and polydispersity of polymers prepared from polymerisation of miniemulsions containing different C₈mimPF₆ concentrations are shown in Table.5.8. The number-average molecular weights are relatively low at low C₈mimPF₆ concentrations (0 wt% ~ 10 wt%), ranging from 283632 g/mol to 331117 g/mol. At high C₈mimPF₆ concentrations, *e.g.* 20 wt% and 30 wt%, the number-average molecular weights become higher, which are 364850 g/mol to 399103 g/mol, respectively. In addition, the polydispersities are relatively high, ranging from 2.64 to 3.47.

Table.5.8 Number-average molecular weight and polydispersity of polymers prepared from polymerisation of miniemulsions containing different C₈mimPF₆ concentration

C ₈ mimPF ₆ concentration (wt%)	Number-average molecular weight (g/mol)	Polydispersity
0	289730	3.38
1	283632	3.47
5	331117	3.20
10	293581	3.34
20	364850	2.98
30	399103	2.64

Fig.5.20 shows molecular weight distributions of polymers prepared from polymerisation of miniemulsions containing different C₈mimPF₆ concentrations. It can be seen that distributions are relatively broad for all C₈mimPF₆ concentrations. The molecular weight distributions shift to higher molecular weights when the concentration of C₈mimPF₆ increases from 10 wt% to 30 wt%.

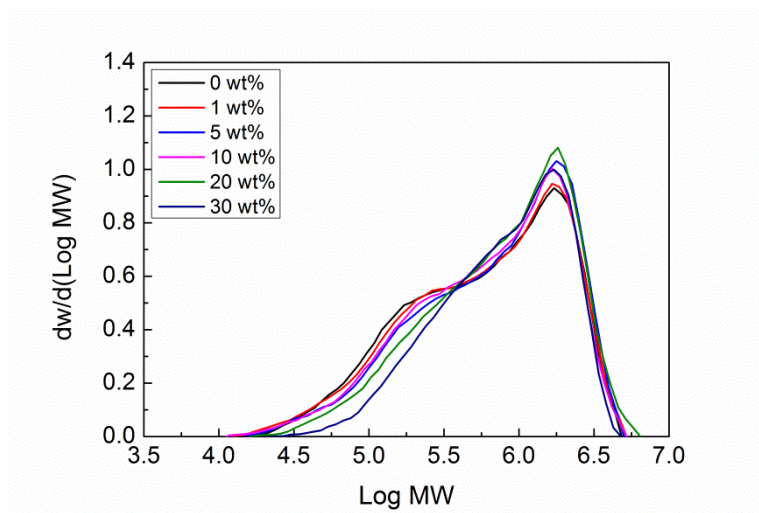


Fig.5.20 Molecular weight distributions of polymers prepared from polymerisation of miniemulsions containing different C_8mimPF_6 concentration.

5.3.2.4 Effect of C_8mimPF_6 concentration on thermal properties of film

In order to investigate the effect of C_8mimPF_6 concentration on the property of final film, latexes were baked at 120 °C within 2 h for film formation. The films formed by latexes containing 0, 10, 20, 30 wt% C_8mimPF_6 all cracked. Their thermal properties were studied according to these cases.

C_8mimPF_6 showed high thermal stability over a wide range of temperature, as the decomposition happened at a temperature as high as 400 °C (Fig.5.21). The film may have a better thermal stability to resist fire hazard in the presence of C_8mimPF_6 . Fig.5.21 shows the TG curves for films formed from latexes containing different C_8mimPF_6 concentrations. The onset of the weight loss for film without C_8mimPF_6 is the same as films containing C_8mimPF_6 . When thermal decomposition of film is not apparent, e.g. 150 °C to 300 °C, weight loss rate of film without C_8mimPF_6 is slow than that of film containing C_8mimPF_6 . However, as thermal decomposition of film becomes remarkable, e.g. 300 °C to 450 °C, weight loss rate of film without C_8mimPF_6 is much faster than that of film containing C_8mimPF_6 , indicating the better

thermal stability of film containing C_8mimPF_6 at this temperature range. It is interesting to note that, the thermal stability of film does not increase with the increase of C_8mimPF_6 concentration, and an optimal concentration, *e.g.* 10 wt% provides a better thermal stability. Similar observations have been reported when studied the composite of networked PMMA/ $C_2mimTFSI$ by Susan *et al.* and was attributed to the thermal stability of RTILs.(Susan et al., 2005b)

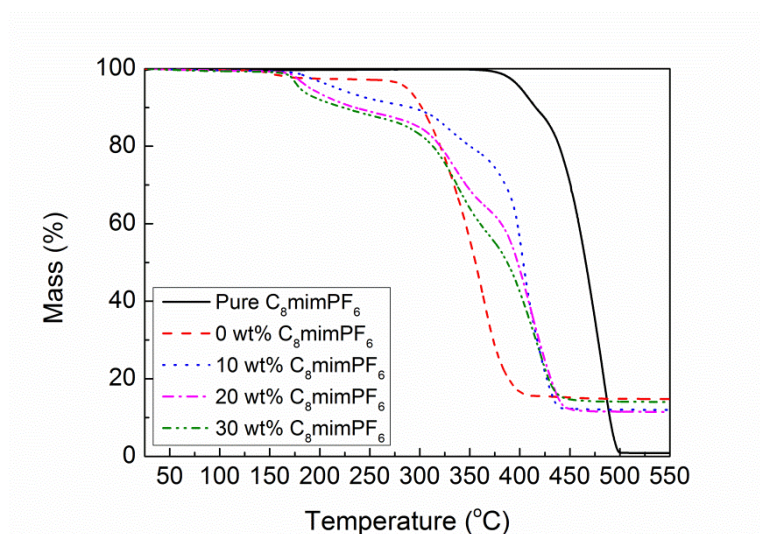


Fig.5.21 TG curves for films formed from latexes containing different C_8mimPF_6 concentrations.

5.4 Conclusion

A new latex containing C_8mimPF_6 , in the stabilisation of surfactant or silica nanoparticle has been developed for low VOCs latex coatings. This was achieved by encapsulating C_8mimPF_6 inside particles via miniemulsion polymerisation. Systematic investigations on C_8mimPF_6 concentration on stability of latex, glass transition temperature of polymer and deformation of particle, thermal stability of film, and mechanical property of film were carried out.

For latex stabilised by surfactant, results were summarised as follows.

The stability of latex decreased with the increase of C_8mimPF_6 when its concentration was reaching 10 wt%, manifesting as the increase in particle size with aging time caused by aggregation. Since the absolute zeta potentials were less than 30 mV for dispersion system containing 20 wt% and 30 wt% C_8mimPF_6 , they were unstable during long term storage. The T_g of polymer decreased and particles deformation were enhanced with the increase of C_8mimPF_6 concentration, providing that C_8mimPF_6 has the potential to be a coalescing agent. The reason why C_8mimPF_6 played such roles was attributed to its function as an external plasticiser with low T_g and compatibility with PMMA inside particles, which had been proven by FTIR spectra and TEM study. A continuous film could be formed when the C_8mimPF_6 was reaching 10 wt%. As the increase of C_8mimPF_6 , the film became more flexible, with better elongation, but lower Young's modulus due to the plasticiser function of C_8mimPF_6 . As compared with the bulk PMMA, films containing C_8mimPF_6 had better thermal stability caused by the thermal stability of C_8mimPF_6 .

For latex stabilised by silica nanoparticle, results were summarised as follows.

During storage, instability occurred for all latexes containing 0, 1, 5, 10, 20, 30 wt% C_8mimPF_6 : coagulation was detected for 0, 1, 5 wt% C_8mimPF_6 ; and sedimentation was detected for 10, 20, 30 wt% C_8mimPF_6 . The T_g of polymer decreased with the increase of C_8mimPF_6 concentration, indicating its function as an external plasticiser which had been proven by FTIR spectra study. However, deformation of particles was limited, probably due to obstacles of silica nanoparticles on the surface of particles. Compared with bulk PMMA, film containing C_8mimPF_6 had a better thermal stability at a temperature ranging from 300 °C to 450 °C.

Chapter 6 Conclusions

6.1 Conclusions

In this study, room temperature ionic liquid (C_8mimPF_6) was proposed as a non-volatile multi-functional additive to replace coalescing agent for the first time. The addition of C_8mimPF_6 in latex was successfully achieved by encapsulating it inside particles *via* miniemulsion polymerisation. Two kinds of emulsifiers, surfactant and silica nanoparticle were employed to stabilise miniemulsion/latex.

The main objectives of this study were achieved. The key outcomes would be summarised in following session.

6.1.1 Preparation of miniemulsion

During the preparation of miniemulsion, factors, including energy input, emulsifier type & concentration, C_8mimPF_6 concentration, and temperature on initial droplet size and stability of miniemulsion were systematically studied. The key outcomes related to this part are as follows:

- Droplet size of miniemulsion could be reduced by increasing energy input of homogeniser (input power or input duration) within certain limits, but further increase in energy input had less effect on reduction of droplet size.
- The choice of emulsifier played a key role in stabilising miniemulsion. For miniemulsion stabilised by surfactant, sodium dodecyl sulfonate (SDSO) is the target emulsifier. For silica nanoparticle, a pH of 3 is suitable to prepare a stable miniemulsion. With a proper emulsifier, initial droplet size sharply decreased as the emulsifier concentration increased, then tended to be stable.

- The presence of C₈mimPF₆ has demonstrated significant impact on initial droplet size of miniemulsion. Adding as little as 1 wt% C₈mimPF₆, resulted in a sharp decline in the droplet size for miniemulsion stabilised by surfactant or silica nanoparticle. Such trend was due to the combined effects of C₈mimPF₆ on the viscosity of oil phase and interfacial tension.

C₈mimPF₆ also affected the stability of miniemulsion during storage. When stabilised by surfactant, miniemulsions containing 20 wt%, 30 wt% C₈mimPF₆ were unstable during long time storage as the absolute zeta potentials were less than 30 mV. For miniemulsion stabilised by silica nanoparticle, instability during storage could be detected for all C₈mimPF₆ concentrations due to their low absolute zeta potentials. Creaming occurred at 0~5 wt% C₈mimPF₆, and sedimentation occurred at 10~30 wt% C₈mimPF₆ concentrations, depending on the density difference between droplet and water phase.

- High temperature was adverse to the stability of miniemulsion during storage. Above 50 °C, droplet size increased apparently independent the type of emulsifier used.

6.1.2 Miniemulsion polymerisation

In the following process, miniemulsion polymerisation, factors, including initiator type, temperature, and C₈mimPF₆ concentration on yield and stability of polymerisation process were systematically investigated. The key outcomes related to this part are as follows:

- Two types of initiators, hydrophobic AIBN and hydrophilic H₂O₂/AAc were chosen to initiate polymerisation at 40 °C, and they mainly had influences on reaction

rate. For miniemulsion stabilised by surfactant, when initiated by AIBN, C₈mimPF₆ had a promoting effect on the reaction rate at low concentrations, but this effect might reverse upon 10 wt% C₈mimPF₆; while initiated by H₂O₂/AAc, this promoting effect faded down even at low C₈mimPF₆ concentration. For miniemulsion stabilised by silica nanoparticle, a much higher yield of polymer could be achieved by AIBN (86.0%), compared with H₂O₂/AAc (28.1%).

- Reaction rate and stability of miniemulsion strongly depended on temperature. Higher temperatures resulted in higher reaction rates regardless of any emulsifier being used. A higher temperature e.g. 50 °C promoted the coalescence of droplet/particle of miniemulsion stabilised by surfactant, and hence produces larger latex particles. While for miniemulsion stabilised by silica nanoparticle, among temperatures ranging from 40 °C to 60 °C, 60 °C was with a product in smaller particle size.

- C₈mimPF₆ concentration not only affected reaction rate, but also stability of miniemulsion during polymerisation.

For miniemulsion stabilised by surfactant, AIBN could initiate polymerisation at a temperature (40 °C) much lower than its efficient decomposition temperature in the presence of C₈mimPF₆. At this temperature, C₈mimPF₆ had a promoting effect on the reaction rate at low concentrations, because it may cause an enhanced chain propagation rate and reduced chain termination rate. This effect might reverse upon certain C₈mimPF₆ concentrations, e.g. 10 wt%. While initiated by H₂O₂/AAc, the presence of C₈mimPF₆ had a negative effect on reaction rates even at low concentration, as C₈mimPF₆ and surfactant may form a tighter interfacial structure between droplet/particle and water phase that slowed down the entry rate of radicals

into droplet/particle. For miniemulsion stabilised by silica nanoparticle, the promoting effect on the reaction rate at low $C_8\text{mimPF}_6$ concentrations could also be observed when initiated by AIBN at 60 °C. Changing of concentrations of $C_8\text{mimPF}_6$ ranging from 0 to 30 wt% had only small effect on product yield, varying from 85wt% to 91 wt%.

For miniemulsion stabilised by surfactant, higher $C_8\text{mimPF}_6$ concentration (20 wt% and 30 wt%) promoted droplets coalescence causing increase in particle size of latex regardless of the type of initiator used. While for miniemulsion stabilised by silica nanoparticle, only above 10 wt% $C_8\text{mimPF}_6$, stable products could be achieved. The difference was due to the factor that the former was mainly stabilised by electrostatic repulsion between droplet/particle which may weaken at high $C_8\text{mimPF}_6$ concentration, while stabilisation of the latter was supported by the absorption of silica nanoparticle on the surface of droplet/particle which was enhanced by $C_8\text{mimPF}_6$ in droplet/particle.

6.1.3 Characterisation of latex

Based on the study of preparation of miniemulsion and miniemulsion polymerisation, latexes containing different concentrations of $C_8\text{mimPF}_6$ were achieved. The function of $C_8\text{mimPF}_6$ on final properties of latexes, including stability of latex, T_g of polymer, deformation of particles, molecular weight, mechanical property of film, and thermal stability of film was evaluated. The key outcomes related to this part are as follows:

- The effect of $C_8\text{mimPF}_6$ on stability of latex depended on the type of emulsifier used. For latex stabilised by surfactant, since the absolute zeta potential were less than 30 mV for latexes containing 20 wt% and 30 wt% $C_8\text{mimPF}_6$, they

were unstable during long term storage, manifesting as the increase in particle size with aging time caused by aggregation. While for latex stabilised by silica nanoparticle, coagulation was detected for 0, 1, 5 wt% C₈mimPF₆, and sedimentation was detected for 10, 20, 30 wt% C₈mimPF₆.

- C₈mimPF₆ could efficiently reduce the T_g of polymer for latex stabilised by surfactant or silica nanoparticle. The reason why C₈mimPF₆ played such roles was attributed to its function as an external plasticiser with low T_g and compatibility with PMMA.

- Deformation of particles strongly depended on the type of emulsifier used. For latex stabilised by surfactant, particles with higher C₈mimPF₆ concentration would efficiently deform at lower temperature. However, deformation of particles for latex stabilised by silica nanoparticle was limited, probably due to obstacles of silica nanoparticles on the surface of particles.

- For latex stabilised by SDSO, the number-average molecular weight continuously decreases with the increase in C₈mimPF₆ concentration from 1 wt% to 30 wt%. While for silica nanoparticle, the number-average molecular weights become higher at high C₈mimPF₆ concentrations, *e.g.* 20 wt% and 30 wt%.

- A continuous film could be formed for latex stabilised by surfactant when the C₈mimPF₆ was reaching 10 wt%. With the increase of C₈mimPF₆, the film became more flexible, with better elongation, but lower Young's modulus due to the plasticiser function of C₈mimPF₆.

- For both latex stabilised by surfactant and latex stabilised by silica nanoparticle, films containing C_8mimPF_6 had better thermal stability due to the thermal stability of C_8mimPF_6 .

6.2 Future work

In this study, some unexpected results were obtained during experiment. Due to the time limitation, further experiment to explain these results has been carried out. On the other hand, to produce latex coating with commercial application, further work based on current product shall be done.

- From the result of Fig.3.13, both C_8mimPF_6 concentration and SDSO concentration had influences on the oil/water phase interfacial tension, thus affecting the initial droplet size of miniemulsion. However, at the study of variation of droplet sizes as a function of C_8mimPF_6 concentration for miniemulsions stabilised with SDSO (Fig.3.11), SDSO concentration was fixed at 30 mM. The effect of C_8mimPF_6 concentration on initial droplet size at other SDSO concentrations, *e.g.* 20 mM, 40 mM, should also be taken into consideration.

Similarly, the effect of C_8mimPF_6 concentration on initial droplet size of miniemulsion stabilised by silica nanoparticles should be studied at other silica nanoparticle concentration, *e.g.* 30 g/L, 70 g/L.

- The reason why initiating temperature of AIBN could be reduced to 40 °C in the presence of C_8mimPF_6 was not clear. Relevant research can be first carried out in solvent polymerisation to study effect of C_8mimPF_6 on decomposition rate of initiator, chain propagation rate and chain termination rate at such low temperature, as solvent polymerisation is a homogeneous reaction which may avoid the effect of mass

transfer on reaction rate. After having a better understanding of C_8mimPF_6 on reaction process, research can be expanded to miniemulsion polymerisation.

Decomposition rate of initiator can be expressed as its consumption as a function of reaction time. This consumption would be reflected by the change of initiator concentration which can be measured by ultraviolet visible light spectrophotometer.(Thurecht et al., 2008) Taking AIBN for example, AIBN has a strong absorption peak at 347 nm, which can be taken as characteristic peak. By measuring absorbance at this characteristic peak, according to Lambert-Beer law shown in Eq.6.1, concentration of AIBN can be calculated, where ϵ is molar absorption coefficient, b is absorption layer thickness, c is AIBN concentration.

$$A = \epsilon bc \quad \text{Eq.6.1}$$

Because the decomposition of AIBN is a first-order reaction, by drawing the figure of $\ln(C_0/C_t)$ as a function of time, decomposition rate of AIBN can be obtained by calculating the slope of the line.

Chain propagation rate constant can be measured by pulsed laser free radical polymerization.(Harrisson et al., 2003) In the process of pulsed laser free radical polymerization, the monomer solution containing photo initiator is irradiated by an equal interval of pulse laser. After a pulse, new radicals formed and propagated the polymer chain. The propagation is then terminated after a subsequent pulse. By detecting the increase in polymer molecular weight, the growth of polymer chain at the dark interval between two times of pulses can be calculated. The chain growth rate, k_p can be calculated by Eq.6.2, where v is inflection point of number average molecular weight distribution peak, $[M]$ is monomer concentration, t_d is the dark time between two pulses.

$$v = k_p[M]t_d \quad \text{Eq.6.2}$$

• MMA was employed as the solo monomer for preparing latex, which may not fulfil the application. From the result of Table.1.1, which shows relationships between monomers and functions of coating layers, combination of different monomers may make it possible to apply latex at different situations. However, due to the incompatibility, some polymers may separate from RTILs.(Susan et al., 2005a) This incompatibility may lead to the formation of particle with a core-shell structure during miniemulsion polymerisation. If some parts of RTILs permeate into the space between polymers and other form a separated phase due to the limited compatibility, only the permeating parts play the plasticising function, thus weakening the function of RTILs as a coalescing agent.(Wypych, 2004) So it is necessary to study the effect of monomer composition on the polymerisation process to achieve a stable latex. After that, the properties of final latex, like morphology of particle, T_g of polymer, molecular weight, and mechanical properties shall be tested for commercial applications.

Reference

- ABISMAÏL, B., CANSÉLIER, J. P., WILHELM, A. M., DELMAS, H. & GOURDON, C. 1999. Emulsification by ultrasound: drop size distribution and stability. *Ultrasonics Sonochemistry*, 6, 75-83.
- AI, Z., DENG, R., ZHOU, Q., LIAO, S. & ZHANG, H. 2010. High solid content latex: preparation methods and application. *Adv Colloid Interface Sci*, 159, 45-59.
- ALDUNCIN, J. A. & ASUA, J. 1994. Molecular-weight distributions in the miniemulsion polymerization of styrene initiated by oil-soluble initiators. *Polymer*, 35, 3758-3765.
- ALDUNCIN, J. A., FORCADA, J. & ASUA, J. M. 1994. Miniemulsion polymerization using oil-soluble initiators. *Macromolecules*, 27, 2256-2261.
- ANDERSON, C. D. & DANIELS, E. S. 2003. *Emulsion Polymerisation and Latex Applications*, Shrewsbury, GBR, Smithers Rapra.
- ARAMENDIA, E., BARANDIARAN, M. J., GRADE, J., BLEASE, T. & ASUA, J. M. 2005. Improving Water Sensitivity in Acrylic Films Using Surfmers. *Langmuir*, 21, 1428-1435.
- ARAMENDIA, E., MALLÉGOL, J., JEYNES, C., BARANDIARAN, M. J., KEDDIE, J. L. & ASUA, J. M. 2003. Distribution of Surfactants near Acrylic Latex Film Surfaces: A Comparison of Conventional and Reactive Surfactants (Surfmers). *Langmuir*, 19, 3212-3221.
- AROCA, R., NAZRI, M., NAZRI, G., CAMARGO, A. & TRSIC, M. 2000. Vibrational spectra and ion-pair properties of lithium hexafluorophosphate in ethylene carbonate based mixed-solvent systems for lithium batteries. *Journal of Solution Chemistry*, 29, 1047-1060.
- ASUA, J. M. 2002. Miniemulsion polymerization. *Progress in Polymer Science*, 27, 1283-1346.
- ASUA, J. M. 2014. Challenges for industrialization of miniemulsion polymerization. *Progress in Polymer Science*, 39, 1797-1826.
- BAŁDYGA, J., ORCIUCH, W., MAKOWSKI, Ł. & MALIK, K. 2008. Dispersion of Nanoparticle Clusters in a Rotor-Stator Mixer. *Industrial & Engineering Chemistry Research*, 47, 3652-3663.
- BALKE, S. & HAMIELEC, A. 1973. Bulk polymerization of methyl methacrylate. *Journal of Applied Polymer Science*, 17, 905-949.
- BARBOSA, J. V., VELUDO, E., MONIZ, J., MENDES, A., MAGALHÃES, F. D. & BASTOS, M. M. 2013a. Low VOC self-crosslinking waterborne acrylic coatings incorporating fatty acid derivatives. *Progress in Organic Coatings*, 76, 1691-1696.
- BARBOSA, J. V., VELUDO, E., MONIZ, J., MENDES, A., MAGALHÃES, F. D. & BASTOS, M. M. S. 2013b. Low VOC self-crosslinking waterborne acrylic coatings incorporating fatty acid derivatives. *Progress in Organic Coatings*, 76, 1691-1696.
- BAZYLIŃSKA, U., KULBACKA, J. & WILK, K. A. 2014. Dicapalic ionic surfactants in fabrication of biocompatible nanoemulsions: Factors influencing droplet size and stability. *Colloids and Surfaces A: Physicochemical and Engineering Aspects*, 460, 312-320.
- BECHTHOLD, N. & LANDFESTER, K. 2000. Kinetics of miniemulsion polymerization as revealed by calorimetry. *Macromolecules*, 33, 4682-4689.
- BEHERA, K. & PANDEY, S. 2007. Modulating properties of aqueous sodium dodecyl sulfate by adding hydrophobic ionic liquid. *J Colloid Interface Sci*, 316, 803-14.
- BERG, J. C. 2010. *An Introduction to Interfaces and Colloids: The Bridge to Nanoscience*, 5 Toh Tuck Link, Singapore, World Scientific Publishing Co. Pte. Ltd.
- BIELEMAN, J. 2000. Additives for coatings.
- BINKS, B. P. 2002. Particles as surfactants—similarities and differences. *Current opinion in colloid & interface science*, 7, 21-41.
- BINKS, B. P. & CLINT, J. H. 2002. Solid wettability from surface energy components: relevance to Pickering emulsions. *Langmuir*, 18, 1270-1273.

- BINKS, B. P. & LUMSDON, S. O. 2000a. Effects of oil type and aqueous phase composition on oil-water mixtures containing particles of intermediate hydrophobicity. *Physical Chemistry Chemical Physics*, 2, 2959-2967.
- BINKS, B. P. & LUMSDON, S. O. 2000b. Influence of Particle Wettability on the Type and Stability of Surfactant-Free Emulsions†. *Langmuir*, 16, 8622-8631.
- BOURSIER, T., CHADUC, I., RIEGER, J., D'AGOSTO, F., LANSALOT, M. & CHARLEUX, B. 2011. Controlled radical polymerization of styrene in miniemulsion mediated by PEO-based trithiocarbonate macromolecular RAFT agents. *Polymer Chemistry*, 2, 355-362.
- BRIX, H. D., EBERSOLD, D., SEMAR, M., BRUNS, J. & VONEND, M. 2013. Ternary fungicidal compositions comprising boscalid and chlorothalonil. Google Patents.
- CANSELIER, J. P., DELMAS, H., WILHELM, A. M. & ABISMAÏL, B. 2002. Ultrasound Emulsification—An Overview. *Journal of Dispersion Science and Technology*, 23, 333-349.
- CAO, Y. & MU, T. 2014. Comprehensive Investigation on the Thermal Stability of 66 Ionic Liquids by Thermogravimetric Analysis. *Industrial & Engineering Chemistry Research*, 53, 8651-8664.
- CAO, Z., SHAN, G., FEVOTTE, G., SHEIBAT-OTHMAN, N. & BOURGEAT-LAMI, E. 2008. Miniemulsion copolymerization of styrene and γ -methacryloxypropyltrimethoxysilane: kinetics and mechanism. *Macromolecules*, 41, 5166-5173.
- CAPEK, I. 2012. On photoinduced miniemulsion polymerization of butyl acrylate with clay. *Designed Monomers and Polymers*, 15, 345-355.
- CAPEK, I. & KOCSISOVÁ, T. 2011. On the preparation of composite poly (butyl acrylate)/carbon nanotube nanoparticles by miniemulsion polymerization of butyl acrylate. *Polymer journal*, 43, 700-707.
- CARDOSO, P. B., ARAÚJO, P. H. H. & SAYER, C. 2013. Encapsulation of Jojoba and Andiroba Oils by Miniemulsion Polymerization. Effect on Molar Mass Distribution. *Macromolecular Symposia*, 324, 114-123.
- CARSON, L., CHAU, P. K. W., EARLE, M. J., GILEA, M. A., GILMORE, B. F., GORMAN, S. P., MCCANN, M. T. & SEDDON, K. R. 2009. Antibiofilm activities of 1-alkyl-3-methylimidazolium chloride ionic liquids. *Green Chemistry*, 11, 492-497.
- CASEY, M. B. 2009. *Study of monomer droplet behavior in miniemulsions*. PhD, Lehigh University
- CHAI, X. S., HOU, Q. X. & SCHORK, F. J. 2004. Determination of residual monomer in polymer latex by full evaporation headspace gas chromatography. *Journal of Chromatography A*, 1040, 163-167.
- CHANG, J., FORTMANN, R., ROACHE, N. & LAO, H. C. 1999. Evaluation of Low - VOC Latex Paints. *Indoor Air*, 9, 253-258.
- CHATZI, E., KAMMONA, O. & KIPARISSIDES, C. 1997. Use of a midrange infrared optical-fiber probe for the on-line monitoring of 2-ethylhexyl acrylate/styrene emulsion copolymerization. *Journal of applied polymer science*, 63, 799-809.
- CHAUMONT, A., SCHURHAMMER, R. & WIPFF, G. 2005. Aqueous Interfaces with Hydrophobic Room-Temperature Ionic Liquids: A Molecular Dynamics Study. *Journal of Physical Chemistry B*, 109, 18964-18973.
- CHEN, M., WU, L., ZHOU, S. & YOU, B. 2004. Synthesis of Raspberry-like PMMA/SiO₂ Nanocomposite Particles via a Surfactant-Free Method. *Macromolecules*, 37, 9613-9619.
- CHEN, M., ZHOU, S., YOU, B. & WU, L. 2005. A novel preparation method of raspberry-like PMMA/SiO₂ hybrid microspheres. *Macromolecules*, 38, 6411-6417.
- CHENG, L., ZHANG, Y., ZHAO, T. & WANG, H. 2004. Free Radical Polymerization of Acrylonitrile in Green Ionic Liquids. *Macromolecular Symposia*, 216, 9-16.

- CHERN, C.-S. & LIOU, Y.-C. 1999a. Kinetics of styrene miniemulsion polymerization stabilized by nonionic surfactant/alkyl methacrylate. *Polymer*, 40, 3763-3772.
- CHERN, C.-S. & LIOU, Y.-C. 1999b. Kinetics of styrene miniemulsion polymerization stabilized by nonionic surfactant/alkyl methacrylate. *Polymer*, 40, 3763-3772.
- CHERN, C.-S. & LIOU, Y.-C. 1999c. Styrene Miniemulsion Polymerization Initiated by 2,2'-Azobisisobutyronitrile. *Journal of Polymer Science: Part A: Polymer Chemistry*, 37, 2537-2550.
- CHERN, C. & CHEN, T. 1997. Miniemulsion polymerization of styrene using alkyl methacrylates as the reactive cosurfactant. *Colloid and Polymer Science*, 275, 546-554.
- CHERN, C. & CHEN, T. 1998. Effect of Ostwald ripening on styrene miniemulsion stabilized by reactive cosurfactants. *Colloids and Surfaces A: Physicochemical and Engineering Aspects*, 138, 65-74.
- CHERN, C. S. 2006. Emulsion polymerization mechanisms and kinetics. *Progress in Polymer Science*, 31, 443-486.
- CHERN, C. S., LIM, H. & CALA, N. A. 2009. Miniemulsion copolymerizations of styrene and methyl methacrylate in the presence of reactive costabilizer. *Journal of Applied Polymer Science*, 112, 173-180.
- CHEUNG, H. M. & GADDAM, K. 2000. Ultrasound-assisted emulsion polymerization of methyl methacrylate and styrene. *Journal of applied polymer science*, 76, 101-104.
- CHOI, E. C., JIN, S. M., PARK, Y. J. & KIM, Y. 2008. Polymerization kinetics for the preparation of poly(p-divinylbenzene) via a miniemulsion polymerization process. *Journal of the Chinese Institute of Chemical Engineers*, 39, 483-488.
- CHOI, S.-S., KIM, I.-S. & WOO, C.-S. 2007. Influence of TESPT content on crosslink types and rheological behaviors of natural rubber compounds reinforced with silica. *Journal of Applied Polymer Science*, 106, 2753-2758.
- COSTA, C. E., SANTOS, V. S. H. S., DARIVA, C., S, A. X. F. S., TUNY, M. R. F., JO, P. H. H. A. & SAYER, C. U. 2013. Ionic Liquid as Surfactant in Microwave-Assisted Emulsion Polymerization. *Journal of Applied Polymer Science*, 448-455.
- DAVIS, J. J. H. & FOX, P. A. 2003. From curiosities to commodities: ionic liquids begin the transition. *Chemical Communications*, 1209-1212.
- DOANE, T. L., CHUANG, C.-H., HILL, R. J. & BURDA, C. 2011. Nanoparticle ζ -Potentials. *Accounts of Chemical Research* 45, 317-326.
- DOCHERTY, K. M. & KULPA, J. C. F. 2005. Toxicity and antimicrobial activity of imidazolium and pyridinium ionic liquids. *Green Chemistry*, 7, 185-189.
- DUPRE, J. 1982. Thickening agent for aqueous compositions. Google Patents.
- ECKERSLEY, S. T. & HELMER, B. J. 1997. Mechanistic considerations of particle size effects on film properties of hard/soft latex blends. *Journal of Coatings Technology*, 69, 97-107.
- FITCHETT, B. D., ROLLINS, J. B. & CONBOY, J. C. 2005. Interfacial tension and electrocapillary measurements of the room temperature ionic liquid/aqueous interface. *Langmuir*, 21, 12179-12186.
- FITZWATER, G., GEISSLER, W., MOULTON, R., PLECHKOVA, N. V., ROBERTSON, A., SEDDON, K. R., SWINDALL, J. & JOO, K. W. 2005. Ionic liquids: sources of innovation. *Report Q002, QUILL, Belfast*.
- FLORY, P. J. 1953. *Principles of polymer chemistry*, Ithaca, New York Cornell University Press.
- FORTUNA, S., COLARD, C. A., TROISI, A. & BON, S. A. 2009. Packing patterns of silica nanoparticles on surfaces of armored polystyrene latex particles. *Langmuir*, 25, 12399-12403.
- FORTUNATO, R., AFONSO, C. A. M., REIS, M. A. M. & CRESPO, J. G. 2004. Supported liquid membranes using ionic liquids: study of stability and transport mechanisms. *Journal of Membrane Science*, 242, 197-209.

- FREDLAKE, C. P., CROSTHWAITE, J. M., HERT, D. G., AKI, S. N. V. K. & BRENNECKE, J. F. 2004. Thermophysical Properties of Imidazolium-Based Ionic Liquids. *Journal of Chemical & Engineering Data* 49, 954-964.
- FREEMANTLE, M. 2010. *An Introduction to Ionic Liquids*, Cambridge, UK, The Royal Society of Chemistry.
- FREIRE, M. G., NEVES, C. M. S. S., CARVALHO, P. J., GARDAS, R. L., FERNANDES, A. M., MARRUCHO, I. M., SANTOS, L. S. M. N. B. F. & COUTINHO, J. O. A. P. 2007. Mutual Solubilities of Water and Hydrophobic Ionic Liquids. *Journal of Physical Chemistry B*, 13082-13089.
- FREZ, C. & DIEBOLD, G. J. 2006. Determination of Thermal Diffusivities, Thermal Conductivities, and Sound Speeds of Room-Temperature Ionic Liquids by the Transient Grating Technique. *Journal of Chemical and Engineering Data*, 1250-1255.
- GALLAGHER, M., DALTON, P., SITVARIN, L. & PRETI, G. 2008. Sensory and Analytical Evaluations of Paints With and Without Texanol. *Environmental Science & Technology*, 42, 243-248.
- GAN, L., CHEW, C. & LYE, I. 1992. Styrene polymerization in oil - in - water microemulsions: kinetics of polymerization. *Die Makromolekulare Chemie*, 193, 1249-1260.
- GRIFFIN, W. C. 1949. Classification of Surface-Active Agents by "HLB". *Journal of the Society of Cosmetic Chemists* 1, 311-326.
- GUNDABALA, V. R., LEI, C.-H., OUZINEB, K., DUPONT, O., KEDDIE, J. L. & F. ROUTH, A. 2008. Lateral surface nonuniformities in drying latex films. *AIChE Journal*, 54, 3092-3105.
- HARRIS, K. R., KANAKUBO, M. & WOOLF, L. A. 2007. Temperature and Pressure Dependence of the Viscosity of the Ionic Liquids 1-Hexyl-3-methylimidazolium Hexafluorophosphate and 1-Butyl-3-methylimidazolium Bis (trifluoromethylsulfonyl) imide. *Journal of Chemical & Engineering Data*, 52, 1080-1085.
- HARRISSON, S., MACKENZIE, S. R. & HADDLETON, D. M. 2002. Unprecedented solvent-induced acceleration of free-radical propagation of methyl methacrylate in ionic liquids. *Chemical Communications*, 2850-2851.
- HARRISSON, S., MACKENZIE, S. R. & HADDLETON, D. M. 2003. Pulsed Laser Polymerization in an Ionic Liquid Strong Solvent Effects. *Macromolecular*, 36, 5072-5075.
- HECHT, L. L., WAGNER, C., LANDFESTER, K. & SCHUCHMANN, H. P. 2011. Surfactant Concentration Regime in Miniemulsion Polymerization for the Formation of MMA Nanodroplets by High-Pressure Homogenization. *Langmuir*, 27, 2279-2285.
- HEZAVE, A. Z., DOROSTKAR, S., AYATOLLAHI, S., NABIPOUR, M. & HEMMATEENEJAD, B. 2013. Investigating the effect of ionic liquid (1-dodecyl-3-methylimidazolium chloride ([C₁₂mim] [Cl])) on the water oil interfacial tension as a novel surfactant. *Colloids and Surfaces A: Physicochemical and Engineering Aspects*, 421, 63-71.
- HOFFARTH, G. 1998. Low-foaming wetting agent consisting of various alkoxyated alcohol mixtures. Google Patents.
- HONG, K., ZHANG, H., MAYS, J. W., VISSER, A. E., BRAZEL, C. S., HOLBREY, J. D., REICHERT, W. M. & ROGERS, R. D. 2002. Conventional free radical polymerization in room temperature ionic liquids: a green approach to commodity polymers with practical advantages. *Chemical Communications*, 1368-1369.
- HONG, R. Y., FENG, B., CAI, X., LIU, G., LI, H. Z., DING, J., ZHENG, Y. & WEI, D. G. 2009. Double-mini-emulsion preparation of Fe₃O₄/poly(methyl methacrylate) magnetic latex. *Journal of Applied Polymer Science*, 112, 89-98.
- HOU, L. X. & WANG, S. 2011. Study on ionic liquid [bmim]PF₆ and [hmim]PF₆ as plasticizer for PVC paste resin. *Polymer Bulletin*, 67, 1273-1283.
- HOUSAINDOKHT, M. R. & NAKHAEI POUR, A. 2012. Study the effect of HLB of surfactant on particle size distribution of hematite nanoparticles prepared via the reverse microemulsion. *Solid State Sciences*, 14, 622-625.

- HULKKO, J., KOSKIMIES, S., KYLAEKOSKI, R., LOEIJIA, M., MARTTINA, M., PAAJANEN, L. & RISSANEN, K. 2005. *Reactive coalescent agents*. PCT/FI2005/050102.
- IIMORI, T., IWAHASHI, T., KANAI, K., SEKI, K., SUNG, J., KIM, D., HAMAGUCHI, H.-O. & OUCHI, Y. 2007. Local Structure at the Air/Liquid Interface of Room-Temperature Ionic Liquids Probed by Infrared -Visible Sum Frequency Generation Vibrational Spectroscopy: 1-Alkyl-3-methylimidazolium Tetrafluoroborates. *J. Phys. Chem. B*, 4860-4866.
- JAFARI, S. M., HE, Y. & BHANDARI, B. 2007. Production of sub-micron emulsions by ultrasound and microfluidization techniques. *Journal of Food Engineering*, 82, 478-488.
- JASIŃSKA, M., BAŁDYGA, J., HALL, S. & PACEK, A. W. 2014. Dispersion of oil droplets in rotor-stator mixers: Experimental investigations and modeling. *Chemical Engineering and Processing: Process Intensification*, 84, 45-53.
- JENSEN, D. & MORGAN, L. 1991. Particle size as it relates to the minimum film formation temperature of latices. *Journal of applied polymer science*, 42, 2845-2849.
- JIA, Z., WANG, Z., XU, C., LIANG, J., WEI, B., WU, D. & ZHU, S. 1999. Study on poly(methyl methacrylate)/carbon nanotube composites. *Materials Science and Engineering A*, 271, 395-400.
- JOHANSSON, K. 2006. Growing greener: ICE 2006-A look at what's driving the industry. *European coatings journal*, 16.
- JOSCELYNE, S. M. & TRÄGÅRDH, G. 2000. Membrane emulsification—a literature review. *Journal of Membrane Science*, 169, 107-117.
- JUMAA, M. & MÜLLER, B. W. 2002. Parenteral emulsions stabilized with a mixture of phospholipids and PEG-660-12-hydroxy-stearate: evaluation of accelerated and long-term stability. *European Journal of Pharmaceutics and Biopharmaceutics*, 54, 207-212.
- KARAM, H. J. & BELLINGER, J. C. 1968. Deformation and Breakup of Liquid Droplets in a Simple Shear Field. *Industrial & Engineering Chemistry Fundamentals*, 7, 576-581.
- KARGAR, M., FAYAZMANESH, K., ALAVI, M., SPYROPOULOS, F. & NORTON, I. T. 2012. Investigation into the potential ability of Pickering emulsions (food-grade particles) to enhance the oxidative stability of oil-in-water emulsions. *Journal of Colloid and Interface Science*, 366, 209-215.
- KEDDIE, J. & ROUTH, A. F. 2010. *Fundamentals of latex film formation: processes and properties*, Springer Science & Business Media.
- KEDDIE, J. L. 1997. Film formation of latex *Materials Science and Engineering*, 21, 101-170.
- KHEZRI, K., HADDADI - ASL, V., ROGHANI - MAMAQANI, H. & SALAMI - KALAJAHI, M. 2012. Synthesis of clay - dispersed poly (styrene - co - methyl methacrylate) nanocomposite via miniemulsion atom transfer radical polymerization: A reverse approach. *Journal of Applied Polymer Science*, 124, 2278-2286.
- KIM, K.-J. 2010. Ethylene-propylene-diene terpolymer/silica compound modification with organosilane [bis(triethoxysilylpropyl)disulfide] and improved processability and mechanical properties. *Journal of Applied Polymer Science*, 116, 237-244.
- KITAGAWA, M. & TOKIWA, Y. 2006. Polymerization of vinyl sugar ester using ascorbic acid and hydrogen peroxide as a redox reagent. *Carbohydrate Polymers*, 64, 218-223.
- KOBAYASHI, M., JUILLERAT, F., GALLETTO, P., BOWEN, P. & BORKOVEC, M. 2005. Aggregation and charging of colloidal silica particles: effect of particle size. *Langmuir*, 21, 5761-5769.
- KÖHLER, K., SANTANA, A. S., BRAISCH, B., PREIS, R. & SCHUCHMANN, H. P. 2010. High pressure emulsification with nano-particles as stabilizing agents. *Chemical Engineering Science*, 65, 2957-2964.

- KOHRI, M., KOBAYASHI, A., FUKUSHIMA, H., KOJIMA, T., TANIGUCHI, T., SAITO, K. & NAKAHIRA, T. 2012. Enzymatic miniemulsion polymerization of styrene with a polymerizable surfactant. *Polymer Chemistry*, 3, 900-906.
- KONG, Y., HU, B., CHOY, K.-L., LI, X. & CHEN, G. 2015. Study of miniemulsion formulation containing 1-octyl-3-methylimidazolium hexafluorophosphate for its application in low-emitting coating products. *Soft Matter*, 11, 1293-1302.
- LAHTINEN, M., GLAD, E., KOSKIMIES, S., SUNDHOLM, F. & RISSANEN, K. 2003. Synthesis of novel reactive coalescing agents and their application in a latex coating. *Journal of Applied Polymer Science*, 87, 610-615.
- LANDFESTER, K., BECHTHOLD, N., TIARKS, F. & ANTONIETTI, M. 1999a. Formulation and Stability Mechanisms of Polymerizable Miniemulsions. *Macromolecules*, 32, 5222-5228.
- LANDFESTER, K., BECHTHOLD, N., TIARKS, F. & ANTONIETTI, M. 1999b. Miniemulsion polymerization with cationic and nonionic surfactants: a very efficient use of surfactants for heterophase polymerization. *Macromolecules*, 32, 2679-2683.
- LE BIDEAU, J., VIAU, L. & VIOUX, A. 2011. Ionogels, ionic liquid based hybrid materials. *Chemical Society Reviews*, 40, 907.
- LEI, Y. D., TANG, Z. H., GUO, B. C., ZHU, L. X. & JIA, D. M. 2010. Synthesis of novel functional liquid and its application as a modifier in SBR/silica composites. *EXPRESS Polymer Letters*, 4, 692-703.
- LI, N., LU, J., XU, Q., XIA, X. & WANG, L. 2007. Reverse atom transfer radical polymerization of MMA via immobilized catalysts in imidazolium ionic liquids. *Journal of Applied Polymer Science*, 103, 3915-3919.
- LIU, Y., WU, G., FU, H., JIANG, Z., CHEN, S. & SHA, M. 2010. Immobilization and melting point depression of imidazolium ionic liquids on the surface of nano-SiO_x particles. *Dalton Trans*, 39, 3190-4.
- LÓPEZ-MARTÍNEZ, E. I., MÁRQUEZ-LUCERO, A., HERNÁNDEZ-ESCOBAR, C. A., FLORES-GALLARDO, S. G., IBARRA-GÓMEZ, R., YACAMÁN, M. J. & ZARAGOZA-CONTRERAS, E. A. 2007. Incorporation of silver/carbon nanoparticles into poly(methyl methacrylate) via in situ miniemulsion polymerization and its influence on the glass-transition temperature. *Journal of Polymer Science Part B: Polymer Physics*, 45, 511-518.
- LÓPEZ, A., CHEMTOB, A., MILTON, J. L., MANEA, M., PAULIS, M., BARANDIARAN, M. A. J., THEISINGER, S., LANDFESTER, K., HERGETH, W. D. & UDAGAMA, R. 2008. Miniemulsification of monomer-resin hybrid systems. *Industrial & Engineering Chemistry Research*, 47, 6289-6297.
- LU, J., YAN, F. & TEXTER, J. 2009. Advanced applications of ionic liquids in polymer science. *Progress in Polymer Science*, 34, 431-448.
- LV, L.-P., ZHAO, Y., ZHOU, H.-X., LANDFESTER, K. & CRESPI, D. 2014. From core-shell and Janus structures to tricompartiment submicron particles. *Polymer*, 55, 715-720.
- MA, J., LU, M., CAO, C. & ZHANG, H. 2013. Synthesis and characterization of PMMA/SiO₂ organic-inorganic hybrid materials via RAFT-mediated miniemulsion polymerization. *Polymer Composites*, 34, 626-633.
- MA, J. & ZHANG, H. 2014. Preparation and characterization of poly (methyl methacrylate)/SiO₂ organic-inorganic hybrid materials via RAFT-mediated miniemulsion Polymerization. *Journal of Polymer Research*, 21, 1-9.
- MAA, Y.-F. & HSU, C. 1996. Liquid-liquid emulsification by rotor/stator homogenization. *Journal of Controlled Release*, 38, 219-228.
- MACCALLUM, J. R. 1989. *Polymer electrolyte reviews*, Springer Science & Business Media.
- MACCHIAGODENA, M., GONTRANI, L., RAMONDO, F., TRIOLO, A. & CAMINITI, R. 2011. Liquid structure of 1-alkyl-3-methylimidazolium-hexafluorophosphates by wide angle x-ray and neutron scattering and molecular dynamics. *J Chem Phys*, 134, 114521.

- MAHDI JAFARI, S., HE, Y. & BHANDARI, B. 2006. Nano-Emulsion Production by Sonication and Microfluidization—A Comparison. *International Journal of Food Properties*, 9, 475-485.
- MANDZY, N., GRULKE, E. & DRUFFEL, T. 2005. Breakage of TiO₂ agglomerates in electrostatically stabilized aqueous dispersions. *Powder Technology*, 160, 121-126.
- MASA, J. A., DE ARBINA, L. L. P. & ASUA, J. M. 1993. A comparison between miniemulsion and conventional emulsion terpolymerization of styrene, 2-ethylhexyl acrylate and methacrylic acid. *Journal of applied polymer science*, 48, 205-213.
- MELIANA, Y., SUPRIANTI, L., HUANG, Y. C., LIN, C. T. & CHERN, C.-S. 2011. Effect of mixed costabilizers on Ostwald ripening of monomer miniemulsions. *Colloids and Surfaces A: Physicochemical and Engineering Aspects*, 389, 76-81.
- MILLER, C., SUDOL, E., SILEBI, C. & EL-AASSER, M. 1995. Polymerization of miniemulsions prepared from polystyrene in styrene Solutions. 3. Potential differences between miniemulsion droplets and polymer particles. *Macromolecules*, 28, 2772-2780.
- MISTRY, M. K., SUBIANTO, S., CHOUDHURY, N. R. & DUTTA, N. K. 2009. Interfacial interactions in aprotic ionic liquid based protonic membrane and its correlation with high temperature conductivity and thermal properties. *Langmuir*, 25, 9240-9251 %@ 0743-7463.
- MOK, M. M., LIU, X., BAI, Z., LEI, Y. & LODGE, T. P. 2011. Effect of Concentration on the Glass Transition and Viscoelastic Properties of Poly(methyl methacrylate)/Ionic Liquid Solutions. *Macromolecules*, 44, 1016-1025.
- MØRK, P. C. & MAKAME, Y. 1997. Compartmentalized polymerization with oil-soluble initiators. Kinetic effect of single radical formation. *Journal of Polymer Science Part A: Polymer Chemistry*, 35, 2347-2354.
- MOSCA, M., CUOMO, F., LOPEZ, F. & CEGLIE, A. 2013. Role of emulsifier layer, antioxidants and radical initiators in the oxidation of olive oil-in-water emulsions. *Food Research International*, 50, 377-383.
- MUHAMMAD, A., ABDUL MUTALIB, M. I., WILFRED, C. D., MURUGESAN, T. & SHAFEEQ, A. 2008. Thermophysical properties of 1-hexyl-3-methyl imidazolium based ionic liquids with tetrafluoroborate, hexafluorophosphate and bis(trifluoromethylsulfonyl)imide anions. *The Journal of Chemical Thermodynamics*, 40, 1433-1438.
- MUSYANOVYCH, A., ROSSMANITH, R., TONTSCH, C. & LANDFESTER, K. 2007. Effect of Hydrophilic Comonomer and Surfactant Type on the Colloidal Stability and Size Distribution of Carboxyl- and Amino-Functionalized Polystyrene Particles Prepared by Miniemulsion Polymerization. *Langmuir*, 23, 5367-5376.
- NAGANO, T., TAKAHASHI, T. & SUGAI, H. 2009. *paint compositions*. United States patent application 11/218,510.
- NAZARZADEH, E. & SAJJADI, S. 2010. Viscosity effects in miniemulsification via ultrasound. *AIChE Journal*, 56, 2751-2755.
- NI, P., ZHANG, M., MA, L. & FU, S. 2006. Poly(dimethylamino)ethyl Methacrylate for Use as a Surfactant in the Miniemulsion Polymerization of Styrene. *Langmuir*, 22, 6016-6023.
- NING, H., HOU, M., MEI, Q., LIU, Y., YANG, D. & HAN, B. 2012. The physicochemical properties of some imidazolium-based ionic liquids and their binary mixtures. *Science China Chemistry*, 55, 1509-1518.
- NIRIELLA, D. & CARNAHAN, R. 2006. Comparison study of zeta potential values of bentonite in salt solutions. *Journal of dispersion science and technology*, 27, 123-131.
- OH, K., LEE, J. Y., LEE, S.-S., PARK, M., KIM, D. & KIM, H. 2013. Highly stretchable dielectric nanocomposites based on single-walled carbon nanotube/ionic liquid gels. *Composites Science and Technology*, 83, 40-46.
- OHSHIMA, H. 2012. *Electrical phenomena at interfaces and biointerfaces: fundamentals and applications in nano-, bio-, and environmental sciences*, John Wiley & Sons.

- OKADA, H., KOMURO, T., SAKAI, T., MATSUO, Y., ONO, Y., OMOTE, K., YOKOO, K., KAWACHI, K., KASAMA, Y., ONO, S., HATAKEYAMA, R., KANEKO, T. & TOBITA, H. 2012. Preparation of endohedral fullerene containing lithium (Li@C60) and isolation as pure hexafluorophosphate salt ([Li@C60][PF6⁻]). *RSC Advances*, 2, 10624.
- OUZINEB, K., LORD, C., LESAUZE, N., GRAILLAT, C., TANGUY, P. A. & MCKENNA, T. 2006. Homogenisation devices for the production of miniemulsions. *Chemical Engineering Science*, 61, 2994-3000.
- P. BINKS, B. & O. LUMSDON, S. 1999. Stability of oil-in-water emulsions stabilised by silica particles. *Physical Chemistry Chemical Physics*, 1, 3007-3016.
- PAL, A. & CHAUDHARY, S. 2013. Effect of hydrophilic ionic liquid on aggregation behavior of aqueous solutions of sodium dodecylsulfate (SDS). *Fluid Phase Equilibria*, 352, 42-46.
- PEI, X., ZHOU, F., YU, B., HU, H., XUE, J. & LIU, W. 2011. *Ionic liquid modified marine antifouling coating*. China patent application.
- PENG, B., ZHANG, J., LU, R., ZHANG, S., ZHOU, W. & GAO, H. 2013. Dispersive micro-solid phase extraction based on self-assembling, ionic liquid-coated magnetic particles for the determination of clofentezine and chlorfenapyr in environmental water samples. *Analyst*, 6834-6843.
- PERCY, M., BARTHET, C., LOBB, J., KHAN, M., LASCELLES, S., VAMVAKAKI, M. & ARMES, S. 2000. Synthesis and characterization of vinyl polymer-silica colloidal nanocomposites. *Langmuir*, 16, 6913-6920.
- PERNAK, J., SOBASZKIEWICZ, K. & MIRSKA, I. 2003. Anti-microbial activities of ionic liquids. *Green Chemistry*, 5, 52-56.
- PERRIER, S., TAKOLPUCKDEE, P. & MARS, C. A. 2005. Reversible addition-fragmentation chain transfer polymerization: End group modification for functionalized polymers and chain transfer agent recovery. *Macromolecules*, 38, 2033-2036.
- PERRIER, S. B., DAVIS, T. P., CARMICHAEL, A. J. & HADDLETON, D. M. 2002. First report of reversible addition-fragmentation chain transfer (RAFT) polymerisation in room temperature ionic liquids. *Chemical Communications*, 2226-2227.
- PHAM, V. H., DANG, T. T., HUR, S. H., KIM, E. J. & CHUNG, J. S. 2012. Morphology and properties of segregated-network chemically converted graphene-poly (vinyl chloride) composite. *Journal of nanoscience and nanotechnology*, 12, 5820-5826.
- PIANELLI, C., DEVAUX, J., BEBELMAN, S. & LELOUP, G. 1999. The micro-Raman spectroscopy, a useful tool to determine the degree of conversion of light-activated composite resins. *Journal of biomedical materials research*, 48, 675-681.
- PLECHKOVA, N. V. & SEDDON, K. R. 2008. Applications of ionic liquids in the chemical industry. *Chem Soc Rev*, 37, 123-50.
- QIAN, C. & MCCLEMENTS, D. J. 2011. Formation of nanoemulsions stabilized by model food-grade emulsifiers using high-pressure homogenization: Factors affecting particle size. *Food Hydrocolloids*, 25, 1000-1008.
- RAHMAN, M. & BRAZEL, C. S. 2006. Ionic liquids: New generation stable plasticizers for poly(vinyl chloride). *Polymer Degradation and Stability*, 91, 3371-3382.
- RAI, R., BAKER, G. A., BEHERA, K., MOHANTY, P., KURUR, N. D. & PANDEY, S. 2010. Ionic Liquid-Induced Unprecedented Size Enhancement of Aggregates within Aqueous Sodium Dodecylbenzene Sulfonate. *Langmuir*, 26, 17821-17826.
- RAJA, T. N., BROUWER, A. M., BIEMANS, K., NABUURS, T. & TENNEBROEK, R. 2010. Detection of coalescing agents in water-borne latex emulsions using an environment sensitive fluorescent probe. *Photochem Photobiol Sci*, 9, 975-84.
- RAJA, T. N., BROUWER, A. M., NABUURS, T. & TENNEBROEK, R. 2012. A fluorescence approach to investigate repartitioning of coalescing agents in acrylic polymer emulsions. *Colloid Polym Sci*, 290, 541-552.

- RAMESH, S., LEEN, K. H., KUMUTHA, K. & AROF, A. K. 2007. FTIR studies of PVC/PMMA blend based polymer electrolytes. *Spectrochimica Acta Part A*, 1237-1242.
- REIMERS, J. & SCHORK, F. 1996a. Miniemulsion copolymerization using water-insoluble comonomers as cosurfactants. *Polymer Reaction Engineering*, 4, 135-152.
- REIMERS, J. & SCHORK, F. 1996b. Robust nucleation in polymer - stabilized miniemulsion polymerization. *Journal of applied polymer science*, 59, 1833-1841.
- RIDUAN, S. N. & ZHANG, Y. 2013. Imidazolium salts and their polymeric materials for biological applications. *Chemical Society Reviews*, 42, 9055-70.
- ROMIO, A. P., BERNARDY, N., LEMOS SENNA, E., ARAÚJO, P. H. H. & SAYER, C. 2009a. Polymeric nanocapsules via miniemulsion polymerization using redox initiation. *Materials Science and Engineering: C*, 29, 514-518.
- ROMIO, A. P., SAYER, C., ARAÚJO, P. H. H., AL-HAYDARI, M., WU, L. & DA ROCHA, S. R. P. 2009b. Nanocapsules by Miniemulsion Polymerization with Biodegradable Surfactant and Hydrophobe. *Macromolecular Chemistry and Physics*, 210, 747-751.
- ROSEN, M. J. & KUNJAPPU, J. T. 2012. *Surfactants and interfacial phenomena*, John Wiley & Sons.
- RUFFOLO, S. A., MACCHIA, A., LA RUSSA, M. F., MAZZA, L., URZÌ, C., DE LEO, F., BARBERIO, M. & CRISCI, G. M. 2013. Marine antifouling for underwater archaeological sites: TiO₂ and Ag-doped TiO₂. *International Journal of Photoenergy*, 2013.
- SACANNA, S., KEGEL, W. K. & PHILIPSE, A. P. 2007. Thermodynamically stable pickering emulsions. *Phys Rev Lett*, 98, 158301.
- SARAC, A. S. 1999. Redox polymerization. *Progress in Polymer Science*, 24, 1149-1204.
- SAYGI-ARSLAN, Ö. 2010. *Aspects of droplet and particle size control in miniemulsions*. PhD, Lehigh University.
- SCHMIDTS, T., DOBLER, D., GULDAN, A. C., PAULUS, N. & RUNKEL, F. 2010. Multiple W/O/W emulsions—Using the required HLB for emulsifier evaluation. *Colloids and Surfaces A: Physicochemical and Engineering Aspects*, 372, 48-54.
- SCHMITZ, J., FROMMELIUS, H., PEGELOW, U., SCHULTE, H.-G. & HÖFER, R. 1999. A new concept for dispersing agents in aqueous coatings. *Progress in organic Coatings*, 35, 191-196.
- SCHOONBROOD, H. A. S. & ASUA, J. M. 1997. Reactive Surfactants in Heterophase Polymerization. 9. Optimum Surfactant Behavior in Emulsion Polymerization. *Macromolecules*, 30, 6034-6041.
- SCHORK, F. J., LUO, Y., SMULDERS, W., RUSSUM, J. P., BUTTÉ, A. & FONTENOT, K. 2005. Miniemulsion Polymerization. *Advanced Polymer Science*, 175, 129-255.
- SCHRADE, A., LANDFESTER, K. & ZIENER, U. 2013. Pickering-type stabilized nanoparticles by heterophase polymerization. *Chem Soc Rev*, 42, 6823-39.
- SCHRADE, A., MIKHALEVICH, V., LANDFESTER, K. & ZIENER, U. 2011. Synthesis and characterization of positively charged, alumina-coated silica polystyrene hybrid nanoparticles via pickering miniemulsion polymerization. *Journal of Polymer Science Part A: Polymer Chemistry*, 49, 4735-4746.
- SCOTT, M. P., BRAZEL, C. S., BENTON, M. G., MAYS, J. W., HOLBREY, J. D. & ROGERS, R. D. 2002. Application of ionic liquids as plasticizers for poly(methyl methacrylate). *Chemical Communications*, 1370-1371.
- SCOTT, M. P., RAHMAN, M. & BRAZEL, C. S. 2003. Application of ionic liquids as low-volatility plasticizers for PMMA. *European Polymer Journal*, 39, 1947-1953.
- SHANG, Y. & SHAN, G.-R. 2012. IBN partition between st monomer/polymer and water and its application in miniemulsion polymerization initiated by AIBN. *AIChE Journal*, 58, 3135-3143.
- SHIBULAL, G. & NASKAR, K. 2012. Exploring a novel multifunctional agent to improve the dispersion of short aramid fiber in polymer matrix. *Express Polym Lett*, 6, 329-344.

- SINGH, M., ESQUENA, J., SOLANS, C., BOOTEN, K. & TADROS, T. F. 2014. Influence of hydrophobically modified inulin (INUTEK NRA) on the stability of vulcanized natural rubber latex. *Colloids and Surfaces A: Physicochemical and Engineering Aspects*, 451, 90-100.
- SMITH, E. A. & CHEN, W. 2008. How to Prevent the Loss of Surface Functionality Derived from Aminosilanes. *Langmuir*, 24, 12405-12409.
- SONAVANE, G., TOMODA, K. & MAKINO, K. 2008. Biodistribution of colloidal gold nanoparticles after intravenous administration: effect of particle size. *Colloids Surf B Biointerfaces*, 66, 274-80.
- STARK, A. & SEDDON, K. R. 2007. *Kirk-Othmer Encyclopedia of Chemical Technology*, Hoboken, New Jersey, John Wiley & Sons, Inc.
- STAUDT, T., MACHADO, T. O., VOGEL, N., WEISS, C. K., ARAUJO, P. H., SAYER, C. & LANDFESTER, K. 2013. Magnetic polymer/nickel hybrid nanoparticles via miniemulsion polymerization. *Macromolecular Chemistry and Physics*, 214, 2213-2222.
- STEINMACHER, F. R., ARAÚJO, P. H. H. & SAYER, C. 2015. Incorporation of high oil content in polyvinyl acetate nanoparticles produced by batch miniemulsion polymerization stabilized with a polymeric stabilizer. *Journal of Applied Polymer Science*, 132.
- STOUT, W. & LOUIS, C. 2005. Molecular defoamers. *European coatings journal*, 4, 132-137.
- STREITBERGER, H.-J. & DÖSSEL, K.-F. 2008. *Automotive Paints and Coatings*, Germany, WILEY-VCH Verlag GmbH & Co. KGaA, Weinheim.
- SUMMERS, M. & EASTOE, J. 2003. Applications of polymerizable surfactants. *Advances in Colloid and Interface Science*, 100-102, 137-152.
- SUN, X., WU, D., CHEN, J. & LI, D. 2007. Separation of scandium(III) from lanthanides(III) with room temperature ionic liquid based extraction containing Cyanex 925. *Journal of Chemical Technology & Biotechnology*, 82, 267-272.
- SUSAN, M. A. B. H., KANEKO, T., NODA, A. & WATANABE, M. 2005a. Ion gels prepared by in situ radical polymerization of vinyl monomers in an ionic liquid and their characterization as polymer electrolytes. *Journal of American Chemical Society*, 127, 4976-4983.
- SUSAN, M. A. B. H., KANEKO, T., NODA, A. & WATANABE, M. 2005b. Ion gels prepared by in situ radical polymerization of vinyl monomers in an ionic liquid and their characterization as polymer electrolytes. *Journal of the American Chemical Society*, 127, 4976 -4983.
- SVEC, F. & FRECHET, J. M. J. 1995. Temperature, a Simple and Efficient Tool for the Control of Pore Size Distribution in Macroporous Polymers. *Macromolecules*, 28, 7580-7582.
- TANIGUCHI, T., TAKEUCHI, N., KOBARU, S. & NAKAHIRA, T. 2008. Preparation of highly monodisperse fluorescent polymer particles by miniemulsion polymerization of styrene with a polymerizable surfactant. *Journal of Colloid and Interface Science*, 327, 58-62.
- TAO, B. & XIAN-HUA, C. 2006. Preparation and characterization of lanthanum-based thin films on sulfonated self-assembled monolayer of 3-mercaptopropyl trimethoxysilane. *Thin Solid Films*, 515, 2262-2267.
- TAUER, K. 2005. Stability of monomer emulsion droplets and implications for polymerizations therein. *Polymer*, 46, 1385-1394.
- TEO, V. L., DAVIS, B. J., TSAREVSKY, N. V. & ZETTERLUND, P. B. 2014. Successful Miniemulsion ATRP Using an Anionic Surfactant: Minimization of Deactivator Loss by Addition of a Halide Salt. *Macromolecules*, 47, 6230-6237.
- THURECHT, K. J., GOODEN, P. N., GOEL, S., TUCK, C., LICENCE, P. & IRVINE, D. J. 2008. Free Radical Polymerization in Ionic Liquids: The Case for a Protected Radical. *Macromolecules*, 41, 2814 -2820.

- TIARKS, F., LANDFESTER, K. & ANTONIETTI, M. 2001a. Preparation of Polymeric Nanocapsules by Miniemulsion Polymerization. *Langmuir*, 17, 908-918.
- TIARKS, F., LANDFESTER, K. & ANTONIETTI, M. 2001b. Silica nanoparticles as surfactants and fillers for latexes made by miniemulsion polymerization. *Langmuir*, 17, 5775-5780.
- TOH, S. L. I., MCFARLANE, J., TSOURIS, C., DEPAOLI, D. W., LUO, H. & DAI, S. 2006. Room - Temperature Ionic Liquids in Liquid - Liquid Extraction: Effects of Solubility in Aqueous Solutions on Surface Properties. *Solvent Extraction and Ion Exchange*, 24, 33-56.
- TOMIDA, D., KUMAGAI, A., KENMOCHI, S., QIAO, K. & YOKOYAMA, C. 2007a. Viscosity of 1-Hexyl-3-methylimidazolium Hexafluorophosphate and 1-Octyl-3-methylimidazolium Hexafluorophosphate at High Pressure. *Journal of Chemical and Engineering Data*, 577-579.
- TOMIDA, D., KUMAGAI, A., KENMOCHI, S., QIAO, K. & YOKOYAMA, C. 2007b. Viscosity of 1-Hexyl-3-methylimidazolium Hexafluorophosphate and 1-Octyl-3-methylimidazolium Hexafluorophosphate at High Pressure. *Journal of Chemical and Engineering Data*, 52, 577-579.
- TOUSSAINT, A., WILDE, M. D., MOLENAAR, F. & MULVIHILL, J. 1997. Calculation of T_g and MFFT depression due to added coalescing agents *Progress in Organic Coatings*, 30, 179-184.
- UCHIYAMA, Y. & SUZUKI, H. 1992. Anti-foaming agent. Google Patents.
- UEDA, J., YAMAGUCHI, H., SHIRAI, K., YAMAUCHI, T. & TSUBOKAWA, N. 2008. Radical polymerization of vinyl monomers in the presence of carbon black initiated by 2,2'-azobisisobutyronitrile and benzoyl peroxide in ionic liquid. *Journal of Applied Polymer Science*, 107, 3300-3305.
- UEMAE, M. & KOMATSU, T. 1995. Dispersion of acrylic particles having core and skin with different glass transition temperatures; chip-resistant coatings. Google Patents.
- URBAN, K., WAGNER, G., SCHAFFNER, D., RÖGLIN, D. & ULRICH, J. 2006. Rotor-Stator and Disc Systems for Emulsification Processes. *Chemical Engineering & Technology*, 29, 24-31.
- VADAMALAR, R., MANI, P., BALAKRISHNAN, R. & ARUMUGAM, V. 2008. Evaluation of Excess Free Volume and Internal Pressure in Binary Mixtures of Methyl Methacrylate(MMA) with Alcohols *E-Journal of Chemistry* 6, 261-269.
- VYGODSKII, Y. S., MEL'NIK, O. A., LOZINSKAYA, E. I., SHAPLOV, A. S., MALYSHKINA, I. A., GAVRILOVA, N. D., LYSENKO, K. A., ANTIPIN, M. Y., GOLOVANOV, D. G. & KORLYUKOV, A. A. 2007. The influence of ionic liquid's nature on free radical polymerization of vinyl monomers and ionic conductivity of the obtained polymeric materials. *Polymers for Advanced Technologies*, 18, 50-63 %@ 1042-7147.
- WANG, C. & BAO, Q. 2005. *Acrylate coatings*, Beijing, Chemical Industry Press.
- WANG, S., POEHLEIN, G. W. & SCHORK, F. J. 1997. Miniemulsion polymerization of styrene with chain transfer agent as cosurfactant. *Journal of Polymer Science Part A: Polymer Chemistry*, 35, 595-603.
- WANG, S., SCHORK, F., POEHLEIN, G. & GOOCH, J. 1996. Emulsion and miniemulsion copolymerization of acrylic monomers in the presence of alkyd resin. *Journal of applied polymer science*, 60, 2069-2076.
- WANG, Y., ZHANG, Y., XIA, T., ZHAO, W. & YANG, W. 2014. Effects of fabricated technology on particle size distribution and thermal properties of stearic-eicosanoic acid/polymethylmethacrylate nanocapsules. *Solar Energy Materials and Solar Cells*, 120, 481-490.
- WEI, R., LUO, Y., ZENG, W., WANG, F. & XU, S. 2012. Styrene-Butadiene-Styrene triblock copolymer latex via reversible addition-fragmentation chain transfer miniemulsion polymerization. *Industrial & Engineering Chemistry Research*, 51, 15530-15535.

- WEYERSHAUSEN, B., LEHMANN, K. & BAKER, G. A. 2005. Industrial application of ionic liquids as performance additives. *Green Chemistry*, 7, 15-19.
- WINKELMANN, M. & SCHUCHMANN, H. P. 2011. Precipitation of metal oxide nanoparticles using a miniemulsion technique. *Particuology*, 9, 502-505.
- WITTMAR, A., RUIZ-ABAD, D. & ULBRICHT, M. 2012. Dispersions of silica nanoparticles in ionic liquids investigated with advanced rheology. *Journal of Nanoparticle Research*, 14, 1-10.
- WYPYCH, G. 2004. *Handbook of plasticizers*, Toronto, Canada, ChemTec Publishing.
- YAGCI, M. B., BOLCA, S., HEUTS, J. P. A., MING, W. & DE WITH, G. 2011. Antimicrobial polyurethane coatings based on ionic liquid quaternary ammonium compounds. *Progress in Organic Coatings*, 72, 343-347.
- YAMAMOTO, T. 2013. Synthesis of nearly micron-sized particles by soap-free emulsion polymerization of methacrylic monomer using an oil-soluble initiator. *Colloid and Polymer Science*, 291, 2741-2744.
- YANG, Y., SHEERIN, R. & SHAVEL, L. C. 2007. Paint Compositions with Low-or Zero-VOC Coalescence Aids and Nano-Particle Pigments. Google Patents.
- YE, Y.-S., RICK, J. & HWANG, B.-J. 2013. Ionic liquid polymer electrolytes. *Journal of Materials Chemistry A*, 1, 2719-2743.
- YILMAZ, O. 2014. A hybrid polyacrylate/OMMT nanocomposite latex: Synthesis, characterization and its application as a coating binder. *Progress in Organic Coatings*, 77, 110-117.
- YIN, Y., ZHOU, S., YOU, B. & WU, L. 2011. Facile fabrication and self - assembly of polystyrene - silica asymmetric colloid spheres. *Journal of Polymer Science Part A: Polymer Chemistry*, 49, 3272-3279.
- YU, B., ZHOU, F., PEI, X., YE, Q. & HU, H. 2011. A kind of ionic liquid based marine antifouling coating. China patent application.
- YUAN, J., BAI, X., ZHAO, M. & ZHENG, L. 2010. C12mimBr Ionic Liquid/SDS Vesicle Formation and Use As Template for the Synthesis of Hollow Silica Spheres. *Langmuir*, 26, 11726-11731.
- YUHONG, Z., QICHAO, Z., XINGWANG, S., QINGQIONG, T., MIN, C. & LIMIN, W. 2009. Preparation of raspberry-like polymer/silica nanocomposite microspheres via emulsifier-free polymerization in water/acetone media. *Journal of colloid and interface science*, 336, 544-550.
- ZENO W. WICKS, J., JONES, F. N., PAPPAS, S. P. & WICKS, D. A. 2007. *Organic Coatings*, Hoboken, New Jersey, John Wiley & Sons.
- ZHANG, H., SU, Z., LIU, P. & ZHANG, F. 2007. Preparation and property of raspberry - like AS/SiO₂ nanocomposite particles. *Journal of applied polymer science*, 104, 415-421.
- ZHANG, Q., SHI, Y., ZHAN, X. & CHEN, F. 2012. In situ miniemulsion polymerization for waterborne polyurethanes: Kinetics and modeling of interfacial hydrolysis of isocyanate. *Colloids and Surfaces A: Physicochemical and Engineering Aspects*, 393, 17-26.
- ZHOU, H., SHI, T. & ZHOU, X. 2013. Preparation of polystyrene/SiO₂ microsphere via Pickering emulsion polymerization: Synergistic effect of SiO₂ concentrations and initiator sorts. *Applied Surface Science*, 266, 33-38.
- ZHOU, Y., SCHATTKA, J. H. & ANTONIETTI, M. 2004. Room-Temperature Ionic Liquids as Template to Monolithic Mesoporous Silica with Wormlike Pores via a Sol-Gel Nanocasting Technique. *Nano letters*, 4, 477-481.
- ZHU, A., CAI, A., YU, Z. & ZHOU, W. 2008. Film characterization of poly(styrene-butylacrylate-acrylic acid)-silica nanocomposite. *J Colloid Interface Sci*, 322, 51-8.

ZHU, G., ZHANG, L., PAN, X., ZHANG, W., CHENG, Z. & ZHU, X. 2012. Facile Soap - Free Miniemulsion Polymerization of Methyl Methacrylate via Reverse Atom Transfer Radical Polymerization. *Macromolecular rapid communications*, 33, 2121-2126.